

**The genomic profile of low frequency  
chromosome 17p deletion sub-clones  
in Chronic Lymphocytic Leukaemia:  
detection and characterisation.**

by

**Cuc Hoang Do, M.D., M.Sc.(Med.)**

*Thesis  
Submitted to Flinders University  
for the degree of*

**Doctor of Philosophy**  
College of Medicine and Public Health

20<sup>th</sup> June 2018

---

---

# Contents

## Contents

<b>CONTENTS.....</b>	<b>I</b>
<b>FIGURES .....</b>	<b>VII</b>
<b>TABLES.....</b>	<b>XI</b>
<b>DECLARATION .....</b>	<b>XIII</b>
<b>ACKNOWLEDGEMENTS.....</b>	<b>XIV</b>
<b>ABBREVIATIONS .....</b>	<b>XVII</b>
<b>STANDARD INTERNATIONAL UNITS OF MEASUREMENT .....</b>	<b>XX</b>
Indicators of magnitude.....	xx
<b>ABSTRACT.....</b>	<b>XXI</b>
<b>PUBLICATIONS AND PRESENTATIONS ARISING DURING CANDIDATURE.....</b>	<b>XXIV</b>
Full publications .....	xxiv
Published abstracts.....	xxiv
Oral presentations.....	xxv
Poster presentations .....	xxvi
<b>1 CHAPTER 1 – INTRODUCTION.....</b>	<b>28</b>
1.1 Normal biology of B lymphocytes - IgHV.....	28
1.1.1 B-cell development .....	28
1.1.2 Somatic hyper-mutation and class switch recombination.....	30
1.1.3 Cell surface immunoglobulin and B cell receptor in normal B-lymphocytes .....	30
1.2 Overview of chronic lymphocytic leukaemia .....	31
1.3 Pathology of CLL.....	32
1.3.1 Cellular origin(s) of CLL.....	32

---

1.3.2	Monoclonal B lymphocytosis (MBL) and familial CLL (F-CLL) .....	34
1.3.3	Infection factors in the origin of CLL .....	35
1.3.4	MicroRNAs in the pathogenesis of CLL .....	36
1.4	Diagnosis of CLL .....	36
1.4.1	Clinical characteristics of CLL patients .....	36
1.4.2	Rai and Binet staging systems .....	37
1.4.3	Laboratory features for diagnosis .....	38
1.4.4	Immuno-phenotype .....	39
1.5	Treatment .....	40
1.5.1	Criteria for initial treatment .....	40
1.5.2	Treatment Components .....	40
1.5.3	Aim of treatment .....	46
1.6	Markers for prognosis .....	46
1.6.1	IgHV gene mutational status .....	47
1.6.2	CD38 .....	48
1.6.3	Cytogenetic markers .....	48
1.6.4	Conventional fluorescence <i>in situ</i> hybridisation (conventional FISH) .....	49
1.6.5	Laser scanning cytometry (LSC) .....	53
1.6.6	Single nucleotide polymorphism array (SNP array) .....	54
1.6.7	Sanger sequencing .....	56
1.6.8	Massive parallel sequencing (MPS) .....	56
1.6.9	Fluorescence <i>in situ</i> hybridisation in suspension (FISH-IS) .....	57
1.7	<i>TP53</i> aberrations in CLL .....	59
1.7.1	Tumour suppressor gene <i>TP53</i> .....	59
1.7.2	Overview of the role of <i>TP53</i> abnormalities in CLL .....	61

---

1.7.3 Clonal evolution of <i>TP53</i> genes defects.....	64
1.7.4 Low frequency del17p sub-clones ( <i>TP53</i> genes loss in small clones).....	68
1.8 Purpose of this study.....	69
<b>2 CHAPTER 2 - MATERIALS AND METHODS .....</b>	<b>72</b>
2.1 Materials.....	72
2.2 Collection of peripheral blood from CLL patients .....	72
2.3 Isolation/cryopreservation of peripheral blood mononuclear cells from whole blood	73
2.4 Counting and viability of PBMCs by trypan blue analysis .....	74
2.5 Thawing cells from liquid nitrogen storage.....	74
2.6 Conventional fluorescence <i>in situ</i> hybridisation (conventional FISH) .....	75
2.6.1 Conventional FISH Buffers.....	75
2.6.2 Conventional FISH method .....	75
2.7 Laser scanning cytometry (LSC).....	77
2.8 Fluorescence <i>in situ</i> hybridisation in suspension (FISH-IS).....	82
2.8.1 FISH-IS buffers .....	82
2.8.2 FISH-IS method .....	83
2.9 Bacterial artificial chromosome (BAC) probe labelling by nick translation.....	86
2.10 Statistical analysis .....	88
<b>3 CHAPTER 3 - GENOMIC ANALYSIS OF CLL5 ARC COHORT .....</b>	<b>89</b>
3.1 Introduction.....	89
3.2 Materials and methods .....	92
3.2.1 Conventional FISH.....	92
3.2.2 Laser scanning cytometry (LSC) .....	93
3.2.3 Massive parallel sequencing (MPS) analysis .....	93
3.2.4 Statistical methods.....	96

---

3.3 Results.....	96
3.3.1 Baseline characteristic of the CLL5 cohort.....	96
3.3.2 Conventional FISH characteristics of the CLL5 cohort and overall outcome. ...	98
3.3.3 Further investigations of conventional FISH data of the CLL5 cohort.....	101
3.3.4 Relationship between 17p deletion and 13q deletion in the CLL5 cohort .....	103
3.3.5 Genomic molecular profiling characteristics of the CLL5 cohort.....	113
3.3.6 Investigations of mutational profile of patients containing <i>TP53</i> mutation .....	115
3.3.1 Assessment of the low frequency del17p detection by analysing MPS data. .	117
3.4 Discussion .....	121
3.5 Conclusion.....	128
<b>4 CHAPTER 4 - DEVELOPMENT OF FISH-IS TO DETECT ANEUPLOIDIES IN CLL.....</b>	<b>129</b>
4.1 Introduction.....	129
4.2 Materials and methods .....	131
4.2.1 FISH-IS with centromere probes protocol .....	131
4.2.2 Laser scanning cytometry.....	131
4.2.3 Statistical methods.....	131
4.3 Results.....	132
4.3.1 Optimisation of the FISH-IS protocol with CLL cells.....	132
4.3.2 FISH-IS protocol produces auto-fluorescence of CLL cells .....	135
4.3.3 FISH-IS is able to detect monosomy in CLL cells .....	137
4.3.4 FISH-IS can detect disomy by fluorescence intensity but not by spot count...	139
4.3.5 FISH-IS signal intensity in CLL cells is not sample dependent .....	143
4.3.6 FISH-IS is able to differentiate between monosomy and disomy in CLL cells	145
4.3.7 FISH-IS is able to differentiate between disomy and trisomy in CLL cells .....	150
4.3.8 Spot Count cannot accurately identify the number of hybridisation signals ....	154

---

4.3.9 Comparison of detection of trisomy 12 in CLL samples by 3 different methods	156
4.4 Discussion .....	158
4.5 Conclusion.....	166
<b>5 CHAPTER 5 - DEVELOPMENT OF FISH-IS TO DETECT DEL17P IN CLL .....</b>	<b>167</b>
5.1 Introduction.....	167
5.2 Materials and methods .....	171
5.2.1 Commercial FISH probes .....	171
5.2.2 Bacterial Artificial Chromosome (BAC) FISH probes .....	171
5.2.3 FISH-IS protocol with 17p BAC probe contig .....	172
5.2.4 Flow sorting and Sanger sequencing .....	173
5.2.5 Cell culture.....	174
5.2.6 Apoptosis analyses.....	175
5.2.7 Investigation of pseudo-nodes.....	175
5.2.8 Statistical analysis .....	176
5.3 Results.....	176
5.3.1 Commercial 17p probes do not generate sufficient signal for use in FISH-IS	176
5.3.2 Development and validation of a custom 17p BAC probe contig .....	179
5.3.3 Increasing the number of BAC probe increases signal fluorescence intensity	182
5.3.4 Optimisation of FISH-IS with the 17p BAC probe contig.....	184
5.3.5 FISH-IS is able to distinguish 17p-deleted cells from wild-type 17p cells .....	209
5.3.6 Sanger sequencing confirms that FISH-IS can discriminate del17p sub-clone.	214
5.3.7 FISH-IS cannot discriminate del17p from wt17p on cryopreserved samples..	217
5.3.8 Alternative analysis to identify del17p sub-clone on cryopreserved samples .	219
5.3.9 Standard media incubation of cryopreserved CLL does not enable FISH-IS analysis	222
5.3.10 Various culture conditions cannot sufficiently restore cryopreserved CLL.....	225

---

5.3.11 FISH-IS results after maintenance in supportive <i>in vitro</i> conditioned media...	229
5.3.12 CLL cells incubated in HS5 co-culture acquired pseudo-nodes.....	231
5.4 Discussion .....	233
5.5 Conclusions .....	247
<b>6 CHAPTER 6 - GENERAL DISCUSSION AND CONCLUSIONS.....</b>	<b>248</b>
6.1 Overview.....	248
6.2 Characteristics of low frequency del17p sub-clone.....	250
6.3 The FISH-IS method provides superior monitoring of del17p sub-clones. ....	251
6.4 The FISH-IS method has the potential to integrate with many other fields.....	253
6.5 Future directions for this project – Other approaches to solving the puzzle .....	255
6.6 Conclusion.....	257
<b>APPENDIX.....</b>	<b>258</b>
<b>REFERENCES.....</b>	<b>277</b>

---

**Figures**

Figure 1.1. A model for different derivations of CLL cells. .... 33

Figure 1.2. Development of CLL model from haematopoietic stem cells. .... 34

Figure 1.3. Kaplan-Meier graph showing overall survival of CLL patients according to five common genetic categories. .... 49

Figure 1.4. A model of inferring the clonal evolution in CLL. .... 67

Figure 2.1. Laser scanning cytometry protocol for FISH analysis. .... 79

Figure 2.2. Analysis workflow of laser scanning cytometry data for centromere 12 probe. .... 81

Figure 2.3. Analysis workflow of laser scanning cytometry data for *DLEU/TP53* probes. .... 82

Figure 3.1. Kaplan-Meier curves demonstrating progression free survival of patient subsets according to del17p status as determined by conventional FISH analysis. .... 100

Figure 3.2. Frequency of co-occurrence of 2 genomic aberrations by conventional FISH in CLL5 cohort. .... 104

Figure 3.3. Kaplan-Meier curves demonstrating progression free survival of del17p patient subsets according to del13q status as determined by conventional FISH analysis. .... 106

Figure 3.4. Sub-clonal frequencies by laser scanning cytometry in cases harbouring both low frequency del17p and del13q. .... 112

Figure 3.5. Normalised MPS coverage of read analysis from the 5 gene panel. .... 119

Figure 3.6. Percentage del17p identified by copy number variant analysis of *TP53* gene region. .... 120

Figure 4.1. Examples of technique failures whilst developing the FISH-IS protocol. .... 133

Figure 4.2. Analysis of FISH-IS data pipeline. .... 134

Figure 4.3. Determination of auto-fluorescence of CLL cells. .... 136

Figure 4.4. FISH-IS is able to accurately detect monosomy Y in CLL cells by fluorescence intensity and spot count. .... 138



---

Figure 4.5. FISH-IS is able to accurately detect disomy 9 in CLL cells by fluorescence intensity but not by spot count. ....	140
Figure 4.6. FISH-IS is able to enumerate centromere 9 spots in CLL cells only by manual correction of the automatic spot count. ....	142
Figure 4.7. Hybridisation of fluorescence probes in CLL cells is not sample-dependent. ....	144
Figure 4.8. FISH-IS is able to accurately differentiate between monosomy and disomy with centromere X probe in CLL samples by fluorescence intensity. ....	146
Figure 4.9. FISH-IS is able to enumerate centromere X spots in CLL cells only by manual curation of the Spot Count Wizard. ....	149
Figure 4.10. FISH-IS is able to accurately differentiate between disomy and trisomy with centromere 12 probe in CLL samples by fluorescence intensity. ....	151
Figure 4.11. FISH-IS is able to enumerate centromere 12 spots in a sample of CLL cells with 95% trisomy 12 by manual correction of the Spot Count Wizard. ....	152
Figure 4.12. Correlation of the observed proportions of spot-count (Spot Count Wizard) analysis and the expected percentage spots of centromere Y, 9, X and 12 probes using FISH-IS. ....	155
Figure 5.1. Commercial <i>TP53</i> probes do not generate sufficient signal for analysis with FISH-IS. ...	177
Figure 5.2. Different masking strategies are unable to distinguish spots with commercial Kit 3. ....	178
Figure 5.3. Schematic representation of 20 BACs surrounding <i>TP53</i> gene on chromosome 17. ....	180
Figure 5.4. Individual BAC clones were tested to ensure specific hybridisation by metaphase and interphase conventional FISH. ....	181
Figure 5.5. Both raw max pixel and fluorescence intensity increase with an increase in the number of 17p BAC probe contig. ....	183
Figure 5.6. Comparison of Carnoy's fixative standard methods with drop-wise on the number of remaining single cells and their morphology. ....	185
Figure 5.7. One µg of BAC probe contig gives optimal hybridisation signal. ....	188
Figure 5.8. Cot-1 optimisation demonstrates that 50x excess Cot-1 DNA results in optimal specific hybridisation. ....	190

---

---

Figure 5.9. Microscopic visualisation confirms an increase in single intact cells with the addition of EDTA in the pre-hybridisation wash buffer 2. ....	192
Figure 5.10. Representative images of different denaturation temperature and time. ....	195
Figure 5.11. Representative images of different hybridisation temperature and formamide concentration. ....	197
Figure 5.12. Twelve hours is the optimal hybridisation time for FISH-IS with the 17p BAC probe contig. ....	198
Figure 5.13. Various features of wash 1 were altered in order to optimise the FISH-IS method. ....	202
Figure 5.14. Various features of wash 2 were altered in order to optimise the FISH-IS method. ....	204
Figure 5.15. Schematic representation of image acquisition optimisation. ....	206
Figure 5.16. Optimisation of the laser power. ....	208
Figure 5.17. Analysis by raw max pixel and fluorescence intensity of the 17p BAC probe contig gives the best discrimination of two separate populations. ....	210
Figure 5.18. FISH-IS is able to accurately differentiate del17p CLL cells within a mixing model based on fluorescence intensity. ....	212
Figure 5.19. Removal of BAC RP11-199F11 from the probe contig does not significantly affect raw max pixel intensity nor fluorescence intensity when analysed by FISH-IS. ....	214
Figure 5.20. FISH-IS can successfully separate the del17p sub-clone in a CLL sample as confirmed by Sanger sequencing. ....	216
Figure 5.21. FISH-IS on a cryopreserved CLL with 41% 17p deletion. ....	218
Figure 5.22. Spot Count Wizard is unable to accurately determine signal number from FISH-IS with 17p BAC probe contig. ....	220
Figure 5.23. Morphology of CLL samples after Carnoy's fixation as assessed by ImageStreamX with brightfield images. ....	222
Figure 5.24. FISH-IS results with centromere X probes on a 50:50 mixture of male and female CLL samples. ....	224
Figure 5.25. Schematic overview of six different culture conditions assessed and EVOS™ images. ....	226

Figure 5.26. The impact of *in vitro* supportive culture conditions on CLL cell survival as determined by different methods. .... 228

Figure 5.27. Evaluation of cryopreserved CLL cells with FISH-IS procedure after maintaining in supportive *in vitro* conditioned media..... 230

Figure 5.28. Comparison of CLL cell survival between cells in suspension and cells contained inside the pseudo-nodes. .... 232

---

**Tables**


Table 1.1. Clinical stage according to the Rai and Binet systems. ....	38
Table 2.1. Properties of fluorochromes used in ImageStreamX analysis. ....	84
Table 2.2. Brief descriptions of features used in IDEAS software analysis. ....	85
Table 2.3. Preparation buffers used in the REPLI-g Midi Kit. ....	86
Table 3.1. CLL5 patients' baseline characteristics at enrolment. ....	97
Table 3.2. Treatment response according to cytogenetic characteristics as determined by conventional FISH. ....	98
Table 3.3. Response to treatment according to the number of genetic abnormalities as characterised by conventional FISH in CLL5 cohort (n=95). ....	102
Table 3.4. List of conventional FISH results of CLL5 samples with 17p deletion (n=20). ....	105
Table 3.5. Laser scanning cytometry results of normal healthy control PBMCs. ....	107
Table 3.6. Analysis of sub-clonal chromosomal architecture in CLL samples with concomitant del17p & del13q and normal-by-FISH. ....	111
Table 3.7. Associations between the genomic mutations identified by targeted sequencing and conventional FISH analysis in the entire CLL5 cohort. ....	114
Table 3.8. Frequency of 5 gene mutations and treatment responses. ....	115
Table 3.9. Patients with <i>TP53</i> mutations and other variant alleles identified by MPS stratified by del17p frequency. ....	116
Table 4.1. Detection of FISH-IS with predictable model of aneuploidy in CLL samples with centromere X probe. ....	147
Table 4.2. Detection of FISH-IS with centromere 12 probe in CLL samples. ....	154
Table 4.3. Comparison of results of three methods analysing centromere 12 probe hybridisation on CLL samples. ....	157
Table 5.1. DNase I treatment does not increase the number of single intact cells. ....	186

---

Table 5.2. The addition of proteinase K does not increase the number of single intact cells or the signal to background ratio. ....	187
Table 5.3. Optimisation of BSA and EDTA concentrations in the pre-hybridisation wash buffer 1. ...	191
Table 5.4. Optimisation of denaturation temperature, denaturation time and formamide concentration in hybridisation buffer. ....	194
Table 5.5. Optimisation of hybridisation temperature and formamide concentration in hybridisation buffer. ....	196
Table 5.6. Summary of optimisation of washing conditions for FISH-IS. ....	199
Table 5.7. FISH-IS analysis based on fluorescence intensity of CLL controlled mixed samples. ....	213
Table 5.8. Results of manual curation of Spot Count Wizard on cryopreserved CLL samples. ....	221
Table 5.9. Intact CLL cells following various time points of standard incubation after cryopreservation. ....	223

**Declaration**

I certify that this thesis does not incorporate without acknowledgment any material previously submitted for a degree or diploma in any university; and that to the best of my knowledge and belief it does not contain any material previously published or written by another person except where due reference is made in the text.

A handwritten signature in blue ink, consisting of a stylized 'm' followed by a horizontal line, positioned above a solid horizontal line.

Cuc Hoang Do

## **Acknowledgements**

The work reported in this thesis would never have been finished without the guidance of my supervisors, help from my colleagues, encouragement from friends, and support of my family. Special thanks are due to CLL patients and people who donated blood for this study and allowed me to access their clinical information.

First and foremost I would like to sincerely thank my principle supervisor, Associate Professor Bryone Kuss, for giving me a chance to undertake this PhD project in her department. I will always appreciate her encouragement for me to develop all of my skills. Thank you for giving me the chance to attend some national/international conferences and to visit interstate laboratories to showcase my work and to learn from others. I thank her deeply for her generosity to my family and the many opportunities that she facilitated for me during the last 4 years.

I would like to acknowledge my co-supervisors Associate Professor Cindy Macardle and Dr Karen Lower. I thank Dr Karen Lower profoundly for all her support and scientific guidance and for inspiring in me the love of genetic science by allowing me to attend her genetic medicine lectures. To Bryone and Karen, thank you for all the time, patience and effort throughout my PhD studies that you have expended to help me, from guidance to designing experiments, and creating figures to helping me to publish two academic papers. I have learnt a lot from you and I will never forget all your support.

The work of this project would have been impossible without the kind and expert assistance of a number of people. I would like to thank the Women's and Children's Hospital (Adelaide) for providing me the BAC DNA and giving me immeasurable help

in labelling the BAC probes. Thanks to Dr Randall Grose (SAMHRI) for inspiring me with his enthusiasm and always helping with flow sorting and laser scanning. I appreciate Dr Sarah Moore and her team (SA Pathology, Adelaide) for their professional advice and support. I thank Dr Orlar Maguire and her team (Roswell Park Cancer Institute, USA) for providing the detailed FISH-IS protocol described in Chapter 4 and much technical advice. Thanks for all the advice from Dr Kathy Fuller during the 2 weeks I visited her laboratory in Perth. Thank you to Dr Giles Best, Dr Badoux Xavier and their research team (University of Sydney) for giving me the raw data of massive parallel sequencing data and extensive advice for my thesis. I also especially thank the CLL5 clinical trial committee for all the sample collections and providing me with the patients' characteristics.

I would like to thank Dr Sinoula Apostolou, Dr Sheree Bailey, Dr Lauren Thurgood, Dr Anya Hotinski and Mrs Dianne Luke for their continued support, their encouragement, advice and friendship. They were always willing to discuss the unclear concepts, read my writing, listen to my difficulties and chat with me about my daily life and family. Thanks for your invaluable friendship.

I would like to particularly thank Ms Rachel Hall and Dr Scott Grist (SA Pathology, Adelaide) for conducting the massive parallel sequencing for 5 patients and IgHV mutational status described in Chapter 3 and their useful advice on data analysis.

I profoundly thank my colleagues Jasmine Wannop, Monica Dreimanis, Duncan Holds and Kristy Nichol, who took me through the techniques during my early candidature. I thank Dr Melanie Hayes, Dr Katherine Morel, Jennifer Washington, Brad Budgen and Sue Latham for sharing much helpful technical advice. My thanks also to all past and



present members and students of the Department of Haematology & Genetic Pathology for their assistance throughout my PhD studies.

My sincere thanks to Professor Pam Sykes for opening the door for me to conduct my PhD in Adelaide. Thanks for doing all the paper work at the beginning of my candidature. Thanks to Pam and Adrian for supporting my family so warmly.

I would like to thank to Dr Maria Flutsch for her help editing my writing. To Maria and Graeme Payne, thanks for sharing their house with my family, for caring for my son and for all of their support, especially in my last “horrible” year.

Personally, to my parents and my siblings, thanks for their unlimited love and for calling me every weekend, caring about my health, my daily life in Adelaide and encouraging me to finish my thesis. Most importantly, a special thanks to my husband Linh and my son Bach for understanding my work, for waiting for dinner every night (due to late experiments), for their willingness to share most of their weekends over the last 4 years with my experiments and for always eating a lot of frozen food to save me time for my PhD project. Their unwavering love and constant belief in me gave me strength to finish my PhD.

---

**Abbreviations**

ALL	acute lymphoblastic leukemia
AML	acute myeloid leukemia
ARC	Australian Research Consortium
ATM	ataxia telangiectasia mutated
BAC	bacterial artificial chromosome
BCR	B cell receptor
BSA	bovine serum albumin
BTK	Bruton's tyrosine kinase
CEP	chromosome enumerate probes
Chr	chromosome
CIRS	cumulative illness rating scale
CLL	chronic lymphocytic leukaemia
CML	chronic myelogenous leukemia
CNV	copy number variation
COSMIC	catalogue of somatic mutations in cancer
CR	complete remission
DAPI	4',6-diamidino-2-phenylindole
del11q	deletion of the long arm of chromosome 11
del13q	deletion of the long arm of chromosome 13
del17p	deletion of the short arm of chromosome 17
dH <sub>2</sub> O	distilled water
DLEU	deleted in lymphocytic leukemia
DNA	deoxyribonucleic acid
DNase I	deoxyribonuclease I
dNTP	deoxynucleotide triphosphate
dsDNA	double strand DNA
EDF	extended depth of field
EDTA	ethylenediaminetetraacetic acid
F	female
F-CLL	family CLL
FCR	fludarabine, cyclophosphamide, rituximab

---

FCS	fetal calf serum
FISH	fluorescence in situ hybridization
FISH-IS	fluorescence <i>in situ</i> hybridization in suspension
GC	germinal center
HS5	human bone marrow stroma 5
HSC	haematopoietic stem cells
Ig	immunoglobulin
IgHV	immunoglobulin heavy chain variable
IL	interleukine
iwCLL	International Workshop on CLL
LDH	lactate dehydrogenase
LDT	lymphocyte doubling time
LPD	lymphoproliferative disorder
LSC	laser scanning cytometry
LSD	least significant difference
LSI	locus-specific identifier
M	male
MBL	monoclonal B lymphocytosis
M-CLL	mutated chronic lymphocytic leukemia
miRNA	microRNA
MPS	massive parallel sequencing
MRD	minimal residual disease
NF- $\kappa$ B	nuclear factor kappa-light-chain-enhancer of activated B cells
NP40	nonidet P-40
nPR	nodular partial remission
ORR	overall response rate
OS	over survival
PBMC	peripheral blood mononuclear cells
PBS	phosphate buffered saline
PCR	polymerase chain reaction
PFS	progression-free survival
PI	propidium iodide

PR	partial remission
RP11	Roswell Park Cancer Institute 11
RT	room temperature
SCT	stem cell transplantation
SD	standard deviation
<i>SF3B1</i>	splicing factor 3b subunit 1
SHM	somatic hypermutation/s
SNPs	single nucleotide polymorphisms
SSC	saline-sodium citrate
<i>TP53</i>	tumour protein 53
tri12	trisomy 12
UM-CLL	unmutated chronic lymphocytic leukemia
VAF	variant allele frequency
wt17p	wild type 17p
ZAP70	Zeta-chain associated protein kinase

**Standard international units of measurement**

°C degree Celsius

g gram (s)

h hour (s)

d day(s)

min minute(s)

s second (s)

L litre (s)

M molar

m meter(s)

V volt

W watt

**Indicators of magnitude**

k kilo ( $\times 10^3$ )

m milli ( $\times 10^{-3}$ )

$\mu$  micro ( $\times 10^{-6}$ )

n nano ( $\times 10^{-9}$ )

**Abstract**

Chronic lymphocytic leukaemia (CLL) is a disease predominantly of elderly people and therefore is becoming increasingly important given Australia's ageing population. One of the most important prognostic markers in CLL is a deletion of the short arm of chromosome 17 (del17p), which harbors a tumour suppressor gene (*TP53*). Loss of function of the encoded p53 protein, either by deletion or mutation, results in aggressive disease. However, it has been hypothesised that low frequency loss of *TP53* genes (<25% of cells carrying del17p) may not carry the same clinical significance, particularly early in the disease course. To further confound this issue, it has not previously been possible to identify the additional genetic mutations which may be contained within these small del17p sub-clones in CLL. Clinicians are faced with these fundamental issues when selecting best therapy, which is usually guided by risk calculations based on the genetics of the disease. Therefore, to address this gap in knowledge, this study investigated primary CLL samples containing del17p low frequency clones, including their baseline characteristics, genomic profiling and relationships with other genetic aberrations.

With respect to the intra-clonal heterogeneity of low frequency del17p CLLs, this study has demonstrated a sub-clonal architecture and hierarchy that is different to current assumptions. From the data presented, it is apparent that del13q associates with low frequency del17p sub-clones; this association is not evident in the patients where del17p forms the dominant or high-risk clone. Additionally, through the application of high-throughput laser scanning FISH analysis, it is evident that del17p sub-clones arise independently or at least simultaneously with del13q clones, which is currently

thought to represent a founder event. Whilst determining the clinical impact of this finding requires larger studies, this finding demonstrates a clear genetic difference between dominant and non-dominant del17p clones, and may help to explain the differences in their clinical course.

A direct comparison of the clinical application of three current FISH techniques was also undertaken, incorporating analysis of trisomy 12 CLL samples with the chromosome 12 centromeric probe. This work clearly demonstrates the clinical applicability of automated approaches to FISH analysis.

In order to identify the underlying driver mutations in low frequency del17p CLL sub-clones, a reliable technique is required to identify and analyse these small sub-clones. This study has demonstrated the ability to utilise fluorescence *in situ* hybridisation in suspension (FISH-IS), a method which combines a state of the art flow cytometer with image analysis of individual cells, to capture and record thousands of cells by ImageStreamX. This study has provided the first demonstration of the sensitivity/accuracy of FISH-IS in distinguishing aneuploidy subgroups at 1% with various centromere enumerate probes (CEP) on CLL samples. This is also the first report of a locus-specific probe set being used to identify low frequency del17p in CLL by FISH-IS, with the fluorescence signal made analysable by the use of a 17p BAC probe contig (consisting of labelled bacterial artificial chromosome DNA from the RP11 library). This method enables a prognostic test to reliably detect very low frequency del17p sub-clones with a reliable number of cells monitored at 3%, with the potential for these cells to be genetically analysed as a separate sub-clone.

Hence, the ultimate aim of this work was to flow sort low frequency del17p sub-clones and genetically analyse these cells specifically. This has been accomplished as a proof of principle experiment, which is the first time the genomic landscape of del17p sub-clones has been able to be interrogated in an unbiased manner. Taking this work forward, this technique will enable, for the first time, a specific and in depth genetic analysis of the untreated low frequency del17p sub-clones, with a view to being able to identify the early genetic abnormalities that accompany this event. This method will thereby provide information regarding the differences between early and late events that may lead to the chemo-refractoriness and aggressive CLL phenotype accompanying higher frequency *TP53* genes loss. Critical to further understanding of the relevance of early minor sub-clones is the determination of the genetic profiles of these sub-clones and the identification of potentially druggable driver mutations.



## **Publications and presentations arising during candidature**

### **Full publications**

Do, CH, Lower, KM, Macardle, C & Kuss, BJ, 2017. Trisomy 12 assessment by conventional fluorescence *in situ* hybridisation (FISH), FISH in suspension (FISH-IS) and laser scanning cytometry (LSC) in chronic lymphocytic leukaemia. *Cancer Genetics*, Vol. 216-217, pp. 142-9.

Do, CH, Bailey, S, Macardle, C, Thurgood, LA, Lower, KM & Kuss, BJ, 2017. Development of locus specific sub-clone separation by fluorescence *in situ* hybridisation in suspension in chronic lymphocytic leukaemia. *Cytometry A*. 2017 Oct 11. DOI: 10.1002/cyto.a.23264 (ahead of print).

### **Published abstracts**

Cuc H. Do, Karen Lower, Cindy Macardle, Bryone Kuss. The detection and determination of the genomic profile of low frequency 17p deletion clones in Chronic Lymphocytic Leukaemia (CLL). 58<sup>th</sup> American Society Haematology Annual Meeting, 3-6<sup>th</sup> December 2016, San Diego, California, USA. *Issue in Blood*, 2016. Vol. 128, No. 22, pp. 2021.

Cuc H. Do, Karen Lower, Cindy Macardle, Bryone Kuss. Flow cytometric karyotyping: from centromeres to locus specific identification. XVI International Workshop on Chronic Lymphocytic Leukemia (iwCLL), 7-9<sup>th</sup> September 2015, Sydney, Australia. *Issue in Leukaemia & Lymphoma*, 2015, Volume 56, Supplementary 1. DOI: <http://www.tandfonline.com/doi/full/10.3109/10428194.2015.1080893>.

Cuc H. Do, Karen Lower, Cindy Macardle, Bryone Kuss. Assessment of trisomy 12 in chronic lymphocytic leukaemia by three methods: conventional fluorescence *in-situ* hybridisation (FISH), FISH in suspension (FISH-IS) and Laser Scanning Cytometry (LSC). XVI International Workshop on Chronic Lymphocytic Leukemia (iwCLL), 7-9<sup>th</sup> September 2015, Sydney, Australia. Issue in Leukaemia & Lymphoma, 2015, Volume 56, Sup1. DOI: <http://www.tandfonline.com/doi/full/10.3109/10428194.2015.1080893>.

Kuss, BJ, Do, HC, Lower, KM, Wannop, J, Macardle, PC. Investigating a New Methodology for the Detection of Low Frequency 17p Deleted Clones in Chronic Lymphocytic Leukaemia (CLL): Impact on Prognostic Outcome and Therapeutic Resistance. 56<sup>th</sup> American Society Haematology Annual Meeting, 4-9<sup>th</sup> December 2014, San Francisco, California, USA. Issue in Blood 2014, Vol. 124, No. 21, pp. 5645.

### **Oral presentations**

Cuc H. Do, Karen M. Lower, Bryone J. Kuss. Isolation of a sub-clone containing a specific chromosomal deletion in CLL cells. ASMR SA Scientific Meeting 2017, Adelaide Convention Centre, Adelaide, Australia, 7<sup>th</sup> June 2017.

Cuc H. Do, Karen M. Lower, Cindy Macardle, Bryone J. Kuss. The novel detection of low-frequency 17p deletion clones In Chronic Lymphocytic Leukaemia (CLL). 19<sup>th</sup> Scientific Meeting Haematology Society of Australia and New Zealand 2016, Victor Harbor, Adelaide, Australia, 9<sup>th</sup> Sep 2016.

Cuc H. Do, Karen M. Lower, Cindy Macardle, Bryone J. Kuss. The genomic profile of low frequency 17p deletion clones in chronic lymphocytic leukemia (CLL), Cancer Clinical Research Day 2016, Flinders Centre for Innovation in Cancer, Adelaide, Australia, 20<sup>th</sup> May 2016.

Cuc H. Do, Karen M. Lower, Cindy Macardle, Bryone J. Kuss. Assessment of Trisomy 12 in Chronic Lymphocytic Leukaemia (CLL) by three methods: conventional Fluorescence in-situ hybridisation (FISH), laser scanning cytometry (iCys) and FISH in suspension (FISH-IS). Flinders University PhD Research Day 2015, Flinders Centre for Innovation in Cancer, Adelaide, Australia, 9<sup>th</sup> Oct 2015.

Cuc H. Do, Karen M. Lower, Cindy Macardle, Bryone J. Kuss. TP53 deleted-clone size in Chronic Lymphocytic Leukaemia: challenging techniques. Blood Club Translational Research Meeting 2015, South Australia Health & Medical Research Institute (SAMHRI), Adelaide, Australia. 21<sup>st</sup> April 2015.

### **Poster presentations**

Anya Hotinski, Cuc Do Hoang, Karen Lower, Bryone Kuss. Purification of Trisomy 12 Sub-clone in Chronic Lymphocytic Leukaemia Using Imaging Flow Cytometry and Fluorescence in Situ Hybridisation in Suspension (FISH-IS), XVII International Workshop on Chronic Lymphocytic Leukemia (iwCLL) 2017, New York, USA, 12-15<sup>th</sup> May 2017.

Cuc H. Do, Karen Lower, Cindy Macardle, Bryone Kuss. Approach to 17p deleted patients by fluorescence in-situ hybridisation in suspension (FISH-IS). New Directions in Leukemia Research Meeting 2016, Peppers Noosa, Australia, 16-19<sup>th</sup> March 2016.

Cuc H. Do, Karen Lower, Cindy Macardle, Bryone Kuss. Flow cytometry karyotyping: from centromeres to locus specific identification in chronic lymphocytic leukaemia (CLL). Australian Society for Medical Research (ASMR) Annual Scientific Conference, Stamford Plaza, Adelaide, Australia, 15-18<sup>th</sup> November 2015.

Cuc H. Do, Cindy Macardle, Bryone Kuss. Low frequency 17p deletion clones in chronic lymphocytic leukaemia by fluorescence in-situ hybridisation in suspension (FISH-IS). Australia Society for Medical Research (ASMR) 2015, National Wine Centre, Adelaide, Australia, 3<sup>rd</sup> June 2015.

Kuss, B., Do C, Lower K, Wannop J, Macardle C. Investigating a new methodology for the detection of low frequency 17p deleted clones in Chronic Lymphocytic Leukaemia (CLL): Impact on prognostic and therapeutic resistance. Haematology Society of Australia and New Zealand Annual Scientific Meeting 2014, Perth, Australia, 19-22<sup>nd</sup> October 2014.

Cuc H. Do, Cindy Macardle, Bryone Kuss. The genomic profile of low frequency 17p deletion clones in Chronic Lymphocytic Leukaemia (CLL): impact on prognostic and therapeutic resistance. Australia Society for Medical Research (ASMR) 2014, Adelaide Conventional Centre, Adelaide, Australia, 4<sup>th</sup> June 2014.

# 1 Chapter 1 – Introduction

## 1.1 Normal biology of B lymphocytes - IgHV

### 1.1.1 B-cell development

B lymphocytes are derived from a hematopoietic lineage and represent an important part of the cognate immune system (Lai et al. 2008, Montecino-Rodriguez et al. 2012). The different pathways of B cell development are regulated by an ordered rearrangement of the antigen receptor genes. Early B cells undergo several gene rearrangements which encode for heavy (H) and light (L) chains, containing variable (V) and constant (C) regions (reviewed in Pieper et al. (2013)). As B-cell development continues, cells with appropriate receptor molecules are selected through an antigen recognition process.

In order to become fully functional, there are two waves of immunoglobulin gene rearrangements, first involving the heavy chain, and then the light chain gene loci to form functional immunoglobulin genes. The heavy chain genes are assembled from one of several V region genes, one of several D segments, and one of several J segments. In the first step, B cell precursors that performed  $D_H-J_H$  rearrangement at their heavy chain genes are named pro-B cells, followed by the rearrangement of  $V_H$  to  $D_H-J_H$  segments that are termed pre-B cells. If successful, these cells will attempt to transcribe and then translate the  $\mu$  chain which feeds back on the complete mechanism of heavy chain gene rearrangements.

The next step is the rearrangement of light chain genes (2 types: kappa and lambda), which will combine from one of several  $V_L$  region genes and one of

several J<sub>L</sub> segments. Once V<sub>L</sub>-J<sub>L</sub> joining has occurred, cells expressing complete B-cell receptor (BCR) (Pinto et al. 2011) on their surfaces depart the bone marrow as naïve B cells. They migrate from the bone marrow to the peripheral blood and the secondary lymphoid organs, including lymph nodes, spleen and Peyer's patch where they encounter antigens. Contact with antigen and helper T-cells triggers B cells to differentiate further. The activated B cells migrate to the germinal centres (GC) and proliferate extensively; they also undergo clonal expansion, somatic hyper-mutation (SHM) (Grubor et al. 2009), affinity selection and class switching (reviewed in Pieper et al. (2013)). During SHM, mutations are acquired in the immunoglobulin (Ig) genes, B cells that acquire disadvantageous mutations or bind with low affinity to their cognate antigen undergo apoptosis, whereas B cells that acquire high affinity are positively selected (Wagner et al. 1996). Finally, antigen-selected B cells can differentiate into memory B cells or terminally differentiated plasma cells which secrete antibody and leave the germinal centre microenvironments (Hagman et al. 1994, Thompson 1995, Oscier 1997).

The control of this process depends on the successful down-regulation of RAG gene expression, that is, RAG1 and RAG 2 proteins (Grawunder et al. 1995, Giachino et al. 1998, Herzog et al. 2009, Chiorazzi et al. 2011, Pieper et al. 2013). Additionally, there are many transcription factors involved in the development of B cells, including Pu.1, E2A, ENF, Pax-5, Bcl-6, IRF4, BLIMP1, XBP1, etc. (Scott et al. 1994, Shen et al. 1998). Recently, it has become obvious that B cell differentiation is not only regulated at the transcriptional level by these transcription factors, but also at the posttranscriptional level by small

noncoding RNA, termed micro-RNAs (mi-RNA) (Chen 2004, Ferrajoli et al. 2013).

### **1.1.2 Somatic hyper-mutation and class switch recombination**

Somatic hyper-mutation in immunoglobulin heavy chain variable region genes (IgHV genes) is a valuable prognostic marker of patient survival in CLL (Grubor et al. 2009). In fact, SHM is a process which allows point mutations to be introduced into productively or non-productively rearranged variable region genes (IgV) at a rate of  $10^{-3}$  per base pair per generation (Kocks et al. 1989). The pattern of SHM is not random, using an intrinsic preference for transitions over transversions and hot-spot motifs. Indeed, V-region gene mutations occur at a high ratio to increase affinity for antigens in SHM. The immunoglobulin heavy chain locus (IgH) is located on chromosome 14q32.33, and the functional genes have been categorized into 7 subgroups depending on their nucleotide homology, including IgHV1 to IgHV7 (Okazaki et al. 2002).

### **1.1.3 Cell surface immunoglobulin and B cell receptor in normal B-lymphocytes**

Lymphocytes (and other leukocytes) express different functionally important molecules on their membranes, termed “cluster of differentiation” (CD). These CD markers can be used to categorise different leukocyte subsets. CD19 and CD20 are the principle markers used to identify human B cells. In adult humans, B cells account for roughly 5-15% of the circulating lymphoid pool and are defined by the presence of surface markers, namely immunoglobulin. This associates with other molecules on the B cell membrane such as CD79a (Ig  $\alpha$ ) and CD79b (Ig  $\beta$ ) which form the BCR.

B lymphocytes expressing CD5 are the predominant population in early life (in the foetus or the first year after birth) and they rarely undergo germinal centre reactions evidenced by unmutated V regions. As a result, in adults, the CD5+ B cells only account for approximately 15% of B lymphocytes in the peripheral blood (Geiger et al. 2000, Pieper et al. 2013).

## **1.2 Overview of chronic lymphocytic leukaemia**

Chronic lymphocytic leukaemia (CLL) is the most common adult leukaemia in western countries, usually affecting individuals in their 7th decade of life and beyond (Altekruse et al. 2010). This disease results from a clonal overgrowth of B-lymphocytes in the blood and bone marrow, but also involves other compartments such as lymph nodes and spleen. In addition, CLL is an extremely heterogeneous disease, and is characterized by a highly variable disease course where survival can range from months to decades.

The development of modern techniques has significantly improved the ability to prognosticate for CLL, thereby impacting the choice and timing of therapy of CLL. The mortality rate for CLL, however, remained unchanged for nearly three decades in Australia with 1.4 deaths per 100,000 people in both 1982 and 2010. The overall survival (OS) five-year rate for CLL remained relatively consistent over these years in Australia and was 70.3% for the period 1982-1987 and 72.6% for the period 2006-2010 (CLL\_statistics 2014).



## **1.3 Pathology of CLL**

CLL is an accumulative disease of B-lymphocytes, which are immature and non-functional with a low rate of proliferation. These CLL cells result from B-lymphocytes arrested at the G0/G1 phase in the cell cycle and failure to undergo apoptosis (Dameshek 1967).

### **1.3.1 Cellular origin(s) of CLL**

It is difficult to understand the origin of CLL even with a good understanding of the normal B lymphocyte life cycle (Chiorazzi et al. 2011). The natural processes of Ig V (D) J rearrangement, somatic hyper-mutation (SHM), and class switching create unique sequences that not only provide a tracking device for tumour detection, but also reveal the clonal history of the cell from its parental B cell. Usually, the immune-phenotype of the tumour cells and/or the identical histology of tumour cells demonstrate their origins. (Kuppers et al. 1999, Chiorazzi et al. 2003, Klein et al. 2010, Fabbri et al. 2016).

The different derivations of CLL cells can be seen in Figure 1.1. According to current hypotheses, these can be divided into two subgroups: one originating from pre-germinal centre B cells, with no somatic hyper-mutations (U-CLL), the other from post-germinal centre B cells with mutations (M-CLL) (Klein et al. 2010, Seifert et al. 2012).

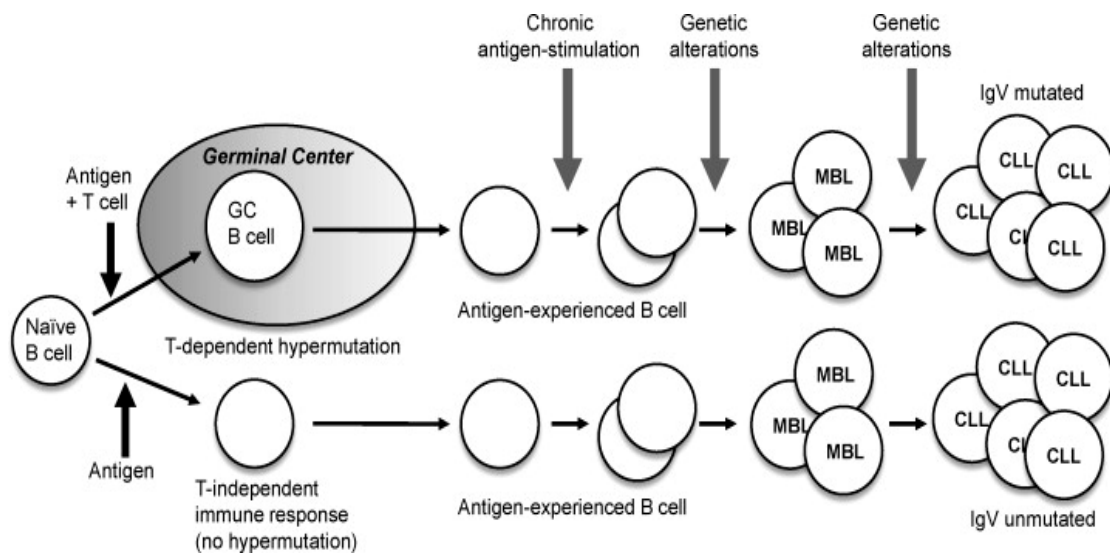


**Figure 1.1. A model for different derivations of CLL cells.**

*Naïve B-cells may migrate to germinal centres (IgHV mutated) or not (IgHV unmutated). Next these cells could receive ongoing activation through antigens and accumulate genetic aberrations. This could lead to multiple clones with an MBL phenotype or result in CLL transformation.*

*Adapted from Klein et al. (2010).*

By contrast, experiments conducted on xenograft mouse models revealed that the genetic aberrations and epigenetic lesions presented in haematopoietic stem cells (HSCs) might develop into CLL clones (Kikushige et al. 2011). Similarly, further reports demonstrated that the somatic mutations acquired in CLL were found in HSCs, suggesting that CLL resulted from an expansion of clonally pre-leukemic HSCs (Figure 1.2) (Damm et al. 2014, Genovese et al. 2014, Jaiswal et al. 2014).

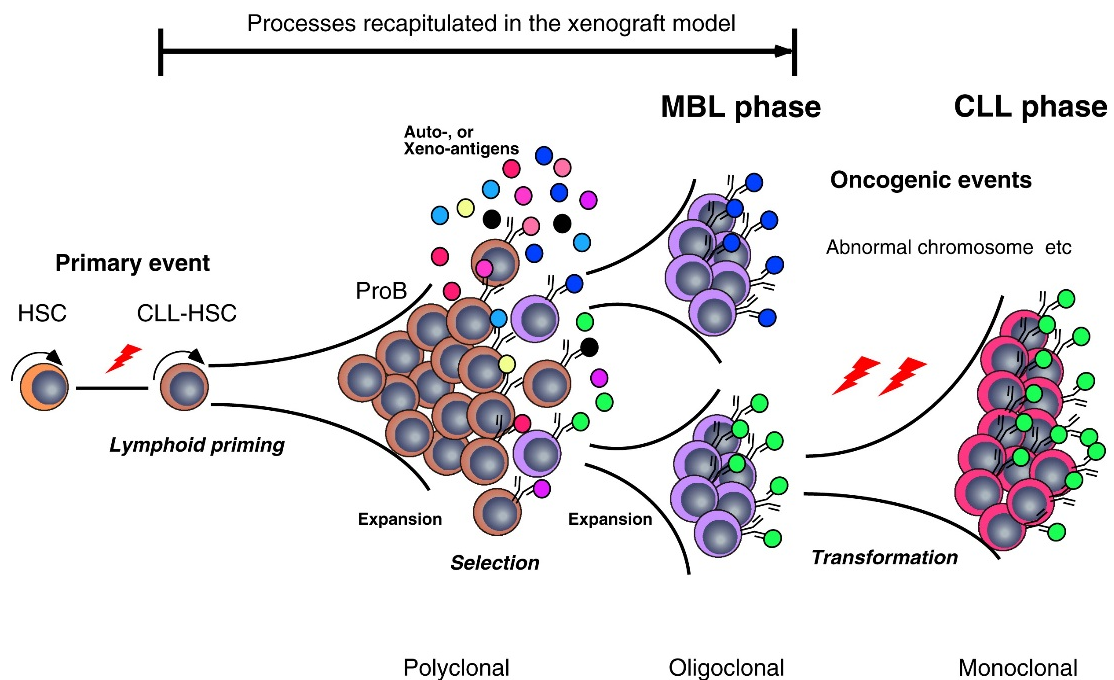


**Figure 1.2. Development of CLL model from haematopoietic stem cells.**

*Adapted from Kikushige et al. (2011).*

### 1.3.2 Monoclonal B lymphocytosis (MBL) and familial CLL (F-CLL)

The presence of monoclonal B cells in peripheral blood without any lymphoproliferative disorder is called monoclonal B-cell lymphocytosis (MBL) (Marti et al. 2007). MBL is an asymptomatic haematological condition characterized by small B cells clones (fewer than 5000 B lymphocytes/ $\mu\text{L}$ ) with similar CD markers on the surface to that of CLL (e.g. CD5 and CD19) (Goldin et al. 2010). The risk of transformation to CLL from MBL is approximately 1% to 2% annually (Rawstron et al. 2008). In addition, this concept allows the separation of two types of CLL: familial CLL (F-CLL), defined as a CLL case with at least three blood relatives with CLL (Goldin et al. 2010).

People of Australia, the USA and Europe (Western countries) show a high incidence of CLL, whereas it is rare in China, Japan, or Southeast Asian countries. The reasons for these differences are not conclusively known. It is probable that additional genes confer a significant risk as part of the inherited susceptibility which is called inherited predisposition (Houlston et al. 2003). The ability to identify these susceptible genes for CLL in large scale genomic studies by screening whole genomes for loci will play an important role in unfolding of the etiologic pathways of CLL (Fuller et al. 2008, Goldin et al. 2010, Tegg et al. 2010).

### **1.3.3 Infection factors in the origin of CLL**

It is hypothesised that CLL may result indirectly from the processes that result in normal B lymphocytes continuing to divide without restraint after they have reacted to an antigen; however, the mechanism is currently not understood (Loeb 1947, Klein et al. 2008). Recently, it was suggested that MBL is an immune trigger from infectious disease exposure (Casabonne et al. 2012). Furthermore, it has been hypothesised that viruses might play an important role in inducing CLL, but there is no evidence for this. Specifically, such a concept presupposes that viruses are present, though in an inactive state, in all specific organs or tissues. These viruses enable the normal cells to undergo a cancerous change if stimulated by unknown sources which can cause somatic mutations or other cancer promoting pathways (Casabonne et al. 2013).

### **1.3.4 MicroRNAs in the pathogenesis of CLL**

MicroRNAs (miRNAs) are small non-coding RNAs (approximately 22 nucleotides) that function as gene expression regulators, including for cell proliferation and apoptosis (Subramanian et al. 2010, Chen et al. 2017). In CLL, miRNA has been reported to act as surrogate tumour suppressor genes and/or oncogenes. Calin et al. (2002) was the first to demonstrate that loss of miR15 and miR16 (located at chromosome 13q14) was correlated with developing CLL tumours. Subsequently, Cimmino et al. (2005) provided evidence that these miRNAs induce cell apoptosis, negatively regulating the BCL2 genes (anti-apoptosis).

## **1.4 Diagnosis of CLL**

### **1.4.1 Clinical characteristics of CLL patients**

Unlike other leukaemia, CLL patients present with a variety of disease behaviours from indolent to aggressive forms; patients might or might not have fever and sweats (or severe infections), weight loss, fatigue, anaemia, or a propensity to bleed (thrombocytopenia). Palpable lymph nodes and hepatosplenomegaly can be present and are a hallmark of clinically progressive CLL (Hallek et al. 2008).

The heterogeneity of the genomic landscape of CLL has been characterized in several large cohorts using SNP array analysis and massively parallel sequencing. In addition to the four common chromosomal alterations (tr12, del13q14, del11q22 and del17p13); Dohner et al. 2000) (see section 1.6.3), A landmark study by Landau (2015) suggested that CLL may be initiated with

large chromosomal abnormalities (eg, del13q, del11q, or tri12) followed by additional mutations which may lead to the CLL clone becoming more aggressive. This study also identified two distinct initiations of del13q and tris12. Landau et al. (2015) identified 44 recurrent mutated genes and 11 recurrent somatic copy number variations in CLL, including NOTCH1, MYD88, TP53, ATM, SF3B1, BIRC3, FBXW7, RPS15, IKZF3, ZNF292, POT1, CHD2, ZMYM3, ARID1A and PTPN11. The five common genes analysed in this study (NOTCH1, TP53, ATM, SF3B1 and BIRC3) were described in section 3.1. A shorter progression free survival (PFS) was reported in cases of TP53, SF3B1, BIRC3, NOTCH1 and RPS15 mutations. The proliferation and/or survival from B-cell malignancies depends on several major pathways including B cell receptor (BCR), inflammatory responses, Wnt signaling and NOTCH signalling.

#### **1.4.2 Rai and Binet staging systems**

Both CLL staging methods, the Rai system (common in North America) and the Binet system (used throughout Europe) are used in daily practice and clinical trials. The original Rai classification (Rai et al. 1975) has five staging groups in CLL, while the Binet staging is defined into three prognostic groups (Binet et al. 1981) (Table 1.1).

Ultimately, both these staging systems, which solely rely on physical examination and blood count, classify CLL patients into three relatively parallel groups with distinct prognoses: low, intermediate and high risk. However, these systems alone are not sufficient to distinguish within these groupings, patients who will have stable disease for some time from those who will have a more aggressive form of disease (Shanafelt et al. 2006). Reliable prognostic markers

are therefore needed to predict disease behavior, responses to therapy and long term patient outcomes that facilitate insight into the biology of the highly variable course of CLL.

**Table 1.1. Clinical stage according to the Rai and Binet systems.**

A. Clinical stage according to Rai (Rai et al. 1975).

0	Blood and bone marrow involvement only, no cytopenia.
I	0 + lymphadenopathy
II	0 + splenomegaly/hepatomegaly with or without lymphadenopathy
III	0 + anaemia with haemoglobin < 110 g/L, with or without organomegaly
IV	0 + thrombocytopenia with platelets count < 100 x 10 <sup>9</sup> /L, with or without anaemia or organomegaly

B. Clinical stage according to Binet (Binet et al. 1981).

	Number of involved lymph node areas*	Haemoglobin (g/L)	Platelets (10 <sup>9</sup> /L)
Binet A	< 3	> 100	> 100
Binet B	> 2	> 100	> 100
Binet C	any	< 100	< 100

\*Each of the following five regions counts as one area: palpable nodes in the neck, axillae and groins, clinically enlarged spleen and liver.

### 1.4.3 Laboratory features for diagnosis

To confirm the diagnosis of CLL, it is typical to evaluate the blood count, examine blood smears by microscopy, and the immuno-phenotype of

peripheral blood lymphocytes using flow cytometry (Hallek et al. 2008, Hallek 2013). In peripheral blood, the threshold for diagnosis is at least  $5 \times 10^9$  B-lymphocytes/L (or 5000/ $\mu$ L), however, a large number of patients develop counts as high as 100,000 - 200,000/ $\mu$ L. The clonality of B-lymphocytes needs to be confirmed by flow cytometry. Then, the most common morphological form of CLL cells found in the blood smear are characterised by their small sized, mature lymphocytes with a narrow border of cytoplasm and a dense nucleus lacking discernible nucleoli and having partially aggregated chromatin.

#### **1.4.4 Immuno-phenotype**

The diagnostic and prognostic assessment of B-cell CLL (B-CLL) requires an immuno-phenotype to be established due to its similar clinical presentations to other B-cell malignant lymphoproliferative disorders, including mantle cell lymphoma, hairy cell leukaemia, follicular, and non-Hodgkin's lymphoma (Jennings et al. 1997).

According to the International Workshop in CLL guidelines (Hallek et al. 2008), CLL cells co-express the T-cell antigen CD5 and B-cell surface antigens CD19, CD20, and CD23. The levels of surface immunoglobulin, CD20, and CD79b are characteristically low compared with those found on normal B cells. Each clone of leukaemia cells is restricted to expression of either kappa or lambda immunoglobulin light chains. In short, CLL B cells typically express an antigen profile including CD5+, CD19+, dim CD20, CD23+, CD27+, CD79b dim, CD22 dim, FMC7-, and low levels of surface membrane Ig (Dillman et al. 2008). However, the percentage of cells within a given clone expressing individual molecules can vary and the expression may offer some prognostic significance



such as CD38. Some surface molecules, FMC7 and CD10 are often not displayed on CLL cells and so their lack of expression helps to distinguish from other lymphomas (e.g. diffuse large B- cell lymphomas) (Uherova 2001, Oscier et al. 2004).

## **1.5 Treatment**

### **1.5.1 Criteria for initial treatment**

In general practice, newly diagnosed CLL patients without any symptoms or at the low risk stage (Rai 0, Binet A), should be monitored. No current standard treatment is effective in prolonging OS at these early stages unless they show evidence of disease progression. This was demonstrated by the French Cooperative Group on CLL (Dighiero et al. 1998), the Cancer and Leukaemia Group B (CALGB) (Shustik et al. 1988), the American group (Raphael et al. 1991), and then confirmed by a meta-analysis.

Patients with both intermediate (Rai Stages I and II or Binet stage A) and high-risk disease (Rai Stages III and IV or Binet Stage B or C) usually benefit from the initiation of treatment or can be monitored without therapy until they show evidence of progressive or symptomatic/active disease as defined by International Workshop on CLL (iwCLL) guidelines (Hallek et al. 2008).

### **1.5.2 Treatment Components**

#### **1.5.2.1 Chemotherapy**

##### **1.5.2.1.1 Alkylating agents**

Historically, chlorambucil is the oldest standard treatment for CLL. It induces partial remission in 60-70% of cases but no complete remissions (Rai et al. 2000, Hallek et al. 2004). Early CLL clinical trials looked at combinational therapy approaches with chlorambucil, such as co-administering corticosteroids and cyclophosphamide, but this was associated with a high incidence of infections (Montserrat et al. 1988, Raphael et al. 1991).

#### **1.5.2.1.2 Purine analogues**

Treatment of CLL was rapidly revised by the introduction of purine analogues (i.e. predominantly fludarabine, also pentostatine and cladribine), which inhibit DNA polymerase and ribonucleotide reductase, promoting apoptosis (Grever et al. 1987). Fludarabine is currently considered the most effective monotherapy in CLL with CR ranging from 7-40%; failure of response to fludarabine has been associated with poor prognosis (Raphael et al. 1991, Rai et al. 2000, Keating et al. 2005). However, in CLL patients the response is short-lived and the disease often becomes refractory to repeated courses of treatment with the same drug, and single agent therapy has not been shown to alter OS in CLL (Keating et al. 2002).

#### **1.5.2.2 Immunotherapy**

##### **1.5.2.2.1 Rituximab**

In theory, the expression of CD20 is reserved to B lymphocytes but its expression is lost once the B cells differentiate to plasma cells, as the antigen is not internalised or shed (Stashenko et al. 1980, Darzentas et al. 2013). Therefore, despite little being known about the natural ligand and its precise *in vivo* function, CD20 has become an ideal target for monoclonal antibody

therapy in lymphoproliferative disorders (LPDs). Its role has been demonstrated as a cell membrane calcium-acting channel (Uchida et al. 2004). Since 1998, the introduction of rituximab to traditional chemotherapy based treatments has improved the response rates in CLL and other LPDs, dramatically changing the standard of care for these conditions (Marcus et al. 2007, Hagemester 2010).

However, the OS rates (the percentage of patients who are alive for a certain period of time from first time of diagnosis or first treatment) are relatively low (23-45%) and complete remission is rare if the therapy contains only the single agent rituximab (Byrd et al. 2001).

#### **1.5.2.2 Alemtuzumab**

Another antibody, campath-1H (or alemtuzumab) is a monoclonal antibody against CD52, which is found on normal/malignant B and T lymphocytes (Treumann et al. 1995). Its mechanism of action has been investigated over several decades and is thought to induce cell death in three different ways: complement activation (Heit et al. 1986), antibody dependent cellular cytotoxicity (Greenwood et al. 1993) and apoptosis (Rowan et al. 1998). Early studies demonstrated that alemtuzumab is an effective therapy in CLL but is significantly associated with the incidence of severe opportunistic infections that are the main cause of death. This is likely due to the presence of CD52 on both B and T cells, which leads to a complete suppression of key components of the immune response. Alemtuzumab has been considered as an alternative option for poor prognosis patients for whom fludarabine treatment has failed (Osterborg et al. 1997, Keating et al. 2002, Wendtner et al. 2004, Ferrajoli et al. 2008). However, recent advances in therapies has relegated alemtuzumab

to an infrequently used modality of therapy. Other studies have taken the approach that alemtuzumab will be more effective in the management of minimal residual disease (MRD) (Hillmen et al. 2007, Hertlein et al. 2013).

### **1.5.2.3 Chemo-immunotherapy**

While the combination of chlorambucil and fludarabine induces a similar response as fludarabine alone, greater toxicity has been observed (Rai et al. 2000). The synergy between fludarabine and cyclophosphamide has proven more effective (Eichhorst et al. 2006, Wierda et al. 2006, Eichhorst et al. 2009).

According to iwCLL guidelines, regimes containing fludarabine, cyclophosphamide and the immunotherapy agent rituximab (FCR) are currently the standard therapy for CLL (Hallek et al. 2008) and have greatly advanced clinical outcomes for CLL patients including increased complete remission (CR) rates, prolonged clinical remissions and evidence of increased OS using the FCR chemotherapy regimen pioneered by Keating et al at the MD Anderson Cancer Centre. (Byrd et al. 2003a, Keating et al. 2005, Tam et al. 2008, Robak et al. 2010a, Robak et al. 2010b, Badoux et al. 2011a, Parikh et al. 2011).

### **1.5.2.4 New drug agents and other combinations in preclinical use or in the clinic.**

Many promising drug agents are still being studied. Most are based on targeting various key proteins in BCR signalling and different pathways of apoptosis (BCL2 and BH3 mimetics) (Hallek 2013). Following the promising results from other haematological malignancies, immunomodulatory drugs are currently being investigated in CLL (Sher et al. 2010) including chimeric antigen receptor (CAR) T cells (Lorentzen et al. 2015).

A huge number of other treatment combinations have been investigated around the world, such as clonidine with rituximab, methylprednisolone with rituximab followed by alemtuzumab, or rituximab plus alemtuzumab, etc. Their detailed

outcomes vary from paper to paper; however, until recently, none has been proven to have higher efficacy than FCR (Elter et al. 2005, Elter et al. 2011, Fischer et al. 2011, Bauer et al. 2012, Lepretre et al. 2012).

Several new agents in CLL treatment have had many successes in preclinical research, which has then led to clinical trials. Examples of these novel treatments include: monoclonal antibodies such as ofatumumab, obinutuzumab (GA101), alemtuzumab (against CD52); targeting B-cell signaling with idelalisib (Class I phosphatidylinositol 3-kinases (PI3Ks)), ibrutinib (bruton tyrosine kinase (BTK)); B-cell lymphoma 2 (Bcl-2) inhibitors with venetoclax (ABT-199). (Hallek, 2017)

#### **1.5.2.5 Stem Cell Transplantation**

Stem cell transplantation (SCT) is not widely used in CLL therapy for a number of reasons. Firstly, more than 80% of CLL patients are aged above 65 years, and due to both their age and the presence of co-morbidities, they are generally not fit enough to suffer the highly toxic and risky SCT procedure (Dreger et al. 2007). Secondly, the cost-effectiveness of SCT and the quality of life are questionable, ranging from the long periods of time waiting for a suitable HLA donor to the isolation protection needed for the patient after the heavy chemotherapy required prior to SCT (Dreger et al. 2007, Le Dieu et al. 2007, Schetelig et al. 2008, Tam et al. 2009a). Furthermore, allo-SCT may overcome the unfavourable effect of unmutated IgHV genes in CLL patients who are in a considerably poor risk group when treated with FCR approaches (Moreno et al. 2005). However, the decision to treat with allogeneic transplantation has

increased during the last 5 years due to the excellent results achieved with new emerging therapies (Montserrat et al. 2015).

### **1.5.3 Aim of treatment**

The iwCLL has given detailed criteria of the different categories/levels of treatment response or definitions of refractory disease. However, whichever available therapies are used, the ultimate aim of treatment is to achieve the maximum disease eradication to less than detectable MRD as soon as and for as long as possible (Nabhan et al. 2007, Varghese et al. 2010).

Regarding the technology to measure MRD, the quantitative methods to assess MRD with flow cytometry are more accurate than consensus polymerase chain reaction (PCR), but allele specific PCR provides the most sensitive results in determining disease response and predicting clonal evolution (Maloum et al. 2002, Moreno et al. 2006). However, this procedure has not yet been taken up in routine practice (Hallek et al. 2008, Bottcher et al. 2012). MPS approaches have also been used but immuno-phenotyping remains the most widely accepted tool for MRD detection.

## **1.6 Markers for prognosis**

While the diagnosis of CLL is quite simple, it is very challenging to prognosticate individual outcomes of CLL due to its highly variable clinical course. Classically, the significant prognostic factors are identified as follows:

1. Clinical characteristics such as age, sex, performance status, lymphadenopathy, and hepato-splenomegaly (Cramer et al. 2010, Shanafelt et al. 2010).

2. Haematological/laboratory parameters: blood lymphocyte count, lymphocyte doubling time (LDT), haemoglobin level, and platelet count. According to Montserrat et al. (1986), an LDT of >12 months is also indicative of the good prognosis associated with longer treatment free period (TFP) and OS.
3. Biochemical laboratory parameters:
  - Markers of tumour burden: serum albumin, calcium, uric acid, lactate dehydrogenase, alkaline phosphatase and creatinine. Increased levels of lactate dehydrogenase have been associated with poor outcomes (Han et al. 1985).
  - Serum parameters (Bergmann et al. 2007):  $\beta$ 2 microglobulin, Thymidine kinase (TK) and soluble CD23 (sCD23) (Hallek et al. 1999).

In recent decades, thanks to significant technological developments, the most prominent molecular markers encompass the mutational status of the IgHV gene, chromosomal aberrations assessed by FISH and also membrane markers (CD38 and ZAP70).

### **1.6.1 IgHV gene mutational status**

The mutational status of the IgHV genes are identified by comparing the homology between DNA sequencing of CLL patients with similar germ line genes. Unmutated is defined as an IGHV sequence  $\geq 98\%$  identity to germ-line (Damle et al. 1999, Hamblin et al. 1999). Patients with unmutated CLL (U-CLL) have inferior prognosis whereas CLL patients with mutated IgHV often have slower progression with long OS. IgHV mutational status is also predictive of



better response to therapy with FCR (Hamblin et al. 1999, Krober et al. 2002, Lin et al. 2003, Thompson et al. 2016).

### **1.6.2 CD38**

During B-lymphocyte development, CD38 expression changes over time, is upregulated before B cells enter the germinal centre, and decreases during differentiation, and is completely absent on memory B cells (Moreno-Garcia et al. 2004). The establishment of appropriate cut-off levels to distinguish CD38 positive and CD38 negative cases has been challenging to define. Indeed, Damle et al. (1999) showed a strong association between IgHV mutation status and CD38 expression with the typical cut-off of 30%. The association between CD38 positivity and poor clinical outcome in CLL has been well documented (Zucchetto et al. 2006, Van Bockstaele et al. 2009, Kempin 2013). This relationship could be explained by the fact that the presence of CD38 is predominately found on cells in the proliferative compartment of CLL, so a high expression of CD38 corresponds with more aggressive disease (Jelinek et al. 2001).

### **1.6.3 Cytogenetic markers**

Cytogenetic markers are now considered the most important prognostic markers in CLL. Döhner et al. (2000) established the use of cytogenetic analysis by standard fluorescence *in situ* hybridisation (FISH), which has shown that more than 80% of CLL patients have genetic aberrations that can be identified among their malignant clones. The most common cytogenetic aberrations are shown in Figure 1.3, including trisomy 12, deletions of 13q14, 11q22 and 17p13 (Dohner et al. 2000). Based on cytogenetics, del13q as sole

abnormality had the superior outcome, median groups had normal-by-FISH and trisomy 12, followed by del11q which had poor prognosis. It is evident that del17p had the worst prognosis with probability of survival less than 20% after 48 months. In addition, this study also showed that the median survival time of sole abnormality del13q, normal karyotype, trisomy 12, del11q and del17p were 133,111, 114, 79 and 32 months, respectively (Figure 1.3).

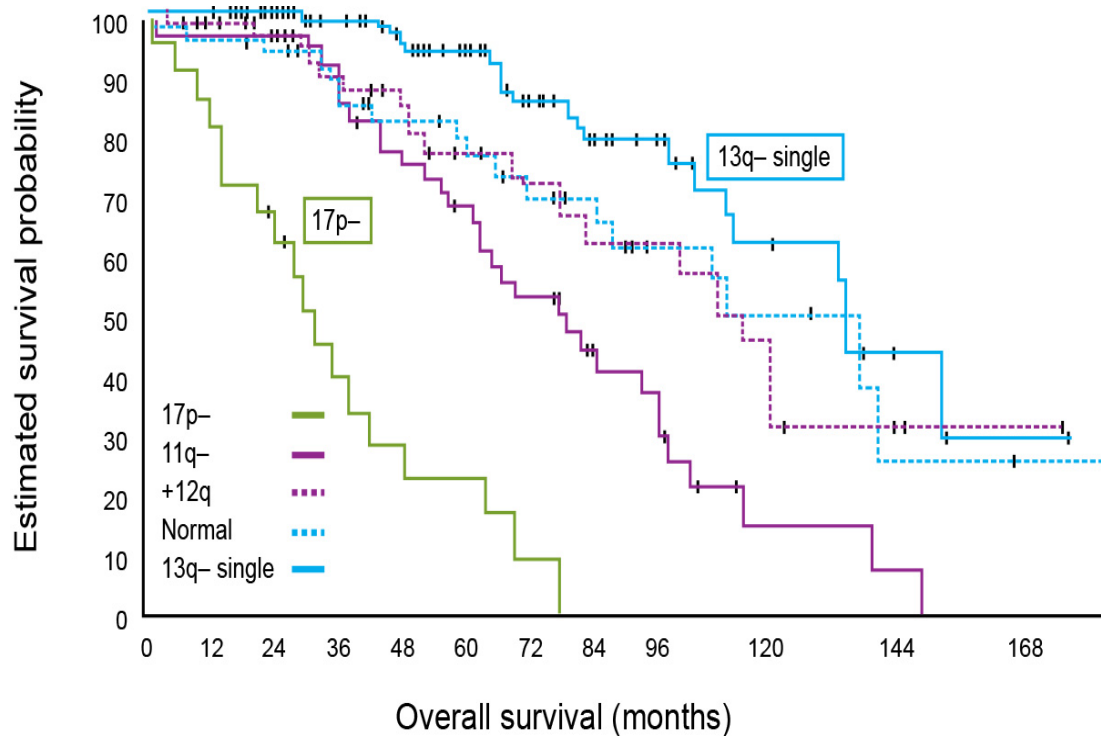


**Figure 1.3. Kaplan-Meier graph showing overall survival of CLL patients according to five common genetic categories.**

*Adapted from Döhner et al. (2000).*

#### 1.6.4 Conventional fluorescence *in situ* hybridisation (conventional FISH)

##### 1.6.4.1 General conventional FISH technique

FISH is a cytogenetic technique used to detect and localize the presence or loss of specific DNA sequences on chromosomes. Labelled probes are used that bind to specific regions of the chromosome with which they show a high degree of sequence complementarity. Either radio-, fluorescence-, or antigen-label can be used to label these probes. The cells labelled with the probes are visualized by autoradiography, fluorescence microscopy, or immunohistochemistry respectively, according to probe type (Jin et al. 1997).

The earliest FISH technique was performed in the late 1960s with radiolabelled probes (Gall et al. 1969). The first report on chromosome identification by fluorescence hybridisation was in 1986 (Pinkel et al. 1986). The FISH technique has been developed continuously as a very powerful tool in both clinical setting genome diagnostics and in scientific research (Heng et al. 1997, Jensen 2014). FISH can be applied to cell samples (smears, cytopins, etc.) or on tissue sections, either frozen or fixed in paraffin. Fixation is required to preserve DNA/RNA and cell/tissue morphology (Jensen 2014).

Fluorescence probes can be labelled by either enzymatic or chemical methods. In addition, there are two types of fluorescence probes: direct and indirect. Direct detection methods after hybridisation use Fluorescein, Rhodamine, Cyanin and Alexa dyes. Indirect visualisation methods detect haptenized probes by subsequent amplification signals including biotin, digoxigenin and fluorescein. (van der Ploeg 2000). Probes directly conjugated with fluorochromes can eliminate background noise compared with secondary detection steps (Gozzetti et al. 2000). Nick translation is the most common technique to label probes with a hapten or modified deoxynucleotide

triphosphate fluorophore (Rigby et al. 1977). Other less common methods include random priming using smaller fragment probes (Feinberg et al. 1984) and digoxigenin introduced as a hapten (Kessler et al. 1990). In general, double strand DNA probes can be classified into three groups: (1) whole chromosome painting probes; (2) chromosome specific repetitive probes, for example, the centromere of chromosomes with  $\alpha$ - and  $\beta$ - satellite sequences and (3) unique (single locus) sequence probes (Gozzetti et al. 2000).

Overall, a conventional FISH procedure contains four major steps: cell fixing and permeabilisation, probe hybridisation to the target sequence, washing away of excess and nonspecific binding probes, and visualisation (Amann et al. 2008). The aim of cell fixing is to preserve the macromolecules and structure of the cytoskeleton to prevent cell lysis and to prevent nucleic acid degradation during subsequent steps. Fixation permeabilises the cell/nuclear membrane allowing probes to enter the cell. Probe hybridization is the main step of the FISH procedure, in which fixed cells are incubated with labelled probes in optimal conditions (pH, temperature, components, etc.). These stringent conditions allow specific binding of probes to targeted sequences with a high degree of homology inside fixed cells during a period of time. The cells are then washed with high stringency to remove unbound probes or non-specific binding of probes. Lastly, hybridised cells are scored by fluorescence microscopy or imaging flow cytometry.

In CLL, FISH is carried out with a specific probe to detect chromosomal abnormalities, such as deletions of the 17p13 region which contains the *TP53* gene. The limitations of this technique however include: false-positive signals

due to probe positioning in a three-dimensional nucleus that allows probe signals to overlap, diffuse probe signals in cells due to the spreading of chromatin, or random loss or gain of fluorescence signals (Gozzetti et al. 2000, Best et al. 2012). Furthermore, accurate interpretation of microscopic imagery is not only dependent on probe size, slide preparation technique, and observer bias, but results can be subjective, qualitative, and laborious (Wiktor et al. 2006, Smoley et al. 2010). Importantly, the sensitivity of these microscopy-based methods is limited by the low number of cells (200 nuclei) evaluated among the abundance of the abnormal cells in the samples.

#### **1.6.4.2 Normal reference ranges of FISH probes**

The FISH method is an essential tool for diagnosis/monitoring of diseases; hence it requires precise and accurate normal cut-offs to interpret the clinical results of each fluorescence probe. The cut-off will vary according to the probes and the methods used. However, the methods to validate the normal reference range of each probe for FISH are not in consensus across the laboratories in the world (Ciolino et al. 2009). Many different statistical methods have been applied to measure the normal cut-off of probes, including a binomial treatment (Ciolino et al. 2009), the  $\beta$  inverse function (Wiktor et al. 2006) and Gaussian statistics (Dewald et al. 2000).

It is notable that the false positive signals in FISH could be minimized by an experienced scientist in carefully performing FISH slide preparation on high quality sample cells, but the problem of false positive signals cannot be eliminated. False positive signals may occur for a variety of reasons. Firstly, the false negative/positive signals during scoring of FISH may be due to the 3D

positions of the probes within the nucleus, resulting in overlapping or/and amalgamated signals, especially where the chromatin is less condensed. Secondly, there are random losses or gain of probe signals during the FISH technique procedure (hybridisation, washing), due to poor specificity or stringency issues, also dependent on sample types, the quality of samples or slide preparation. Thirdly, observer bias could give a miscounted result due to lack of experience or tiredness (Wiktor et al. 2006).

A review by Ciolino et al. (2009) compared the results of several available statistical tests in calculating the normal reference cut-off of conventional FISH. This review suggested that Gaussian distribution statistics (mean, standard deviation) were able to evaluate the cut-off with 95% confidence interval. Dohner et al. (1995) used the mean plus three times of SD to calculate the cut-off level of *TP53* probe. In this present study, the average scores (mean) plus three times of the SD on normal healthy (control) samples were used to determine the normal cut-off.

### **1.6.5 Laser scanning cytometry (LSC)**

In an attempt to overcome these limitations, the microscope-based laser scanning cytometer (LSC) was developed in the mid-1990s by Dr. Louis Kametsky (Kametsky et al. 1991, Kametsky et al. 1997, Kametsky 2001), and has since been updated with the new iGeneration of LSC Research Imaging Cytometer (e.g. iCys by Compucyte) and complemented by analysis software (Luther et al. 2004, Holden et al. 2005, Henriksen et al. 2011). These advances have allowed large-scale automated quantification of conventional FISH data. The two main advantages of the LSC method, compared to the

conventional FISH method, is that LSC is able to analyse a significantly larger number of cells, and the process of automated spot counting solves the problem of scorer fatigue and human error, resulting in more consistent results (Pozarowski et al. 2013).

Furthermore, LSC has been widely applied across a number of fields, ranging from cell cycle analysis (Zhao et al. 2008, Darzynkiewicz et al. 2011), enumeration of fluorescence probes within the nucleus (Kobayashi et al. 2000, Baumgartner et al. 2001), immuno-phenotyping (Gerstner et al. 2000, Al-Za'abi et al. 2008, Takahashi et al. 2009), interactions of *in situ* cells-cells (Claytor et al. 2001), to supporting the new drug discoveries (Krull et al. 2011).

#### **1.6.6 Single nucleotide polymorphism array (SNP array)**

FISH can only detect known genetic aberrations with designed probes. It cannot identify other unknown changes nor can it screen all chromosomes, unlike SNP arrays, a type of DNA microarray, which can perform these functions. Similar to the FISH technique, SNP array generally contains allele specific oligonucleotide probes and fragments target sequences. However, SNP array uses solid surface DNA capture during the hybridisation step and different hybridisation signal detection systems. In the last decade, the most advanced SNP array technique uses approximately 950,000 probes and can cover >90% of known copy number of variants (Song et al. 2016). SNP array enables genome-wide analysis of genetic abnormalities in terms of copy number alterations and allelic imbalances in cancer cells, including in acute lymphoblastic leukaemia (ALL) (Irving et al. 2005, Mullighan et al. 2007), in acute myeloid leukemia (AML) (Bullinger et al. 2010), and in CLL (Edelmann et

al. 2012). However, SNP array is unable to detect chromosomal translocations, and the identification of small clones less than 25% can be compromised (Mao et al. 2007, Gondek et al. 2008).



### **1.6.7 Sanger sequencing**

Sanger sequencing was developed by Frederick Sanger and his group in 1977 (Sanger et al. 1977a, Sanger et al. 1977b). This method of DNA sequencing is based on the incorporation of chain terminating di-deoxynucleotides during DNA replication by DNA polymerase. The different oligonucleotides are then recorded with four colour labels and identified by size using gel electrophoresis (Maxam et al. 1977). From raw data, sequencing scanner software (Applied Biosystems) can display the nucleotide chromatograms and compare them with reference sequences to detect abnormalities, representing polymorphisms or mutations.

For nearly 40 years, Sanger sequencing has become the gold standard for confirming genomic variations because it can provide unbiased sequence data with mutations in the targeted region. However, this technique has all the limitations of PCR amplifications and limited sensitivity, as variants with a lower allele frequency (less than 20%) may be indistinguishable from noise or sequencing errors (Dong et al. 2011, Chin et al. 2013, Hagemann 2015).

### **1.6.8 Massive parallel sequencing (MPS)**

Sanger sequencing was considered as the “first generation” of sequencing. New high throughput genome-wide sequencing applications, namely massively parallel sequencing (MPS) methods (also known as next generation sequencing) are replacing Sanger sequencing. The reason for this is that in the last decade, the benefits of the MPS technique outweigh Sanger sequencing, especially in haematological malignancies (Hutchison 2007, Gupta et al. 2014). Sanger sequencing is limited to a few genes at one time within targeted DNA

regions of 800-1000 bp. On the other hand, MPS can produce the data of thousands of genes in megabases or gigabases rapidly and efficiently in one assay at lower cost (Lee et al. 2014a).

In addition, MPS approaches can be used to detect low frequency clones with additional information regarding genome wide mutational events. MPS instruments capable of generating vast quantities of sequencing data at modest cost have enabled scanning for somatic mutations across the exome, transcriptome or even the entire genome (Rehm et al. 2013).

In this study, my original intention was to employ the Illumina platform to sequence the exomes of patients enrolled in the CLL5 clinical trial expression profiling to better understand the biology of low frequency *TP53* deleted clones in CLL.

#### **1.6.9 Fluorescence *in situ* hybridisation in suspension (FISH-IS)**

In flow cytometry, cells can be measured by fluorescence intensity, forward scatter and side scatter; however, this technique preferences plasma membrane analysis. Images from standard microscopes are able to demonstrate many subcellular structures, locations and other features (Basiji et al. 2007). As a consequence, there has been continuous development of the techniques combining microscopy and flow cytometry.

Over the last 40 years, various techniques have been reported for this combination of imaging and flow cytometry (IFC) (Baerlocher et al. 2002, Han et al. 1987). One of the earliest applications using the combination of FISH and flow cytometry was published in 1988 (Trask et al. 1988) to quantify the amount

of target DNA in male diploid cells. However there has been a paucity of publications in this field since, despite the potential utility of this method. The emergence in the last decade of the ImageStreamX Mark II imaging flow cytometer has enabled integration of the rapid analysis of large cell populations with the utility of the fluorescence microscope, bringing FISH-IS (FISH in suspension) back to the fore.

Based on conventional FISH, the new technology, namely FISH in suspension (FISH-IS), combines conventional FISH images with the high-throughput detection afforded by flow cytometry. The ImageStreamX instrument merges the speed, statistical power, and fluorescence sensitivity of flow cytometry with the collection of multi-parameter images. 12 high-resolution images of each cell can be seen directly at flow rates of 1000 cells per second, enabling the quantification of genetic abnormalities and retaining the fluorescence sensitivity of standard flow cytometry. This also implies that more than 10,000 cells can be analysed per experiment. Interestingly, the detection of rare cells (small sub-clones) can be tracked at levels below 0.001%, as these instrument systems can capture images of millions of cells in minute (Basiji et al. 2015). In addition, IDEAS software accompanies the ImageStreamX system to investigate data, in which each image can be used to calculate more than 40 quantitative features, allowing roughly 250 different masking features. As a result, this new technology could potentially enable an advance in cytogenetic research with the capacity to demonstrate low frequency clones, e.g. containing loss of 17p, and possibly facilitate co-characterisation with immuno-phenotyping.

In terms of the methods, the major difference between conventional FISH methods and FISH-IS is the immobilization of cells. In FISH, the cells are fixed and then mounted onto slides, whereas with the new FISH-IS technique the cells are in suspension as they are visualised by flow cytometry. One of the first ideas about imaging in flow cytometry was introduced by Kay et al. (1979). It took over 25 years for the first commercial imaging flow cytometry to emerge from this work. By 2015, it had been applied in over 500 peer-reviewed scientific research papers (Basiji et al. 2015).

Research to date has demonstrated the application of FISH-IS using probes to telomeres (Baerlocher et al. 2006) or chromosome-specific centromere probes (CEP) (Minderman et al. 2012). Such repetitive targets provide high fluorescence intensity at the target site due to a large number of bound probes. Minderman et al. (2012) reported the limit of detection of monosomies by FISH-IS with CEPs as 1%. However, adaption of this assay to single locus-specific targets (locus-specific identifier (LSI)) has not been demonstrated.

## **1.7 *TP53* aberrations in CLL**

### **1.7.1 Tumour suppressor gene *TP53*.**

In 1979, the p53 protein was discovered by two independent groups studying SV40-transformed cells showing a 55-kDa protein co-precipitated with the large-T antigen (Lane et al. 1979, Linzer et al. 1979). Since then, many researchers have investigated the role of p53 in tumour cells, but it took nearly 10 years to determine its tumour suppressor behaviour (Eliyahu et al. 1989, Finlay et al. 1989).

The p53 protein is encoded by the *TP53* gene, which is located on chromosome 17p13.1 with a length of 19144 bp, and 11 exons (UCSC Genome Library). It is obvious from the published literature that *TP53* provides an important link between DNA damage and apoptosis (Wang 2001, Bartkova et al. 2005, Bartkova et al. 2006, Bartek et al. 2007a, Bartek et al. 2007b). Faced with stress, the p53 protein induces cell-cycle arrest, DNA repair, and apoptosis (Wattel et al. 1994, Vousden et al. 2002, Goh et al. 2012). Therefore, it has been considered as “the guardian of genome” since 1992 due to its role as a checkpoint for DNA damage, preventing genome mutations (Lane 1992, Wattel et al. 1994).

Normally, p53 exists at low levels in cells, and then rises rapidly (overexpression) when damage to the DNA occurs (e.g. due to genotoxic exposure). This induces apoptosis by transcriptional regulation in circumstances of irreparable damage (Xu-Monette et al. 2012).

Regarding *TP53* target genes, there are several microRNAs involved (Mraz et al. 2009b, Suzuki et al. 2009, Subramanian et al. 2010). For instance, Chin et al. (1992) showed that mutated *TP53* enhances the upregulation of miRNAs involved in regulating the expression of multidrug-resistance gene 1 (MDR1), which inhibits therapy efficacy. It is reported that the promoters of miR-34 bind to *TP53* to stimulate the expression of miR-34 (Merkel et al. 2010).

There are three members in the miR-34 family, including miR-34b and miR-34c, which are both not expressed in CLL, while miR-34a has high level expression in cases with normal *TP53* and is down regulated in cases with defective *TP53*

(Mraz et al. 2009a). For this reason, low expression of miR-34a in CLL is linked to worse prognosis and chemo-refractoriness (Zenz et al. 2009b).

Furthermore, the *ATM*-*p53*-miR-34a pathway has been commonly proposed for CLL pathogenesis (Zenz et al. 2009a, Balatti et al. 2013b). In detail, del11q leads to loss of the ataxia telangiectasia mutated (*ATM*) gene. *ATM* deletion causes an unbalanced post cleavage complex and misguided checkpoint in the cell cycle, normally necessary for VDJ rearrangements. These broken BCR genes may lead to malformations in B lymphocytes (Bredemeyer et al. 2006). However, without the effects of oncogenic stress, *ATM* produces *ATM* kinase to stabilise DNA complexes during V(D)J rearrangement (Bredemeyer et al. 2006). Under activation stress, *ATM* phosphorylates *p53* through check point kinase 2 (*CHK2*), which inhibits *p53* from binding to *MDM2* (murine double minute-2) and being degraded by proteasomes (Michael et al. 2002, Michael et al. 2003, Stommel et al. 2004, Vassilev et al. 2004, Deng et al. 2005, Meulmeester et al. 2005, Stommel et al. 2005, Vassilev 2007). Next, *MDM2*, located on chromosome 12 (12q15), directly inhibits *p53* in the *MDM2*-*p53* auto-regulatory feedback cycle as a negative regulator (Haidar et al. 1997, Harris et al. 2005, Gryshchenko et al. 2008).

### **1.7.2 Overview of the role of *TP53* abnormalities in CLL**

The Cancer Genome Atlas study revealed that in various human cancers, *TP53* was the most common mutated gene (42% of samples) among 3218 tumours from 12 cancer types by MPS (Kandoth et al. 2013). Many studies also confirmed the associations between *TP53* mutations and aggressive outcomes in many different kinds of tumours (Wattel et al. 1994, Harutyunyan et al. 2011,

Cleary et al. 2013, Churi et al. 2014, Tirode et al. 2014, Moreira et al. 2015, Parry et al. 2015).

Interestingly, *TP53* mutations are less frequent in haematological malignancies, varying from 5-20%, compared to solid tumours at over 40% (<http://p53.iarc.fr/SelectedStatistics.aspx>) (Soussi et al. 1994, Olivier et al. 2010). However, the prognostic value of *TP53* mutations is very significant in haematological malignancies (Zenz et al. 2008a, Zenz et al. 2008c, Olivier et al. 2010, Stengel et al. 2014, Parkin et al. 2015). Particularly in CLL, studies showed that *TP53* mutations are found in approximately 8.5 – 17.5% of patients and confirmed the association of these mutations with chemo-refractoriness and poor clinical outcome (Malcikova et al. 2009, Zenz et al. 2010a, Seiffert et al. 2012). Similar to *TP53* mutations, patients with 17p deletion (i.e. loss of *TP53* gene) had the worst prognosis with a median survival of 2 to 3 years from initial diagnosis (Dohner et al. 1995, Cordone et al. 1998, Döhner et al. 2000, Stilgenbauer et al. 2010, Stilgenbauer et al. 2014). It is noted that the incidence of del17p was found to be around 5-10% at CLL diagnosis, which increased up to 50% in refractory/relapse stages (Tam et al. 2007, Malcikova et al. 2015).

Regarding the relationship between del17p and *TP53* mutations in CLL, mono-allelic *TP53* mutations were identified in about 4-23% without del17p, as assessed by FISH (Dal-Bo et al. 2009, Malcikova et al. 2009, Rossi et al. 2009, Butler et al. 2010, Zenz et al. 2010a). 80% of del17p samples had bi-allelic *TP53* inactivation (Zenz et al. 2008c, Rossi et al. 2009, Gonzalez et al. 2011).

In addition, according to many studies, CLL lymphocytes with del17p are resistant to treatment with either sole purine analogues or combined with

alkylating agents (Wattel et al. 1994, Dohner et al. 1995, O'Brien et al. 2001, Pettitt 2003, Eichhorst et al. 2006, Catovsky et al. 2007, Ricci et al. 2009), and Rituximab (Silber et al. 1994, Byrd et al. 2003b, Robak 2005, Byrd et al. 2006, Hallek et al. 2010, Keating 2010). The combination of fludarabine, cyclophosphamide and rituximab (FCR) (standard treatment for CLL) has not improved the OS rates (Wierda et al. 2005, Hallek et al. 2010, Hallek 2013). The explanation is that loss of the *TP53* gene induces a defect in activating pro-apoptotic responses after DNA damage including that elicited by chemotherapy (Stankovic et al. 2004).

Consequently, despite del17p now being widely accepted as a unique powerful prognostic marker in resistance to therapy (chemo- refractoriness) and poor outcomes in CLL, there are currently no standard protocols for the first line treatment of symptomatic patients with del17p CLL, unless patients are eligible for an allogeneic hematopoietic cell transplant (Schetelig et al. 2008, Dreger et al. 2014, Kharfan-Dabaja et al. 2016). Many different new drugs with p53 independent pathways have been tested either alone or in combined approaches, including antibody-based treatment (alemtuzumab), ofatumumab, immuno-modulating drugs (lenalidomide), CDK inhibitors (flavopiridol), an inhibitor of Bruton's tyrosine kinase (BTK) (ibrutinib), B-cell receptor (BCR) inhibitors (idelalisib) and an inhibitor of BCL-2 (venetoclax) (Zenz et al. 2009b, Choi et al. 2012, Jain et al. 2012, Byrd et al. 2013, Furman et al. 2014, Wiestner 2015, Stilgenbauer et al. 2016).



### 1.7.3 Clonal evolution of *TP53* genes defects

Nowell (1976) foundation paper of established the landmark of the evolutionary somatic mutation process in cancer cells and sub-clonal selections. Since then, it has been demonstrated that these mutations cause genomic instability in tumour cells and clonal evolution and are the main characteristic of most cancers (Lengauer et al. 1997, Hanahan et al. 2000, Sieber et al. 2003, Eyfjord et al. 2005, Gorgoulis et al. 2005, Negrini et al. 2010, Hanahan et al. 2011, Shen 2011, Greaves et al. 2012, Yates et al. 2012, Burrell et al. 2014).

In this sense of dynamic genomics, there are two types of genetic alterations: transient (passenger mutations) and persistent state (driver mutations) (Bozic et al. 2010). As a result, the driving mutations of tumorigenesis which are substantially modified in cancer cells promote further acquired DNA aberrations, resulting in heterogeneity within (sub) clonal progression in tumours (Hackett et al. 2002, Sieber et al. 2003, Schwartz et al. 2006, Halazonetis et al. 2008, Loeb 2011, Gerlinger et al. 2012, Fisher et al. 2013, Apostoli et al. 2016, Gatenby et al. 2017).

Recently, based on sequencing data, massive studies of multiple types of cancers have explored the somatic mutations (sub) clonal phylogeny underlying tumour progression, for instance, in breast cancer (Goswami et al. 2015), ovarian cancer (Bashashati et al. 2013), small cell lung cancer (McFadden et al. 2014), acute lymphoblastic leukaemia (Li et al. 2001), acute myeloid leukaemia (Ding et al. 2012, Parkin et al. 2013), and in CLL (Schuh et al. 2012, Landau et al. 2013, Landau et al. 2015, Puente et al. 2015).

Particularly in CLL, many common crucial driver genes have been identified, involving the following pathways: DNA damage/repair or cell cycle control (*TP53*, *ATM*, *BIRC3* genes), NOTCH signalling (*NOTCH1* gene), and RNA splicing (*SF3B1* gene) (Wang et al. 2011, Campregher et al. 2014). Interestingly, despite the detection of novel driver genes in CLL, *TP53* mutations stand out as the most frequent driver mutations (Zenz et al. 2010a, Puente et al. 2011, Wang et al. 2011, Rossi et al. 2014).

As already stated, regarding the evolution of *TP53* loss clones, they are uncommon at diagnosis (5% to 10%), but their frequency significantly increases to 40%-50% as detected by conventional FISH in relapsed or treatment-refractory patients (Stilgenbauer et al. 2007, Tam et al. 2007, Rossi et al. 2009, Zenz et al. 2009a, Badoux et al. 2011a). This results from the fact that chemotherapy treatments are able to eradicate the drug sensitive clones and the normal cells, but small clones harbouring *TP53* loss persist due to the central role of *TP53* in cell death following chemotherapy (Joerger et al. 2008). A report of Landau et al (Nature 2015) was demonstrated that there was a significant increase of *TP53* and del17p in relapse cases. The frequency of *TP53* deleted sub-clones increases presumably due to the exposure to DNA damaging drugs and the inherent genomic instability associated with the loss of *TP53* and/or the selection of clonal evolution/chemotherapy pressure; they possibly also acquire other genetic abnormalities or may transform to Richter's syndrome (Rossi et al. 2011b).

Despite genomic studies which depict the landscape of the del17p clonal complexity of CLL, little is known about the dynamics of small subclones that

may be present and which are commonly undetected or unappreciated in the abundance of the leukemic cell population (Schuh et al. 2012, Landau et al. 2013, Ouillette et al. 2013). The prognostic clinical impact of having del17p depends on the time when it was identified: del17p CLL patients within one year of diagnosis had a OS of 4.7 years (Shanafelt et al. 2006), whereas those who had acquired del17p at a later stage had OS of 1.3 years (Shanafelt et al. 2008). *TP53* mutations can be classified as late driver mutations in CLL clonal evolution (Figure 1.4). This is in agreement with many longitudinal analyses, where small del17p clones identified at pre-treatment become the predominant clones at the time of CLL relapse and predict the development of chemo-refractoriness (Tam et al. 2008, Zenz et al. 2009b, Rossi et al. 2011b, Pospisilova et al. 2012, Rossi et al. 2014, Stilgenbauer et al. 2014).

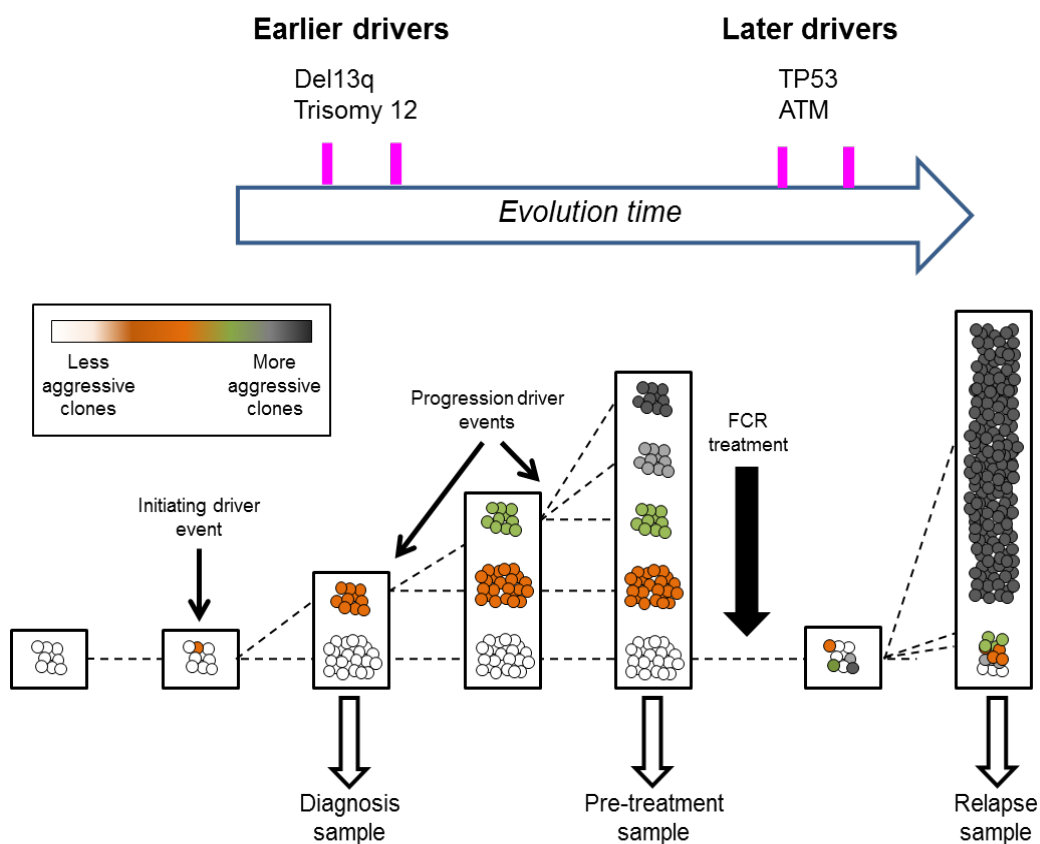


**Figure 1.4. A model of inferring the clonal evolution in CLL.**

*Adapted from Landau et al. (2013).*

#### **1.7.4 Low frequency del17p sub-clones (*TP53* genes loss in small clones)**

Currently, there is a large changeable threshold for detection of del17p nuclei in conventional FISH. According to the German CLL Study Group (Stilgenbauer et al. 2014), there are no relevant clinical outcomes matching the threshold of del17p nuclei; they used the normal cut-off (5-10%) to classify positive or negative del17p. In contrast, a study at the MD Anderson Cancer Center and the Mayo Clinic (Tam et al. 2009b) identified and followed up treatment naïve CLL patients who were reported to have del17p by FISH. They found that CLL patients with less than 25% 17p-deleted nuclei had the best prognosis; those with 25% to 74% 17p-deleted nuclei had intermediate outcomes, and the worst prognosis was in those who had at least 75% 17p-deleted nuclei. Similarly, a United Kingdom study (Catovsky et al. 2007) showed that the percentage of 17p-deleted nuclei resulting in inferior OS was >20%. Furthermore, Best et al. (2012) demonstrated that two out of three major groups failed to find an accurate predictive threshold for del17p nuclei by conventional FISH techniques.

Conversely, Rossi et al. (2014) used ultra-deep massive parallel sequencing to retrospectively confirm very minor *TP53* mutated clones (down to 0.3% of all CLL cells) that were missed by Sanger sequencing due to their very low frequency. These minority sub-clones present at diagnosis developed into the predominant population over time as the disease progressed, resulting in the development of chemo-refractoriness at relapse. This evidence showed the importance of *TP53* as a driver mutation.

As a result, patients with low frequency del17p sub-clones are in the “grey zone” of prognosis and decisions regarding treatment (including whether to treat or not) and the initial therapeutic regime for these patients are serious challenges that the clinical physician faces in treating patients with this disease.

With respect to the classification of del17p clone size, the cohort study by Tam et al. (2009b) showed that the cut-off point of 25% was able to demonstrate different outcomes and an OS rate of 92% compared with 54% for < 25% and ≥ 25% 17p-deleted nuclei, respectively. In this present study, less than 25% of del17p nuclei were classified as low frequency, from 25% to 75% of del7p nuclei as mid-frequency and more than 75% of del7p nuclei as high frequency del17p.

## **1.8 Purpose of this study**

Currently, there is a gap in knowledge about how to predict treatment outcomes in CLL with a low percentage of 17p-deleted cells as identified by conventional FISH. Thus, the accuracy in calculating the percentage of *TP53* loss in CLL appears significant for outcome, and this question has been debated by many researchers (Sturm et al. 2003, Zenz et al. 2008b, Tam et al. 2009b, Best et al. 2012, Stilgenbauer et al. 2014). According to the UKCLL4 cohort study (Catovsky et al. 2007), the defined cut off was 20%; however, in this trial, it was reported that there was one case with del17p in less than 20% of cells identified by FISH initially, but the patient did not respond to therapy (FCR as first line treatment) and after 5 months, the proportion of del17p increased significantly to 77% of nuclei. In another study, the percentage of del17p nuclei identified by conventional FISH rose from 16% at diagnosis to >95% at the time of relapse (after 8 months) (Zenz et al. 2008b). At the other extreme Rossi et al. (2014)

demonstrated that clones detectable at 0.3% of all CLL cells present at diagnosis are capable of resulting in chemo-refractoriness at relapse. While this is thought to be due to the genotoxic stress of alkylator and fludarabine therapy, clearly the genomic instability of the sub-clone, resulting from lack of *TP53* gene function is important. Therefore, Zenz et al. 2008b questioned, “how little is too much?” of the percentage of del17p. Hence, patients with low frequency 17p deletion sub-clones are in the “grey zone” of prognostics and treatment decisions and present serious challenges. As a result, there is a need to further study the low frequency del17p CLL underlying genomic landmarks.

The overall aims of this study were to seek evidence to explore the following hypotheses. Firstly, that minor del17p sub-clones detected in CLL at diagnosis are an important driver of the subsequent disease course in association with other genetic events that have occurred within that sub-clone. Secondly, that low frequency del17p sub-clones in CLL demonstrate lower levels of genomic instability than present in patients with high frequency clones at the time of first treatment. In order to address these hypotheses, the aim of the work contained in this thesis were to characterise the genomic profile of low frequency del17p sub-clones in CLL.

The broad aims of this study were as followings:

1. To analyse the baseline clinical and genetic characteristics (using a variety techniques: conventional FISH, LSC and MPS) of the CLL5 clinical trial cohort, with a specific focus on all del17p cases including patients with low frequency del17p CLL (Chapter 3).
2. To determine the lower limit of sensitivity of the FISH-IS technique on primary CLL samples with centromere probes (Chapter 4).
3. To develop a FISH-IS technique to detect and enrich CLL cells based on the del17p status (Chapter 5).



## 2 Chapter 2 - Materials and Methods

This chapter describes the general materials and methods used in this study. Specific or novel methods are presented in the relevant chapters.

### 2.1 Materials

Lymphoprep™ (Stemcell™ technologies, Norway); Trypan blue (Sigma-Aldrich, Australia); DMSO (Chem-supply, Australia); RPMI 1640 (Roswell Park Memorial Institute) medium (ThermoFisher, Australia); Penicillin, Streptomycin (ThermoFisher, Australia); Fetal Calf Serum (Bovogen, Australia); phosphate buffered saline (PBS) (Sigma-Aldrich, Australia); methanol (chem-supply, Australia), acetic acid (Chem-supply, Australia); potassium chloride (KCl) (Sigma-Aldrich, Australia); saline-sodium citrate (SSC) (Sigma-Aldrich, Australia); NP-40 (IGEPAL® CA-630, Sigma-Aldrich, Australia); sodium hydroxide (NaOH) (Sigma-Aldrich, Australia); hydrochloric acid (HCl) (Sigma-Aldrich, Australia); mounting medium with DAPI (Vectashield, USA); CEP Y, CEP X, CEP 9, CEP 12 probes (Abbott Molecular, USA); CEP hybridisation buffer (Abbott Molecular, USA); spectrum orange (or spectrum green-dUTP) (Life Science, Australia); salmon sperm (Life Technology, Australia); 3M sodium acetate (pH 5.5) (ThermoFisher, Australia); Tris–EDTA (pH 8) (Sigma-Aldrich, Australia).

### 2.2 Collection of peripheral blood from CLL patients

All CLL samples were collected before treatment. The sample sizes were calculated based on the aims of CLL5 clinical trial. These samples were obtained from the Australian Leukaemia and Lymphoma Group (ALLG) clinical

trial CLL5, in which participant patients signed informed consent forms for the ALLG Tissue Bank. In addition, CLL samples from Flinders Medical Centre (FMC) patients with the written consent forms (FCREC 216.56) and blood from healthy donors with written consent forms (FCREC 136.067) were also collected as required. Whole peripheral bloods from CLL patients were collected in 10 mL Lithium Heparin and 10 mL EDTA coated tubes.

### **2.3 Isolation/cryopreservation of peripheral blood mononuclear cells from whole blood**

Whole blood was diluted 1:2 in sterile PBS and then layered on 10 mL of Lymphoprep™ and centrifuged at 500 x g for 20 mins. The interphase layer was collected by transfer pipette, washed in PBS, and then centrifuged at 1000 x g for 5 mins. Cell pellets were resuspended at 4 x10<sup>7</sup> cells/mL in 50% RPMI 1640 media and 50% FCS for immediate use, or frozen. Following PBMC isolation and cell counting, lymphocytes from Lithium Heparin tubes were aliquoted into cryovials at a maximum concentration of 4 x10<sup>7</sup> per vial, then resuspended in RPMI 1640 media containing 25% FCS and 15% DMSO, in 2 mL total volume. Vials were preserved in the vapour phase in a liquid nitrogen tank for a minimum of 24 hours, and transferred to liquid nitrogen (-196°C) until required.

Peripheral blood mononuclear cells (PBMCs) for subsequent DNA extraction were divided into 1.5 mL microcentrifuge Eppendorf tubes at a maximum concentration of 1 x 10<sup>7</sup> cells/tube, then washed in PBS followed by centrifugation at 500 x g for 5 mins. The supernatant was removed and the pellet was stored at -80°C until required.

## **2.4 Counting and viability of PBMCs by trypan blue analysis**

Cells were diluted 1:2, 1:10 or 1:100 (depending on the predicted concentration of cells) in 0.4% trypan blue in PBS and 10  $\mu$ L was added to a Neubauer chamber haemocytometer. Cells were visualised with a microscope (Leitz Wetzlar, Germany) at 40x magnification and the number of both blue cells (dead cells) and unstained cells (viable cells) was counted in two 1 mm<sup>2</sup> areas. The number of cells per mL was calculated by the following formula: concentration of cells/mL = average number of cells/mm<sup>2</sup> area x dilution ratio x 10<sup>4</sup>.

## **2.5 Thawing cells from liquid nitrogen storage**

The vials from the liquid nitrogen tank were removed and transferred immediately into a water bath pre-warmed at 37°C until all ice crystals in the cell suspension had disappeared. The cell suspension was then transferred to a 15 mL sterile tube and 1 mL media was slowly added in a drop-wise manner over 5 mins, followed by an additional 10 mL media. The cells were then centrifuged at 500 x g for 5 mins. The supernatant was removed and the cell pellet was resuspended in 1 mL RPMI 1640 media supplemented with 10% FCS.

## **2.6 Conventional fluorescence *in situ* hybridisation (conventional FISH)**

### **2.6.1 Conventional FISH Buffers**

Carnoy's fixative buffer – 75% (v/v) 4°C methanol and 25% v/v acetic acid. Buffer was freshly prepared prior to each use.

5.6 g/L KCl: 5.6 g KCl (Sigma-Aldrich, Australia) was resuspended in 1000 mL dH<sub>2</sub>O. Prior to use, an aliquot was taken and warmed to 37°C.

20X SSC: 132 g 20X SSC (Sigma-Aldrich, Australia) was resuspended in 500 mL purified H<sub>2</sub>O (Milli-Q) and pH was adjusted to 5.3 with 1M HCl as required.

Wash 1 (0.4X SSC + 0.3% NP-40): 20mL 20X SSC was combined with 980 mL purified H<sub>2</sub>O, followed by the addition of 3 mL of NP-40 (Sigma-Aldrich, Australia). The pH was adjusted to 7.0 with 1M NaOH or 1M HCl (Sigma-Aldrich, Australia) as required.

Wash 2 (2X SSC, 0.1% NP-40): 100 mL 20X SSC was combined with 900 mL purified H<sub>2</sub>O, followed by 1mL of NP-40, then adjusted to pH 7.0.

### **2.6.2 Conventional FISH method**

Chromosome Enumerate Probes (CEP) were as follows: CEP Y (DYZ1) Spectrum Orange probe, CEP 9 Spectrum Orange probe, CEP X (DXZ1) Spectrum Green probe, and CEP 12 (D12Z3) Spectrum Green probe. All probes and CEP hybridisation buffer were obtained from Abbott Molecular (USA).

Conventional FISH was carried out on CLL patient PBMCs. On day 1, cells were fixed by resuspending PBMCs in 500  $\mu$ L of RPMI 1640 media + 10% FCS, followed by the addition of 9 mL 0.075M KCl, pre-warmed to 37°C. The tube was inverted several times and then incubated at 37°C for 30 min in a water bath. Following the incubation, 1 mL of Carnoy's fixative was added and cells were mixed by inversion, then centrifuged at 300 x g for 10 mins. The supernatant was then discarded, leaving approximately 500  $\mu$ L of fixative in the tube which was gently vortexed to resuspend the pellet. Ten millilitres of fresh fixative was added. The tube was then inverted 2-3 times, followed by centrifugation at 300 x g for 10 mins. This step was repeated twice, and the pellet was finally resuspended in 1 mL of Carnoy's fixative and stored at -20°C for a minimum of 4 hours or until required.

On the following day, slides were placed in 100% methanol for a minimum of 10 mins, then removed and wiped clean. Slides were then placed in a coplin jar containing dH<sub>2</sub>O. To prepare the samples, fixed cells were removed from the -20°C freezer and centrifuged at 300 x g for 5 mins, followed by resuspension in fresh fixative to form a slightly cloudy solution of approximately 1 x 10<sup>7</sup> cells/mL. Cleaned slides from the dH<sub>2</sub>O coplin jar were stood upright and allowed to drain until only a thin film of water covered the slides. Sample specimens were dropped onto the slides using a Pasteur pipette (1 drop/slide area), and then slides were tapped on the bench (hard) 4-5 times to allow draining (maximum of 2 mins). Once dry, a black dot was made on the reverse side of the slides in the centre of the sample drop, and used as a guide for cover placement and scoring. Two microlitres of probe was added to each slide and covered with 12 x 12 mm glass coverslips (Sigma-Aldrich) and pressed gently

to remove any bubbles. The edges of the coverslip were then sealed with rubber cement. Sealed slides were then heated to 78°C for 4 mins, followed by incubation in a dark humidified box at 37°C for 14 hours for probe hybridisation.

On the following day, coverslips were removed and slides were washed (wash 1) (pre-warmed to 73°C) for 2 mins. Slides were then transferred to room temperature and wash 2 was performed for 30 seconds, and slides dried by standing upright in a dark box for 15 mins. 20 µL of Vectashield® (Vector Laboratories) containing DAPI was loaded onto the slides and coverslips were placed on the cells. The excess DAPI was removed with blotting paper and the edges of the coverslip were sealed with transparent nail polish. To score the hybridised nuclei, 200 nuclei were manually scored by two independent scorers by visualisation with the appropriate fluorescence channel on a BX50 fluorescence microscope (Olympus, Japan). The DAPI signal was used to locate the nuclei, then the 100x magnification lens was used to score fluorescence signals with appropriate fluorescence channels. The average of the two scores was taken as the final result. If the two scores differed more than 10%, a third scorer was required for the final results.

## **2.7 Laser scanning cytometry (LSC)**

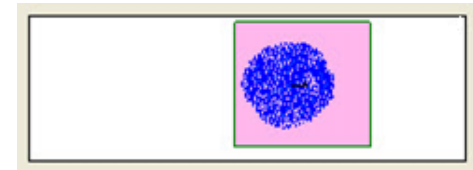
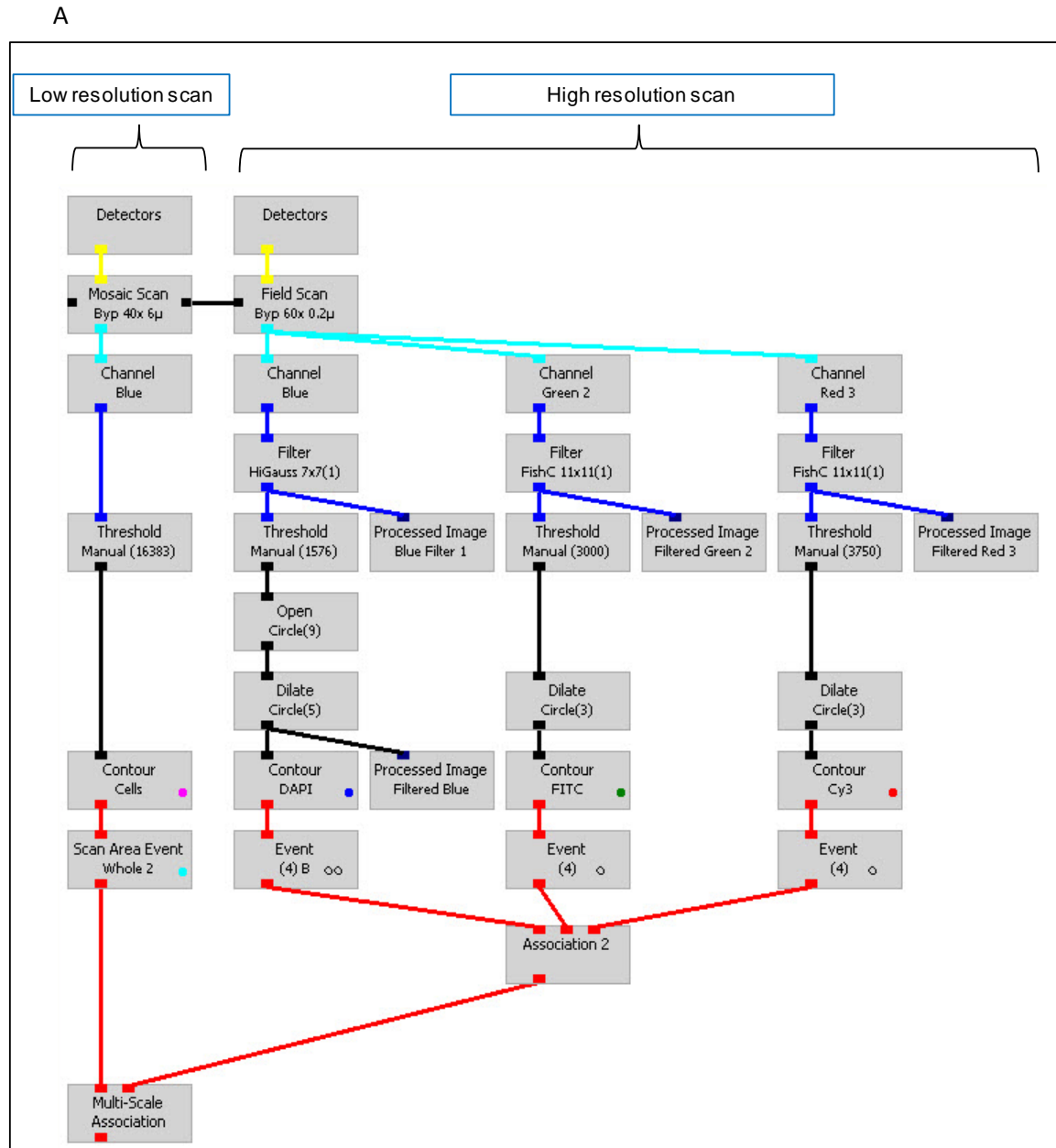
A CompuCyte iCys™ laser scanning cytometer (Thorlabs, USA) was used to analyse the slides which were similarly prepared for conventional FISH. This machine was located at the South Australian Medical Health Research Institute (SAHMRI) (<https://www.sahmriresearch.org/our-research/research-facilities-and-equipment/flow-and-laser-scanning-cytometry-facility>).

A brief outline of the LSC protocol is shown in Figure 2.1A. An initial low-resolution scan at 405 nm (channel blue for detecting nuclei staining of DAPI) was performed to determine the location of the nuclei (Figure 2.1A, B). For high-resolution scanning, the appropriate wavelength for DAPI and each of the hybridised probes, including 488 nm for spectrum green probe (FITC) and 561 nm for spectrum orange probe (Cy3) were used. Regions were then randomly selected for high-resolution scanning as indicated by a blue rectangle (Figure 2.1C, D). The threshold, laser voltage, offset, focus and any required additional filtering were slightly adjusted on a slide-by-slide basis, resulting in images such as those shown in Figure 2.1E. The selected areas of the slides were automatically scanned in 0.2  $\mu\text{m}$  sections until the scan was completed.

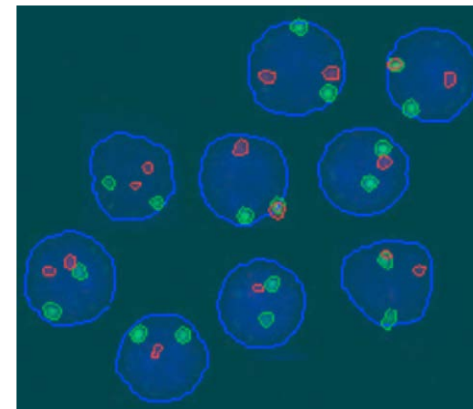
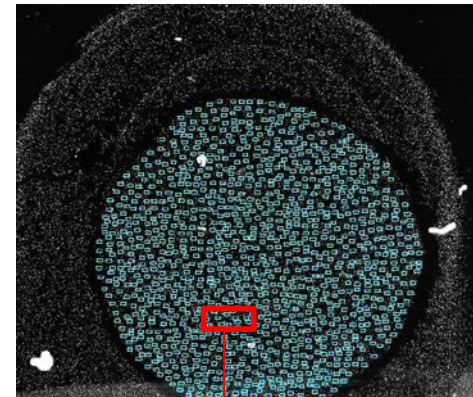
**Figure 2.1. Laser scanning cytometry protocol for FISH analysis.**

*(A) FISH analysis using laser scanning cytometer protocol. (B) A slide containing cells for analysis with the scanning area gates in blue colour on a computer-generated image (low-resolution scan). (C) Areas were randomly selected for high resolution scanning demonstrated by cyan boxes in (D). (E) Final high-resolution scan images with nuclear contour of DAPI (blue), 13q14-FITC probes (green) and 17p13-Cy3 probes (red).*





**C**



The acquired data was analysed by the iCys software, which carries out a detailed statistical analysis and displays the data using scatterplots and histograms (similar to flow cytometry analysis). Single cells were first gated on the nuclear marker (DAPI) based on their size and perimeter (Figure 2.2 A and Figure 2.3 A). In the single cells gate, an event table containing information on each cell, including an ID number and the number of green or red spots, is generated (Figure 2.2B and Figure 2.3B). The software also provides the in-slide position of each cell, enabling the user to cross check the morphology images of individual nuclei ((Figure 2.2C and Figure 2.3C). This also permitted the exclusion of those cells in which spots were outside the contour of DAPI. This analysis enabled data to be recorded for more than 2000 nuclei per slide.

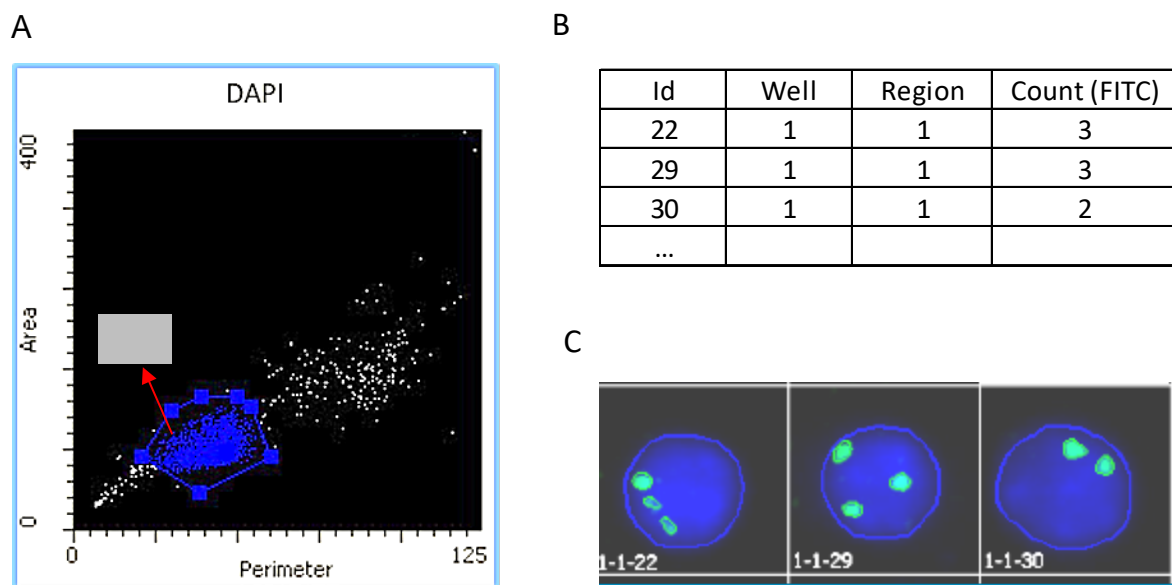


**Figure 2.2. Analysis workflow of laser scanning cytometry data for centromere 12 probe.**

(A) Single nuclei (R1) gated based on perimeter versus area (size) of nuclei (DAPI). Cells above this region are doublet nuclei and DAPI staining below is debris. (B) Examples of data exported to Excel. Numbers represent the identification of individual images. (C) Representative images of centromere 12 probes (FITC, in green) and nuclei (in blue), with location annotated as in (B).

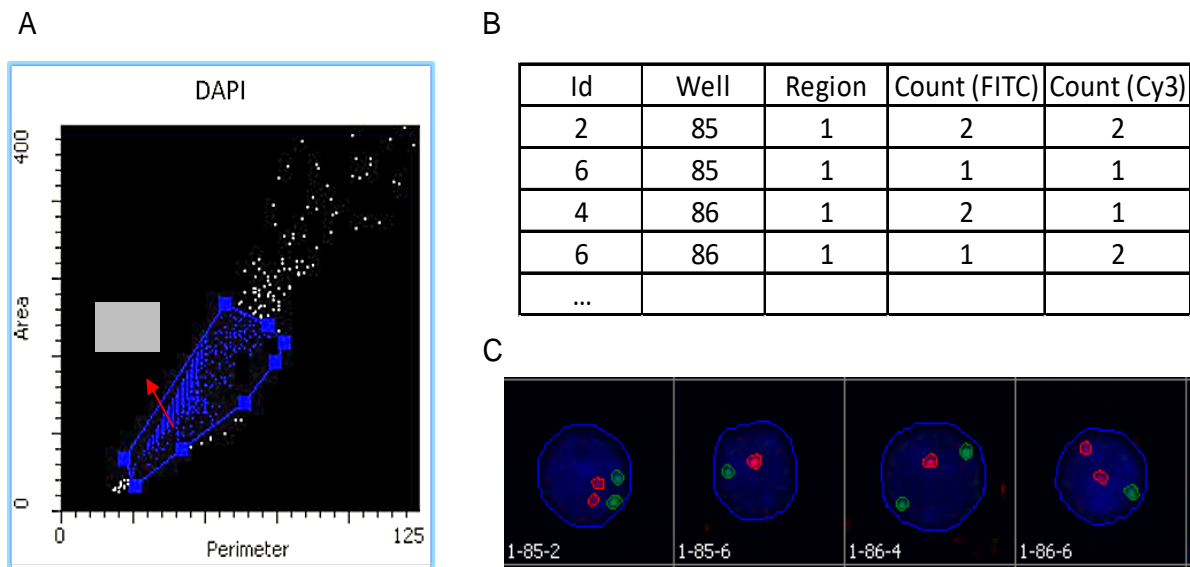


**Figure 2.3. Analysis workflow of laser scanning cytometry data for *DLEU/TP53* probes.**

(A) Single nuclei (R1) gated based on perimeter versus area (size) of nuclei (DAPI). Cells above this region are doublet nuclei and DAPI staining below is debris. (B) Examples of data exported to Excel. Numbers represent the identification of individual images. (C) Representative images of *DLEU* (13q) probes (FITC, in green), *TP53* (17p) probes (Cy3, in red) and nuclei (DAPI, in blue), with location annotated as in (B).

## 2.8 Fluorescence *in situ* hybridisation in suspension (FISH-IS)

### 2.8.1 FISH-IS buffers

All of the following buffers were freshly prepared for each experiment.

1X PBS + 1% BSA: 0.5 g BSA was added to 50 mL 1X PBS at 4°C.

2X SSC + 0.1% NP-40: 4 mL of 20X SSC and 40  $\mu$ L of NP-40 were combined and made up to 40 mL with 1X PBS. The pH was adjusted to 7.0 with 1M NaOH or 1M HCl as required.

0.4X SSC + 0.3% NP-40: 800  $\mu$ L of 20X SSC and 120  $\mu$ L of NP-40 were combined with 40 mL of 1X PBS. The pH was adjusted to 7.0 as required.

### **2.8.2 FISH-IS method**

The FISH-IS protocol used in this study was adapted from the report by Minderman et al. (2012). PBMCs were fixed according to the day 1 protocol described in section 2.6.2. Three million fixed cells were washed in 5 mL of 1X PBS + 1% BSA followed by centrifugation at 300  $\times$   $g$  for 4 mins, and repeated. Cells were then washed in 2 mL of 2X SSC + 0.1%NP-40 followed by centrifugation at 300  $\times$   $g$  for 4 mins, and the supernatant was removed. Cells were counted on a haemocytometer (see section 2.4) and  $1.5 \times 10^6$  cells (per each hybridisation tube) were transferred to a 1.5 mL non-stick microfuge tube. Cells were then resuspended in 500  $\mu$ L of 2X SSC + 0.1% NP-40, centrifuged at 1000  $\times$   $g$  for 4 mins and the supernatant discarded. The cell pellet was resuspended in a master mix containing 28  $\mu$ L of CEP hybridisation buffer, 2  $\mu$ L of CEP probe and 10  $\mu$ L of nuclease-free water, then transferred to a 0.2 mL tube. Samples were then incubated at 80°C for 5 mins, followed by incubation at 42°C for 13 hours. On the following day, the samples were washed in 200  $\mu$ L of 2X SSC + 0.1% NP-40 at room temperature, followed by centrifugation at 2000  $\times$   $g$  for 5 mins. Cells were then resuspended into 200  $\mu$ L of 0.4X SSC + 0.3% NP-40, pre-warmed to 73°C and incubated at 73°C for 2 mins in order to degrade any remaining excess probe. Cells were then centrifuged at 2000  $\times$   $g$  for 5 mins at room temperature. The supernatant was discarded and cells were resuspended in 30  $\mu$ L of 2% FCS + PBS and 10  $\mu$ L of 5  $\mu$ g/mL DAPI. Prior to analysis on the ImageStreamX Mark II (Amnis, Seattle, USA), samples were carefully resuspended by drawing through a 25G needle several times in order to prevent cells clumping.

Details of fluorochrome laser settings used for ImageStreamX analysis are presented in **Table 2.1**. The Compensation Wizard instructions (INSPIRE) were followed to create a compensated matrix file for each colour used. Briefly, all channels were enabled and brightfield and scatter laser were turned off. A file (\*.ctm) was created whilst recording 500 events, and the compensation file (\*.ctm) was applied to the .rif file when analysing. For each analysis, 20,000 events were imaged at 60x magnification with slow flow speed. All imaging data were collected with extended depth of field (EDF), which enabled analysis of in-focus spots ranging from 4 to 16  $\mu\text{m}$  (Ortyn et al. 2007).

**Table 2.1. Properties of fluorochromes used in ImageStreamX analysis.**

Channel	Bands (nm)	Laser (nm)	Laser Power (mW)	Applicable Fluorochrome	Excitation (nm)	Emission (nm)
Channel 1	420-480	-	-	Brightfield	-	-
Channel 2	480-560	488	50-100	Spectrum Green	496	520
Channel 3	560-595	561	100-200	Spectrum Orange	560	576
Channel 7	430-505	405	30-80	DAPI	358	460

*Fluorochromes are analysed within channels which analyse a certain band width. Lasers are then selected according to wavelength. The power, fluorochrome excitation/emission wavelengths are noted.*

Following data collection, hierarchical gating strategies were established with IDEAS Software version 6.1 by using Spot Count Wizard. In brief, cells were gated for best focus, single intact cells were selected, and fluorescence spots were assigned with both low and high range intensity. The IDEAS V6 Spot Count Wizard software automatically calculated the number of spot counts by scoring the fluorescence FISH signals. Features utilised in the IDEAS software analysis are summarized in Table 2.2.

**Table 2.2. Brief descriptions of features used in IDEAS software analysis.**

Feature name on IDEAS software	Meaning
Gradient root mean square (RMS)	A measure of pixel value variation. Used to select the cells in focus.
Aspect Ratio	Minor Axis divided by the Major Axis. Indicates the roundness of the cell and is used to discriminate single cells from doublets.
Area	Number of microns squared to determine single cells.
Intensity	The background subtracted pixel values within the masked area of the image.
Raw Max Pixel	The largest value of the pixels contained in the input mask.
Spot count	The algorithm examines each pixel based on the masks input.
Bright detail intensity R3	Intensity of the bright spots that are 3 pixels in radius or less with the background around the spots removed.

## 2.9 Bacterial artificial chromosome (BAC) probe labelling by nick translation

Prior to labelling, the REPLI-g Midi Kit (QIAGEN, Germany) was used to replicate each RP11 BAC clone (<https://bacpacresources.org>). In brief, approximately 1 µg of BAC DNA was made up to 2.5 µL with water, briefly centrifuged, and 2.5 µL of buffer D1 (Table 2.3A) was then added. The solution was briefly vortexed and then centrifuged, and samples were incubated at room temperature for 3 mins, after which 5 µL of Buffer N1 (Table 2.3B) was added and mixed well by gently vortexing. The master mix (Table 2.3C) was prepared and 20 µL was added to each reaction, and incubated at 30°C for 16 hours, followed by 65°C for 10 mins to inactivate the REPLI-g Mini DNA Polymerase. The amplified DNA was stored at -20°C.

**Table 2.3. Preparation buffers used in the REPLI-g Midi Kit.**

### A. Preparation Buffer D1

Component	Volume
Reconstituted Buffer DLB	9 µL
Nuclease-free water	32 µL
Total volume	41 µL

### B. Preparation Buffer N1

Component	Volume
Stop solution	12 µL
Nuclease-free water	68 µL
Total volume	80 µL

## C. Preparation of Master Mix

---

Master mix per reaction	Volume
Nuclease-free water	6 $\mu$ L
REPLI-g Midi Reaction Buffer	13.5 $\mu$ L
REPLI-g Midi DNA Polymerase (thawed on ice)	0.5 $\mu$ L
Total volume	20 $\mu$ L

---

Nick translation labelling of the BAC DNA was carried out as per manufacturer's instructions (Abbott Molecular, USA). Briefly, 2  $\mu$ L of replicated DNA was combined with 15.5  $\mu$ L of nuclease-free water, 2.5  $\mu$ L of 0.2 mM spectrum orange (or spectrum green-dUTP) (Life Science, Australia), 5  $\mu$ L of 0.1 mM dTTP, 10  $\mu$ L of dNTP mix and 5  $\mu$ L of 10x nick buffer. The solution was quickly vortexed and pulse centrifuged. 10  $\mu$ L of REPLI-g midi DNA polymerase was then added and the solution was gently pipetted up and down to mix, followed by incubation at 15°C for 16 hours, 75°C for 5 mins to inactivate this enzyme, and finally, stored at 4°C. 5  $\mu$ L of 10 mg/mL salmon sperm (Life Technology, Australia) and 5.5  $\mu$ L of 10% 3M sodium acetate (pH 5.5) (Thermo Fisher, Australia) were added to the sample, followed by the addition of 151  $\mu$ L of 100% ice cold ethanol. Samples were then placed at -70°C for 1 hour, followed by centrifugation at 15,000 x g for 15 mins at 4°C. The supernatant was discarded and DNA was washed in 900  $\mu$ L of 70% ethanol, followed by centrifugation at 15,000 x g for 15 mins at room temperature. The supernatant was discarded, and the DNA was desiccated at 45°C for 30 mins, followed by resuspension in 45  $\mu$ L of Tris-EDTA (pH 8) (Sigma-Aldrich, Australia) and storage at -20°C until required.



## 2.10 Statistical analysis

Statistical analysis of data was carried out with GraphPad Prism Version 6.0 (GraphPad Inc, USA) and SPSS version 22 (IBM Corporation, USA). A minimum of 2 or 3 samples were used in each experiment, and experiments were repeated a minimum of two or three times. In all tables and figures, data are presented as mean  $\pm$  the standard deviation (SD) unless otherwise stated. The differences in the geometric means were calculated by a student t-test or ANOVA test. Statistically significant differences were reported when  $p < 0.05$ .

## **3 Chapter 3 - Genomic analysis of CLL5 ARC cohort**

### **3.1 Introduction**

The clinical impact of the presence of low frequency del17p clones is an area of ongoing research and a fundamental research question in this study. It is clear that some patients with low frequency clones do well and even require no treatment while in other patients the presence of these sub-clones results in early disease progression and also treatment failure (Tam et al. 2009b). To explore this question, analysis of patients enrolled in the CLL5 clinical trial was performed to further understand clinical and genetic characteristics of patients with low frequency del17p clones.

The CLL5 clinical trial was conducted by the CLL Australian Research Consortium (ARC) of which our laboratory is a founding member and one of the two central investigative laboratories for the clinical trials. 120 patients who were treatment-naïve, fit and elderly, with symptomatic CLL, were enrolled with standard inclusion and exclusion criteria (Appendix Table 1) and randomized to receive fludarabine based therapy with either fludarabine, cyclophosphamide, rituximab (FCR) 3 or 5 days, or fludarabine and rituximab (FR) (Appendix Figure 1 and Appendix Table 2) and monitored for toxicity. The primary end-point of the study was tolerability and safety of delivering fludarabine based therapy in an elderly population of patients. However, clinical response has also been determined.

The translational research aim of this part of the study was to characterise the study patients in terms of their baseline clinical characteristics, IgHV mutational status, genomic molecular profiling and FISH analysis of deletions of chromosomes 17p, 13q, 11q and trisomy 12. With respect to the more specific aims of this chapter, the cohort

was analysed with a focus on the low frequency del17p subgroups, including methods of detection and better characterisation of their clinic-pathological features. Genomic mutational assessment of 5 commonly mutated genes in CLL (*TP53*, *ATM*, *BIRC3*, *SF3B1* and *NOTCH1*) (Campregher et al. 2014, Landau et al. 2015, Nadeu et al. 2016) was conducted in this subgroup and analysed by massive parallel sequencing. The targeted genes are outlined below.

- The tumour suppressor ***TP53*** gene is located on chromosome 17p13.1, and plays a key role in controlling cell cycle and apoptosis through DNA damage response pathways (Pietsch et al. 2008, Trbusek et al. 2013). In a cohort analysed by Rossi et al. (2014), approximately 14% of CLL patients had *TP53* disruption (mutation and/or deletion), and *TP53* mutations were an independent predictor for shorter OS and being refractory to chemo-immunotherapy, conferring the worst outcomes (see further detail in section 1.7.2).

- Ataxia telangiectasia mutated (***ATM***) gene is located on chromosome 11q22.3 and *ATM* mutations result in impaired DNA damage responses (Austen et al. 2005, Stankovic et al. 2014). *ATM* genetic alterations accounted for approximately 11% of CLL patients (Nadeu et al. 2016), whereas in comparison with the high frequency of *TP53* mutations, *ATM* mutations were only identified in 36% of CLL patients having del11q (Austen et al. 2007, Wang et al. 2011). CLL patients with bi-allelic *ATM* disruption had shorter survival and worse response to chemotherapeutics (Austen et al. 2007).

- A gene located near the *ATM* gene is the ***BIRC3*** gene (at 11q22.2). The *BIRC3* gene plays a role as a negative regulator of the alternative NF- $\kappa$ B signalling pathway (Rossi et al. 2012a). This mutation was found in only 4% of CLL patients prior to

treatment but up to 24% of cases of fludarabine refractory CLL patients (Puiggros et al. 2014). Furthermore, Rossi et al. (2012a) also confirmed that *BIRC3* mutations were associated with fludarabine chemo-refractory CLL patients.

- The splicing factor 3b subunit 1 (***SF3B1***) gene is located on chromosome 2q33.1, and encodes a component of the ribonucleoprotein (spliceosome) which helps to form the mature mRNA (Scott et al. 2013). The study of Te Raa et al. (2015) revealed *SF3B1* mutation is associated with increased direct DNA damage and results from DNA damage response aberrations. Several recent studies have found that *SF3B1* mutation is associated with poorer clinical outcome (Quesada et al. 2011, Rossi et al. 2011a, Wan et al. 2013).

- ***NOTCH1*** gene is located on chromosome 9q34.3 and encodes a type 1 transmembrane protein, which affects the development of numerous cells and organs, especially lymphoid systems (Kojika et al. 2001, Yuan et al. 2010). Several recent studies have examined the tumour suppressor role of *NOTCH1*, in which the *NOTCH1* gene was considered as an oncogene in specific diseases (Lobry et al. 2014). In T-cell ALL, the deregulation of the *NOTCH1* signalling pathway was found in nearly 50% of patients (Paganin et al. 2011, Tzoneva et al. 2012). In CLL, *NOTCH1* plays a key role in B cell apoptosis (Rosati et al. 2009). *NOTCH1* mutations have been found in 4% to 10% of CLL patients at diagnosis and up to 30% of relapsed and/or refractory CLL patients (Oscier et al. 2013). Interestingly, *NOTCH1* mutation is increased in the subgroup of CLL with unmutated IgHV genes, and in the trisomy 12 subgroup: trisomy 12 CLL patients carrying *NOTCH1* mutations associate with a significantly worse outcome compared with those with wild type *NOTCH1* (Del Giudice et al. 2012, Lopez et al. 2012, Balatti et al. 2013a). Additionally, Rossi et al. (2012b) demonstrated that *NOTCH1* mutations were solely able to confer an inferior outcome in CLL patients

irrespective of other factors, and this poor prognosis was similar to *TP53* defective patients.

Detail analysis of the CLL5 cohort affected by *TP53* aberrations and *TP53* mutation status are presented in this chapter.

The specific aims of this chapter were:

1. To characterise the CLL5 cohort baseline characteristics, conventional FISH analysis and genomic molecular profiles, more specifically in all del17p and low frequency del17p CLLs (section 3.3.1-3.3.3, 3.3.5-3.3.6);
2. To determine using laser scanning techniques the correlation between del17p and other chromosomal events in individual primary CLL cells in the CLL5 cohort (section 3.3.4); and
3. To determine if the low frequency del17p sub-clones can be detected by MPS in the CLL5 cohort (section 3.3.7).

## **3.2 Materials and methods**

### **3.2.1 Conventional FISH**

Of the 120 patients in the CLL5 clinical trial, 95 patients underwent FISH analysis. The standard protocol (see Methods 2.2.1) of conventional FISH was performed on CLL5 clinical trial patient samples. These samples were collected at diagnosis before treatment and FISH was conducted with the diagnostic XL CLL kit probes (MetaSystems, Germany) (see mapping in Appendix Figure 2), including four genetic categories to identify trisomy 12 (12p11.1-q11), deletions at 13q14.2-q14.3 (D13S319, including DLEU2, miR15a/miR16-1), 11q22.3 (*ATM*) and 17p13.1 (*TP53*). Cut-off values were determined by calculating the average scores plus three times the

standard deviation for six normal healthy (control) samples (performed in our laboratory by Dr Melanie Hayes): for the 13q14 probe and the centromere 12 probe, the cut-off level was 4% and for the 17p13 and 11q22 probes, the cut-off level was 5%. Data were interpreted as positive with a specific genetic aberration if the final values were above these cut-off values. All CLL5 conventional FISH results are presented in Appendix Table 3.

### **3.2.2 Laser scanning cytometry (LSC)**

To further investigate the co-occurrence of del13q and del17p sub-clones, LSC was performed on the FISH slides (according to the conventional FISH protocol, see section 2.6) of the 11 patients with both low frequency del17p and del13q, following the LSC protocol (see Methods 2.7) with XL DLEU/TP53 probes (Metasystems, Germany) (see mapping in Figure 7.3). This technique enables analysis of thousands of interphase nuclei, increasing the ability to detect small sub-clones in these patients. Five normal controls and patients who were normal by conventional FISH analysis were also examined by this method to independently establish cut-offs. Mean plus 3 standard deviations of the 5 healthy normal controls was used as a cut-off for each sub-clone.

### **3.2.3 Massive parallel sequencing (MPS) analysis**

Raw CLL5 sequencing data (\*fastq) and quality control were conducted by Dr Xavier Badoux and his research team (University of Sydney). DNA extraction and DNA purification of all of the CLL5 samples were undertaken using the Wizard Genomic DNA Purification kit (Promega). A NanoDrop (ThermoScientific, Wilmington, USA) with OD260/OD280 values was used to measure the concentration and optimal quality of extracted DNA. The DNA was sequenced on an Illumina MiSeq sequencer following

the manufacturer's protocol. This was targeted sequencing with a custom amplicon panel designed by Illumina to cover well-known recurrent mutations in CLL prognostic genes. The quality control of data was rechecked by Illumina Analysis Viewer (Illumina, Hayward, USA). The sequencing panel undertaken by Dr. Xavier Badoux contained 8 CLL target genes including *TP53*, *ATM*, *NOTCH1*, *SF3B1*, *BICR3*, *MYD88*, *XPO1* and *FBXW7*, whilst the sequencing carried out as part of this study contained 5 CLL target genes including *TP53*, *ATM*, *NOTCH1*, *SF3B1*, *BICR3* which were previously described in section 3.1. Therefore, for the purposes of this analysis, only the sequence data from the 5 genes that both panels had in common were analysed. NextGENe software V2.4.2 (Next generation sequencing software for biologists) was used to analyse these raw data (.fastq) files for trimming, mapping and variant analysis and copy number variation (CNV) (see manual instruction on website: [http://www.softgenetics.com/PDF/NextGENe\\_UsersManual\\_web.pdf](http://www.softgenetics.com/PDF/NextGENe_UsersManual_web.pdf)).

The FASTQ format file containing both reverse and forward reads (R1, R2) was trimmed by converting them into \*\_1.fasta and \*\_2.fasta files. The aim of this step was to filter out the low-quality sequences (based on PHRED score < 20 (< 1:100), a read length of less than 20 bases), and the quality filtering was implemented with other FASTQ files. Both of these trimmed files were mapped by aligning them to the human reference genome (Human\_V37p10\_dbsnp135) and the amplicons (\*bed file). Data were generated by allowing mapping of 100 bp sequences with the default value 85% of read matching to the reference genome for the read to be aligned to the reference. The resulting variants were lined up to the reference sequence (shown in Alignment Viewer), and this project was saved under \*ngjob file. Otherwise, variants that did not map were recorded under \*\_unmatched file. For variant calling, files were also exported to \*vcf file for further analysis by Illumina Variant Studio™ 3.0 software.

To generate the Copy Number Variation (CNV) report, the CNV tool carried out parallel comparisons of the copy number variations in projects that were aligned independently to the same reference sequence. One project file (\*.pjt) must be the sample and multiple other project files (of the disomic 17p samples) must be the control. Finally, the normalised coverage ratio value and the amount of noise in each region were measured based on the length of the reference region and the total number of aligned reads, in order to create the CNV classifications for each region, including duplication, normal, deletion, or uncalled.

For the process of the potential genetic mutations identification, Illumina VariantStudio™ 3.0 software was used (see instruction in the website: [https://support.illumina.com/content/dam/illumina-support/documents/documentation/software\\_documentation/variantstudio/variant-studio-v3-0-user-guide-1504890-01.pdf](https://support.illumina.com/content/dam/illumina-support/documents/documentation/software_documentation/variantstudio/variant-studio-v3-0-user-guide-1504890-01.pdf)). The variants in >5% populations were filtered out. Furthermore, identified variants were compared to the catalogue of somatic mutations in cancer (COSMIC) (<http://cancer.sanger.ac.uk/cosmic>): the SNP database (<http://www.ncbi.nlm.nih.gov/SNP/>), the IARC TP53 database (<http://p53.iarc.fr/TP53GeneVariations.aspx>), and the ClinVar database website (<https://www.ncbi.nlm.nih.gov/clinvar/>). According to the guidelines of interpretation of MPS variants recommended by American College of Medical Genetics and Genomics and the Association for Molecular Pathology (Richards et al. 2015), there are five categories of clinical significance: pathogenic, likely pathogenic, uncertain significance, likely benign, and benign.

In addition, the mutational status of the IgHV gene was determined using the LymphoTrack IGH assay on the Illumina MiSeq platform. Unmutated CLL (UM-CLL)



was defined as an IgHV sequence with  $\geq 98\%$  identity to the most homologous germline sequence. The follow up IgHV data were not received until now.

### **3.2.4 Statistical methods**

Baseline characteristics were analysed using descriptive statistics including counts, frequencies, median, mean, and SD. The outcome (complete remission and overall response rate) of each subset was compared using the Cox proportion hazard model, log-rank (Mantel-Cox) test, Fisher's exact test, and multi-way tables for the Pearson's chi-square test. Progression free survival (PFS) was then calculated from the start of therapy until CLL progression or death; OS was calculated from the date of the start of therapy until death. The Kaplan-Meier curve was performed in PFS analyses among different subsets of the cohort with 95% confidence intervals. A hierarchical log linear statistical test was applied to evaluate the correlation between each matching aberration(s) co-occurrence among the CLL5 cohort.

## **3.3 Results**

### **3.3.1 Baseline characteristic of the CLL5 cohort**

CLL untreated patients were characterized by age, gender, Binet and Rai stages (according to criteria in Chapter 1, Table 1.1), physical fitness (CIRS score), serum concentrations of  $\beta 2$  micro-globulin, concentrations of lactate dehydrogenase (LDH), zeta-chain associated protein kinase (ZAP-70) expression, white blood cell, platelet and IgHV mutational status, as shown in Table 3.1. Mean patient age was 71 years (range 65 to 80 years); two thirds were male (66.4%); a nearly equal proportion of each stage was present according to the Binet stage (ranging A-C), and most were fit

(Cumulative Illness Rating Scale (CIRS) score of  $\leq 6$ ). CIRS scores criteria are described in detail in Appendix Table 4.

In addition, the mutational status of the IgHV gene was determined using the LymphoTrack IGH assay on the Illumina MiSeq platform. Unmutated CLL (UM-CLL) was defined as an IgHV sequence with  $\geq 98\%$  identity to the most homologous germline sequence. Of the 67 cases with IgHV sequence information, 54% had a mutated IgHV and 46% had an unmutated IgHV.

**Table 3.1. CLL5 patients' baseline characteristics at enrolment.**

Characteristic	Number (%) (n=116)	
Age group	65-69	44 (37.9)
	70-74	44 (37.9)
	75-79	20 (17.2)
	80-84	8 (6.9)
Age (years)	Mean $\pm$ SD	71.4 $\pm$ 4.9
	Median [range]	71 [65 – 82]
Gender	Female	39 (33.6)
	Male	77 (66.4)
Binet stage	A	37 (31.9)
	B	39 (33.6)
	C	40 (34.5)
RAI stage	0	6 (5.20)
	I	24 (20.9)
	II	37 (32.2)
	III	26 (22.6)
	IV	22 (19.1)
CIRS score group	0-2	62 (53.4)
	3-4	37 (31.9)
	5-6	17 (14.7)

Beta-2 microglobulin (mg/L)	Mean $\pm$ SD	4.3 $\pm$ 1.9
	Median [range]	3.9 [0.1 - 10.7]
LDH (U/L)	Mean $\pm$ SD	300.8 $\pm$ 169.6
	Median [range]	259 [111 – 1355]
ZAP-70 expression	Mean $\pm$ SD	30.5 $\pm$ 26.3
	Median [range]	19.1 [0 – 91]
White blood cell ( $\times 10^9/L$ )	Mean $\pm$ SD	104.8 $\pm$ 82.2
Platelet ( $\times 10^9/L$ )	Mean $\pm$ SD	154.5 $\pm$ 77.4
IgHV	Mutated	36/67 (53.7)
	Unmutated	31/67 (46.3)

### 3.3.2 Conventional FISH characteristics of the CLL5 cohort and overall outcome.

CLL5 trial outcome data (CR, ORR) were recorded for 116 patients (out of 120 patients in total) and FISH analyses were performed on 95 patients (Table 3.2). Of 95 patients, 34.7% had del13q, 15.8% had trisomy 12, 9.5% had del11q, 21.1% had del17p, and no abnormality was detected in 18.9% of patients. Furthermore, del17p patients with a clone size of <25% deleted nuclei (low frequency del17p) accounted for 15.8% of patients, and del17p with clone size  $\geq$ 25% accounted for 5.3%.

The data of treatment response of each genetic abnormality subgroup are shown in Table 3.2. All the response criteria are described in Appendix Table 5, including complete remission (CR) and overall response rate (ORR). ORR is inclusive of CR, nPR, or PR (nodular partial remission (nPR), partial remission (PR)).

**Table 3.2. Treatment response according to cytogenetic characteristics as determined by conventional FISH.**

Conventional FISH	Number (%)	Number CR (%)	Number ORR (%)
-------------------	------------	---------------	----------------

All patients	120 (100)	65/116 (56 [47-64])	105/116 (90.5 [89-92])
Not Done	25/120 (20.8)	14/24 (58.3 [40-75])	24/24 (100 [100-100])
Del17p	20/95 (21.1)	10/19 (52.6 [30-74])	16/19 (84.2 [76-91])
Del17p (<25%)	15/95 (15.8)	8/14 (57.1 [33-80])	13/14 (92.9[89-97])
Del17p (>25%)	5/95 (5.3)	2/5 (40 [18-98])	3/5 (60[20-99])
Del11q	9/95 (9.5)	1/9 (11.1 [50-72])	8/9 (88.9[81-97])
Trisomy 12	15/95 (15.8)	9/15 (60 [39-80])	14/15 (93.3[89-96])
Del13q	33/95 (34.7)	18/33 (54.6 [38-70])	32/33 (97[95-98])
Normal-by-FISH	18/95 (18.9)	13/16 (81.3 [71-90])	16/16 (100[100-100])

*Complete Remission (CR), Overall response rate (ORR) (any CR, nPR or PR).*

*Results represented as n (% [95% Confidence Interval]).*

*One patient can have more than one aberration.*

It is noted that there were no statistically significant differences in the PFS time between del17p patients and non-del17p patients ( $p=0.25$ ) (Figure 3.1A) or with other aberration subsets. However, the study was not designed for outcome determination as a primary aim and not prospectively powered for subset analysis. The monitoring time is relatively short (24 months), therefore the CR of TP53 deleted cases is high; it is predicted that this will reduce with a longer follow-up time. With this limitation in mind, it is noted that patients with low frequency del17p had similar response rates (CR and ORR) as all patients, with CR of 57% versus 56% and OR 93% versus 90% respectively, whereas patients with >25% del17p nuclei deleted had the worst response rates with 40% of CR and 60% of ORR. These subsets were analysed by Kaplan-Meier curve survival demonstrating a trend to superior PFS of patients with low frequency del17p compared to high frequency del17p, but the difference was not statistically significant ( $p = 0.07$ ) (Figure 3.1B).

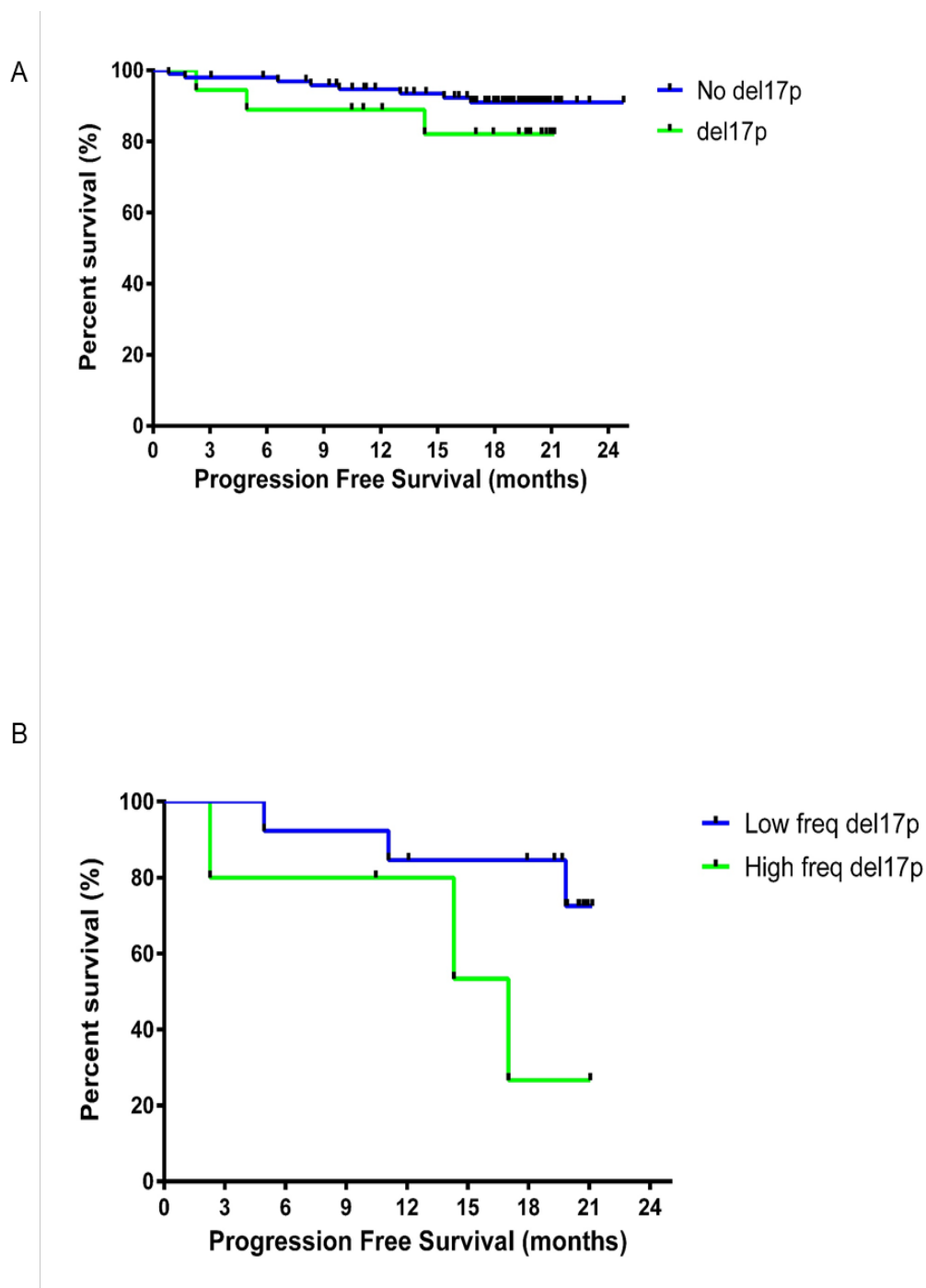


**Figure 3.1. Kaplan-Meier curves demonstrating progression free survival of patient subsets according to del17p status as determined by conventional FISH analysis.**

(A) There was no progression free survival difference for patients with ( $n=18$ ) or without del17p ( $n=95$ ) ( $p=0.25$ ). (B) There was a trend to superior progression free survival in patients with low frequency del17p ( $n=13$ ) versus high frequency del17p ( $n=5$ ) ( $p=0.07$ ).

### 3.3.3 Further investigations of conventional FISH data of the CLL5 cohort

Our cohort showed that 77/95 (81.1%) CLL patients had at least one genomic aberration. Of these, 44 (46.3 %) had a sole aberration, 19 (20%) had 2 concomitant aberrations and 14 (14.8%) had  $\geq 3$  aberrations (complex karyotype) (Table 3.3). In the sole aberration group, del13q mono-allelic abnormalities accounted for 28.4%, followed by trisomy 12 for 10.5%, while there were few del17p, del11q and bi-allelic del13q patients at approximately 2.1% to 3.2%. (Table 3.3). Bi-allelic 13q deletion was classified as only one genetic aberration as the deletion has affected the same chromosome and the same genes.

The data in Table 3.3 demonstrate that the response rate to treatment of complex karyotype was 78.6%, which was inferior to the response rates of patients with no, sole or 2 aberration(s) ( $p=0.023$ ). There were no statistical differences in CR or ORR between other groups ( $p>0.05$ ).

In the literature, certain sole aberrations have clear prognostic impact, as discussed in Chapter 1 (section 1.6.3). It has been reported that complex karyotypes result in the worst outcomes (Döhner et al. 2000, Thompson et al. 2015). However, the determination of 3 chromosomal events representing a specific subgroup is likely only to be a marker of wider genetic instability. The presence of 2 aberrations has unclear impact on prognosis and clinical outcomes and may be dependent on the serendipity of 2 individual genetic events. Therefore, I further investigated in detail the presence of two co-existent chromosomal aberrations in patients enrolled in the study, in particular the poor prognostic variant del17p in association with the good prognostic abnormality del13q, to further delineate any potential associations of the two events. G-banding data of CLL5 were not available for analyse complex karyotype.

**Table 3.3. Response to treatment according to the number of genetic abnormalities as characterised by conventional FISH in CLL5 cohort (n=95).***The number was too low to interpret any significant comparisons.*

Conventional FISH	Number (%)	Number CR (%)	Number ORR (%)
No abnormality	18 (18.9)	13/16 (81.3)	16/16 (100)
Sole aberration	44 (46.3)	22/42 (52.4)	38/42 (90.5)
Del17p only	3 (3.2)	1/2 (50)	1/2 (50)
Mono-allelic del13q only	27 (28.4)	15/26 (57.7)	25/26 (96.2)
Bi-allelic del13q only	2 (2.1)	1/2 (50)	2/2 (100)
Del11q only	2 (2.1)	0/2 (0)	1/2 (50)
Tri12 only	10 (10.5)	5/10 (50)	9/10 (90)
2 aberrations	19 (20)	9/19 (47.4)	16/19 (84.2)
Del17p + mono-allelic del13q	5 (5.3)	3/5 (60)	4/5 (80)
Del17p + bi-allelic del13q	2 (2.1)	1/2 (50)	1/2 (50)
Del17p + del11q	1 (1.1)	0/1 (0)	1/1 (100)
Del17p+ tri12	2 (2.1)	2/2 (100)	2/2 (100)
Mono-allelic del13q + del11q	4 (4.2)	0/4 (0)	4/4 (100)
Mono-allelic del13q + tri12	3 (3.2)	2/3 (66.7)	3/3 (100)
Bi-allelic del13q + del11p	2 (2.1)	1 /2 (50)	1 /2 (50)
≥ 3 aberrations	14 (14.7)	8/14 (57.1)	11/14 (78.6)
Total	95 (100)	52/91 (57.1)	81/91 (89)

### 3.3.4 Relationship between 17p deletion and 13q deletion in the CLL5 cohort

#### 3.3.4.1 17p deletion and 13q deletion in the CLL5 cohort

Nineteen out of 95 patients had 2 concomitant chromosomal aberrations (20%). Within this subgroup, the most frequent association was between del17p and mono-allelic del13q at 26% (5 patients) (**Figure 3.2**). A hierarchical log linear statistical analysis was applied to explore the co-occurrence among the five chromosomal aberrations; mono-allelic del13q, bi-allelic del13q, trisomy 12, del11q and del17p in CLL5 samples. There was a significant relationship between del17p and del13q mono-allelic ( $p < 0.001$ ) (Appendix Table 6). Although Dohner et al (2000) reported the association between 13q and 17p, no further analyses on this relationship has been done. Furthermore, we found a higher percentage of this co-occurrence than expected by chance

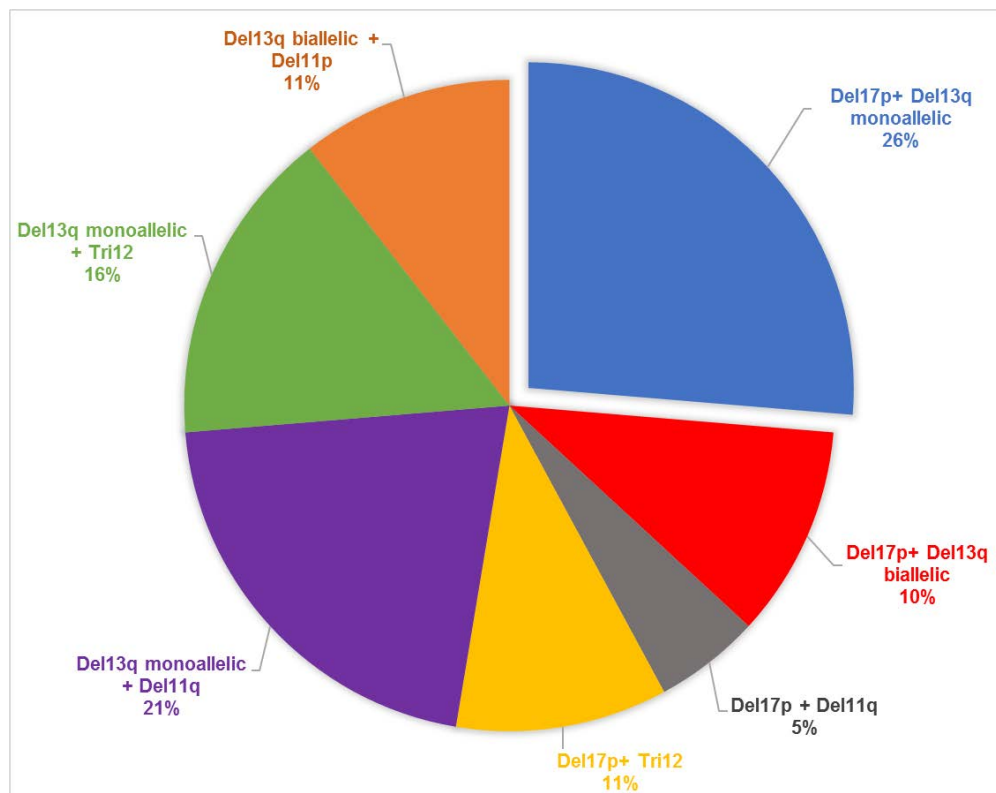




**Figure 3.2. Frequency of co-occurrence of 2 genomic aberrations by conventional FISH in CLL5 cohort.**

*Concomitant del17p and del13q accounts for the greatest percentage of genomic aberrations.*

**3.3.4.2 17p deletion and 13q deletion in del17p samples in the CLL5 cohort**

To investigate this association further, the CLL5 cohort was reviewed for specific associations between del17p and del13q. There were 20 patients in whom del17p was apparent: 15 samples had low frequency del17p (defined by having less than 25% of 17p-deleted nuclei (Tam, C.S et al 2009b); one sample with mid- frequency del17q (41% of the total cell population) and four other samples with high frequency ranging from 85% to 91% del17p nuclei deleted (Table 3.4).

In the specific group of low frequency del17p (15 samples), 11 samples had concomitant del13q (73%). Specifically, within this subgroup, there were 9 samples with co-occurrence mono-allelic del13q, 1 sample with concomitant bi-allelic del13q and 1 sample with co-occurrence of both mono-allelic and bi-allelic del13q in different sub-clonal populations (Table 3.4).

According to Dohner et al (2000), del13q has the highest frequency and del17p has the lowest; therefore, their co-occurrence cannot be explained by the prevalence of each individual lesion.

Regarding other prognostic factors, of the cases with del17p samples, 50% (10 of 20 samples) had an unmutated IgHV, 40% had a mutated IgHV, while the IgHV rearrangement failed to amplify in the remaining 10% (Table 3.4). There was no statistical difference in mutational status between the del17p subgroups ( $p>0.05$ ).

**Table 3.4. List of conventional FISH results of CLL5 samples with 17p deletion (n=20).**

ID	IgHV	del13q (%) mono-allelic	del13q (%) bi-allelic	trisomy12 (%)	del11q (%)	del17p (%)	
Low frequency del17p (<25%) (n=15)							
1	RNS011	M	4	0	55	2	6
2	STV004	UM	9	0	<1	2	7
3	HOB012	UM	13	0	51	9	7
4	STV059	UM	4	0	1	9	8
5	RNS030	M	79	0	<1	2	8
6	HOB031	M	88	0	<1	9	8
7	PAH008	UM	4	0	2	4	9
8	QEH101	UM	95	0	<1	95	9
9	RNS021	M	96	0	<1	5	10
10	RNS019	UM	6	0	2	88	11
11	SCG018	ND	4	93	1	5	12
12	GEE016	UM	96	0	3	9	12
13	CAN037	M	95	0	1	4	12
14	MMN046	M	60	27	<1	4	22
15	GCH058	UM	4	0	73	5	22
Mid/High frequency del17p (≥25%) (n=5)							
16	SCG063	M	4	95	<1	9	41
17	FMC089	M	0	89	<1	<1	85
18	SCG054	ND	2	0	<1	3	88
19	STG066	UM	10	0	<1	4	90
20	MMC085	UM	1	0	<1	2	91

All data are showed in percentages. M: mutated, UM: unmutated, ND: poor quality sample. Cut-off value for del13q mono-allelic & bi-allelic: 4%, trisomy 12: 4%, del11q: 5%, and del17p: 5%. All positive results (above the cut-off value) are shown in red.

While there was no statistically significant survival advantage with del17p and del13q concomitance as opposed to del17p alone at the 24 months analysis time-point ( $p=0.31$ ), further follow-up of those patients is awaited with interest (**Figure 3.3**).

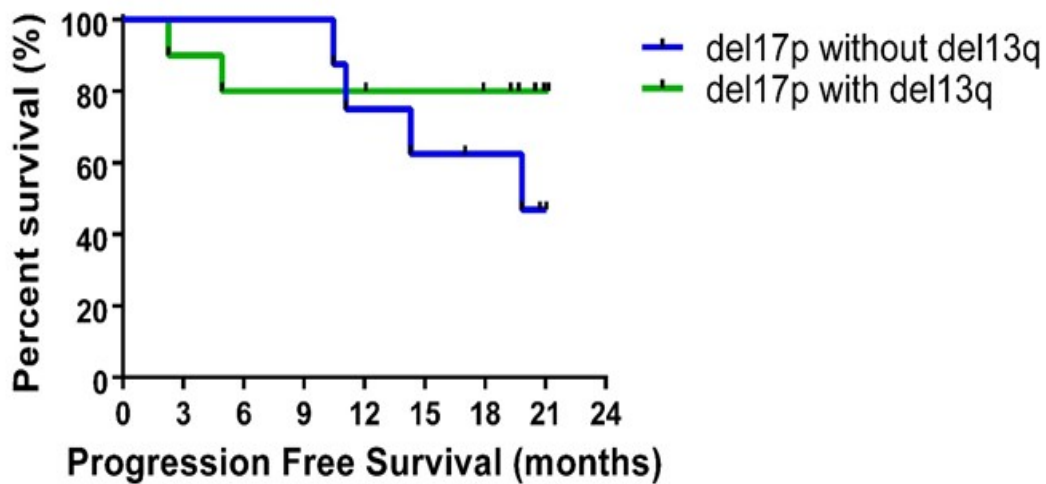


**Figure 3.3. Kaplan-Meier curves demonstrating progression free survival of del17p patient subsets according to del13q status as determined by conventional FISH analysis.**

*The graph demonstrates progression free survival in patients with concomitant del17p and del13q ( $n=12$ ) at a time point of 21 months, compared to del17p as a sole abnormality ( $n=8$ ) ( $p=0.31$ ). Although there appears to be a plateau on the del17p with concomitant 13q curve, the short follow-up of patients and low total patient numbers precludes further interpretation.*

### 3.3.4.3 Investigation of *del17p* and *del13q* intra-tumour sub-clones by laser scanning cytometry

Prior to carrying out LSC on CLL samples, the normal cut-off reference of XL DLEU/TP53 probes on LSC was determined. This was determined by identifying five healthy normal controls (age matching > 65 years old) from the blood bank. Conventional FISH analyses of these individual samples confirmed that they had normal karyotypes. Cells from each of these five healthy samples were hybridised with the above probes (in duplicate) and then scored with LSC. The data are presented in Table 3.5.

**Table 3.5. Laser scanning cytometry results of normal healthy control PBMCs.**

	Total cells	17p+/+ 13q+/+	17p+/+ 13q+/-	17p+/+ 13q-/-	17p+/- 13q+/+	17p+/- 13q+/-	17p+/- 13q-/-	17p-/- 13q+/+	17p-/- 13q+/-	17p-/- 13q-/-
1	5907	97.02	1.79	0.03	0.96	0.07	0.02	0.03	0.02	0.05
2	6966	95.35	0.26	2.20	1.29	0.52	0.32	0.04	0.03	0.00
3	8654	95.32	1.46	0.66	0.65	1.18	0.14	0.13	0.24	0.23
4	9378	92.98	1.24	1.14	1.65	1.78	0.55	0.32	0.29	0.04
5	3564	92.45	3.03	1.82	1.60	0.45	0.36	0.08	0.06	0.14
<b>Mean+3SD</b>	<b>99.67</b>	<b>4.25</b>	<b>3.51</b>	<b>2.38</b>	<b>2.62</b>	<b>0.84</b>	<b>0.44</b>	<b>0.47</b>	<b>0.36</b>	

All data are shown in percentages (%), except for the first column which shows total number of cells.

Following the LSC analysis in normal samples, this analysis was performed with XL DLEU/TP53 probes on 11 patients who had a concomitant loss of del17p and del13q by conventional FISH. The intention of this LSC analysis was to analyse vastly increased numbers of cells per sample in order to better interrogate the sub-clonal frequencies and co-occurrences at an individual cell level. In addition, three normal karyotype by FISH CLL samples were also analysed in parallel as additional controls (MMN013, PAH026 and AUS079). Data are presented in Table 3.6.

It can be seen in Table 3.6 that the majority of the values in the three normal-karyotype CLL samples were less than the normal cut-off reference for each sub-clone; only in MMN013 was there 0.57% (17p-/- & 13q+/-) (normal cut-off is 0.44%). This suggests that normal-by-FISH karyotyping probably identifies a subgroup of CLL with very stable genomes and truly low incidence of chromosomally abnormal sub-clones, within the restricted analysis of chromosomes applied by the currently employed conventional FISH method. The confidence of interpreting very low sub-clone numbers was increased by LSC methodology with 10.5 to 45 times the number of cells evaluated and the achievement of consistently low cut-offs even under stringent statistical analysis.

Of the 11 CLL patient samples which had previously been identified to have both del17p and del13q sub-clones, there were 3 clones which were found to exist at high frequency: a normal clone (17q+/+ & 13q+/+; patients 1, 2 and 7), a mono-allelic del13q clone (17p+/+ & 13q+/-; patients 3-6 and 8-10) or a bi-allelic del13q clone (17p+/+ & 13q-/-; patients 10 and 11) (Table 3.6 and Figure 3.4).

- In the cases where the normal clone predominated (patients 1, 2 and 7), the low frequency (17p+/+ & 13q+/-) and (17p+/- & 13q+/+) sub-clones were in similar frequencies, suggesting that these sub-clones were arising and competing at similar levels.

- Where the predominant clone was mono-allelic del13q (17p+/+ & 13q+/-; patients 3-6 and 8-10), the co-occurrence of del17p and del13q (17p+/- & 13q+/-) was present at a lower but substantial level, suggesting that hierarchically the (17p+/- & 13q+/-) sub-clone was arising secondarily and that the del17p event was occurring within the del13q dominant clone. This scenario best fits the current paradigm of the later development of del17p sub-clones.
- Two samples had a high frequency bi-allelic del13q clone (17p+/+ & 13q-/-; patients 10 and 11). In patient 11, the bi-allelic del13q sub-clone was the predominant clone at a frequency of 87.6%. However, it was found that the sub-clone containing del17p (present at 8.8%) occurred in association with a mono-allelic loss of 13q. This suggests that the second loss of 13q occurred after the 17p loss, but that the bi-allelic del13q has a survival advantage over the mono-allelic 13q deletion. Likewise, in patient 10, the clones with mono and bi-allelic loss of 13q were approximately equal (43.5% and 41.8%); however, the del17p clone (8.2%) occurred essentially only in the setting of mono-allelic loss of 13q. From these observations, it can be inferred that the del17p event in these CLL patients happened in the same clone as the mono-allelic del13q event, but the bi-allelic del13q event occurred in separate clonal events.

In addition, it was evident that the sub-clone containing both del17p and mono-allelic del13q (17p+/- & 13q+/-) was seen at the next highest frequency, ranging from 6% to 12% in all samples (Table 3.6 and Figure 3.4). Again, these findings are consistent with mono-allelic del13q and del17p events occurring early in the evolution of the sub-clones. In comparison, with respect to the order of these 2 events, in samples 1, 2 and 3 the clone with both abnormalities (17p+/- & 13q+/-) was slightly larger than the clones with mono-allelic del13q alone (17p+/+ & 13q+/-). In these cases, it remains possible that del17p was acquired as a second-hit within the del13q clone.

The most interesting finding from this targeted analysis is that del17p did not always occur within the clone harbouring the del13q, and in each patient containing levels of the del17p 13q+/+ above background, 2.5-3% of nuclei bearing del17p alone was observed in a minimum 1000 cell analysis (Table 3.6 and Figure 3.4). It is therefore possible that del17p had arisen independently of the del13q, which is traditionally considered a founder event. This depth of analysis has not previously been possible and it is likely that further analysis of these individual clones at a genomic level would provide information about other non-chromosomal mutational events occurring in these sub-clones.

In conclusion, these analyses demonstrate that there are potentially more branched evolutionary patterns evident within the sub-clonal populations and highlight the complex intra-clonal heterogeneity of these concomitant del17p and del13q samples. These warrant further evaluation to understand the early molecular events in CLL.

**Table 3.6. Analysis of sub-clonal chromosomal architecture in CLL samples with concomitant del17p & del13q and normal-by-FISH.**

ID	Total cells	17p+/+ & 13q+/+	17p+/+ & 13q+/-	17p+/+ & 13q-/-	17p+/- & 13q+/+	17p+/- & 13q+/-	17p+/- & 13q-/-	17p-/- & 13q+/+	17p-/- & 13q+/-	17p-/- & 13q-/-
1 STV004	1648	83.13	4.37	1.45	3.00	5.95	1.40	0.20	0.20	0.30
2 HOB012	1448	74.50	8.50	2.11	2.90	10.10	0.69	0.40	0.30	0.50
3 RNS030	1863	13.00	74.85	1.30	1.00	9.30	0.10	0.30	0.10	0.05
4 HOB031	3463	2.70	82.00	1.67	2.50	10.50	0.50	0.00	0.05	0.08
5 QEH101	3123	1.20	81.30	2.60	3.00	10.70	0.80	0.05	0.30	0.05
6 RNS021	1803	2.23	82.35	0.60	2.70	10.75	0.50	0.07	0.75	0.05
7 RNS019	1257	82.30	3.89	2.02	2.94	7.95	0.07	0.45	0.08	0.30
8 GEE016	1632	1.10	83.52	1.70	1.90	10.20	0.08	0.40	0.50	0.60
9 CAN037	1587	0.30	83.45	0.80	1.45	11.80	0.90	0.70	0.40	0.20
10 MMN046	3005	3.00	43.50	41.80	1.80	8.20	1.10	0.30	0.10	0.20
11 SCG018	2062	0.50	0.40	87.60	2.05	8.80	0.30	0.05	0.20	0.10
12 MMN013	1965	93.00	1.58	0.46	2.10	1.72	0.25	0.57	0.27	0.05
13 PAH026	2164	95.90	0.69	0.09	1.70	1.02	0.23	0.05	0.14	0.18
14 AUS079	2309	93.55	2.16	0.82	1.47	1.34	0.13	0.17	0.22	0.13
<b>Normal cut-off (mean+3SD)</b>		<b>99.67</b>	<b>4.25</b>	<b>3.51</b>	<b>2.38</b>	<b>2.62</b>	<b>0.84</b>	<b>0.44</b>	<b>0.47</b>	<b>0.36</b>

Samples 1 – 11 contained a low frequency del17p sub-clone in addition to varying levels of del13q, as determined by conventional FISH analysis. Samples 12 – 14 did not carry deletions of 13q or 17p, as determined by conventional FISH analysis. The cut-offs for normal healthy controls are shown in comparison (taken from Table 3.5). All data are shown in percentages, except for the first column with total number of cells. All the positive results (above the normal cut-off value) are shown in red.



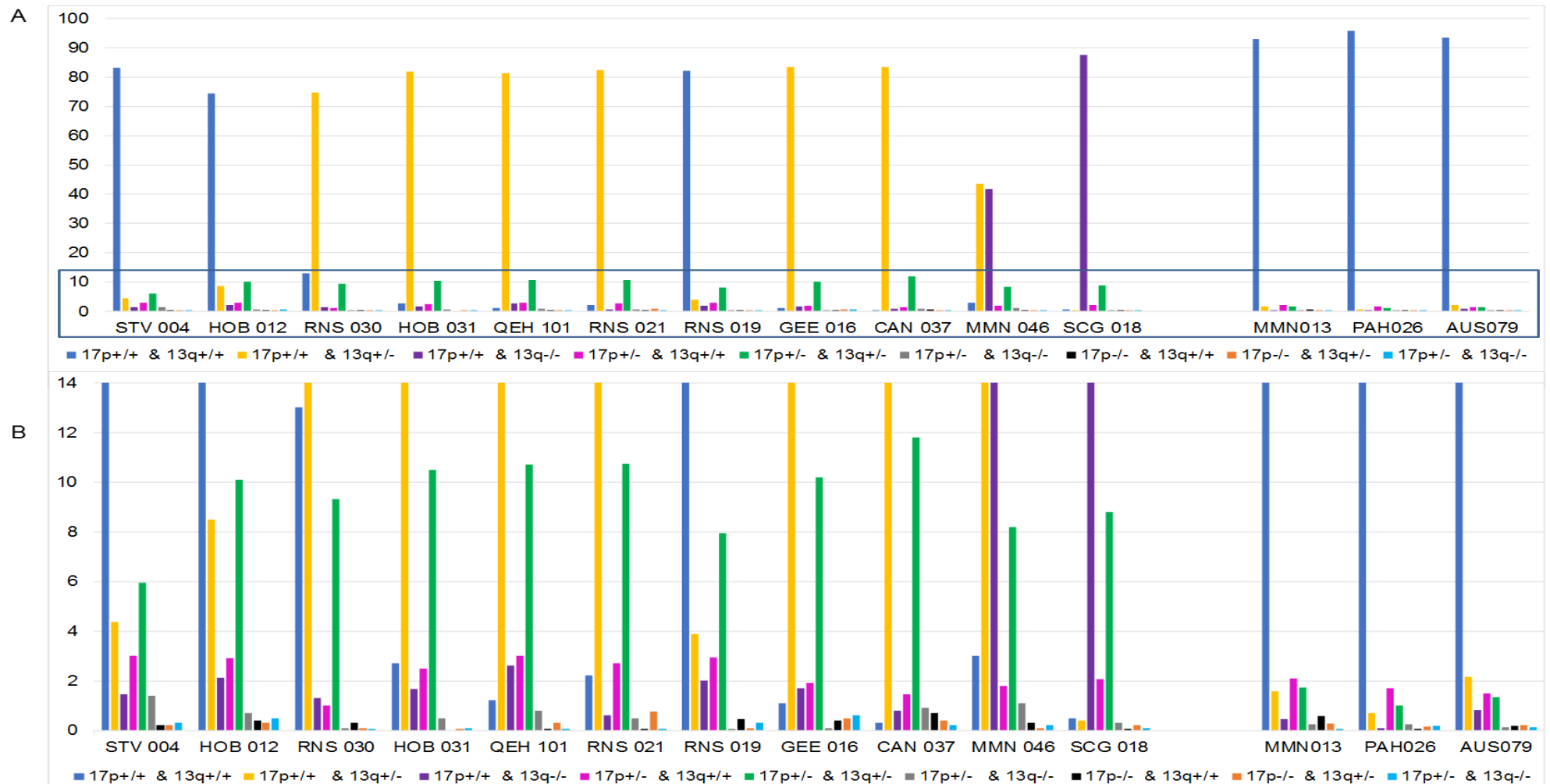


**Figure 3.4. Sub-clonal frequencies by laser scanning cytometry in cases harbouring both low frequency del17p and del13q.**

(A) Full data of sub-clonal distributions, the part of the graph in the blue box data are displayed enlarged in (B). (B) Expanded section of graph (A) defined by the blue box in A.

### 3.3.5 Genomic molecular profiling characteristics of the CLL5 cohort

DNA sequencing data was available for 83 patients. The MPS were analysed using Nextgene software with human reference genome (Hg19). The workflow analysis detail is reported in the Methods (section 3.2.3). From this analysis, the data demonstrated many potential mutations in the whole cohort. The mutations and FISH data are combined in Table 3.7 and show that 5/5 (100%) mid/high frequency del17p samples had *TP53* mutations, while only 3/15 (20%) low frequency del17p patients had *TP53* mutations, 2/14 (14.3%) of normal-by-FISH had *TP53* mutations and 1/4 (25%) of those not analysed by FISH.

Furthermore, the distribution of mutations overall in the genes analysed was at greatest frequency in the del17p high frequency group, followed by the trisomy 12 group. The low frequency del17p, del11q, del13q and other groups had similar distributions (Table 3.7).

Looking at mutational status of each of the 5 genes in the CLL5 cohort, these mutations ranged from 12% to approximately 13%, except 2.4% of *BIRC3* mutation (Table 3.8). The worst outcomes were found in *TP53* mutation, patients only 27% reaching CR and 82% ORR. Neither of the 2 patients with the *BIRC3* mutation achieved CR (Table 3.8). No statistically significant association between OS and 5 genetic mutations were found in this small cohort ( $p>0.05$ ).



**Table 3.8. Frequency of 5 gene mutations and treatment responses.**

Mutation	Number (%)	Number CR (%)	Number ORR (%)
<i>TP53</i>	11/83 (13.3)	3/11 (27.3)	9/11(81.8)
<i>ATM</i>	10/83 (12.1)	4/10 (40)	10/10 (100)
<i>NOTCH1</i>	11/83 (13.3)	6/10 (60)	9/10 (90)
<i>SF3B1</i>	11/83 (13.3)	10/11 (90.9)	10/11 (90.9)
<i>BIRC3</i>	2/83 (2.4)	0/2 (0)	2/2 (100)

### 3.3.6 Investigations of mutational profile of patients containing *TP53* mutation

The 20 del17p samples containing mutations in *TP53* or other genes and all samples harbouring *TP53* mutations in the CLL5 cohort were analysed and are shown in Table 3.9. Among the low frequency del17p subgroup, there were a total of 5 variant mutations (4 *TP53* mutations and 1 *ATM* mutation), whereas twice the number of mutations was found in the high frequency del17p subgroup (5 *TP53* mutations, 2 *ATM* mutations, 2 *NOTCH1* mutations and 1 *SF3B1* mutation). In addition, 2 samples normal-by-FISH (RMH001, PAH048) had *TP53* mutations and 1 sample with no FISH analysed results (WES029) also harboured *TP53* mutations. It was also noted that all mutations harboured the variant allele frequency (VAF) at a higher than 20%. All variants were analysed *in depth* by the Illumina Variant software, ClinVar database, COSMIC database and IARC *TP53* database. The results are summarised in Table 3.9 and showed that 11 of 12 (92%) *TP53* mutations were missense, and only 1/12 (8.3%) was nonsense. Most of the variants were located in exon-7 (42%) and exon-6 (25%), while only one was located in each of the following exons: 4, 5, 8 and 11. Out of 15 low frequency del17p CLLs, only 4 samples had mutations, of which only half had pathogenic mutations, while all 5 high frequency del17p CLLs contained pathogenic mutations. This interesting data needs to be validated by Sanger sequencing and a larger cohort.

**Table 3.9. Patients with *TP53* mutations and other variant alleles identified by MPS stratified by del17p frequency**

ID	del17p /FISH (%)	Gene	Transcript variant	Amino acid alteration	VAF	Exon number	Translation Effect	Clinical Significance	Citation Source
Low frequency del17p									
STV004	7	<i>TP53</i>	c.776A>T	p.D259V	0.47	7-exon	Missense	Uncertain significance	ClinVar
		<i>TP53</i>	c.637C>T	p.R213*	0.45	6-exon	Nonsense	Pathogenic	ClinVar
QEH101	9	<i>ATM</i>	c.1537C>T	p.Q513*	0.56	10-exon	Nonsense	Pathogenic	ClinVar
SCG018	12	<i>TP53</i>	c.646G>A	p.V216M	0.21	6-exon	Missense	Uncertain significance	ClinVar
MMN046	22	<i>TP53</i>	c.1129A>C	p.T377P	0.23	11-exon	Missense	Benign	ClinVar
Mid/High frequency del17p									
SCG063	41	<i>TP53</i>	c.395A>G	p.K132R	0.43	5-exon	Missense	Uncertain significance	ClinVar
		<i>ATM</i>	c.4324T>C	p.Y1442H	0.48	29-exon	Missense	Uncertain significance	ClinVar
FMC089	85	<i>TP53</i>	c.743G>A	p.R248Q	0.38	7-exon	Missense	Pathogenic	ClinVar
SCG054	88	<i>TP53</i>	c.818G>A	p.R273H	0.52	8-exon	Missense	Pathogenic	ClinVar
		<i>NOTCH1</i>	c.7560G>A	p.W2520*	0.41	34-exon	Nonsense	Pathogenic	COSMIC
STG066	90	<i>TP53</i>	c.742C>T	p.R248W	0.86	7-exon	Missense	Pathogenic	ClinVar
		<i>ATM</i>	c.2548G>T	p.E850X	0.17	20-exon	Missense	Pathogenic	COSMIC
		<i>SF3B1</i>	c.2098A>G	p.K700E	0.47	15-exon	Missense	Likely pathogenic	ClinVar
		<i>NOTCH1</i>	c.7537_7538insC	p.E2515fs*	0.49	34-exon	Insertion - Frameshift	Not reported	COSMIC
MMC085	91	<i>TP53</i>	c.733G>A	p.G245S	0.84	7-exon	Missense	Pathogenic	ClinVar
No del17p containing <i>TP53</i> mutations									
RMH001	0	<i>TP53</i>	c.707A>G	p.Y236C	0.89	7-exon	Missense	Likely pathogenic	ClinVar
		<i>NOTCH1</i>	c.931A>C	p.T311P	0.21	6-exon	Missense	Pathogenic	COSMIC
PAH048	0	<i>TP53</i>	c.215C>G	p.P72R	0.99	4-exon	Missense	Uncertain significance	ClinVar
WES029	NA	<i>TP53</i>	c.596G>A	p.G199E	0.41	6-exon	Missense	Benign	COSMIC

VAF, variant allele frequency. NA: not analysed by conventional FISH.

### 3.3.1 Assessment of the low frequency del17p detection by analysing MPS data.

A MPS approach has been used widely to identify mutations in patient samples. However, my research question is whether this MPS method can ascertain the presence of del17p sub-clones, especially at low frequency. To answer this question, the raw sequencing data was analysed to detect the low frequency del17p samples. Based on the designed panel, only 8 amplicons were used for the short arm of chromosome 17 sequencing, spanning the *TP53* exomic regions. For the long arm of chr17, 17 amplicons were used spanning *GRB2* exon region and 7 amplicons were used for *CD79B* exon region (Appendix Table 7.7). In short, there were a total of 3 genes covering the chr17 exon region, including *TP53*, *GRB2* and *CD79B*.

In 2013, due to some limitations of the CLC Genomics software, Dr Gareth Elvidge (Illumina sequencing specialist) helped to generate the graph in Figure 3.5. The CLL5 samples with low, mid and high frequency del17q, especially two females and one male in the low frequency group, were analysed to identify the deleted proportion based on MPS data. In this analysis, the data showed the normalised coverage of each amplicon, and a 50% drop in chromosome X for male samples when compared to the female sample could quite clearly be detected (blue box). Chromosome 18 amplicon regions demonstrated clustered lines between samples representing or demonstrating the pattern where there is no loss or gain of the chromosome. Whereas a 90% del17p sample (STG066, orange line) was quite separate from other samples in the *TP53* amplicons (blue box), a mid/low frequency del17p sub-clone could not be distinguished from a wild type 17p sample (AUS084, green line), as all sample lines were clustered in most of the amplicons covering the *TP53* exon region.

Subsequently, new analysis software became available for MPS data, namely Nextgene software, allowing re-analysis of these amplicons by an alternative method which utilises copy number variant (CNV) analysis. On chromosome 17 (blue box) in Figure 3.6, most of the SNPs were located on the average line in AUS084 (3% del17p sample, control) compared with other chromosome regions. There was a clear decline in SNPs (in red dots) in the case of STG066 with 90% del17p, with the CNV dropping to approximately 30% compared with the average line. However, CNV in 41% del17p (SCG063) did not decline consistently, and there were no measurable differences in 10% and 22% del17p in CNV changes, compared with normal del17p. These results exhibited similarity with my previous normalised coverage analysis despite the upgraded software (Figure 3.7).

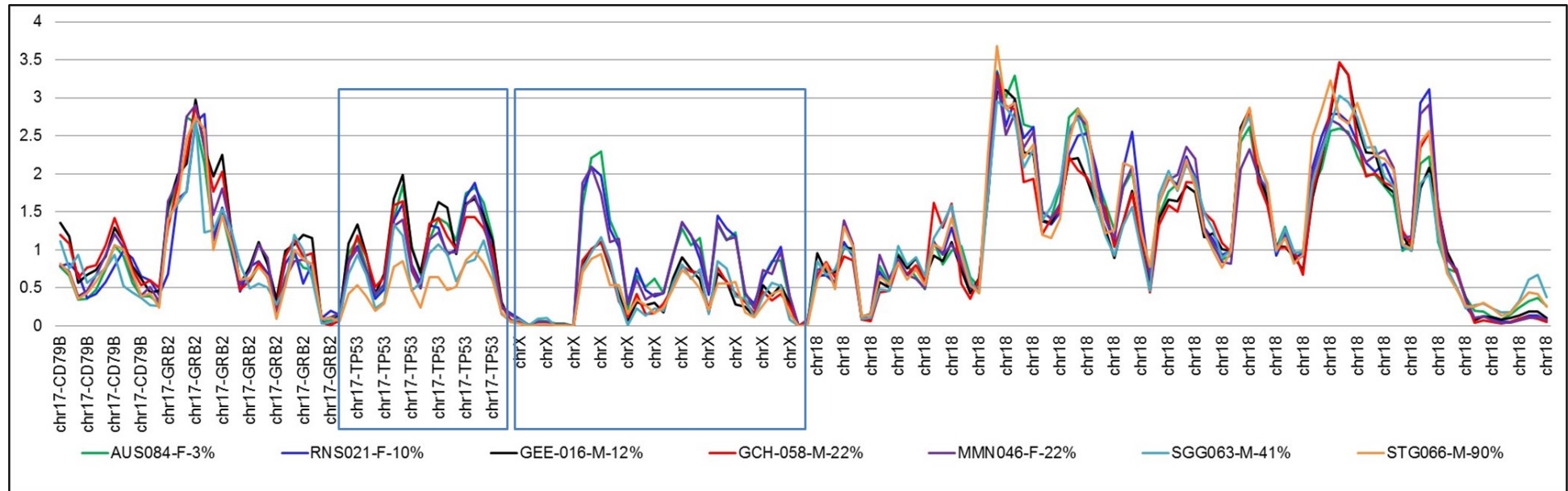


**Figure 3.5. Normalised MPS coverage of read analysis from the 5 gene panel.**

*This graph was generated the normalised coverage of read on chromosome 17, 18 and X region, with the help of Illumina sequencing applications specialist (Dr Gareth Elvidge) on the following samples. AUS084 (3% del17p), RNS021 (10% del17p), GEE016 (12% del17p), GCH058 (22% del17p), MMN046 (22% del17p), SCG063 (41% del17p) and STG066 (90% del17p).*

*AUS084, RNS021 and MMN046 are female (F); GEE016, GCH058, SCG063 and STG066 are male (M).*



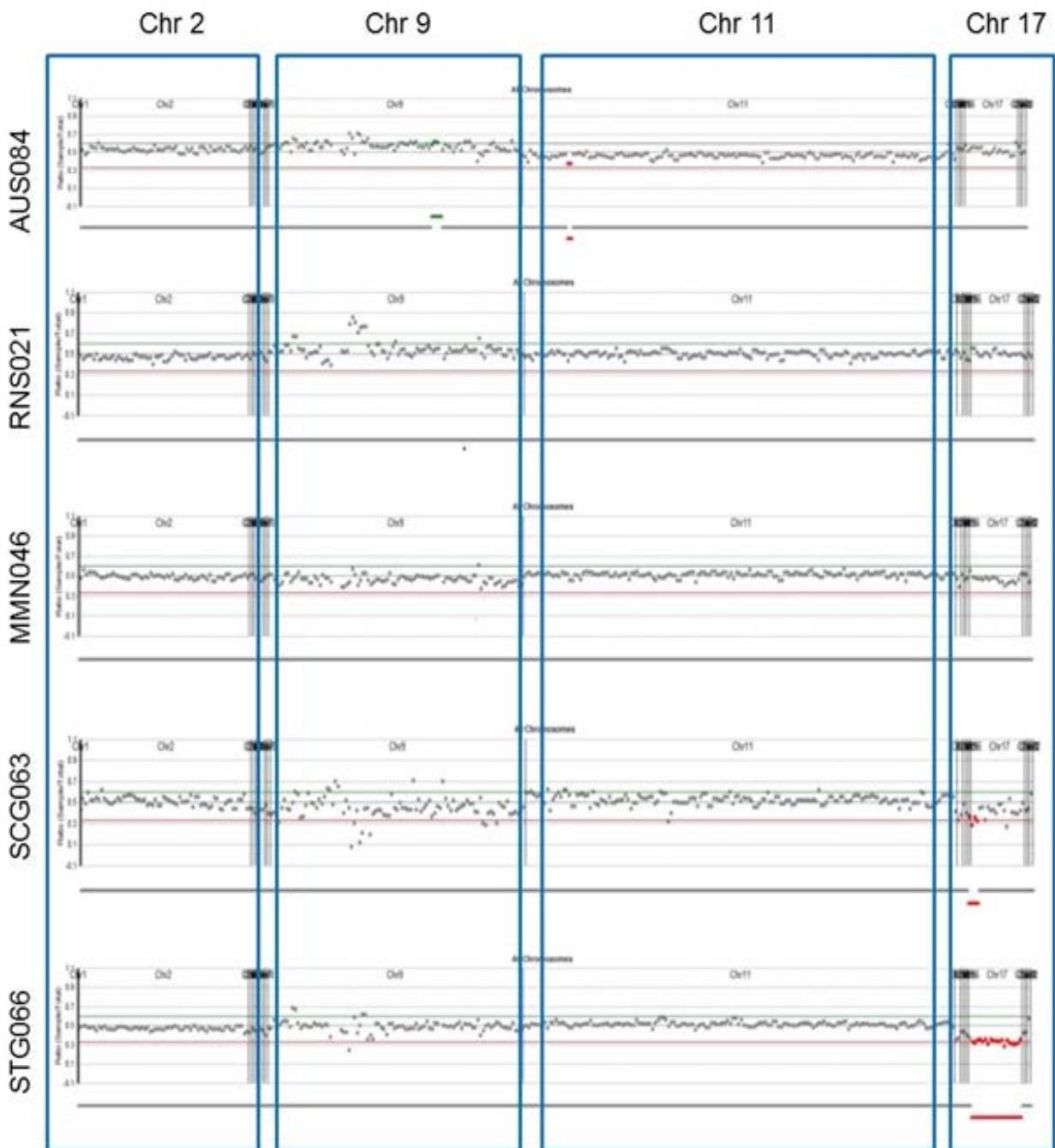


**Figure 3.6. Percentage del17p identified by copy number variant analysis of *TP53* gene region.**

*This graph was generated by copy number variation (CNV) report tools of NextGENe software V2.4.2 (see section 3.2.3) on the following samples: AUS084 (3% del17p), RNS021 (10% del17p), MMN046 (22% del17p), SCG063 (41% del17p) and STG066 (90% del17p); del17p percentages were determined by conventional FISH.*

*X-axis, ratio of sample/total. Small gray dots show the CNV at individual SNPs. CNV which fall below the average line indicate deletion and are shown in red.*

### 3.4 Discussion

In the Döhner et al. (2000) study, patients were aged between 30 to 87 years (median at 62 years) while my cohort age range was 65 to 82 years (median at 71 years). It is evident in the published literature that the level of chromosomal aberrations increases with increasing age (Sinclair 2003, Wojda et al. 2006, Mladinic et al. 2010). Laurie et al. (2012) analysed over 50,000 DNA samples from peripheral blood of normal individuals of all ages. They found that the number of people less than 50 years of age with one or more mosaic DNA aberrations within 5 life-years was less than 0.5%, whereas this increased to 3.2% in subjects more than 80 years old. Consequently, it was expected that more genomic aberrations would be identified in our elderly CLL cohort.

Our FISH data identified that our cohort (Table 3.2) demonstrated the specific genomic aberration(s) in similar distributions as expected compared with the Döhner et al. (2000) study, with some notable exceptions: 18% had no abnormality, 36% del13q, 14% trisomy 12. However, in our cohort, del11q had a lower percentage than expected at 9.5%, and del17p accounted for a higher proportion at 21.1% in comparison with 17% and 7%, respectively in the Döhner et al. (2000) study.

In comparison, Van Dyke et al. (2016) demonstrated that there were up to 12% del17p and 11% del11q among 1585 patients with treatment naïve CLL. Of note, the majority of the identified del17p samples in my study were low frequency with 25% (5/20) of samples containing greater than 25% del17p cells, which is thought to be the more clinically significant threshold for deletion of 17p by conventional FISH. The increase in the low frequency clones may be age related. However, there are insufficient age relevant published data at this level of analysis of sub-clonal architecture by conventional FISH to allow direct comparison.

Additionally, the low frequency del17p clones are likely to be under-represented in the reported literature and few manuscripts actually outline their technical cut-offs. In a comprehensive technical study of five laboratories reporting conventional FISH for CLL, the technical cut-offs varied from 5-8% (Smoley et al. 2010). The clinically significant cut-offs varying from 20-25% have been reported (Tam et al. 2009b, Oscier et al. 2010), while low frequency del17p (<25% deleted nuclei by FISH) patients were not associated with poor outcomes (Catovsky et al. 2007, Rudenko et al. 2008, Tam et al. 2009b, Oscier et al. 2010, Badoux et al. 2011b).

Our data showed that approximately 16% (15/95) had low frequency del17p (<25% of nuclei deleted). This ratio is similar to the report by Tam et al. (2009b) with approximately 17.% (11/64). A publication by Van Dyke et al. (2016) demonstrated that 49% (59/120) CLL patients had low frequency del17p (defined as  $\leq 20\%$  nuclei deleted). Therefore, these reports suggest that the low frequency del17p accounts for a significant proportion in the del17p population. In both of these published papers the outcome of low frequency del17p patients is superior to high frequency del17p. A recent paper of Yu et al. (2017) identified other concomitant driver genetic aberrations besides *TP53* mutations in the del(17p) CLL subgroups. However, they did not identify the CLL patients as low or high frequency del17p. Hence the question of whether the low frequency del17p CLL subgroup may behave differently with distinct pathogenic mechanism compared with high frequency del17p in CLL, remains unanswered.

In terms of the complexity of chromosomal aberrations, our cohort data (Table 3.3) showed a similar proportion of the number of aberration(s) in individual samples to the Döhner et al. (2000) study. Of the 325 patients, they analysed by interphase FISH, 268 had abnormal FISH analyses (82%), including 175 (54%) having one aberration, 67 (20.6%) with 2

aberrations and 26 (8%) with  $\geq 3$  aberrations. However, of note, there were slightly more complex karyotypes in our cohort with 14.8%  $\geq 3$  aberrations found, which may again be explained by the age of our cohort population or may simply be due to the smaller cohort size. Gentile et al. (2016) studied 279 elderly, previously untreated CLL patients from up to 33 centres (29 Italian, 3 Israeli and 1 German) to test the safety and efficacy of bendamustine-rituximab (BR). This study had a similar median age of 70 compared to the 71-year-old median in our study, as well as similarity in the follow-up time of 24 months. In their study, they showed 18/192 (9.4%) cases had del17p and these del17p had an ORR of 66.7%, which is comparable with our ORR ratio in the high frequency del17p group. Again, these results parallel the CLL10 clinical trial (Eichhorst et al. 2016).

There was no statistical significance in any outcome (OS or PFS) analysis associated with the underlying FISH abnormalities in our study, also most likely confounded by the small sample size and short follow-up, resulting in no differences in individual cytogenetically defined subgroups. Within the recognised constraints of the trial being powered to answer the question of toxicity and tolerability and not outcome, the lowest ORR to treatment was observed in the subgroup of complex karyotype by FISH (78.6%) when compared with the no, sole or 2 aberration(s) groups. This corresponds with the literature (Travella et al. 2013, Thompson et al. 2015, Le Bris et al. 2016, Rigolin et al. 2016, Puiggros et al. 2017, Yu et al. 2017).

Additionally, in our data, among 14 patients with complex karyotype, there were 6 patients with the co-presence of complex karyotypes and del17p (43%) despite these samples being naïve to treatment. Hence, our data demonstrated the enrichment of del17p in the complex karyotype subgroup, which was in accordance with many previously observed frequencies ranging from 26.7% up to 50% (Haferlach et al. 2007, Jaglowski et al. 2012, Baliakas et al.

2014b, Herling et al. 2016, Collado et al. 2017, Puiggros et al. 2017, Yu et al. 2017). The usual explanation for this finding is that the loss of 17p or loss of *TP53* causes underlying genomic instability, correlating with a defective DNA damage response, leading to complex karyotype (Bartek et al. 2007a, Dicker et al. 2009).

Nevertheless, Puiggros et al. (2017) found that the prognosis of CLL patients with complex karyotype was independent of 17p deleted status. This report also mentioned that current conventional FISH analyses may cause underestimation of the real complex karyotype, compared with chromosome banding analysis; this has also been claimed in several other reports (Jaglowski et al. 2012, Travella et al. 2013, Baliakas et al. 2014, Herling et al. 2016, Puiggros et al. 2017).

A number of researchers have recently reported that besides clinical characteristics, *TP53* disruption, complex karyotype, and IgHV status are the most significant prognostic markers in CLL (Delgado et al. 2014, Rossi et al. 2015, International-C.L.L.I.P.I.group 2016, Le Bris et al. 2016, Yu et al. 2017). Regarding the IgHV mutational status of our entire cohort, the interpretation of data was restricted, as I lacked the results of many patients (nearly half). But, all of the patients in the del17p subgroup were examined for IgHV mutational status, and our data showed that only 50% had an unmutated status. This proportion is compared with other reports, in which the unmutated IgHV in the del17p group ranged from 44% to 81% (Hamblin et al. 1999, Gladstone et al. 2012, International-C.L.L.I.P.I.group 2016). Additionally, it has been reported that mutational status may influence the response to therapy in del17p CLL cases (Kröber et al. 2006, Quijano et al. 2008, Rassenti et al. 2008, Puiggros et al. 2014). This apparent discrepancy may be another reason for the favourable performance in our cohort in terms of response to therapy, besides the restriction of the small sample size.

Our finding revealed the highest frequency of variant mutations for the 5 genes analysed, in the high frequency del17p subgroup compared with other chromosomal aberration subgroups and this subgroup conferred the worst outcome. This finding is in accordance with the finding of Yu et al. (2017), in which the increase of somatic mutation number was associated with poor outcome. In addition, Yu et al. (2017) also revealed that del17p was not the only driving event in CLL progression, especially as the other driving clones could compete with del17p clones. Therefore, an unbiased technique was needed to unravel the genomic landscape of del17p sub-clones, which would afford detailed analysis of each of the sub-clones. Single cell sequencing with its associated expense and potential bias may be only one solution to the problem of understanding complex sub-clonal mutational landscapes (discussed further in Chapter 6).

Different gene mutations associated with specific cytogenetic alterations strongly suggest synergy in driving pathogenesis. Our data showed that the highest frequency of *NOTCH1* aberrations was found in the trisomy 12 group, while *ATM* alterations harboured a higher frequency in the group of del11q patients. In particular, 100% of the high frequency del17p samples had *TP53* mutations, but the coincidence of low frequency del17p and *TP53* mutations was only 20%. This latter finding is in contrast with literature which found that >80% of the remaining *TP53* allele in del17p samples were mutated (Dicker et al. 2009, Zenz et al. 2010b, Seiffert et al. 2012). However, sub-clonal frequencies are not always stated.

Our 5 gene panel mutations have been considered as major and common gene drivers in CLL (Rossi et al. 2014, Sutton et al. 2015, Nadeu et al. 2016, Rasi et al. 2016, Rossi et al. 2016). Our data additionally showed that 43% (36/83) of patients were harbouring at least one of these five mutations, compared with 63% in the Sutton et al. (2015) study; and 23%

in Nadeu et al. (2016) research. The Nadeu et al. (2016) study was a clinical study on untreated CLL, and the same 5 genes as in our study were investigated by targeted ultra-deep sequencing. Their results showed that there were 10.6% of *TP53* mutations, 11.1% of *ATM* mutations, 21.8% of *NOTCH1* mutations, 12.6% of *SF3B1* mutations and 4.2% of *BIRC3* mutations among 406 CLL patients. These results were similar to our data which had *TP53* mutations (13%), *ATM* mutations (12%), *SF3B1* mutations (13%), *BIRC3* mutations (2.4%). However, the observed *NOTCH1* mutations in our data were noticeably lower at 13%. This could be explained by the fact that the ultra-deep panel in the Nadeu et al. (2016) study had higher average sequencing coverage of read at 2310x, compared with 1000x in our assays. For *in silico TP53* variant analysis, our findings correspond with those of Malcikova et al. (2015) who found 79% missense mutations, 4% nonsense mutations and 6/330 (1.8%) patients identified with more than one *TP53* variant.

To date, the relationship to outcome of the concomitance of del13q and del17p has not been explored. This study provides the first demonstration of a positive association of del13q and del17p concomitant sub-clones in CLL. Studies confirmed that LSC can replace manual scoring for conventional FISH (Adler et al. 1996, Baumgartner et al. 2001). The number of cells analysed and the reduction in bias that occurs with a manual scoring technique may provide greater reassurance of sub-clonal frequencies compared with purely manual methods of only 200 cell counts. Through the detailed intracellular analysis by laser-scanning cytometry on FISH slides, the intra-patient clonal heterogeneity of CLL has been clearly demonstrated. Our data pointed out a different sub-clonal architecture and hierarchy than has been previously recognised: and del17p sub-clones appeared to occur independently of del13q. However, the frequencies were always low and would require further analysis to confirm. If found to be valid these findings would challenge the assumption that acquisition of del17p is necessarily a late-driver event in leukaemogenesis

(Baliakas et al. 2014a, Landau et al. 2015, Winkelmann et al. 2015) and may precede or co-occur in parallel with deletion 13q in some cases. The literature reports that many CLLs start with a del13q (considered as indolent) and then develop other aberrations (Balatti et al. 2013b, Balatti et al. 2016). Our data supports the novel assumption that it is possible that del17p occurred first, or as a simultaneously competing clone (presuming that these are del17p CLL indolent or have not acquired other damaging mutations at that early time point), and then possibly another hit (mutational event) occurs to stimulate cell division/survival and change the CLL phenotype. These multi-hit processes are likely to be similar to other cancer genome patterns (Bozic et al. 2010, Davoli et al. 2013, Truger et al. 2015). However, it is clear that in an elderly previously untreated cohort, a not insignificant percentage of patients have low frequency loss of 17p, and that this is associated with a higher than by chance alone association with mono-allelic del13q, which is not seen once the del17p clone predominates.

Currently the extensive MPS approach is being applied in routine CLL clinical practice to detect mutational frequency in the IgHV gene. However, the wholesale use of genomic analysis by MPS is far from established and the cytogenetic tests such as FISH or SNP array still need to be conducted to assist with treatment decisions. Therefore, my question was whether MPS can replace conventional FISH to identify del17p, especially low frequency del17p. The mid/low frequency del17p were unable to analyse based on my available raw MPS data. This can be explained in that the amplicons covering the 17p arm were likely insufficient for determining low frequency allele loss.

To identify the low frequency del17p samples based on the coverage and read depths a specific calculation needs to occur. The assumption is that, 10% del17p means that 10% of cells have a deletion on the short arm of one chr17 (*TP53* exon region), which equates to a



5% read loss. In an ideal situation, to cover the non-deleted 17p sample with 30x coverage using 8 amplicons (*TP53*) implies 240 reads spanning *TP53*; while the 10% del17p would mean a 5% reduction in the *TP53* exon region that has loss, and equal 228 reads spanning the *TP53* region. The difference of 240 reads versus 228 reads comprises the limit of detection for counting read differences.

Another reason for the insensitivity of MPS in detecting CNV is that MPS uses short sequences (approximately 100 bases), and therefore, large deletion at 17p demonstrates the limitations of this technique, and also in PCR reactions. In addition, the method to normalise coverage of the genome was not very accurate in the case of targeted exome sequencing, but would be more precise in the case of whole exome sequencing.

### 3.5 Conclusion

The techniques described in this chapter (conventional FISH, LSC, MPS) have limited power to detect very small sub-clones of del17p and even less capacity to determine what mutations are co-occurring within individual cells in this early phase of CLL. It is clear from the work of Rossi et al. (2014) that the patients who relapse after therapy do so with the clones that harbour *TP53* mutations. However, this analysis was performed retrospectively and does not identify the early events that accompany with the *TP53* mutations in a prospective manner that help us predict an individual patient's course. Therefore, a new technique was needed to develop in order to identify and separate, or purify, the low frequency del17p sub-clone in del17p CLL samples, to better understand what the early events are driving the change from indolent CLL not requiring treatment to aggressive CLL, subsequently seen at relapse or sometimes at time of first treatment.

## **4 Chapter 4 - Development of FISH-IS to detect aneuploidies in CLL**

### **4.1 Introduction**

Cytogenetic analysis currently plays a vital role in identifying chromosomal abnormalities. Conventional FISH has been the gold standard for the diagnostic test since the first application in the early 1980s (Bauman et al. 1980). In addition, conventional FISH was reported with better analytical power in genetic aberrations detection compared to conventional karyotyping (Cox et al. 2003). However, FISH results are based on analysis of 200 nuclei per patient sample, meaning that potentially clinically relevant sub-clones of cells carrying a specific chromosomal abnormality may be missed (Dewald et al. 1998a). Furthermore, the only regions of the chromosomes that can be examined are those to which the designated probes bind. Currently, SNP array techniques are set to take over the role of FISH with whole genome coverage; however sub-clones less than 20% will be variably identified according to the techniques employed (Hagenkord et al. 2010, Puiggros et al. 2014).

Another technique that has not yet been applied in routine diagnosis is using laser scanning cytometry to score the conventional FISH slides. This microscope-based laser scanning cytometry has the advantage of increasing the larger number of cells evaluated due to the automated scoring. However, due to the vast number of cells evaluated, a high throughput technique, perhaps in suspension (rather than on a slide) is better suited, especially for the evaluation of the presence of low frequency sub-clones amongst a high number of cells. Conventional flow cytometry can provide very rapid data with a large number of cells, with an average speed of approximately 5000 cells/seconds (Basiji et al. 2007). The major disadvantage of conventional flow cytometry is the absence of any information about sub-

cellular fluorescence localization and cell morphology; it only provides fluorescence intensity-based data. Hence, a fluorescence microscope can help to overcome these instrument compromises with the ability of characterised sub-cellular visualisation and quantification. Many studies have attempted to combine fluorescence microscopy and flow cytometry, but the development of imaging cells in flow only began in 1979 (Kay et al. 1979). The first imaging flow cytometry instrument, ImageStream100 was commercially launched in 2005, to be followed in early 2010 by the next generation of imaging flow cytometers, ImageStreamX Mark II manufactured by Amnis Corp. (Seattle, USA). This new machine provides high-throughput flow cytometry combined with imaging to generate high-resolution digital images of individual cells. As a result, a new technique, FISH in suspension (FISH-IS) was developed based on this new instrument. FISH-IS is able to analyse thousands of cells per second and the generated images are captured by a computer. The associated IDEAS software enables automated analysis of the captured data, quantifying characteristics such as cell shape, cell size, fluorescence intensity of the hybridised signal, and colocalization of signals. At the commencement of this study (in 2013), there was only one publication (Minderman et al., 2012) which reported the application of the FISH-IS technique to determine chromosomal abnormalities in both healthy and disease cells, demonstrating the utility of this method in detecting the presence of trisomy 8 in acute myeloid leukaemia (AML) samples. However, their analysis was limited to this specific abnormality in this single disease.

The objective of this research was to detect clinically relevant chromosomal abnormalities in CLL and determine whether the FISH-IS technology can be utilised in CLL disease, with the potential to replace conventional FISH in the detection of low frequency sub-clones.

The specific aims of this chapter were:

1. To optimise and to apply the FISH-IS protocol using various centromere probes in CLL samples (section 4.3.1 – 4.3.4);
2. To determine the lower limit of detection of FISH-IS to accurately identify aneuploidy sub-clones in CLL (section 4.3.5 – 4.3.7);
3. To apply Spot Count Wizard software for automated annotation of the hybridisation signals inside CLL cells (section 4.3.8); and
4. To compare the detection of trisomy 12 by three available cytogenetic methods (conventional FISH, LSC and FISH-IS) to establish relative clinical utility (section 4.3.9).

## **4.2 Materials and methods**

### **4.2.1 FISH-IS with centromere probes protocol**

See Methods section 2.8.

### **4.2.2 Laser scanning cytometry**

See Methods section 2.7. Slide FISH were hybridised with centromere 12 probe and scored by two different scorers. Then, slides were scanned by LSC twice for each slide.

### **4.2.3 Statistical methods**

To directly compare between the observed and the expected data in individual case, uncorrected Fisher's Least Significant Difference (LSD) test was applied. Any significant difference is considered if  $p < 0.05$ .

## 4.3 Results

### 4.3.1 Optimisation of the FISH-IS protocol with CLL cells

The FISH-IS protocol used in this study was adapted from the method of Minderman et al. (2012). The details of the FISH-IS protocol with commercial centromere probes were described in section 2.8. Figure 4.1 gives some examples of the type of issues which were encountered (and resolved) when developing this method for CLL cells. The final critical modifications to the original method were as follows:

- Cells must be treated gently, not vortexed and the centrifuge speed must not exceed 2000 x *g*, otherwise there is a higher incidence of cell membrane damage leading to loss of interpretable data (Figure 4.1A).
- In the wash steps, the cells must be resuspended very carefully to remove as much of the adherent probes as possible to reduce background staining. The procedure is highly temperature dependent and wash steps must be performed quickly so as to minimise the loss of temperature. A loss of temperature increases background staining through non-stringent hybridisation of the probe. This leads to multiple “false” spots in the spot-count analysis (Figure 4.1B) and increased background staining (Figure 4.1C).

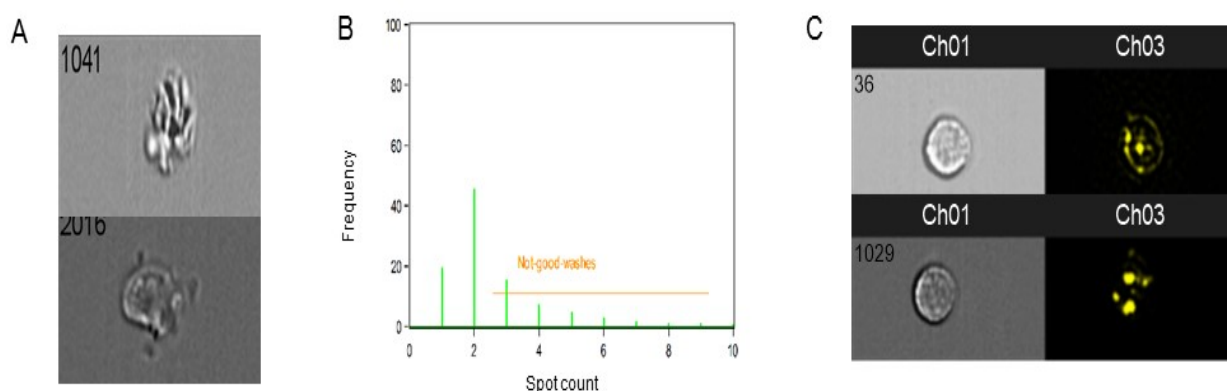


**Figure 4.1. Examples of technique failures whilst developing the FISH-IS protocol.**

(A) Brightfield shows cell morphology, which have been damaged due to either vortexing or high-speed centrifugation. (B) Spot count analysis incorrectly interpreted as increased spots due to shorter washing time. (C) Images of cells with a high background signal.

In order to carry out a consistent analysis, a pipeline for analysis with the IDEAS V6 software was also developed (Figure 4.2). Initially, cells are visualised with the brightfield channel, and data are represented as a histogram, with the contrast gradient root mean square (RMS) on the x-axis and frequency of cells on the y-axis (Figure 4.2A). Cells which are in focus will have a higher RMS, and previous research has shown that selection of cells with an RMS greater than 55 is optimal (Minderman et al., 2012). The ‘in-focus’ cells are then analysed with a scatter plot, with the brightfield area on the x-axis and aspect ratio on the y-axis (Figure 4.2B). Single cells will have a high aspect ratio (from 0.5 to 1) and a low area (50-200). Upon visual inspection, the cell populations contained within these parameters were found to be single, round, and have high contrast morphology, all of which indicate good quality cells suitable for further analysis. The fluorescence intensity of the FISH signal from the single in-focus cells is then recorded and can be displayed relative to cell frequency (Figure 4.2C) or the brightest pixel in the signal (raw max pixel, Figure 4.2D). In addition, the Spot Count Wizard program, contained within the IDEAS V6 software, can then be trained for spot detection by manual identification of cells with a specific number of spots

(Figure 4.2E). An example of the generated data is shown in Figure 4.2F. This optimised method and analysis pathway was subsequently used for all FISH-IS experiments.

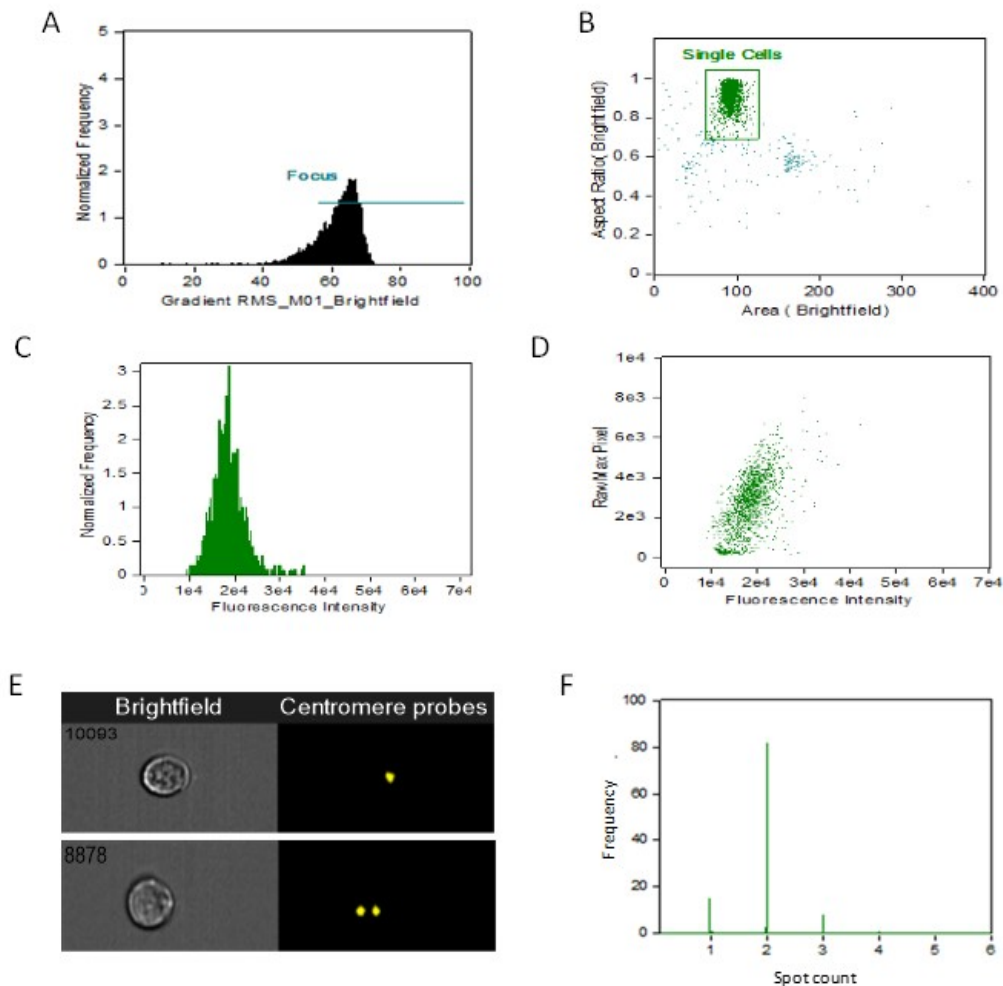


**Figure 4.2. Analysis of FISH-IS data pipeline.**

(A) Histogram enables identification of the cells in best focus (higher contrast gradient RMS), which are then selected for further analysis. RMS: root mean square. (B) Dot plot of best in focus cells, with single cells selected as indicated by the boxed region (brightfield area of 100-200 and aspect ratio of 0.5 to 1). (C) Overall fluorescence can be represented relative to the normalised frequency of the cells, or (D) the single highest pixel intensity (raw max pixel). (E) The Spot Count Wizard is trained for spot detection by manual identification of appropriate cells (for example, the top image is recorded as representative for cells with one spot-count; the bottom image is recorded as being representative for cells with two spot-count). (F) The Wizard then analyses all single cells based on the representative cells in order to gate cells according to spot count.

### 4.3.2 FISH-IS protocol produces auto-fluorescence of CLL cells

CLL cells have a very densely packaged nucleus and aggregated chromatin (Hallek et al. 2008), which can result in an increase in autofluorescence of cells after fixation (Stewart et al. 2007). Therefore, the auto-fluorescence of CLL samples in FISH-IS without probe hybridisation was measured. The auto-fluorescence of CLL cells within the emission/excitation range of spectrum green was found to be greater than that of spectrum orange with or without hybridisation buffer  $1.6 \times 10^3$  versus  $1 \times 10^3$  and  $6.3 \times 10^3$  versus  $5.1 \times 10^3$ , respectively (Figure 4.3). It is interesting to note that the addition of hybridisation buffer resulted in an increase to nearly double the number of intact cells for analysis; 8953 cells versus 4351 cells (Figure 4.3).



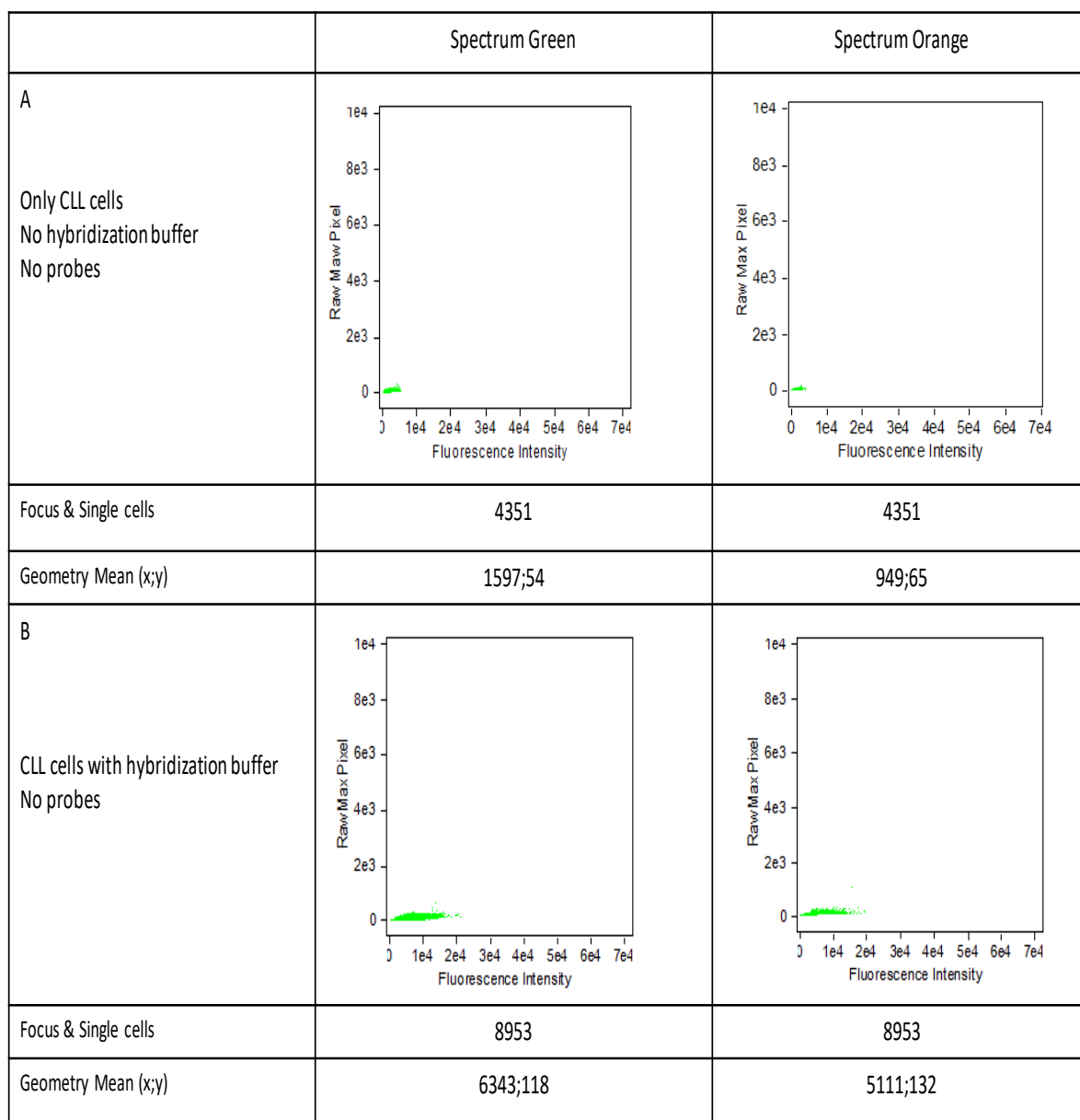


**Figure 4.3. Determination of auto-fluorescence of CLL cells.**

(A) No hybridisation buffer and (B) with hybridisation buffer. X-axis, mean fluorescence intensity of cells; y-axis, raw max pixel. Focus & single cells represent the number of intact cells counted. Data are representative of 3 different CLL samples analysed in triplicate.

### **4.3.3 FISH-IS is able to detect monosomy in CLL cells**

As FISH-IS analysis had only previously been applied to healthy and AML cells (Minderman et al. 2012), it needed to be established that CLL cells would be amenable to analysis with this method. The simplest analysis for determining chromosome ploidy is the identification of a monosomy. Therefore, a model of FISH-IS analysis of monosomy was tested in CLL cells, consisting of hybridisation with a commercial probe to the centromere of chromosome Y on male CLL samples. This probe detects the highly repetitive satellite DNA present at the Y chromosome centromere, resulting in an extremely strong signal (recorded as maximum pixel intensity). Results of this analysis found that all cells discriminated into one population based on fluorescence, and 100% of best-focus intact single cells had one spot count when analysed with Spot Count Wizard (Figure 4.4). This confirmed that CLL cells can be analysed with the high-throughput FISH-IS method and that this method accurately detects monosomy in CLL samples.

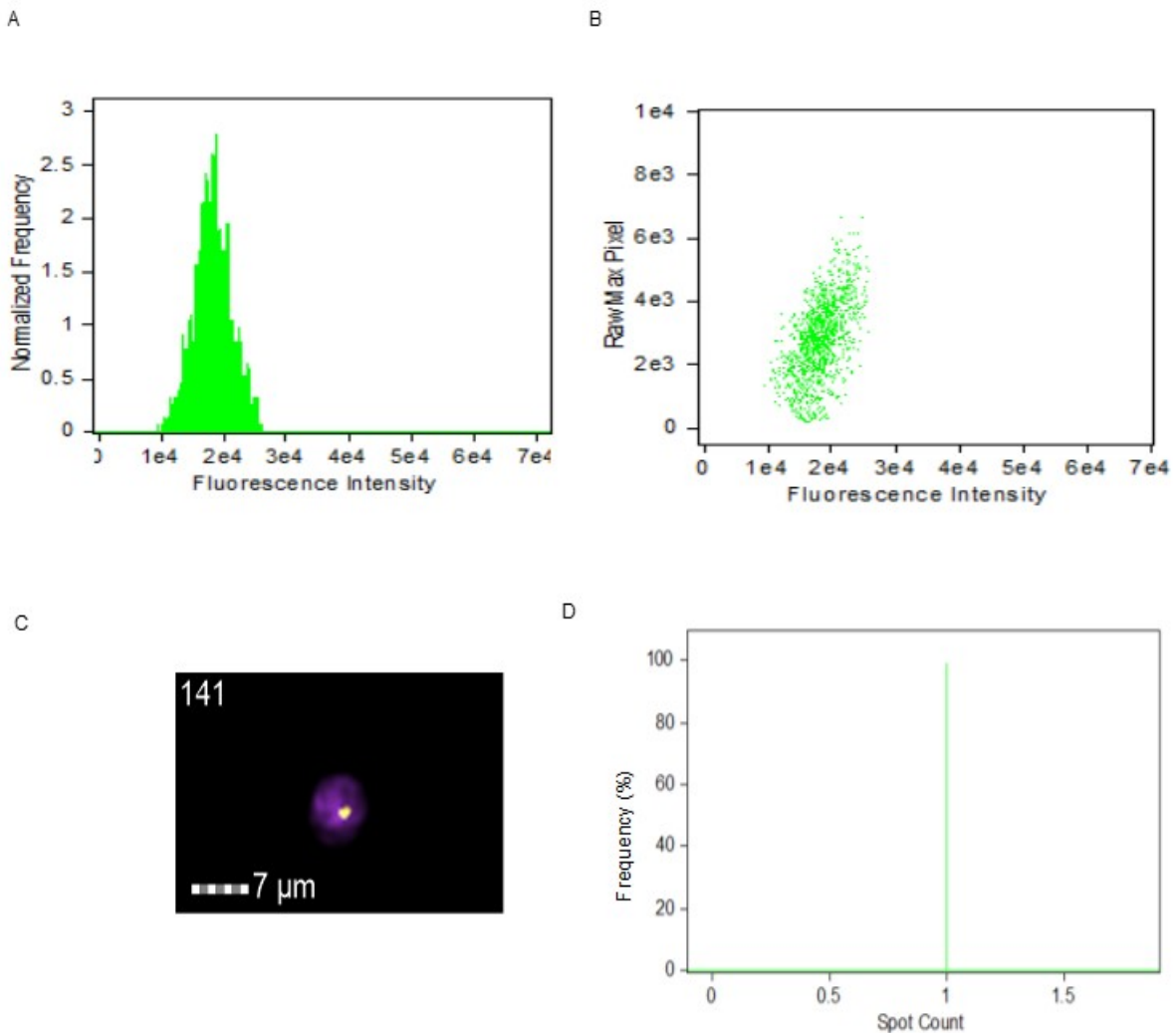


**Figure 4.4. FISH-IS is able to accurately detect monosomy Y in CLL cells by fluorescence intensity and spot count.**

(A) Fluorescence intensity and normalised frequency indicate a single population of cells. (B) Single CLL cells discriminate into one population based on raw max pixel and fluorescence intensity of the Spectrum Orange Y chromosome centromere probe. Each spot represents a cell. (C) An example of a male CLL cell from this FISH-IS analysis. Nuclear staining (DAPI) is shown in purple, centromere Y is shown in yellow (Spectrum Orange). (D) Spot Count Wizard indicates 100% of cells have one spot. Data are representative of 3 different CLL samples analysed in triplicate.

#### **4.3.4 FISH-IS can detect disomy by fluorescence intensity but not by spot count**

Chromosome 9 aneuploidy aberrations are not commonly found in CLL (Döhner et al. 2000). Therefore, FISH-IS was carried out with the chromosome 9 centromere probe on CLL cells in order to confirm that FISH-IS is able to detect disomy in CLL cells. When analysed based on fluorescence intensity, the cells clustered in one population (Figure 4.5A, B) and all of the individual cells contained 2 spots (Figure 4.5C). However, the spot count algorithm found that 22.3% of cells contained only 1 spot, indicating monosomy of chromosome 9 in these cells (Figure 4.5D). As this was unexpected, these cells were interrogated further.

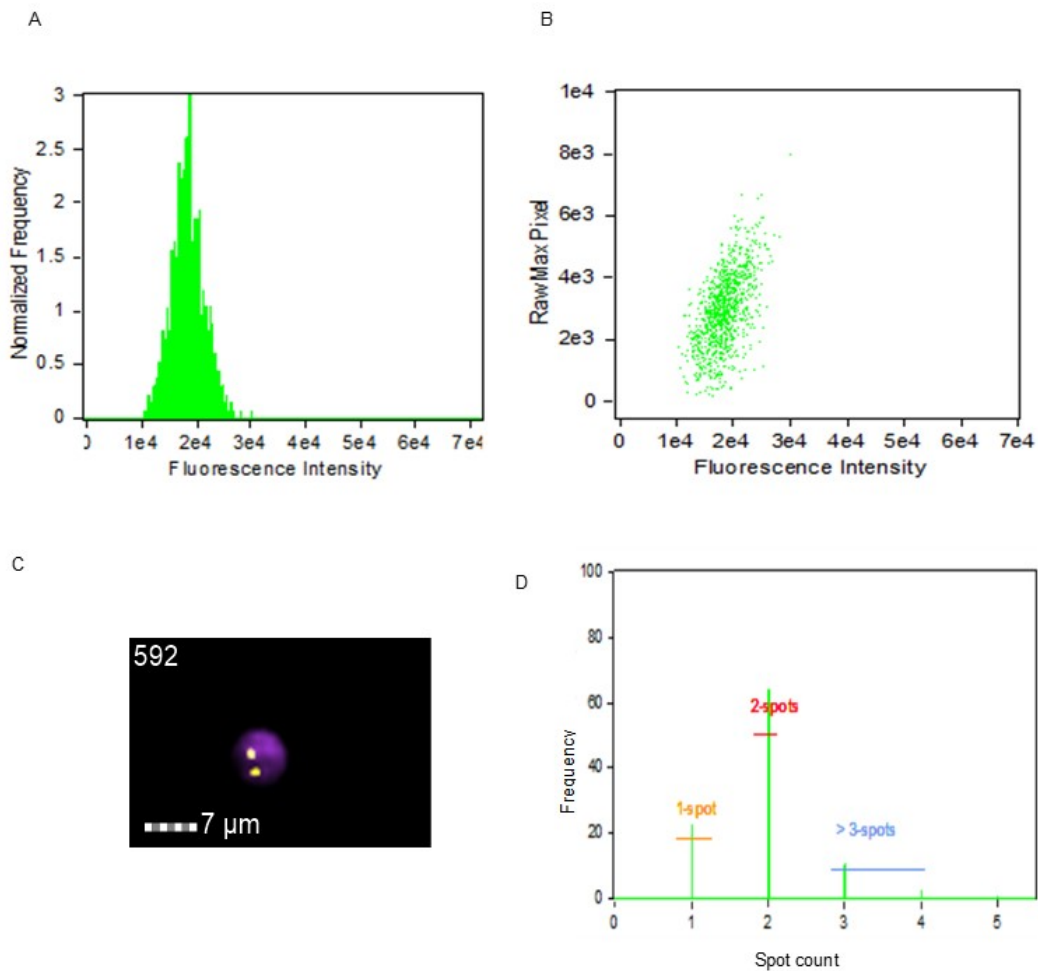


**Figure 4.5. FISH-IS is able to accurately detect disomy 9 in CLL cells by fluorescence intensity but not by spot count.**

(A) Fluorescence intensity and normalised frequency indicates a single population of cells. (B) Single CLL cells discriminate into one population based on raw max pixel and fluorescence intensity of the Spectrum Orange chromosome 9 centromere probe. Each spot represents a cell. (C) An example of a CLL cell from FISH-IS analysis. Nuclear staining (DAPI) is shown in purple, centromere 9 are shown in yellow (Spectrum Orange). (D) Spot Count Wizard indicates only 64% of cells have the expected two spots. Data are representative of 3 separate experiments with 3 different CLL samples in duplicate.

Comparison of the total fluorescence intensity within individual cells revealed that cells that were classified as having one spot had the same overall fluorescence as cells that were classified as having 2 spots (Figure 4.6A-C). This suggested that these cells had the same amount of probe hybridisation, indicating they were likely to be disomic for chromosome 9. Furthermore, visual interrogation of cells which were annotated as having 1 spot found that 98.4% of these cells did, in fact, have 2 hybridisation signals. However, these signals were found to be either partially or entirely overlapping, or adjacent to each other, causing the Spot Count Wizard software to inaccurately identify the two signals as one spot (Figure 4.6D).

Additionally, reanalysis of the 3-spot population also identified using the Spot Count Wizard found that 93% of these cells had either 2 spots within the cell which were incorrectly annotated as 3 spots or spots located outside of the cell were incorrectly included in the spot count (Figure 4.6D). After comprehensive manual curation of the images of all cells was carried out, it was determined that 96.4% of the total cells analysed were indeed diploid for the centromere 9 signal (Figure 4.6E).

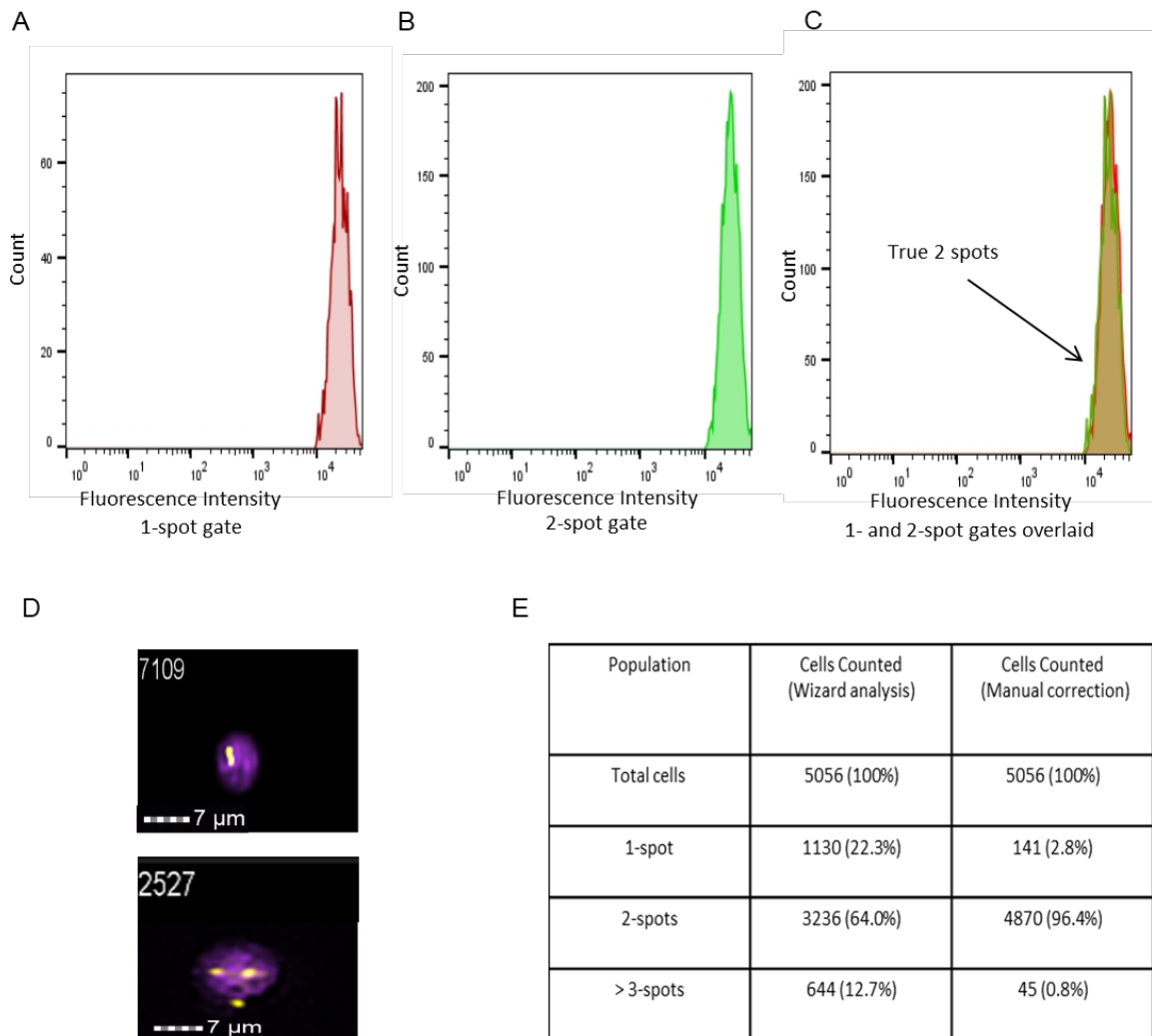


**Figure 4.6. FISH-IS is able to enumerate centromere 9 spots in CLL cells only by manual correction of the automatic spot count.**

(A) Histogram of fluorescence intensity of hybridised probe for cells automatically identified as having 1-spot. (B) Histogram of fluorescence intensity of hybridised probe for cells automatically identified as having 2-spots. (C) Overlapping fluorescence intensity of (A) and (B), indicating that the cells automatically identified as having 1-spot actually have 2-spots based on fluorescence intensity. (D) Examples of cells that were automatically recorded as having one (top) or three (bottom) hybridisation signals by the Spot Count Wizard software. Nuclear staining (DAPI) is shown in purple, centromere 9 is shown in yellow. (E) Manual correction of automatic gating based on spot count shows 96.4% of cells have the expected two spots. Data are representative of 3 separate experiments with 3 different CLL samples in duplicate.

#### 4.3.5 FISH-IS signal intensity in CLL cells is not sample dependent

The sensitivity and robustness of this method could be determined by a number of samples analysed with a wide range of known ratios of diploid:aneuploid cells. To this end, an artificial mixing assay was used, combining CLL cells from different patient samples with known genetic content, in known ratios. For example, mixing of male and female cells in known ratios, followed by hybridisation with a centromere X probe enables assessment of the ability of FISH-IS to discriminate between monosomy (the male cells) and disomy (the female cells). However, a complicating factor is the possibility that CLL samples from different individuals may react differently to hybridisation; one sample may respond better to the hybridisation process than another, resulting in a brighter signal from these cells, irrespective of their genetic content. In order to confirm that any results from the artificial mixing assays were a direct result of the genetic content of the cells and not due to other features of the individual samples, mixing experiments were undertaken combining two male CLL samples in known ratios (80:20 and 50:50), followed by hybridisation with a probe to the centromere of the Y chromosome. As Figure 4.7 clearly shows, these combined CLL cells cluster together in one population, based on both raw maximum pixel intensity (left) and normalised frequency (right) compared to the total cellular fluorescence intensity. Therefore, the mixing model appears to be a valid assay to be used to determine the ability of the FISH-IS assay to accurately determine aneuploidies in CLL cells using centromeric probes.



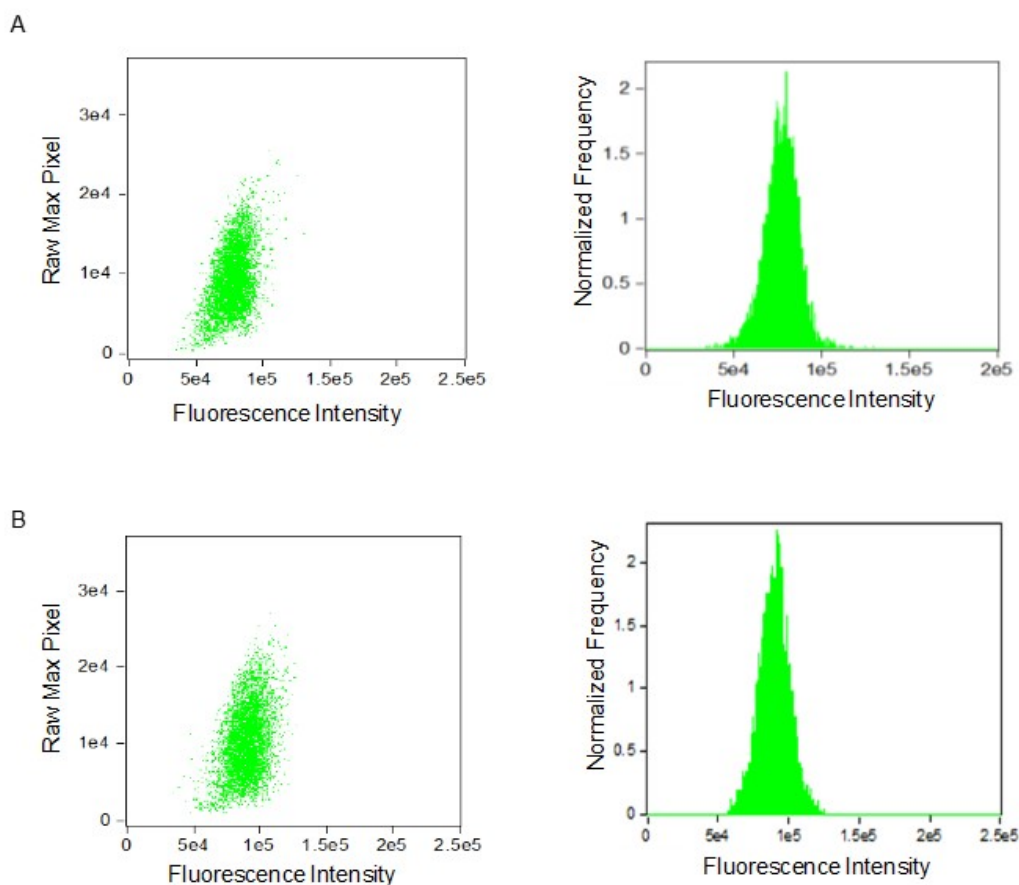


**Figure 4.7. Hybridisation of fluorescence probes in CLL cells is not sample-dependent.**

*(A) Two male CLL samples were combined in 50:50 ratios and hybridised with the centromere X probe. (B) As for (A), two male CLL samples were combined in an 80:20 ratios. Data are representative of 3 separate experiments.*

#### **4.3.6 FISH-IS is able to differentiate between monosomy and disomy in CLL cells**

In order to determine if FISH-IS can differentiate aneuploidies within a single sample, male and female CLL cells were combined in known ratios to generate a mixing model containing both monosomy and disomy of the X chromosome. Analysis of these mixed samples with FISH-IS following hybridisation with the X chromosome centromere probe was carried out. The mixing experiments were carried out from 0.1 to 100% monosomy. An example of FISH-IS carried out on a 10% male: 90% female mixed CLL sample is shown in Figure 4.8. It is clear that cells discriminate into 2 populations based on their chromosomal content when analysed by fluorescence intensity (Figure 4.8 A-B). Figure 4.8C shows examples of cells which were contained within the monosomic population (top panel) and the disomic population (bottom panel), each containing the expected number of hybridisation signals. This analysis demonstrates that FISH-IS is indeed able to discriminate between monosomy and disomy by fluorescence intensity. However, as with the chromosome 9 analysis, the automatic spot-count application within the IDEAS software did not give the expected 10: 90 ratios of 1- and 2-spot cells (Figure 4.8D).

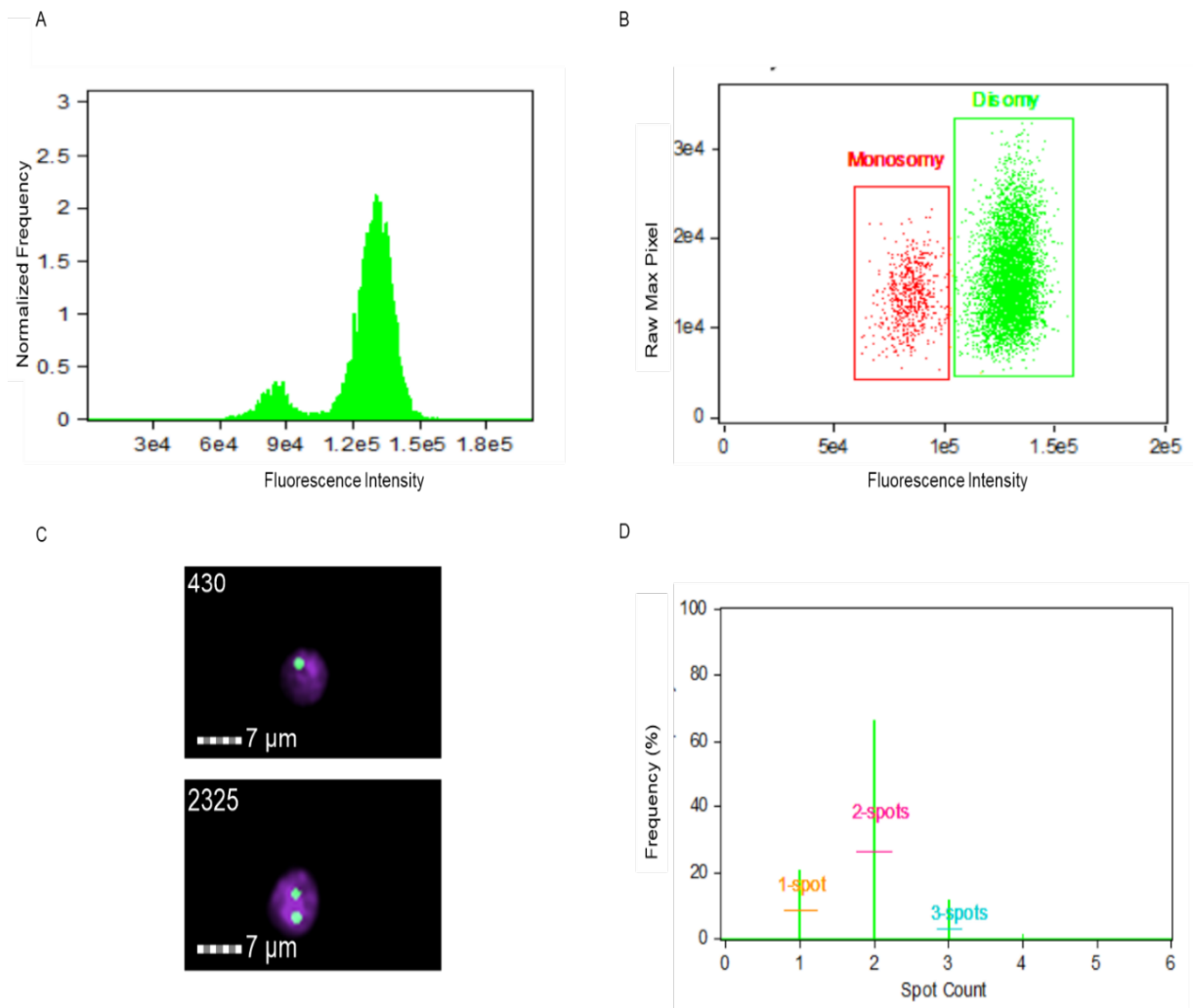


**Figure 4.8. FISH-IS is able to accurately differentiate between monosomy and disomy with centromere X probe in CLL samples by fluorescence intensity.**

(A) Fluorescence intensity and normalised frequency indicate two populations of cells. (B) Single CLL cells discriminate into two populations based on raw maximum pixel intensity of the spectrum green centromere X probe and the total cellular spectrum green intensity. Each spot represents a cell. (C) Examples of CLL cells with monosomy X (top) and disomy X (bottom). Green, centromere X signal from hybridised probes; purple, DAPI nuclear staining. (D) FISH-IS spot count with centromere X probes. Representative results shown are from mixed 10% male CLL and 90% female CLL PBMCs. Data are representative of 3 separate experiments.

Statistic test (uncorrected Fisher's Least Significant Difference (LSD) was applied, it was reported that none of the first six mixing samples were statistically significant ( $p > 0.05$ ), while the last two mixing ratios were statistically significance with  $p < 0.05$  (Table 4.1). As a result, based on the fluorescence intensity of probe, the data demonstrated that FISH-IS is able to accurately identify the sub-clone at low threshold at 1% and higher percentages; however, at a level of 0.1% and 0.01%, the level of observed was greater than expected, by approximately 10 times and 40 times, respectively (Table 4.1).

**Table 4.1. Detection of FISH-IS with predictable model of aneuploidy in CLL samples with centromere X probe.**

CLL mixes (%) Male: Female	Monosomy X expected (%)	Monosomy X observed (%) (mean $\pm$ SD)	p value
100: 0	100	99.61 $\pm$ 0.50	0.08
50: 50	50	49.34 $\pm$ 0.40	0.19
30: 70	30	30.11 $\pm$ 1.4	0.66
10: 90	10	9.96 $\pm$ 0.61	9.87
5: 95	5	4.90 $\pm$ 0.42	0.66
1: 99	1	1.10 $\pm$ 0.18	0.66
0.1: 99.9	0.1	0.91 $\pm$ 0.30	<b>0.03</b>
0.01: 99.99	0.01	0.46 $\pm$ 0.12	<b>0.01</b>

*Data are the mean of 3 separate experiments  $\pm$  SD. The differences between percentages of monosomy X observed and expected were determined by uncorrected Fisher's LSD statistic. Significance ( $p$  value  $< 0.05$ ) is indicated in bold.*

In addition, it can be seen in Figure 4.8D, 21.8% of cells were automatically classified as having 1-spot. Using flow cytometry analysis software (Flow Jo 10), the analysis of the overall fluorescence intensity of cells within the 1-spot gate revealed that there were, in fact, two populations of cells contained within this group, each with clearly separate fluorescence intensities (Figure 4.9A). The cells with the higher overall fluorescence intensity from the 1-spot gate actually had equivalent overall fluorescence intensity to the cells in the 2-spot gate (Figure 4.9A-C). This suggests that these cells were incorrectly assigned as having 1-spot, due to the inability of the Spot Count Wizard software to accurately differentiate spots in some situations. Manual curation of the image of each cell was again carried out and revealed that 54.2% of cells (R1) contained within the 1-spot gate, in fact, have 2 spots, and therefore had been incorrectly annotated by the software. The images of these miscounted cells are displayed in Figure 4.9D.

Reanalysis of the 7.3% of cells classified as having >3-spots found, as had been found previously, that this group was largely made up of cells for which extraneous hybridisation signals had been counted (Figure 4.9E). After carrying out the manual corrections as described above, the percentage of cells contained within the 1-spot population based on fluorescence intensity was 10.0%, as expected (Figure 4.9F).

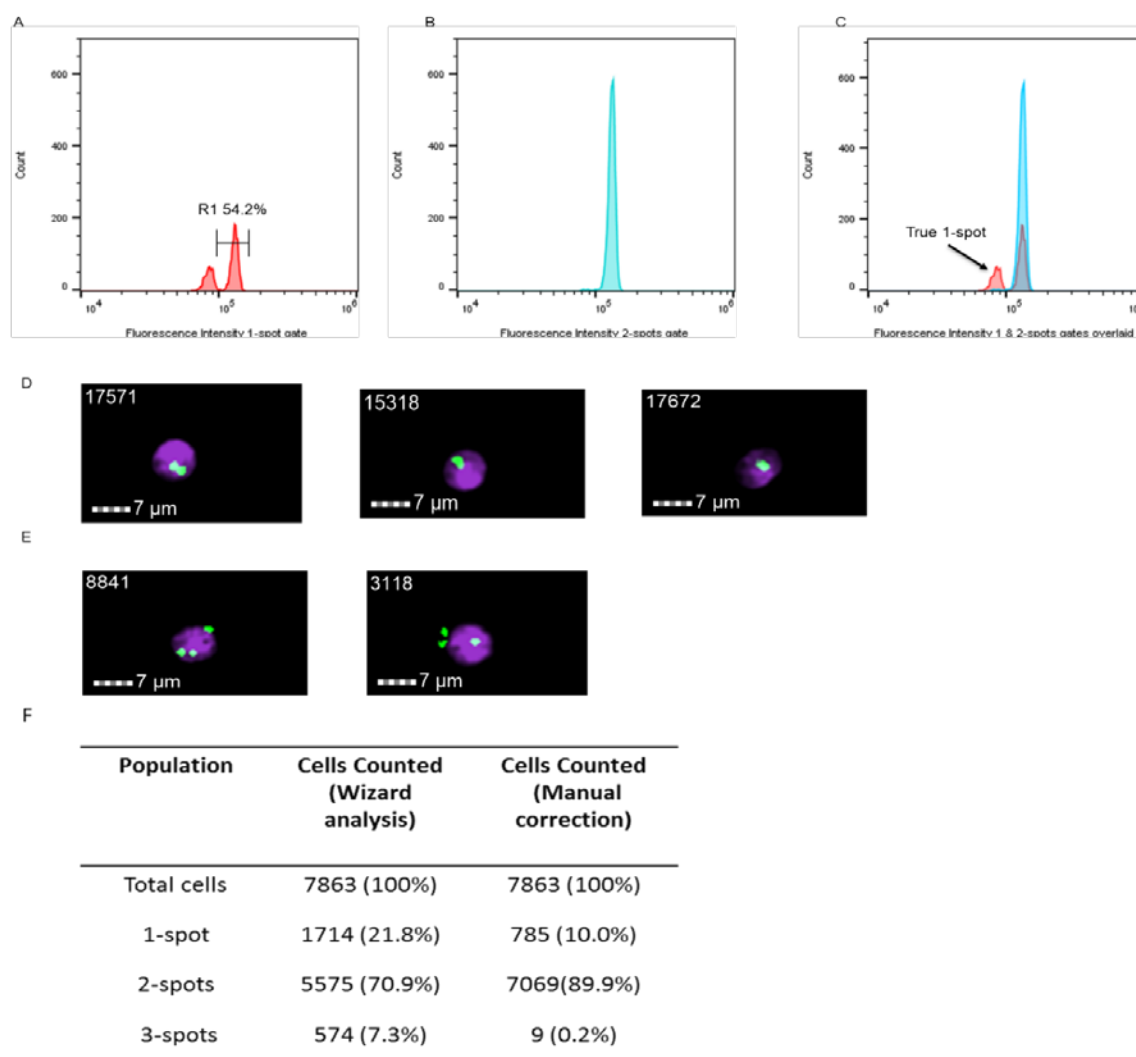


**Figure 4.9. FISH-IS is able to enumerate centromere X spots in CLL cells only by manual curation of the Spot Count Wizard.**

(A) Histogram of fluorescence intensity of hybridised probe gated for cells automatically identified as having 1-spot by Spot Count Wizard. (B) Histogram of fluorescence intensity of hybridised probe gated for cells automatically identified as having 2-spots by Spot Count Wizard. (C) Overlapping fluorescence intensity of (A) and (B), indicating that the majority of cells automatically identified as having 1-spot actually have 2-spots based on fluorescence intensity. (D) Examples of cell images in R1 gate, two juxtaposed spots (left panel), two spots partially (middle panel) or completely (right panel) overlapping. (E) Examples of cells that were inaccurately recorded as having three hybridisation signals by Spot Count Wizard software as the spot(s) located outside the nuclei. (F) Manual correction of gating based on Spot Count Wizard shows 10.0% of cells have one spot and 89.9% of cells have two spots. Nuclear staining (DAPI) is shown in purple, centromere X probes are shown in green (Spectrum Green). Data are representative of 3 separate experiments.

#### **4.3.7 FISH-IS is able to differentiate between disomy and trisomy in CLL cells**

While there is not a common chromosomal monosomy in CLL cells, trisomy 12 is well established as a common aneuploidy occurring in CLL patients (Döhner et al., 2000).

Therefore, in order to assess the ability of FISH-IS to discriminate between disomy and trisomy, this common aneuploidy was analysed with a chromosome 12 centromere probe. Hybridisation was carried out on a sample from a CLL patient (CLL1415) who had previously been diagnosed by conventional FISH with 5% disomy and 95% trisomy chromosome 12 (200 cells analysed). When analysing this sample by FISH-IS based on fluorescence intensity, 95.1% of cells were contained within the trisomic population with 3 spots, and 4.9% of cells were contained within the disomic population with two spots (Figure 4.10A-C). As in previous experiments, the automated spot count was not able to consistently characterise cells based on hybridisation signals (Figure 4.10D).

Assessment of overall fluorescence intensity combined with manual curation was again required in order to accurately characterise cells by spot count (Figure 4.11).

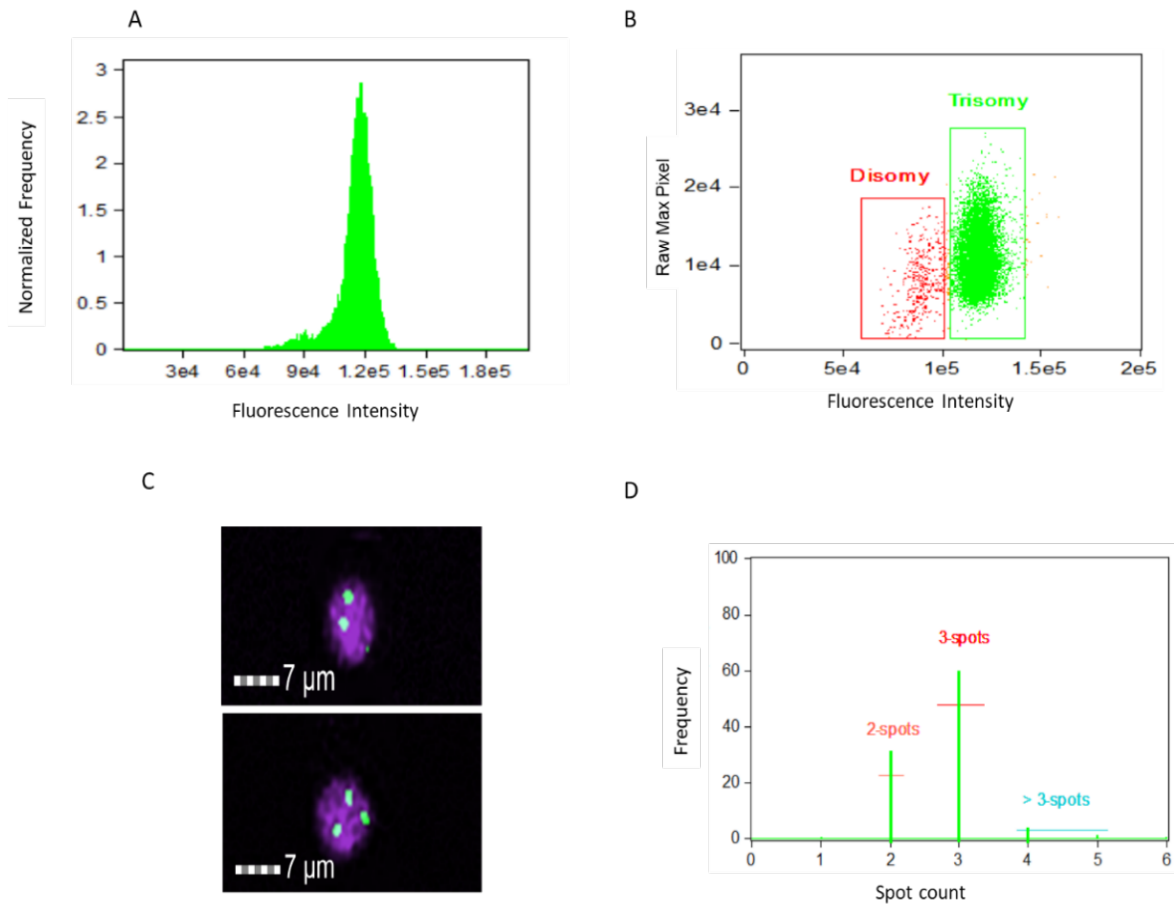


**Figure 4.10. FISH-IS is able to accurately differentiate between disomy and trisomy with centromere 12 probe in CLL samples by fluorescence intensity.**

(A) Fluorescence intensity and normalised frequency indicate two populations of cells. (B) Single CLL cells discriminate into two populations based on raw maximum pixel intensity of the spectrum green centromere 12 probe and the total cellular spectrum green intensity. Each spot represents a cell. (C) Examples of CLL cells with disomy 12 (top) and trisomy 12 (bottom). Green, chromosome 12 centromere signal from hybridised probes; purple, DAPI nuclear staining. (D) FISH-IS spot count with centromere 12 probes. Data are representative of 3 separate experiments.



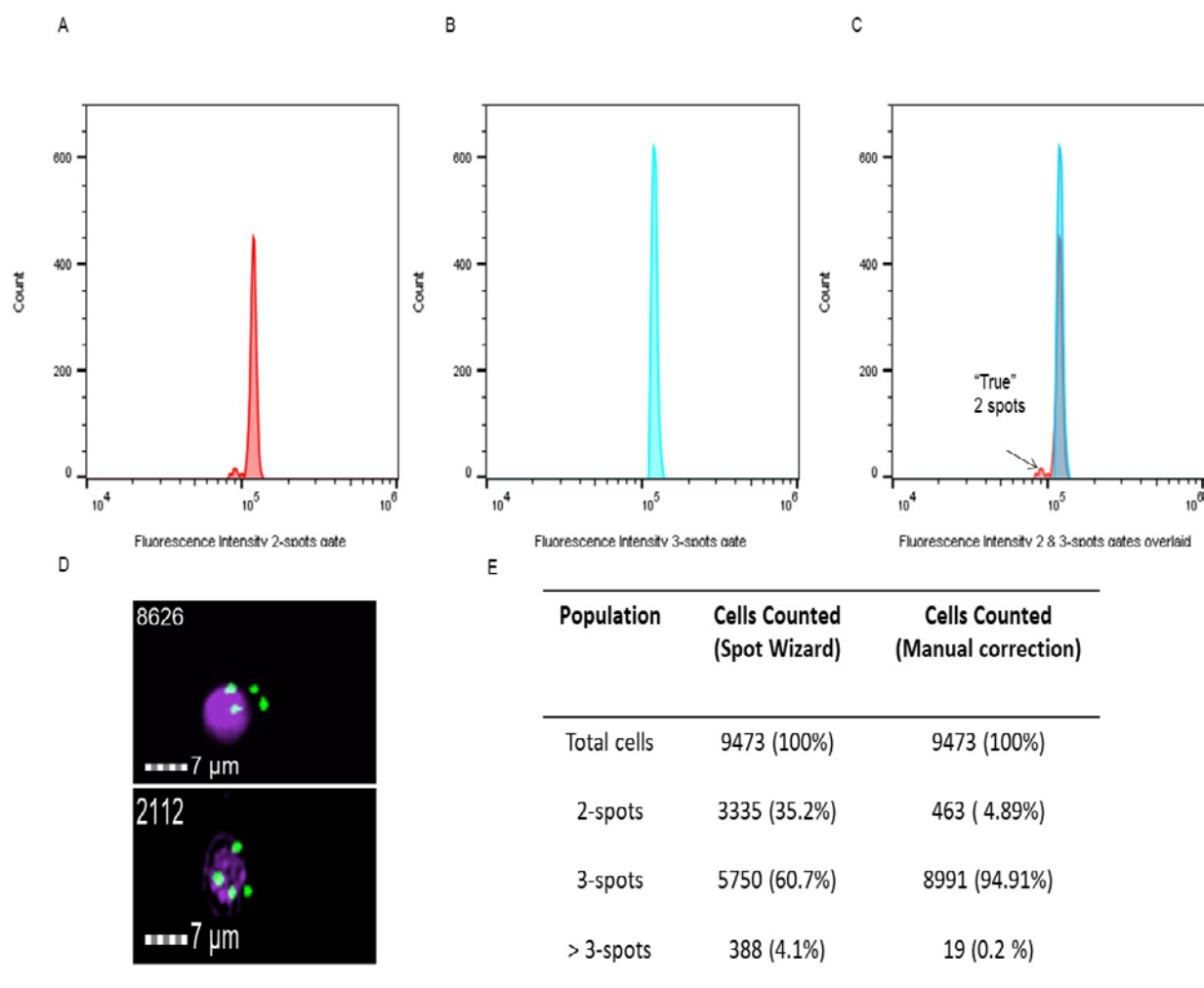


**Figure 4.11. FISH-IS is able to enumerate centromere 12 spots in a sample of CLL cells with 95% trisomy 12 by manual correction of the Spot Count Wizard.**

(A) Histogram of fluorescence intensity of hybridised probe for cells automatically identified as having 2-spots. (B) Histogram of fluorescence intensity of hybridised probe for cells automatically identified as having 3-spots. (C) Overlapping fluorescence intensity of (A) and (B), indicating that the majority of cells automatically identified as having 2-spots actually have 3-spots based on fluorescence intensity. (D) Examples of cells that were inaccurately identified as having > 3-spots by Spot Count Wizard software as the spot(s) located outside the nuclei. Nuclear staining (DAPI) is shown in purple, centromere 12 probes are shown in green. (E) Manual correction of gating based on Spot Count Wizard shows 4.89% of cells have two spots and 94.91% of cells have three spots. Data are representative of 3 different experiments.

In order to determine the level of detection of trisomy 12 in individual CLL samples, there were only four CLL patient samples with various percentages of trisomy 12 available at that time: sample 1 (95% trisomy 12), sample 2 (80% trisomy 12), sample 3 (75% trisomy 12), sample 4 (5% trisomy 12). Hence, samples 1-3 served as high frequency trisomy 12, sample 4 as low frequency trisomy 12, a mid-frequency 50% trisomy 12 sample (sample 5) was generated by combining cells from sample 1 with cells from a CLL patient with 100% disomy chromosome 12 (sample 6).

The data for different individual CLL samples with various disomy: trisomy ratios analysed are presented in Table 4.2. Using an uncorrected Fisher's LSD test, there were no statistically significant differences between the results of trisomy 12 identified by FISH-IS and the expected result in various CLL samples, demonstrating the ability to accurately detect trisomy 12 in individual CLL patient samples. However, the number of samples is small, and further trisomy 12 patient samples with various percentages would benefit this analysis.

**Table 4.2. Detection of FISH-IS with centromere 12 probe in CLL samples.**

CLL mixes (%) disomy 12: trisomy 12	Trisomy 12 expected (%)	Trisomy 12 observed (%) (mean $\pm$ SD)	p value
5: 95	95	94.67 $\pm$ 0.48	0.74
20: 80	80	78.10 $\pm$ 1.59	0.65
25: 75	75	76.47 $\pm$ 1.60	0.15
50: 50	50	50.80 $\pm$ 2.32	0.43
95: 5	5	3.93 $\pm$ 1.69	0.31
100: 0	0	1.23 $\pm$ 0.83	0.22

*Data are the mean of 3 separate experiments  $\pm$  SD. The differences between percentages of trisomy 12 observed and expected were determined by uncorrected Fisher's LSD statistic.*

#### **4.3.8 Spot Count cannot accurately identify the number of hybridisation signals**

The Spot Count Wizard was compared with fluorescence intensity as a means of discriminating between monosomic, disomic and trisomic CLL sub-clones. However, to compare and contrast the inaccuracies which had been found with the Spot Count Wizard, the data obtained from all previous FISH-IS analyses with four different chromosome centromere probes have been combined and are presented in Figure 4.12. In all cases, except for the detection of 100% monosomy with the centromere Y probe on a male sample, the calculated Spot Count Wizard did not accurately estimate the expected signal.

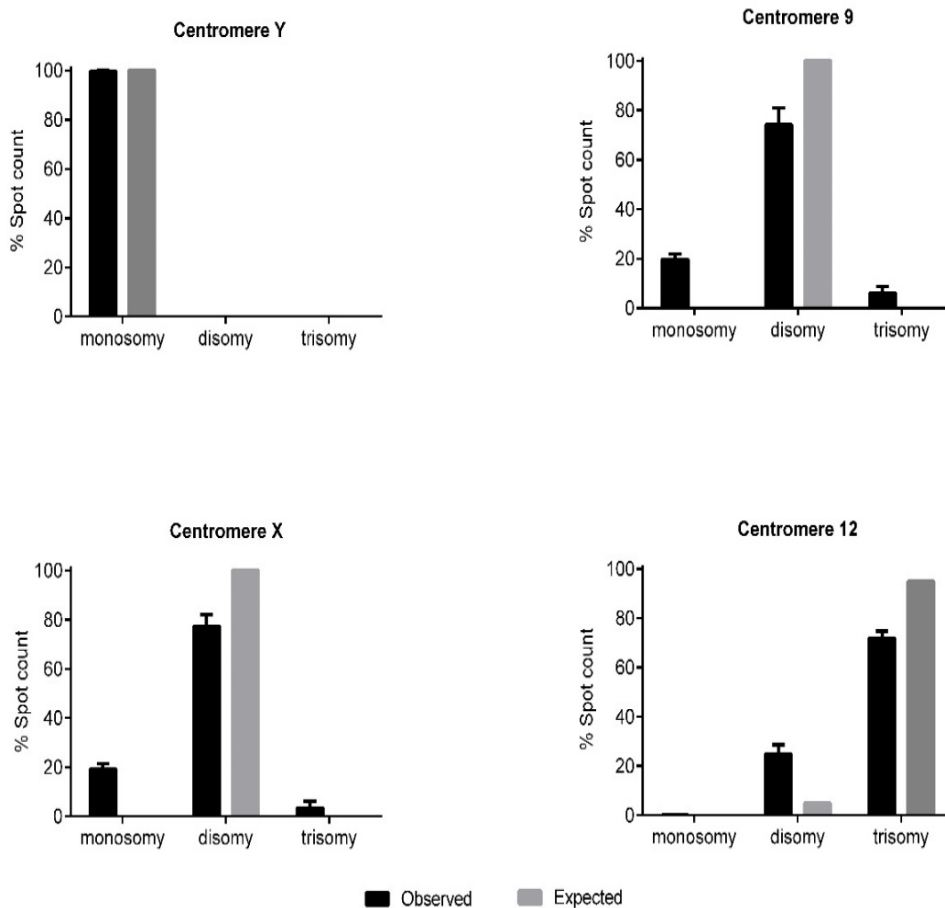


**Figure 4.12. Correlation of the observed proportions of spot-count (Spot Count Wizard) analysis and the expected percentage spots of centromere Y, 9, X and 12 probes using FISH-IS.**

*Data are combined from previous analysis. Data are the mean of 3 separate experiments  $\pm$  SD.*

#### **4.3.9 Comparison of detection of trisomy 12 in CLL samples by 3 different methods**

Given that every technique has its own limitations, three methods were assessed utilising FISH technologies in terms of accuracy and applicability to a diagnostic service in order to accurately detect trisomy 12 in CLL samples. The three available cytogenetic methods: conventional FISH, LSC and FISH-IS were evaluated. Six CLL patient samples with different percentages of trisomy 12, served as high, mid- and low frequency trisomy 12 (as above) were analysed in duplicate (Table 4.3). Although LSC and FISH-IS analysed 10-times to 68-times more cells per sample, all methods were found to be similar in the percentage of trisomy cells detected but were dependent on sub-clonal frequency (Table 4.3). With high and mid- frequency sub-clones, the percentages of trisomy 12 were comparable using the three methods, while greater disparity in the estimated frequency of low frequency trisomy 12 sub-clones was evident, in which, FISH-IS showed lower estimates while LSC showed higher estimates compared with conventional FISH (Table 4.3).

**Table 4.3. Comparison of results of three methods analysing centromere 12 probe hybridisation on CLL samples.**

Sample	Conventional FISH (average of two scores)			Laser scanning cytometry (in duplicated)			FISH-IS (in duplicated)		
	Cells evaluated	Trisomy (%)	Disomy (%)	Cells evaluated	Trisomy (%)	Disomy (%)	Cells evaluated	Trisomy (%)	Disomy (%)
1	200	95	5	1824	94.21	5.79	11461	95.13	4.87
				1986	93.62	6.38	10549	94.88	5.12
2	200	80	20	2041	80.03	19.97	5253	78.12	21.88
				2400	78.94	21.06	3445	79.87	20.13
3	200	75	25	1397	75.76	24.24	2569	75.67	24.33
				1038	75.67	24.33	2068	75.04	24.96
4	200	50	50	2774	52.24	47.76	7596	49.78	50.22
				3673	48.93	51.07	8057	48.64	51.36
5	200	5	95	1623	6.68	93.32	13604	2.47	97.53
				2389	6.88	93.12	9879	3.28	96.72
6	200	0	100	2516	1.87	98.13	10263	0.63	99.37
				3789	1.46	98.54	9867	0.72	99.28

## 4.4 Discussion

The FISH-IS method has been shown to be effective in limited cell types thus far, including AML primary cells and the Jurkat and Ramos cell lines (Minderman et al. 2012, Fuller et al. 2016, Maguire et al. 2016, Grimwade et al. 2017). This research has applied the method to primary CLL cells for the first time. Compared with AML or the other two cell lines noted above, CLL cells are characteristically small lymphocytes with a mean diameter of 6  $\mu\text{m}$  versus 14  $\mu\text{m}$  (Creutzig et al. 2012). Furthermore, most CLL cells contain clumped and dense nuclear chromatin and very little cytoplasmic border, with highly aggregated chromatin (Matutes et al. 2000, Hallek et al. 2008) which has the potential to lead to an increase in auto-fluorescence. ImageStreamX is able to detect small spots with high resolution of spot images within the nuclei of lymphocytes by utilising EDF mode (Ortyn et al. 2006).

This study showed that the centromere Y probe is the only one that the algorithm of spot count was able to accurately enumerate. As a result, the data showed that 100% of single focus intact cells have one spot count; this is to be expected and can be explained by the highly repetitive sequences on the centromere Y creating numerous binding sites for the probes making the spots more discernible as a monosomy. In addition, the centromere Y is acrocentric, and therefore, it may be easier for probes to bind to the target DNA. Furthermore, it is easier to distinguish between one spot and no spot, while it requires equal intensity and separation of location are required to separate two spots from one spot.

To compare conventional FISH with FISH-IS, it is first necessary to acknowledge that both of these methods rely on the successful and accurate hybridisation of a labelled probe to the target DNA within a cell. The efficiency of hybridisation of probes to target DNA in both assays can be affected by various factors, including target sequence density, probe affinity,

sequence characteristics of the target DNA, and hybridisation conditions such as pH, temperature, salt concentration, buffers, etc. These methods, whether high-throughput or not, are all affected by these factors, and a non-specific probe or a poor hybridisation process cannot be improved by merely increasing the number of cells analysed.

The main advantage of conventional FISH is that it is technically simple and relatively inexpensive, only requiring access to basic tissue culture facilities and a fluorescence microscope. However, this technique has a number of limitations. Firstly, due to the lack of automation and its reliance on manual scoring, conventional FISH results are highly operator dependent and the process of data acquisition is relatively laborious and time consuming. Typically, an experienced observer needs to spend over 30 to 60 mins to analyse only 100 nuclei on slide FISH (Halling et al. 2000). Secondly, data misinterpretation and scoring inconsistencies may be the result of operator fatigue, inexperience and subjectivity. In particular, there is inevitable bias for a human reader to be “subjective” and select “good” cells for scoring. This may reduce the sensitivity/specificity in detection of high heterogeneity sub-clones samples, especially in MRD quantification in cancer (Dewald et al. 1998b). A study by Schmid et al. (2001) found that there were 2-fold differences in frequencies between two trained scorers in scoring FISH. Another group also reported that the discordance for inter-reader variability was up to 24% (Paik et al. 2002).

Of most relevance for this work is that the sensitivity of conventional FISH is limited by the low number of cells able to be evaluated. A single analysis will assess approximately 200 nuclei per slide, which represents only a small sample of the potentially complex mixture of cytogenetically abnormal cells often found in CLL samples. Therefore, conventional FISH is limited in its capacity to reliably detect small sub-clones, which may become clinically relevant during the course of the disease. This sub-clonal analysis can potentially be



strengthened by simultaneous immuno-phenotyping of the same cells which is another potential advantage of the ImageStreamX and the subject of ongoing research.

By contrast, FISH-IS is able to provide accurate data on intracellular fluorescence at a minimum speed of a thousand cells per second, meaning that even very small subclones can be detected and the frequency calculated in a single analysis. However, this method relies heavily on maintaining the original morphology of the cells, as damaged or disrupted cells are automatically excluded from the analysis. For the CLL samples, the analysis was compromised when using previously frozen and/or older fixed samples. It is unclear if this is a feature of CLL cells specifically, or a more general issue with this method. Regardless, at this stage, it appears that the applicability of the FISH-IS method may be limited by fresh sample availability. On the other hand, the morphology of cells is not as critical in the slide FISH assay as the cells spread and adhere to the slide, assisting in the maintenance of the morphology of cells. It is evident however, that morphology is significantly affected by the following experimental conditions:

- Buffer: osmolality, pH, temperature, viscosity of the hybridisation buffer, concentration of detergent, salts and other components.
- Pipette size, gentle mixing of cells while ensuring adequate mixing without introduction of air bubbles.

In the FISH-IS procedure, cells are heated up to 80°C (denaturing) and 73°C (high stringency wash). As a result, some fragile cells burst releasing DNA which is viscous and sticky causing the cells to clump or bind non-specifically to the fluorescence probes.

From this work, it is clear that the morphology of the cells is an important determinant for the successful hybridisation of probe and cellular identification. In addition, specificity of probe hybridisation is also critical to prevent non-specific binding, even more so for the in-

suspension FISH compared to conventional FISH, due to the greater dependence on the robustness of the cells which is influenced by their pre-analytical storage. The effect of a coverslip on conventional FISH assists in the even distribution of probe suspension over the area of fixed cells. However, clumping of cells is a concern with both methods. To recap, although FISH-IS is potentially a powerful technique for the detection of gene aberrations visualised at the individual cell level, the procedure has critical steps which need to be accurately performed to achieve a satisfactory outcome.

Regarding the financial costs, the consumable costs for these two methods is approximately the same. In contrast to conventional FISH, the FISH-IS method requires the ImageStreamX machine itself, representing expensive (approximately half of million dollars) and highly specialised equipment. On the other hand, FISH-IS is less labour-intensive in terms of the analysis and is not subject to human error and subjective determination in scoring but must still undergo some manual curation. The data can be analysed by IDEAS software with individual cellular images for subsequent ratification and other software determined features as well as long-term storage of the primary data. The results of scoring conventional FISH are dependent on the scorer in terms of training, experience and fatigue due to the time required for scoring, which is also operator dependent (Kennelly et al. 1995, Perry et al. 2011). In comparison, when a template analysis for FISH-IS is created and a fresh diagnostic sample is available, the results can be automatedly achieved with some curation of the collected data.

An experimental design using known ratios of male: female CLL cells was used to determine the level of detection of FISH-IS for numerical monosomy X aneuploidies based on fluorescence intensity. The data revealed that FISH-IS allowed accurate and affordable detection of a monosomy to a level of 1% when the workflow established in analysis was

applied. At levels below 1% in the serial diluted cells, the monosomy was detectable but was overestimated by the FISH-IS method with increased variance and reduced precision of measurement. Scoring 50 cells permits a lower limit of potential detection of only 1/50 (2% increments), but the analytical sensitivity of 60,000 cells increases the precision to 1/1000 (0.001%) ((Dewald et al. 1998a, Wiktor et al. 2006)). For example, to detect a sub-clone of 8.1%, with high analytical sensitivity, more than 1000 nuclei are required to be assessed.

Besides using mixing experiments, the FISH-IS technique was applied to individual CLL patient samples with various ratios of aneuploidy. As there is not a common monosomy aneuploidy in CLL samples, trisomy 12 was used as it is common in CLL (Döhner et al., 2000). Therefore, the FISH-IS technique was performed on the available trisomy 12 CLL samples at that time. Using the six available samples, the lowest frequency of trisomy 12 analysed was 5% which is likely to be above the lower limit of detection of the methodology. Hence it was not possible to confirm the lower limit of trisomy 12 detection by the FISH-IS technique in a patient sample. Larger studies with more samples would be required to further explore the sensitivity of this FISH-IS technique and translate it into a robust diagnosis test.

IDEAS software employs the Spot Count Wizard which is an ImageStreamX analysis algorithm. The Spot Count Wizard algorithms are based on two user-input-dependent variables of “spot-mask”: the spot-to-background ratio and spot radius area. The spot-to-background ratio is the spot pixel value divided by background in the image, while the radius value of  $x$  implies the image containing spots with thickness of  $2x+1$  pixels. This Spot Count Wizard software will automatically enumerate the spot count optimised for each sample. However, to date the issue with this software is the inability of the associated software to accurately ‘count’ the number of hybridisation signals per cell. There are several aspects of this system which may be causing inaccuracy of the current spot count algorithm.

Firstly, the software records a 2-dimensional image of a 3-dimensional object (the cell). Therefore, if spots are at different depths along the same axis as the camera, the conversion to a 2-dimensional image may cause them to be partially or entirely merged with the front signal. To overcome these limitations, manual curation was applied to adjust the spot count. Cell images are very informative and interpretation by eye unfortunately remains the more efficient analysis than any software analysis approaches. When manually curating images of cells, which had been counted as having 'one-spot', some cells clearly contained two spots that were very close to each other and easily discernible by eye; however, the software was unable to discriminate them as two distinct spots. Secondly, extracellular DNA adheres to the external surface of the cytoplasmic membrane of analysed cells causing wrongly enumerated spots. The nuclear staining marker (DAPI) was used to identify nuclear area when manual curation was performed. The spots located outside of the nuclear region were excluded. In addition, when images of cells were studied, whilst the majority of cells had two or three well-resolved FISH signals, a proportion of cells appeared to have FISH signals which were superimposed partially/entirely due to the orientation of the cell to the camera. Therefore, it is more likely to have 3 spots appear as 2 and 2 spots appear as 1. This could account for the reduced ability to enumerate spot count in the algorithm software.

Previous studies have found a similar level of miscounting of spots with the current algorithm spot count software (Minderman et al. 2012, Fuller et al. 2016). There is a pressing need for further development of this software so that spot counting is an accurate and reproducible analysis step, without requiring manual curation and confirmation, which is a significant limitation of this methodology.

Dohner et al. (2000) reported that trisomy 12 CLL conferred an intermediate outcome, but other studies have since found that trisomy 12 may actually be associated with either a good

or a poor prognosis (Rossi et al. 2009, Gunnarsson et al. 2011). These conflicting findings may be due to differences in the proportion of CLL cells carrying trisomy 12 and additional mutations present in the sub-clones. Furthermore, Gonzalez-Gascon et al. (2015) found that trisomy 12 had to be present in >60% of CLL cells (high frequency) to confer a poor outcome and Van Dyke et al. (2016) showed a significantly shorter time to first treatment in patients with >60% trisomy 12 cells. However, to date, the effect of low frequency trisomy 12 in CLL itself is not fully understood.

From our limited data due to small sample size on the detection of low frequency trisomy 12 by three methods (conventional FISH, LSC and FISH-IS), there was a trend towards overestimates by LSC and underestimates by FISH-IS at a level of 5% trisomy 12, compared with conventional FISH. The reason for this discrepancy of LSC may be that the split FISH spots were recorded as three spots (instead of two spots) due to the uncondensed chromosomes in interphase in a few cells (Wang et al. 2009); and this might not be easy to distinguish if there is a lack of focus depth (Wang et al. 2012b). Basiji et al. (2007) also reported that the spot image data might have increased sensitivity by dwelling over the cell for a longer time period. Also, a plausible explanation for the decrease in FISH-IS as compared to monosomy detection is that the difference in FISH probe fluorescence intensity between two and three signals (in disomy and trisomy) is a 50% increase, compared to a 100% increase when discriminating between one and two signals (in monosomy and disomy). Therefore, this smaller differentiation between the two groups of cells increases the difficulty in distinguishing these two populations and reduces the sensitivity.

The microscope-based laser scanning cytometer emerged in the mid-1990s (Kamentsky et al. 1991, Kamentsky et al. 1997, Kamentsky 2001), allowing automated quantification of FISH slides with a significantly larger number of cells, (Luther et al. 2004, Holden et al. 2005,

Henriksen et al. 2011). This LSC method is not, however, without its limitations. Firstly, the LSC machine itself represents expensive and highly specialised equipment; therefore access will be the limiting factor for most researchers or diagnostic centres in applying this method. In terms of the actual method of signal detection, LSC detects cells by the primary contour (visualised as DAPI-stained nuclei) and enumerates any hybridised probes by the secondary contour. However, both the hybridised probes and the nuclei can vary in relative fluorescence intensities and size, requiring a large training range of acceptable contours to be established to ensure correct detection of all cells and hybridised probes. The fluorescence signals can also occur at variable depths along the optical axis, which can also lead to incorrect spot counting per cell. Therefore, the accuracy of the spot counting analysis needs to be checked by manually scoring a random sample of the cells, in order to ensure that these factors are not resulting in a flawed automated analysis. In addition, there are several parameters which need to be established prior to scanning the slides, for example, the focal length of the camera needs to be adjusted according to the thickness of the covering glass and the sample itself. Considering these factors, the application of LSC in FISH analysis is considered a semi-automated procedure (Kamentsky 2001, Pozarowski et al. 2013).

By contrast, FISH-IS is able to provide accurate data generated from thousands of cells by analysing the fluorescence intensity of the samples. However, this method relies heavily on maintaining the original morphology of the cells, as damaged or disrupted cells are automatically excluded from the analysis. For our CLL samples, analysis was compromised when using previously frozen and/or long term fixed samples. This may be a feature of CLL cells specifically, or a more general issue with this method. Regardless, the applicability of the FISH-IS method may be limited by sample availability.

With respect to the financial cost of these three methods, the obvious difference is the specialised equipment required for the two high-throughput methods. That factor aside, all methods cost approximately the same for consumables; however the LSC and FISH-IS methods are less labour-intensive than conventional FISH. Experienced scorers spend approximately 2 hours to score 200 nuclei on conventional FISH, whilst the LSC and FISH-IS need 30 mins to 1 hour for analysis of up to 3000 cells in LSC and up to 10,000 cells in FISH-IS. Therefore, the labour time of the latter method is reduced significantly and the results do not depend heavily on experienced scorer.

#### **4.5 Conclusion**

FISH-IS is a dynamic methodology which is able to accurately analyse chromosome genetic aberrations in CLL and hence provides an important research tool and potential diagnostic assay with automation of cytogenetic analysis. Furthermore, it is clear that the ability to detect low frequency clones at a level of detection of 1% in CLL has potential translational impact on clinical care. Continued research in the area of low frequency sub-clones is vital to improve understanding of the biological relevance of these clones and to assist in prognostic determination and treatment decision making in the future.

## 5 Chapter 5 - Development of FISH-IS to detect del17p in CLL

### 5.1 Introduction

Due to the broad spectrum of clinical course which CLL can take (ranging from indolent to rapidly progressive disease), the correct decision about treatment for CLL patients is a remarkably challenging task, requiring consideration not only of clinical characteristics and previous experience, but also of a variety of genetic and cellular prognostic markers. According to the latest revised iwCLL guidelines, genetic abnormalities play a definite role in stratification of risk in CLL and selection of treatments now and into the future (Hallek 2013). In support of this concept, up to 80% of CLL patients have been shown to harbour recurrent cytogenetic alterations which have been identified by conventional fluorescence *in situ* hybridisation (FISH). As identified by Dohner et al. (2000), the common genetic defects can be arranged in five hierarchical classifications which are strongly predictive of survival, including 17p deletion, 11q deletion, trisomy 12, 13q deletion, and a normal karyotype. Patients who carry a deletion of the short arm of chromosome 17 (del17p) have been shown to have the worst outcome of all groups, with OS of 2-3 years post diagnosis (Lens et al. 1997, Dohner et al. 2000). These patients have a phenotype which may rapidly progress to symptomatic disease, demonstrate chemo-refractoriness, and undergo earlier relapse. The 17p deletion in CLL usually encompasses the whole short arm, including the *TP53* gene (Edelmann et al. 2012), a tumour suppressor gene that plays a critical role in CLL progression and sensitivity to therapy. The reason for the poor response to treatment in the del17p group is most likely due to the fact that the current standard treatment (fludarabine, cyclophosphamide, and rituximab) aims to trigger cell death via *TP53*-dependent pathways (Stilgenbauer et al. 2007, Rossi et al. 2009). Therefore, the del17p genomic aberration is



the only current marker which has distinct predictive value with regards to response to treatment, therefore influencing therapeutic decisions.

As mentioned in Chapter 1 (section 1.7.4), there is no consensus on the prognostic impact of the size of *TP53* defective sub-clones in CLL. Rossi et al. (2014) indicated that very small *TP53* defective sub-clones (0.3% of all CLL cells by ultra-deep MPS) led to greater disease progression, whereas Tam et al. (2009b) assumed that the low frequency del17p (< 25% 17p-deleted nuclei by conventional FISH) resulted in a favourable prognosis. Several other studies have also shown a favourable prognosis with low frequency del17p in CLL patients, displaying a longer time to first treatment and longer OS (Delgado et al. 2012, Van Dyke et al. 2016).

Therefore, to clarify this issue, there was a need to develop a reliable high-throughput cytogenetic technique to accurately identify del17p small sub-clones. It is very important to accurately quantify the percentage of del17p cells within a sample, particularly the low frequency sub-clones, not only before initial treatment but also during subsequent treatment decisions in order to monitor for clonal evolution in relapsed and chemo-refractory patients, enabling tailoring of effective treatment. However, currently cytogenetic tests including karyotype and FISH analysis are used to identify the presence of a 17p deletion in CLL samples. Both of these microscope-based tests have limitations in providing information on low frequency sub-clones which have potential clinical relevance for subsequent disease evolution. Slide-based detection methods have a relatively low level of sensitivity due to the small number of cells assessed: in traditional karyotyping 20-30 metaphase cells are counted, and conventional FISH usually involves two scorers independently analysing up to 200 nuclei. Considering these relatively low numbers of cells, it is clear that these methods are not able to accurately detect and monitor low frequency del17p sub-clones. It is however

evident that accurate information is required regarding the presence of this deletion, due to the fact that identification of the existence of small *TP53* deletion clones is clinically critical (Best et al. 2012).

Other novel detection techniques for chromosomal copy number changes include SNP array analysis and massive parallel sequencing. However, whilst SNP array analysis can give precise information on exact sizes of deletions and duplications, it is not significantly more sensitive than microscopy based methods, with a detection limit of approximately 20%-30% (Gondek et al. 2008, Gunn et al. 2008). MPS is able to accurately detect sub-clones of less than 1%; however this approach requires gene target enrichment followed by ultra-deep sequencing (Goodwin et al. 2016). This requirement means that MPS is both significantly more expensive than the other methods, and also requires specific information on the target sequence prior to analysis (Sun et al. 2015).

In response to the clinical necessity for detecting low frequency sub-clones and the low sensitivity of conventional cytogenetic tests, an alternative methodology to those currently available is clearly required. One such methodology is FISH-in suspension (FISH-IS), consisting of conventional FISH combined with a flow cytometry-based imaging platform (Amnis ImageStream<sup>X</sup> MkII) and analysis software (IDEAS<sup>TM</sup>; Amnis Cooperation Seattle, WA). This relatively novel methodology has been shown to enable quantification of genetic abnormalities with high accuracy in up to 1000 cells/second (Minderman et al. 2012). This method is therefore able to stratify tumour clonal heterogeneity with high sensitivity. The morphometric visualisation of fluorescence microscopy merged with the statistical power of flow cytometry (e.g. mean fluorescence intensity - MFI) has been remarkably enhanced by algorithm spot count and extended depth of field (EDF) mode in order to enumerate fluorescence spots associated with FISH (Ortyn et al. 2007).

At the commencement of this research in 2013, all FISH-IS published studies had utilised probes to highly repetitive sequences (telomere or chromosome-specific centromere probes (CEP)). These probes generate a signal with a very high fluorescence intensity due to the enormous number of labelled probes which bind to the target sequence. Examples of such applications include telomere length analysis (Baerlocher et al. 2006) and detection of aneuploidy based on centromere probe analysis (Minderman et al. 2012). The data presented in Chapter 4, in accordance with a report by Minderman et al. (2012), demonstrated the capacity of accurate detection of monosomies by FISH-IS to be as low as 1%.

However, it remains unclear whether or not this assay is able to be applied to non-repetitive probes, such as the *TP53* region on the short arm of chromosome 17. To this point in time there have been no reports which have successfully developed FISH-IS with locus-specific probes. Therefore, this study is the first to successfully apply FISH-IS analysis to a 17p locus-specific probe, and to be carried out for the clinically relevant application of identifying 17p deletions in CLL samples.

Therefore, the aims of this chapter were:

1. To apply the commercially available locus-specific 17p probes to the FISH-IS method (section 5.3.1);
2. To develop and optimise FISH-IS using a fluorescently labelled 17p BAC probe contig (section 5.3.2 – 5.3.4);
3. To apply FISH-IS with 17p locus-specific probes to fresh CLL patient samples and to determine the level of sensitivity of detection (section 5.3.5);

4. To flow sort the FISH-IS with 17p locus-specific probes on fresh CLL patient samples, confirming the enrichment of the 17p sub-clone by Sanger sequencing (section 5.3.6); and
5. To optimise FISH-IS with 17p locus-specific probes on cryopreserved CLL samples (section 5.3.7 – 5.3.12).

## 5.2 Materials and methods

### 5.2.1 Commercial FISH probes

Three commercial FISH probe kits were trialled and will be referred to as Kit 1 (ATM/*TP53* CLL probe kit, Metasystems, Germany), Kit 2 (ATM/*TP53* CLL probe kit, Abbott Molecular, Australia) and Kit 3 (*TP53* probe, Abbott Molecular, Australia).

### 5.2.2 Bacterial Artificial Chromosome (BAC) FISH probes

Seventeen BAC clones mapping to the short arm of chromosome 17 (17p) and spanning the *TP53* region were selected from the RP11 DNA BAC library (Osoegawa et al. 2001) (Table 7.8). A nick translation kit (Abbott Molecular, Australia) was used to label BAC DNA with spectrum orange-dUTP or spectrum green-dUTP. The ratio of labelled - dUTP : dTTP was 6:1 and the method of labelling was adjusted from the manufacturer's protocol to achieve the highest possible labelling levels (Cox et al. 2004) (see detailed protocol in section 2.9). Following labelling, unincorporated dUTP and probe fragments were removed by gel filtration micro-spin G50 (GE Healthcare, Australia). Probes were analysed on an agarose gel to confirm final fragment sizes between 200 bp and 400 bp. Probes were labelled with one fluorophore per every 30-80 bp as recommended by manufacturer's protocol, and the concentration of probes was 20 ng/ $\mu$ L (Yu et al. 1994, Vermeesch et al. 2005).

### 5.2.3 FISH-IS protocol with 17p BAC probe contig

The initial method for FISH-IS with 17p BAC probes was adapted from a previously published FISH-IS protocol (see section 2.8) in combination with the laboratory's standard conventional FISH protocol. Further optimisation of this method formed part of this chapter.

Sixty nanograms of each BAC clone was combined (giving a total of 1 µg) with 50 µg Cot1 DNA (Abbott Molecular, Australia). The solution was desiccated at 45°C for 30 mins, followed by resuspension in 20 µL of locus-specific identifier (LSI) hybridisation buffer (Abbott Molecular, Australia). Probes were denatured at 80°C for 5 mins, placed on ice for 2 mins, vortexed, and then placed at 42°C for 30 mins (pre-annealing) before applying to denatured cells.

Three hundred thousand cells were used for each hybridisation reaction. Cells were incubated in 9 mL 0.075 M KCl for 30 mins at 37°C. The reaction was stopped with 1 mL of Carnoy's fixative, followed by centrifugation at 300 x g for 10 mins. The pellet was resuspended in 10 mL of Carnoy's fixative and centrifuged at 300 x g for 10 mins. This was repeated twice more, and the pellet was finally resuspended in 1 mL of Carnoy's fixative and stored at -20°C for a minimum of 4 hours. Samples were then centrifuged at 300 x g for 5 mins and the supernatant removed. Cells were then washed in Wash 1 (1X PBS with 0.5% BSA and 5 mM EDTA) twice, followed by once in Wash 2 (2X SSC with 0.1% NP-40 and 5 mM EDTA).

In order to generate the control mix samples containing different proportions of 17p-deleted cells, CLL samples with 95% of del17p cells (as ascertained by conventional FISH) were mixed with wild-type 17p CLL samples (100% wt17p) in various ratios prior to hybridisation. Cells were then centrifuged 300 x g for 5 mins and resuspended in 20 µL LSI hybridisation

buffer and denatured at 80°C for 5 mins. The probes and cells were then combined and hybridised at 42°C for 12 hours.

Following hybridisation, cells were washed in 2X SSC + 0.1% NP40 at room temperature, centrifuged at 2000 x g for 5 mins, followed by the addition of 200 µL of 0.3% NP-40 in 0.4X SSC pre-warmed to 73°C. Cells were incubated at 73°C for 3 mins, then 200 µL of ice cold 2% FBS in PBS was added to immediately lower the temperature, followed by centrifugation at 2000 x g for 5 mins at room temperature. The supernatant was discarded and cells were resuspended in 50 µL 2% FBS in cold Hank's buffer (Sigma-Aldrich, Australia) and 10 µL 5 µg/mL DAPI through a 25G needle and syringe to prevent cells clumping before analysis.

#### **5.2.4 Flow sorting and Sanger sequencing**

Samples hybridised with the FISH-IS protocol were sorted on a BD FACSAria™ Fusion flow sorter (BD Biosciences, Australia) which discriminates and sorts samples based on the fluorescence intensity of individual cells. The flow sorting procedures were provided by Dr Randall Grose at the South Australian Health and Medical Research Institute.

DNA was extracted from the collected cells by QIAGEN Midi blood kits (QIAGEN, Australia). PCRs were carried out under standard conditions in a 2720 Thermal Cycler (Applied Biosystems, Australia). Primer sequences and cycling conditions are provided in Appendix Table 8. Following amplification, 5 µL of PCR product was prepared for sequencing via enzymatic treatment with 1 unit Shrimp Alkaline Phosphatase (Affymetrix, Australia) and 4 units exonuclease I (New England Biolabs, Australia) in 1x Shrimp Alkaline Phosphatase buffer (Affymetrix, Australia) in a total volume of 7.5 µL, then incubated at 37°C for 60 mins and the enzyme inactivated at 80°C for 20 mins in a 2720 Thermal Cycler (Applied Biosystems, Australia). The purified PCR product was sequenced at the Flinders Sequencing Facility (SA Pathology, Flinders Medical Centre) using BigDye Terminator

chemistry (Life Technologies, Australia) and a Prism 3100 Genetic Analyzer (Life Technologies, Australia). Sequence analysis was carried out with the Sequence Scanner Software 2 (Applied Biosystems, Australia).

### 5.2.5 Cell culture

Cryopreserved cells were thawed by heating to 37°C in a water bath by the dropwise addition of warmed media (Yokoyama et al. 2012). Standard media consisted of RPMI 1640 media supplemented with 5 mL of 200 mM L-glutamine, 5000 units penicillin and 5 mg/mL streptomycin solution and 10% fetal calf serum. All cells were incubated at 37°C, 10% CO<sub>2</sub>, in a fully humidified atmosphere. Cells were cultured using the following methods.

1. Co-culture. Bone-marrow derived stromal cell line, HS5 (CRL-11882™) was obtained from the American Type Culture Collection (ATCC®, USA). HS5 was seeded in a 24 well plate at  $1.2 \times 10^5$  cells/mL and incubated for 48 hours. When cells reached confluence, they were washed with standard media, then CLL cells were seeded at high density onto this feeder layer in a total volume of 1 mL of standard media. For harvesting, CLL cells were gently agitated and removed from the feeder layer with the supernatant.
2. Conditioned media. HS5 cells were incubated in standard media for 48 hours, and media was collected and 0.22 µm filtered. This conditioned media is enriched for soluble factors secreted by the HS5 cells.  $1 \times 10^7$  CLL cells were incubated in 1 mL of the conditioned media and were harvested by centrifugation at the indicated time.
3. High-density. CLL cells were cultured in standard media at a concentration of  $1 \times 10^7$  cells/mL.

4. AIM-V serum-free media. CLL cells were cultured at high density in AIM-V serum-free media supplemented with 5 mL of 200 mM L-glutamine, 5000 units penicillin and 5 mg/mL streptomycin solution.
5. McCoy's 5A media. CLL cells were cultured at high density in McCoy's 5A media supplemented with 5 mL of 200 mM L-glutamine, 5000 units penicillin and 5 mg/mL streptomycin solution and 10% fetal calf serum.
6. Low density. CLL cells were cultured in standard media at a concentration of  $2 \times 10^6$  cells/mL.

For all culture conditions, 50% of the media volume was removed and replaced with fresh media every 24 hours. The number of cells, cell morphology and cell viability were analysed at various time points (0, 6, 24, 48, 72, 96 and 120 hours) with visualisation by an EVOS™ inverted microscope (brightfield), trypan blue exclusion assay (viability), and annexin V/propidium iodine detection (for apoptosis: see below).

### **5.2.6 Apoptosis analyses**

The percentage of apoptosis was determined by annexin V/propidium iodine assay. In brief, following isolation, CLL cells were washed twice with cold PBS and resuspended in 100  $\mu$ L of binding buffer containing 2  $\mu$ L of FITC-conjugated annexin V and 10  $\mu$ g/mL of propidium iodide (PI). Samples were incubated for 15 mins at room temperature whilst protected from light. Cells were analysed immediately with a flow cytometer using FITC (annexin V) and PE (PI) lasers.

### **5.2.7 Investigation of pseudo-nodes**

Pseudo-nodes are defined later in section 5.3.12. CLL cells were co-cultured and collected at 3 time-points (72, 96 and 120 hours) by two different methods. Method 1 involved



collection of CLL cells in suspension only, which did not include cells contained within the observed pseudo-nodes. Method 2 involved collection of all cells contained within the entire well, consisting of all suspension cells, pseudo-nodes and HS5 cells. Cells were then physically dissociated from the psuedo-node structures with repeated pipetting. Cells collected by both methods were assayed for viability with the annexin V/PI assay.

### **5.2.8 Statistical analysis**

Results are shown as a mean  $\pm$  SD, calculated from 3 separate experiments data. Statistical significance was determined by a students paired /unpaired t-test, 2-way ANOVAR test for multiple comparison.

## **5.3 Results**

### **5.3.1 Commercial 17p probes do not generate sufficient signal for use in FISH-IS**

To date, FISH-IS has only been successfully carried out using highly-repetitive commercially available centromere probes (Minderman et al. 2012). Therefore, I first determined whether it is also possible to use a commercially available single-locus probe in this method. Three commercial probe kits which span the *TP53* gene and are currently used in CLL analysis (Kit 1 and Kit 2 are dual probes, also containing a probe for the *ATM* gene; Kit 3 only probe for the *TP53* gene) were tested in the FISH-IS protocol. This analysis revealed that all kits gave a strong hybridisation signal with low background in conventional FISH (Figure 5.1A). Unfortunately, the strength of this signal was not sufficient for the FISH-IS method (Figure 5.1B-C). The locus-specific commercial probes demonstrated a low level of fluorescence from the hybridisation signal combined with a high background of non-specific nuclear fluorescence (Figure 5.1C).

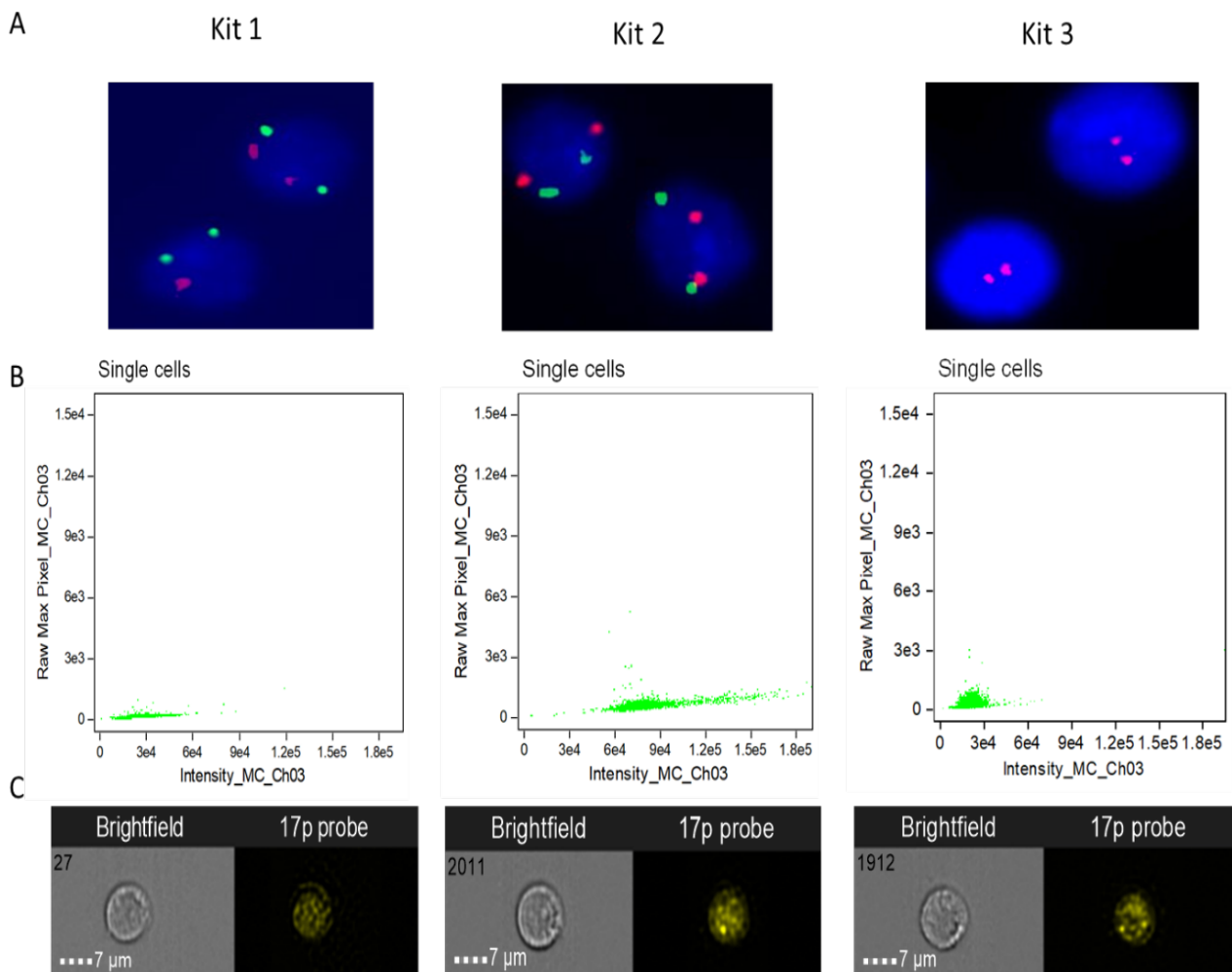


**Figure 5.1. Commercial *TP53* probes do not generate sufficient signal for analysis with FISH-IS.**

(A) Representative images of conventional FISH with the indicated commercial probe kit. Red, *TP53* probe; green, *ATM* probe (kits 1 and 2 only); blue, nuclear staining as shown by DAPI. (B) Distribution of cells based on signal fluorescence intensity (y-axis, raw max pixel) and overall fluorescence intensity (x-axis, total fluorescence intensity of individual cell). (C) Representative cell images by FISH-IS with a 17p commercial probe showing an intact cell (brightfield) and multiple signals for the 17p probes (17p probes). All images were normalised with the same scale. Data are representative of 3 separate experiments in triplicate.

As Kit 3 was the only commercial kit which contained solely a probe to *TP53*, further analysis was undertaken on this hybridisation sample, in order to determine if automated masking and Spot Count Wizard analysis might render the hybridisation signals informative. However, analysis of the data with various masking strategies through the IDEAS software was unable to distinguish the signals (spots) from background noise (Figure 5.2).

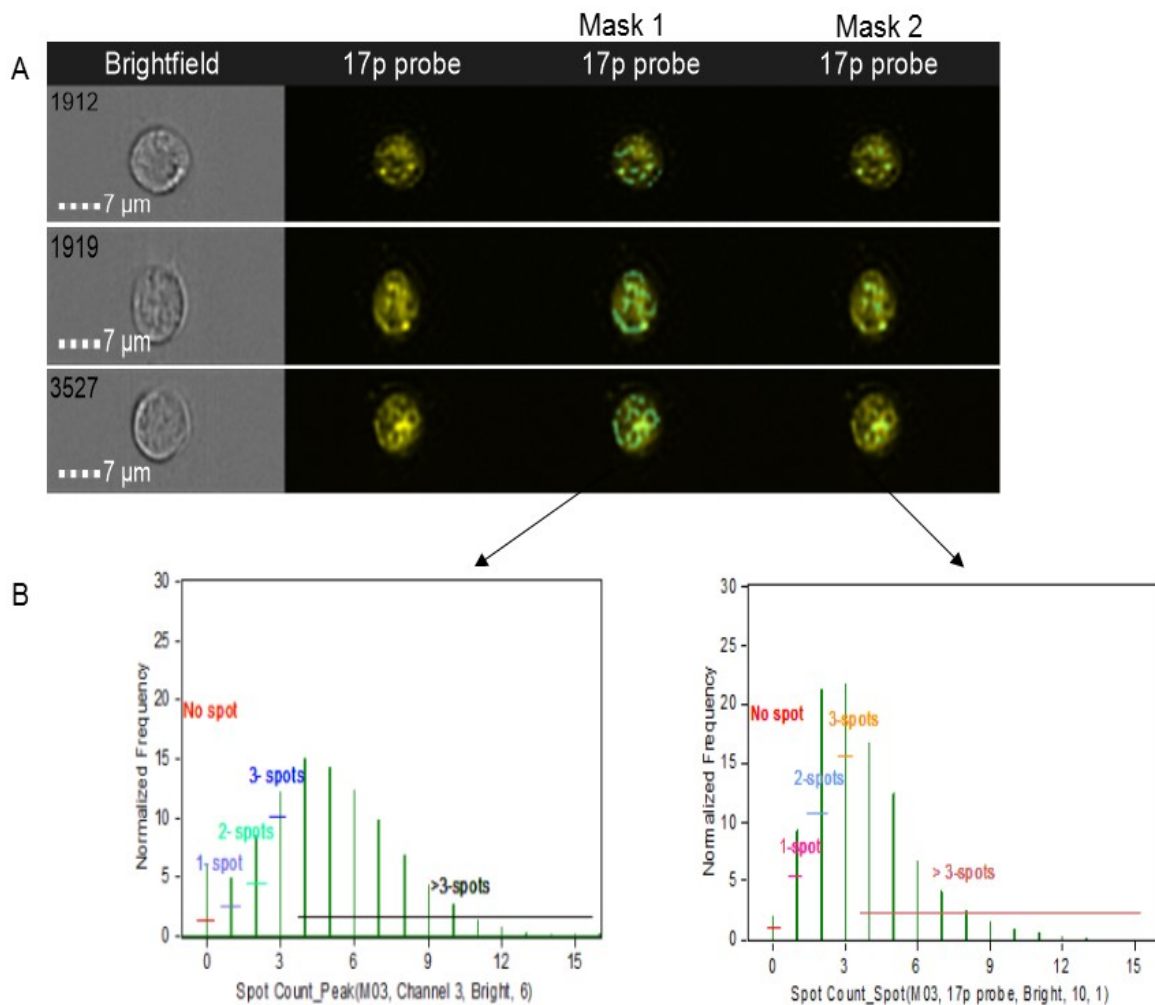


**Figure 5.2. Different masking strategies are unable to distinguish spots with commercial Kit 3.**

(A) Representative images from FISH-IS with a commercial 17p probe (Kit 3), 17p probe in yellow and masking features in light blue. (B) Mask 1 is the mask of Spot Count Wizard spot count versus an optimised mask (Mask 2).

Given that FISH-IS has been successful with probes which have targeted repetitive sequences within the centromere (Minderman et al. 2012), I hypothesised that the size difference and therefore opportunity for multiple probes to bind to the repetitive centromere target sequence and the locus-specific target sequence might be responsible for this difference in signal intensity. An increase in the size of the target region for the locus-specific probes should increase the fluorescence signals to a level that may be used in FISH-IS. The following sections describe the panel of custom 17p BAC contig probes to the 17p region spanning the *TP53* gene which I developed.

### **5.3.2 Development and validation of a custom 17p BAC probe contig**

Microarray analysis has demonstrated that 17p deletions in CLL are quite uniform and encompass not only the *TP53* gene, but are actually a deletion of the whole short arm of chromosome 17 (Edelmann et al. 2012). Therefore, I hypothesised that utilising a BAC contig centred around the *TP53* gene on 17p as a probe would provide the required increase in the size of the probe target region without causing a reduction in specificity of detection. Therefore, 20 BACs surrounding the *TP53* gene were identified from the RP-11 library (Figure 5.3 and Appendix Table 9). The total BAC contig spans approximately 2.5 Mb, making it approximately 15 times greater than the commercial *TP53* probes (Kit 1 probe is 145 kb; Kit 2 and 3 probes are 172 kb) and approaching the size of the target sequence of the highly-repetitive centromere probes.

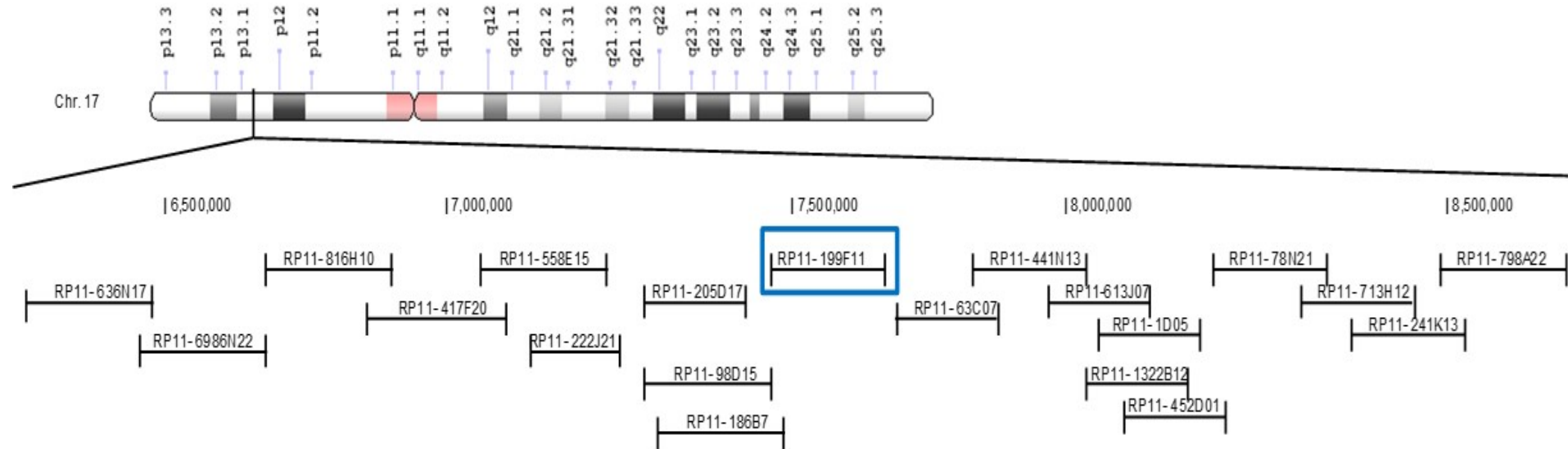


**Figure 5.3. Schematic representation of 20 BACs surrounding *TP53* gene on chromosome 17.**

*BAC RP11-199F11 (indicated by a blue box) contains the *TP53* gene.*

*Genomic co-ordinates of each BAC can be found in Appendix Table 9.*

The individual specificity of each BAC as a probe to 17p was determined by nick translation labelling (see section 2.9) and analysis with interphase/metaphase conventional FISH. Only BAC probes which had specific binding to 17p were used in the final probe contig (example shown in Figure 5.4A). Three BAC probes which showed cross-hybridisation to other chromosomes by interphase/metaphase FISH (RP11-205D17, RP11-417F20 and RP11-816H1) were therefore excluded from further analysis (example shown in Figure 5.4B).

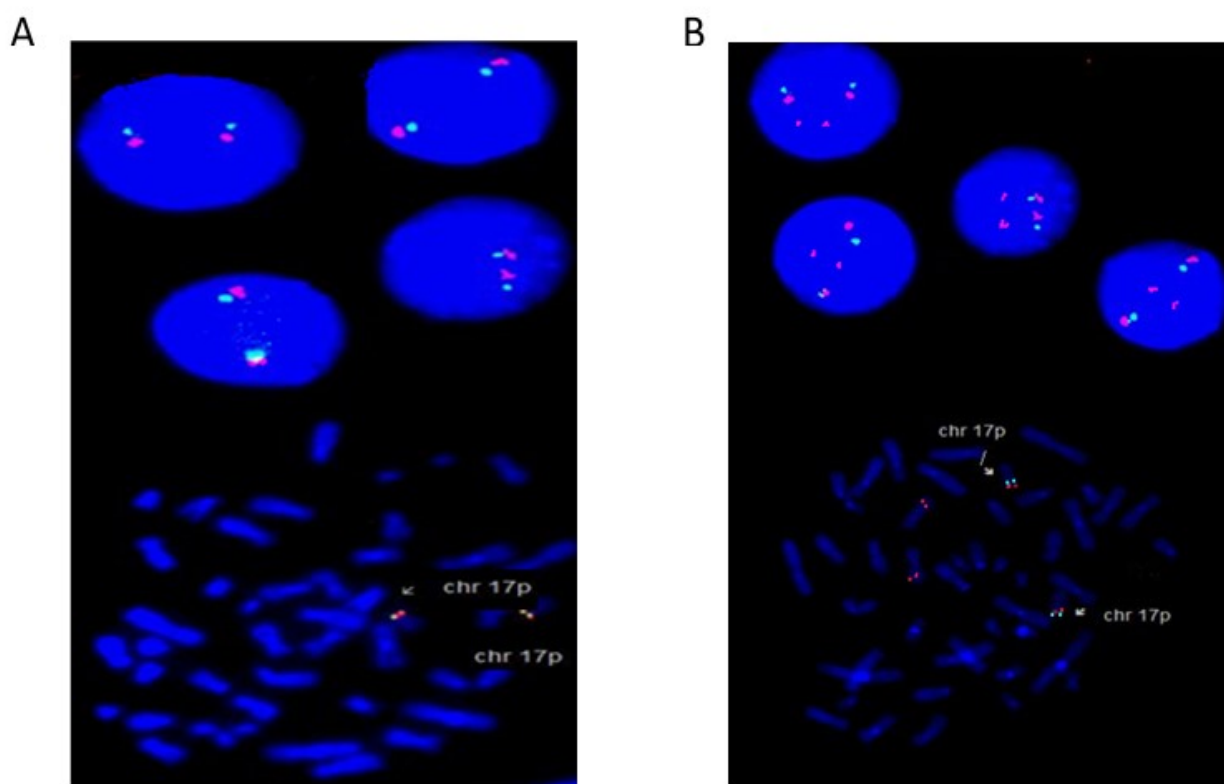


**Figure 5.4. Individual BAC clones were tested to ensure specific hybridisation by metaphase and interphase conventional FISH.**

(A) An example of a BAC with specific hybridisation to 17p, as the BAC being tested (RP11-63C07, red signal) shows punctate signals in close proximity to the guide 17p probe (RP11-199F11, green signal). (B) An example of a BAC probe (RP11-205D17, red signal) which is showing non-specific hybridisation when compared to the guide 17p probe (RP11-199F11, green signal).

### 5.3.3 Increasing the number of BAC probe increases signal fluorescence intensity

An analysis was carried out combining increasing numbers of BAC probes in order to determine the optimal number of BAC probes for FISH-IS. Figure 5.5 shows FISH-IS analyses ranging from a single BAC probe, increasing in number until the entire 17 labelled BAC probes were hybridised simultaneously. A comparison was made with previously utilised commercial probes (*TP53* Kit 3 and CEP X), with CEP X representing optimal signal and background intensity. The analyses were based on the fluorescence intensity generated by FISH-IS and their images (Figure 5.5). From these data, it is clear that as the number of BAC clones increased, the 17p signal intensity also increased (black bars, Figure 5.5). However, this also resulted in a slight increase in overall background fluorescence (grey bars, Figure 5.5). Compared to the commercial *TP53* probe, the BAC contig probes displayed a significant increase in signal intensity; however the CEP X signal intensity remained the highest (Figure 5.5). The 17 BAC contig probes signal intensity was 15-fold greater than commercial *TP53* probes but 50% less than centromeric probe intensity (Figure 5.5). Even though there was no significant statistical difference between hybridisation with 10 and 17 BACs ( $p=0.32$ ), the highest ratio of raw max pixel to fluorescence intensity was found with 17 BAC probes. Therefore, the final BAC probe contig consisted of 17 BAC probes (Table 7.7) and was used in all future 17p FISH-IS analyses. The next step was to determine if the FISH-IS methodology could be optimised for application with the BAC probe contig.

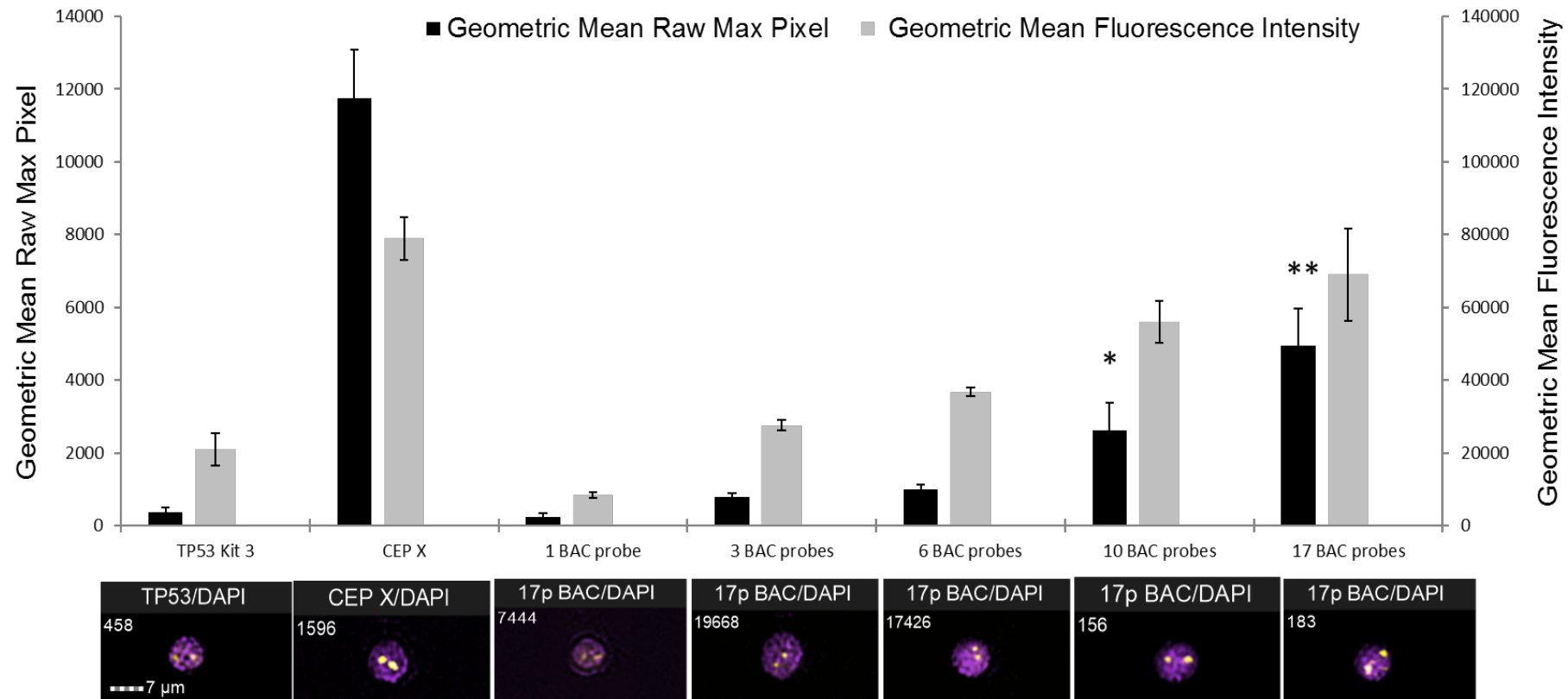


**Figure 5.5. Both raw max pixel and fluorescence intensity increase with an increase in the number of 17p BAC probe contig.**

An example of a single cell hybridised with the indicated probe(s) is shown directly under the respective column; probes are shown as yellow signals (spectrum orange, Ch03), nuclear staining (DAPI, Ch07) is shown in purple. The ratio between raw max pixel and fluorescence intensity is equivalent to the ratio of signal to background. Student's *t*-test was performed and the only significant differences were found between the commercial TP53 kit 3 vs 10 BAC probes (\* $p=0.018$ ) and the commercial TP53 kit 3 vs 17 BAC probes (\*\* $p=0.001$ ). Data are representative of the geometric mean of 3 separate experiments  $\pm$  SD on normal karyotype CLL samples.



### 5.3.4 Optimisation of FISH-IS with the 17p BAC probe contig

Given that 17 BAC probes were found to produce the highest signal to background ratio in FISH-IS, protocol optimisation was then undertaken to determine if this ratio could be improved. Optimisation of the FISH-IS method was addressed at four major steps in the protocol: fixation/permeabilisation, hybridisation, washing and visualisation. Due to the large number of steps in the protocol, it was not feasible to optimise all steps in all possible combinations. Therefore, for each parameter being tested, all other parameters remain as standard (as described in section 5.2.4) unless otherwise noted.

#### 5.3.4.1 Fixation and permeabilisation optimisation

*Carnoy's fixative.* The standard process of fixation consists of incubating cells in a hypotonic solution (9 mL KCl 0.075M) at 37°C for 30 mins, followed by the addition of 1 mL of Carnoy's fixative to stop the reaction. The cells are then pelleted and resuspended in 1 mL Carnoy's fixative, repeated three times. Studies in the literature have shown that this methodology gives optimal fixation and preserves the integrity of both nucleic acids and cell morphology (Urieli-Shoval et al. 1992, Murrell-Bussell et al. 1998, Srinivasan et al. 2002, Chao et al. 2011). However, other studies have carried out a simplified method of fixation, consisting of resuspending the cell pellet with gentle vortexing whilst Carnoy's fixative is added in a drop-wise manner (Minderman et al. 2012).

In order to determine which method is more appropriate for CLL cells, both approaches were undertaken. Analysis revealed that the proportion of intact cells significantly declined when Carnoy's fixative was added in a drop-wise manner compared to the standard method (63% compared to 83%; Figure 5.6A). Visual inspection of the cells post fixation reveals that the drop-wise method of fixation clearly results in more cells with poor morphology compared to the standard method of fixation (Figure 5.6B-C).

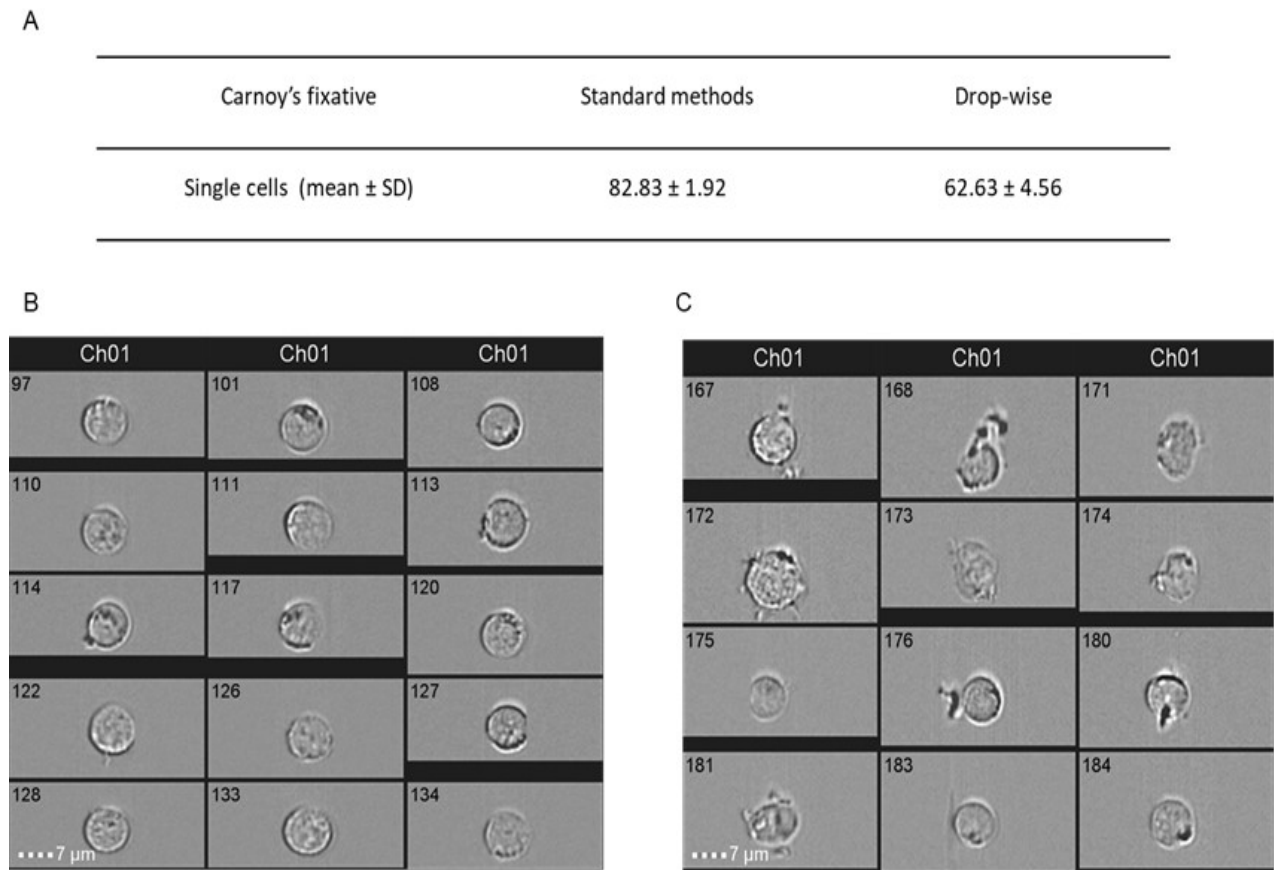


**Figure 5.6. Comparison of Carnoy's fixative standard methods with drop-wise on the number of remaining single cells and their morphology.**

(A) Percentage of intact single cells when fixed with the standard and drop-wise methods. Examples of FISH-IS images following the standard method (B) and drop-wise addition (C) of Carnoy's fixative. Data are representative of the mean  $\pm$  SD of 3 separate experiments.

*DNase I.* Many studies have included the addition of an endonuclease deoxyribonuclease (specifically DNase I) in order to minimize clumping of cells following fixation (Campbell et al. 1980, Renner et al. 1993, Garcia-Pineros et al. 2006). To test if DNase I would be beneficial for the FISH-IS method, cells were incubated with 0, 20, 50, or 100  $\mu\text{g}/\text{mL}$  DNase I at 37°C for 15 mins prior to fixation. Analysis of the treated cells revealed that the highest percentage of intact single cells were yielded in the absence of DNase I incubation (Table 5.1), and therefore this treatment was not included in the optimised protocol.

**Table 5.1. DNase I treatment does not increase the number of single intact cells.**

DNase I ( $\mu\text{g/mL}$ )	Single cells (%) (mean $\pm$ SD)
<b>0</b>	<b>81.57 <math>\pm</math> 2.26</b>
20	78.67 $\pm$ 2.18
50	79.23 $\pm$ 2.56
100	75.56 $\pm$ 3.79

*The optimal condition (no DNase I) is indicated in bold. Data are the mean of 3 separate experiments  $\pm$  SD.*

*Proteinase K.* Andersen et al. (2001), Schurter et al. (2002) and Pineau et al. (2006) have shown that the addition of proteinase K can improve the specificity of the DNA-DNA hybridisation efficiency. Therefore an additional step consisting of incubation with 10 or 20  $\mu\text{g/mL}$  Proteinase K for 15 mins at 37°C was added to the FISH-IS protocol prior to fixation. Analysis revealed that there was no improvement in terms of the proportion of single cells or the hybridisation efficiency (as determined by signal to background ratio) with either proteinase K concentration (Table 5.2). Therefore, proteinase K was not added to the final FISH-IS protocol.

**Table 5.2. The addition of proteinase K does not increase the number of single intact cells or the signal to background ratio.**

Proteinase K ( $\mu\text{g/mL}$ )	Single cells (%) (mean $\pm$ SD)	Signal to background* (mean $\pm$ SD)
<b>0</b>	<b>82.53 <math>\pm</math> 3.06</b>	<b>0.044 <math>\pm</math> 0.000</b>
10	78.83 $\pm$ 1.65	0.043 $\pm$ 0.000
20	72.13 $\pm$ 2.69	0.034 $\pm$ 0.001

\*Signal to background ratio is calculated by the geometric mean of fluorescence intensity divided by the geometric mean of raw max pixel following hybridisation with the 17 BAC probe contig. The optimal condition (no proteinase K) is indicated in bold. Data are the mean of 3 separate experiments  $\pm$  SD.

#### 5.3.4.2 Hybridisation optimisation

*Probe amount.* As FISH-IS has only previously been published with commercial centromeric probes (Minderman et al. 2012) for which probe concentrations are propriety information and therefore unavailable, it was not clear how much BAC contig probe would be optimal for a FISH-IS hybridisation. Various amounts of probe are used in standard conventional FISH, ranging from 0.2-1  $\mu\text{g}$  of probe. However these values are calculated depending on the area of hybridisation (normally 22 x 22 mm) (Leitch et al. 1991, Morrison et al. 2003, Bayani et al. 2004, Serakinci et al. 2009, Weise et al. 2009), a consideration which is clearly not relevant to FISH-IS. Therefore, in order to determine the optimal probe concentration of the 17p BAC contig probes, 0.68 to 1.4  $\mu\text{g}$  of the total BAC contig were tested (which is the equivalent of 2  $\mu\text{L}$  to 4  $\mu\text{L}$  of each BAC clone). For each amount of probe contig tested, each individual BAC was added in equal amounts. Analysis showed that spot

signals were not clear for less than 1  $\mu\text{g}$  of BAC contig (Figure 5.7A-B) and the background level became too high when the amount of BAC contig was above 1  $\mu\text{g}$  (Figure 5.7D-E). Therefore, it was determined that 1  $\mu\text{g}$  of total BAC contig (consisting of 60 ng per individual BAC probe) was the optimal amount of probe to use in FISH-IS (Figure 5.7C).

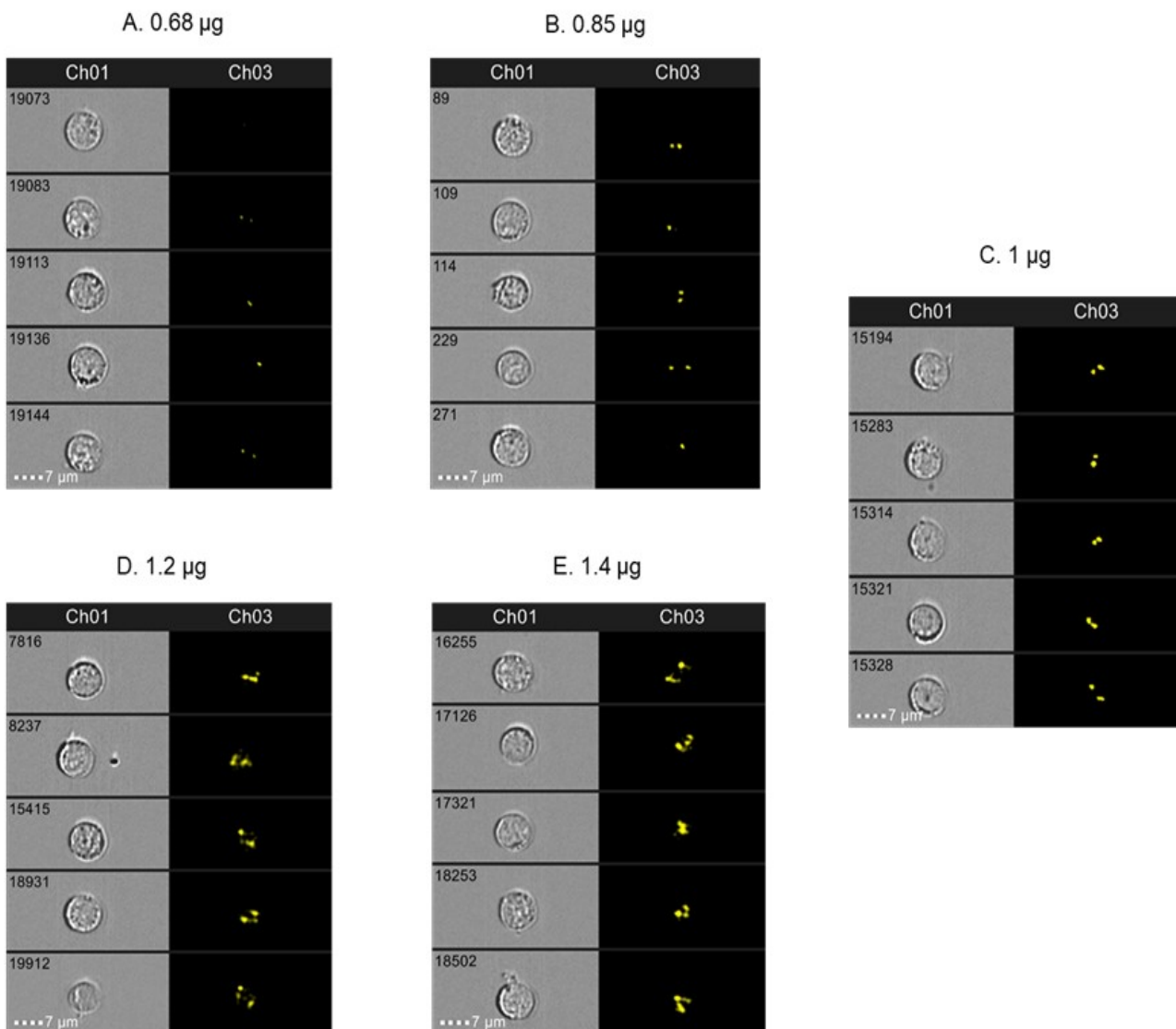


**Figure 5.7. One  $\mu\text{g}$  of BAC probe contig gives optimal hybridisation signal.**

*Brightfield images of cells captured by FISH-IS. The yellow dots represent signal generated from the hybridisation of probe to the chromosome 17p in increasing amounts of probe: (A) 0.68  $\mu\text{g}$ , (B) 0.85  $\mu\text{g}$ , (C) 1  $\mu\text{g}$ , (D) 1.2  $\mu\text{g}$ , (E) 1.4  $\mu\text{g}$  of the labelled BAC probe contig.*

*Cot-1 DNA.* Publications have reported using Cot-1: probe ratios ranging from 20-fold up to 100-fold in order to block nonspecific binding of labelled probes (Trask et al. 1988, Rauch et al. 2000, Dugan et al. 2005, Trifonov 2009, Bogomolov et al. 2014). Therefore, different amounts of Cot-1 DNA were tested in combination with the 17p BAC probes contig in order to determine the optimal Cot-1: BAC probe ratio for this FISH-IS methodology. The optimal Cot-1: BAC probe ratio was determined by analysing the signal to background ratio, calculated by the highest ratio of raw max pixel to fluorescence intensity. Hybridisation with either no Cot-1 or less than 50x Cot-1 resulted in signals which were dim and highly variable, presumably due to inadequate blocking of the repetitive sequences (Figure 5.8A-C). When analysing Cot-1 ratios at 50x and above, no significant improvement in signal to background ratio was seen (Figure 5.8D-F). Therefore, optimal specific hybridisation was achieved with the addition of 50x Cot-1 DNA.

*Addition of BSA and EDTA to pre-hybridisation wash buffer 1.* The addition of BSA and EDTA prior to hybridisation assists with centrifugation of cells whilst preventing clumps from forming. In order to determine the optimal concentration of both BSA and EDTA, a comparison of 0.25-1% BSA with 0-5 mM EDTA was undertaken (Table 5.3). Initial experiments were performed without BSA; however fixed cells were not able to be centrifuged to a pellet in the absence of BSA and therefore 0% BSA was not included as part of this analysis. Analysis revealed that the combination of 0.5% BSA + 5 mM EDTA in PBS provided the optimal wash buffer, giving 84.1% of single intact fixed cells in suspension for hybridisation (Table 5.3).

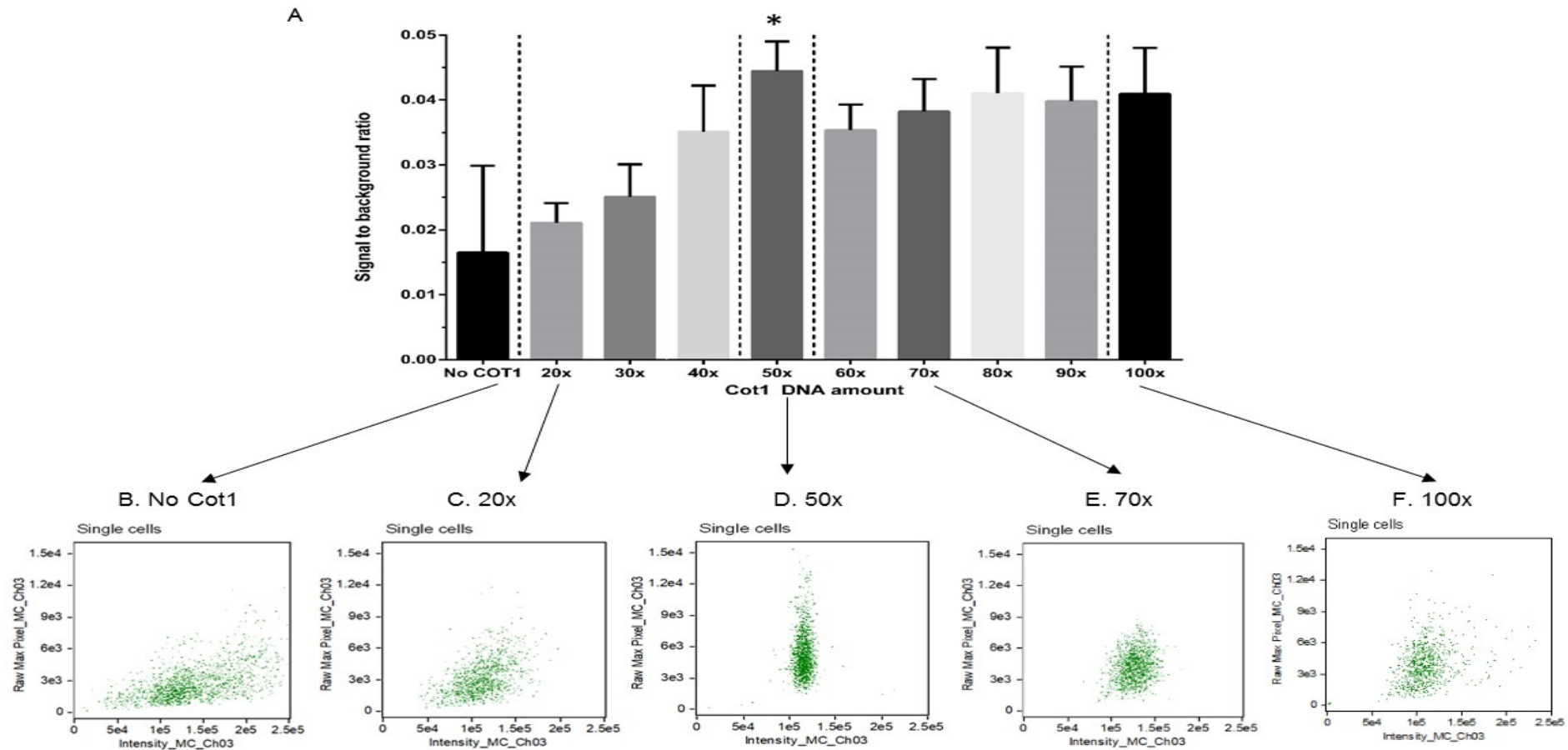


**Figure 5.8. Cot-1 optimisation demonstrates that 50x excess Cot-1 DNA results in optimal specific hybridisation.**

(A) Signal to background ratio is determined by fluorescence intensity and raw max pixel  $\pm$  SD. The only significant difference was found between no Cot-1 DNA vs 50x (\*  $p=0.02$ ; Student's *t*-test). (B - F) Dot plot of the fluorescence intensity (x-axis) and raw max pixel (y-axis) show FISH-IS results with various amounts of Cot-1 DNA. CLL samples with 100% wt17p (as determined by conventional FISH) were used. Data are representative of 3 separate experiments with normal-by-FISH CLL samples.

**Table 5.3. Optimisation of BSA and EDTA concentrations in the pre-hybridisation wash buffer 1.**

	0.25% BSA	0.5% BSA	0.75% BSA	1% BSA
0mM EDTA	76.32 ± 2.31	80.53 ± 1.31	80.03 ± 0.52	79.03 ± 1.52
1mM EDTA	74.43 ± 2.82	77.43 ± 1.82	79.20 ± 3.49	77.20 ± 1.49
2mM EDTA	75.63 ± 3.91	78.63 ± 1.91	81.60 ± 2.67	79.80 ± 0.67
3mM EDTA	76.43 ± 0.22	79.43 ± 1.22	79.33 ± 0.83	80.33 ± 1.83
4mM EDTA	74.93 ± 1.35	81.93 ± 1.31	82.40 ± 0.98	81.40 ± 0.88
<b>5mM EDTA</b>	78.53 ± 1.45	<b>84.10 ± 0.78</b>	76.73 ± 1.35	82.93 ± 1.32

The number of single intact cells percentages are shown. The optimal conditions (5mM EDTA and 0.5% BSA) are indicated in bold. Data are the mean of 3 separate experiments ± SD.

*Addition of EDTA to pre-hybridisation wash buffer 2.* Following the above BSA and EDTA treatment, cells were washed in a second buffer with a similar makeup to the hybridisation buffer (2X SSC+ 0.1% NP-40). Conventional FISH protocols include a wash in 2X SSC prior to hybridisation in order to stabilise cell and chromosome structure and increase tolerance to the high temperature of denaturation. Cells are incubated with this buffer to minimize non-specific binding and cross-hybridisation, whilst maximising the rate of probe binding to the target sequence (Mladinic et al. 2014). In addition, this step facilitates the evaporation of ethanol which may have remained from the fixation step, and removal of



BSA, as this can prevent probes from binding to their target sequences. The addition of 5 mM EDTA to 2X SSC + 1% NP40 was found to reduce cell clumping, as seen by visualisation under light microscope with 0.4% trypan blue staining (Figure 5.9).

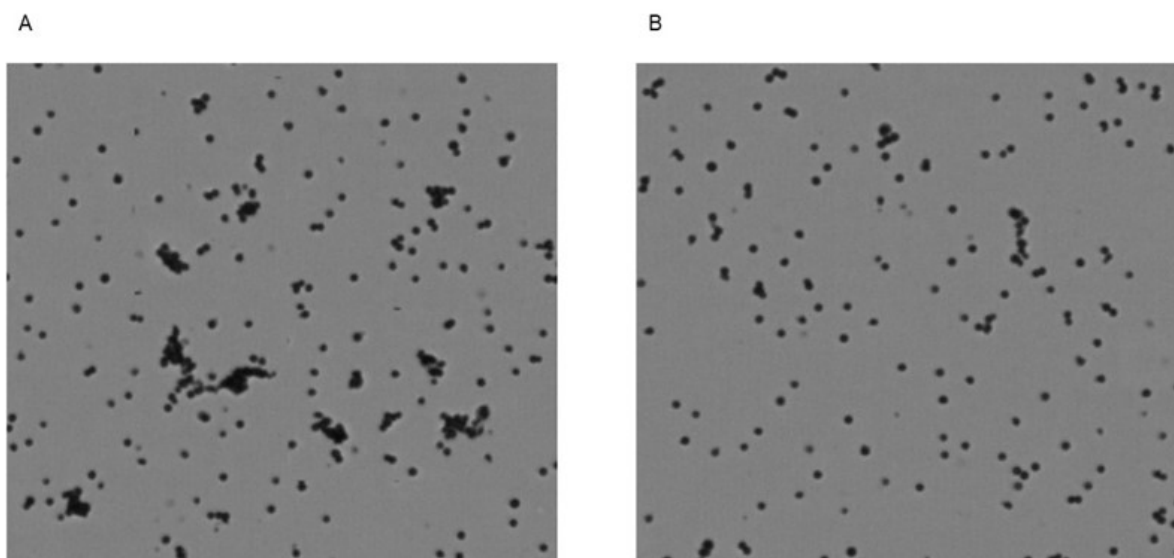


**Figure 5.9. Microscopic visualisation confirms an increase in single intact cells with the addition of EDTA in the pre-hybridisation wash buffer 2.**

*(A) No EDTA. (B) 5 mM EDTA with magnification 40x.*

*Denaturation.* There are several options for probe denaturation, including temperature denaturation, chemical denaturation, or a combination of both simultaneously. Mladinic et al. (2014) reported that chemical denaturation resulted in reduced probe binding specificity and a lower hybridisation success rate due to the fact that acid denaturation may result in damage to the probe fluorophores and hybridisation efficiency. This publication also showed that temperatures above 75°C (temperature could be raised up to 90°C) and longer denaturation times (up to 5 mins) resulted in better signals compared to background noise. Chin et al. (2003) noted that denaturation at 80°C for 10 mins resulted in improved

conventional FISH results. Optimisation of the denaturation temperature requires that it be high enough to unmask the target sequences to allow nucleotides to be exposed for probe binding, but not at a temperature which will cause damage to cell morphology and integrity. To determine optimal denaturation conditions, optimisation was based on methods (specifically temperatures, times and formamide percentage) which are widely used in conventional FISH protocols. A range of denaturation temperatures were tested (75°C, 80°C, 85°C, 90°C) at 2 time-points (2 mins or 5 mins) with various formamide percentages (50%, 55% and 60%). Identification of the most appropriate denaturation temperature was determined by the percentage of single intact cells of the total analysed population and the signal to background of the identified spots (Table 5.4).

This analysis revealed that regardless of other factors, there was a decline in the percentage of intact cells when treated with the higher denaturation temperatures (85°C or 90°C). Conversely, probe hybridisation efficiency was ineffective at 75°C/5 mins or 80°C/2 mins, presumably because denaturation was incomplete and therefore affected the hybridisation efficiency. Additionally, spot intensity was very dim in the presence of 60% formamide; analysis revealed that 50% formamide gave the best result with respect to spot intensity (Figure 5.10). Therefore, based on the percentage of intact single cells and the highest signal to background ratio, 80°C for 5 mins with LSI hybridisation buffer containing 50% formamide was selected as the appropriate denaturation conditions for the 17p BAC probe contig.

**Table 5.4. Optimisation of denaturation temperature, denaturation time and formamide concentration in hybridisation buffer.**

Denature temperature	Duration time (mins)	Formamide (%) in hybridisation buffer	Single cells (%) (mean $\pm$ SD)	Signal to background ratio* (mean $\pm$ SD)
75°C	5	50	79.07 $\pm$ 0.26	0.02 $\pm$ 0.01
		55	79.83 $\pm$ 0.96	0.02 $\pm$ 0.01
		60	80.77 $\pm$ 2.50	0.01 $\pm$ 0.02
80°C	2	50	80.37 $\pm$ 1.39	0.02 $\pm$ 0.00
		55	78.20 $\pm$ 4.23	0.02 $\pm$ 0.01
		60	78.9 $\pm$ 0.16	0.01 $\pm$ 0.00
	5	<b>50</b>	<b>79.57 <math>\pm</math> 0.53</b>	<b>0.05 <math>\pm</math> 0.00</b>
		55	76.73 $\pm$ 8.66	0.03 $\pm$ 0.01
		60	78.43 $\pm$ 5.42	0.02 $\pm$ 0.01
85°C	2	50	59.63 $\pm$ 10.30	0.02 $\pm$ 0.00
		55	61.27 $\pm$ 6.45	0.02 $\pm$ 0.01
		60	52.41 $\pm$ 3.52	0.01 $\pm$ 0.00
	5	50	44.43 $\pm$ 2.91	0.02 $\pm$ 0.00
		55	40.45 $\pm$ 5.58	0.02 $\pm$ 0.01
		60	51.3 $\pm$ 9.08	0.00 $\pm$ 0.00
90°C	2	50	41.9 $\pm$ 6.78	0.01 $\pm$ 0.00
		55	32.87 $\pm$ 4.87	0.01 $\pm$ 0.01
		60	38.40 $\pm$ 8.22	0.00 $\pm$ 0.00

\*Signal to background ratio is calculated by geometric mean of fluorescence intensity divided by the geometric mean of raw max pixel. The optimal conditions (80°C, 5 mins, and 50% formamide) are indicated in bold. Data are the mean of 3 separate experiments  $\pm$  SD.

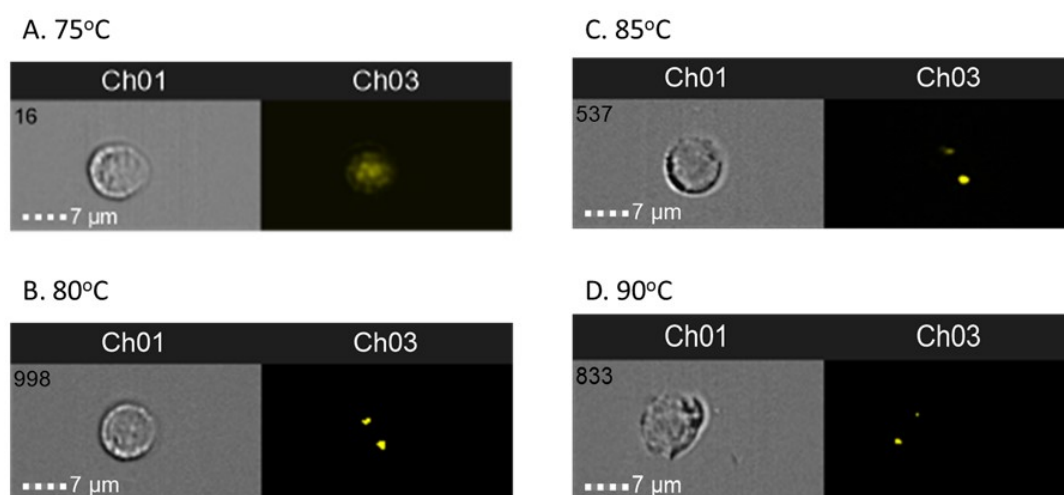


**Figure 5.10. Representative images of different denaturation temperature and time.**

(A) 75°C/5 mins, (B) 80°C/5 mins, (C) 85°C/5 mins and (D) 90°C/2 mins, all with 50% formamide.

*Hybridisation conditions.* Optimisation of hybridisation conditions requires assessment of hybridisation temperature, duration, pH, formamide concentration, salt concentration and dextran sulfate concentration. The majority of conventional FISH protocols are in agreement that the following conditions are optimal for DNA BAC probes: pH  $7 \pm 0.2$ , 2X SSC, 10% dextran sulfate (Bradley et al. 2009, Serakinci et al. 2009, Weise et al. 2009, Liehr et al. 2017). However, these publications detailed a variety of formamide concentrations, temperature and hybridisation duration depending on the probes applied. Analysis was therefore undertaken in order to determine which hybridisation temperature and time were required for optimal signal from the 17p BAC probe conmtig used here. Experiments were carried out with a range of hybridisation temperatures (37°C to 45°C) and a range of formamide percentages in the hybridisation buffer (50%, 55% and 60%) (Table 5.5). This analysis revealed that hybridisation at 42°C with 50% formamide buffer gave the greatest specificity of probe hybridisation with a reasonable level of single intact cells (Figure5.11).

**Table 5.5. Optimisation of hybridisation temperature and formamide concentration in hybridisation buffer.**

Hybridisation temperature	Formamide concentration (%)	Single cells (%) (mean $\pm$ SD)	Signal to background ratio* (mean $\pm$ SD)
37°C	50	80.97 $\pm$ 1.78	0.02 $\pm$ 0.01
	55	81.03 $\pm$ 0.96	0.02 $\pm$ 0.01
	60	81.13 $\pm$ 2.52	0.01 $\pm$ 0.00 (Figure 5.11A)
38°C	50	80.02 $\pm$ 1.42	0.02 $\pm$ 0.00 (Fig 5.11B)
	55	78.73 $\pm$ 9.66	0.02 $\pm$ 0.01
	60	79.43 $\pm$ 2.32	0.01 $\pm$ 0.01
39°C	50	78.73 $\pm$ 2.34	0.03 $\pm$ 0.01
	55	80.93 $\pm$ 3.91	0.03 $\pm$ 0.00
	60	75.43 $\pm$ 7.62	0.02 $\pm$ 0.01
40°C	50	79.53 $\pm$ 1.56	0.03 $\pm$ 0.00 (Figure 5.11C)
	55	78.13 $\pm$ 1.57	0.02 $\pm$ 0.01
	60	77.43 $\pm$ 1.49	0.01 $\pm$ 0.01
41°C	50	78.53 $\pm$ 2.14	0.03 $\pm$ 0.00
	55	76.13 $\pm$ 3.59	0.03 $\pm$ 0.01
	60	77.43 $\pm$ 5.49	0.02 $\pm$ 0.01
<b>42°C</b>	<b>50</b>	<b>79.96 <math>\pm</math> 3.53</b>	<b>0.05 <math>\pm</math> 0.00 (Figure 5.11D)</b>
	55	77.77 $\pm$ 7.66	0.03 $\pm$ 0.01
	60	75.53 $\pm$ 8.42	0.02 $\pm$ 0.01
43°C	50	65.57 $\pm$ 3.53	0.04 $\pm$ 0.00 (Figure 5.11E)
	55	72.29 $\pm$ 7.66	0.03 $\pm$ 0.01
	60	58.23 $\pm$ 9.42	0.02 $\pm$ 0.01
44°C	50	38.57 $\pm$ 5.96	0.02 $\pm$ 0.00
	55	46.73 $\pm$ 0.66	0.02 $\pm$ 0.01
	60	49.49 $\pm$ 9.45	0.01 $\pm$ 0.00
45°C	50	39.97 $\pm$ 3.45	0.02 $\pm$ 0.01
	55	30.53 $\pm$ 9.86	0.01 $\pm$ 0.01
	60	35.73 $\pm$ 1.42	0.00 $\pm$ 0.00 (Fig 5.11F)

\*Signal to background ratio is calculated as Table 5.4. The optimal conditions (42°C, 50% formamide) are indicated in bold. Data are the mean of 3 separate experiments  $\pm$  SD.

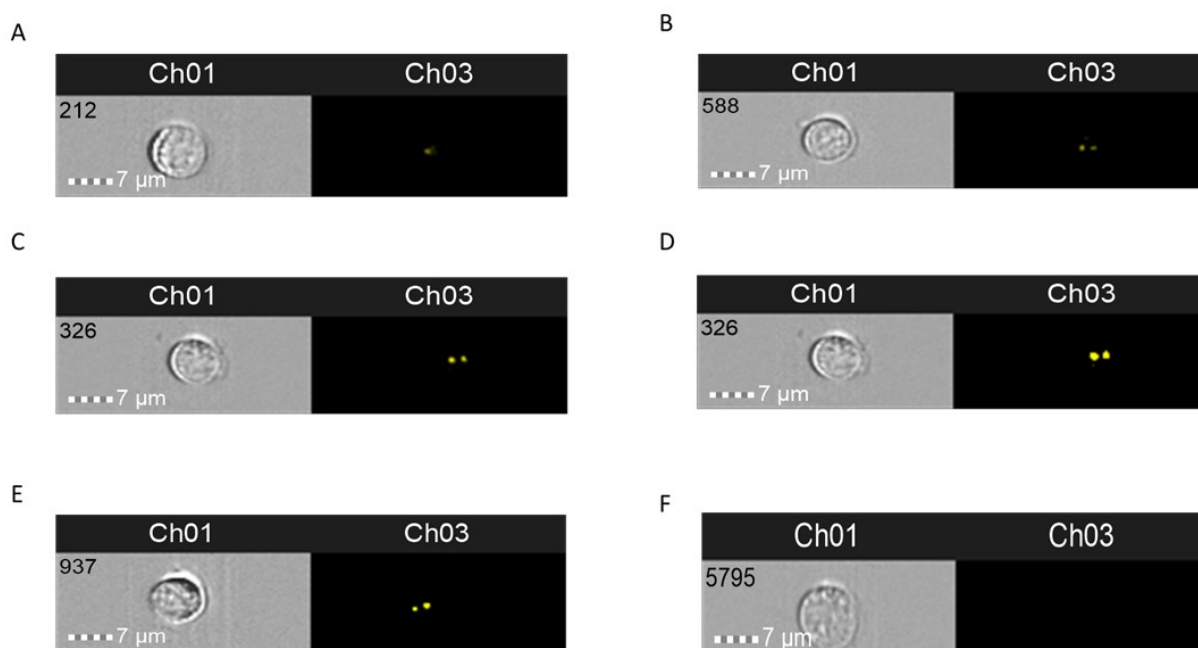


**Figure 5.11. Representative images of different hybridisation temperature and formamide concentration.**

(A) – (F) as annotated in Table 5.5.

Furthermore, Minderman et al. (2012) concluded that there were no significant differences in FISH-IS results when the hybridisation incubation time ranged from 9-14 hours.

Therefore, a comparison of duration of probe hybridisation was undertaken, ranging from 9 to 15 hours in 1-hour increments. This analysis revealed that with 11 hours or less hybridisation, the signal was dull and non-specific (Figure 5.12A). Following 15 hours or more of probe hybridisation, the signals were inconsistent with more non-specific binding and also resulted in fading of the fluorescence signals (Figure 5.12B) when compared to 12 hours hybridisation (Figure 5.12C) with punctuated two signals in each cell. Therefore, 12 hours was determined the optimal incubation time for hybridisation.

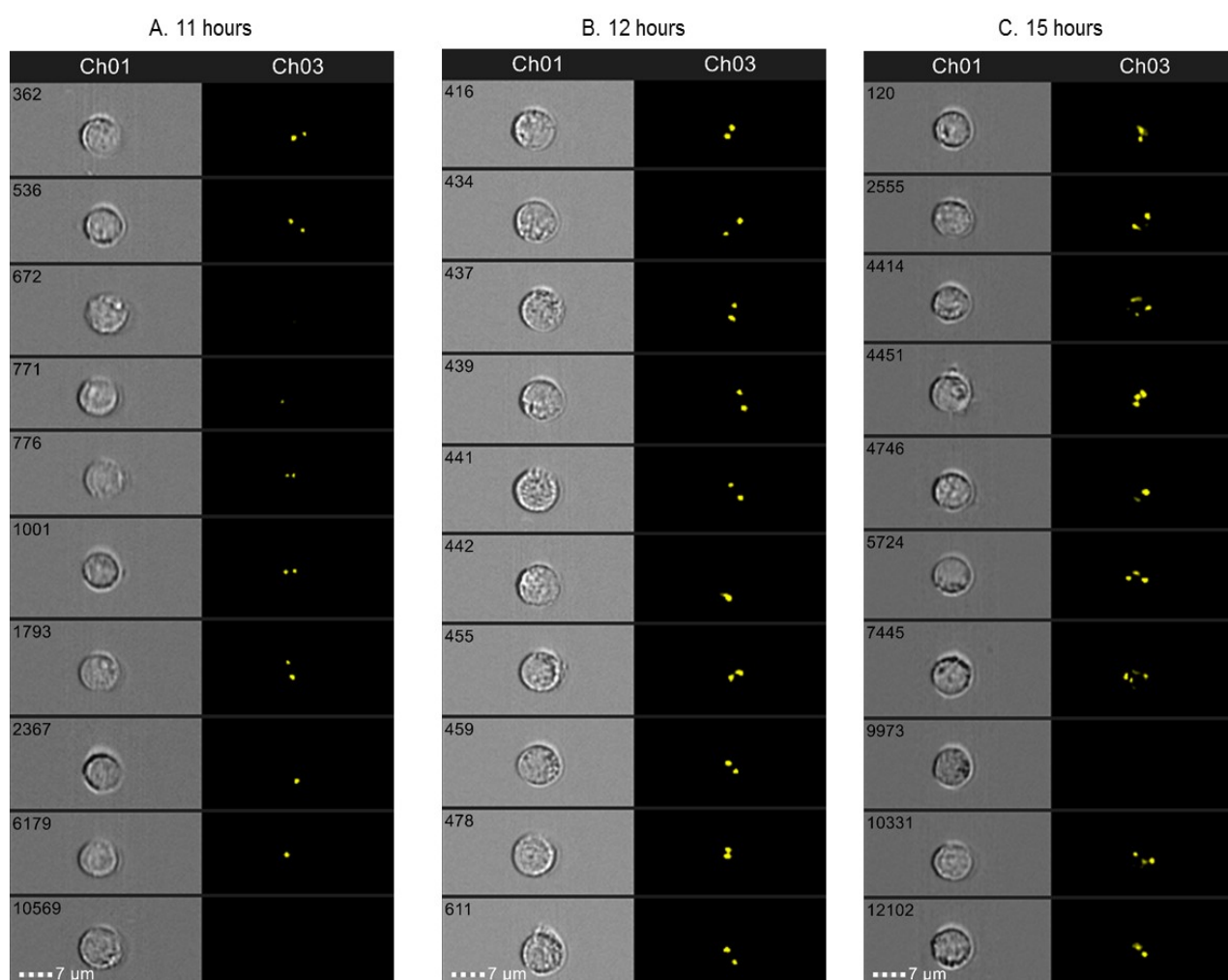


**Figure 5.12. Twelve hours is the optimal hybridisation time for FISH-IS with the 17p BAC probe contig.**

(A) Representative FISH-IS results of 11 hours probe hybridisation. Similar results were obtained with 9 and 10 hours probe hybridisation. (B) Representative FISH-IS results of 12 hours of probe hybridisation. Similar results were obtained with 13 and 14 hours probe hybridisation. (C) Representative FISH-IS results of 15 hours probe hybridisation. Similar results were obtained with 16 and 17 hours probe hybridisation. Data are representative of 3 separate experiments.

#### 5.3.4.3 Wash optimisation

Two wash steps are included in the FISH-IS protocol. Wash 1 is a low stringency wash which removes the unbound excess probe and wash 2 is a high stringency wash which removes non-specific and cross hybridised probes. In addition to removing unwanted probes, both

washes are required to be mild enough to maintain good cell morphology. To optimise individual aspects of each wash, the following method was employed: each post-hybridisation sample was divided into two aliquots, the first aliquot was treated with the standard wash conditions and the second aliquot was treated with the standard conditions plus one variation as listed in Table 5.6. The results of these comparisons are described below, and the optimal final conditions are annotated in Table 5.6.

**Table 5.6. Summary of optimisation of washing conditions for FISH-IS.**

	Variable optimisation	Final method
<b>Wash 1</b>		
SSC	1X, 2X	<b>2X</b>
NP40	0.1%, 0.2%, 0.3%	<b>0.1%</b>
Time	5, 10 mins	<b>5 mins</b>
Temperature	RT, 37°C, 42°C, 48°C, 55°C, 65°C	<b>RT</b>
Formamide	0%, 10%, 20%, 30%	<b>0%</b>
Number of washes	1, 2, 3	<b>1</b>
<b>Wash 2</b>		
SSC	0.1X, 0.2X, 0.3X, 0.4X	<b>0.4X</b>
NP40	0.3%, 0.4%, 0.5%	<b>0.3%</b>
Time	2, 2½, 3, 3½, 4, 4½, 5 mins	<b>3 mins</b>
Temperature	73°C, 74°C, 75°C, 76°C	<b>73°C</b>
Formamide	0%, 10%, 20%	<b>0%</b>
Number of washes	1, 2	<b>1</b>

*The optimal final methods for wash1 and wash 2 are indicated in bold.*



*SSC concentration.* The concentration of salt in a wash buffer, in the form of saline-sodium citrate (SSC), provides ionic strength for the removal of non-specific and cross-hybridised probes. A lower SSC concentration will yield a higher stringency wash, resulting in higher probe binding specificity to the target DNA (Pinkel et al. 1986). Initial optimisation experiments involved altering the SSC concentrations of wash 1 (2X (standard), Figure 5.13A; 1X, Figure 5.13B) and wash 2 (0.4X (standard), Figure 5.14A; 0.1X, Figure 5.14B; 0.2X, Figure 5.14C; 0.3X, Figure 5.14D). The resultant FISH-IS images demonstrated that reducing SSC concentration in either wash 1 or wash 2 resulted in a higher stringency wash and loss of the specific signals as the probe dissociated from its target sequence. Therefore, standard SSC concentration in both washes were found to be optimal (Figure 5.13A and Figure 5.14A).

*NP40 concentration.* Another component of the wash solutions which can be manipulated to alter stringency is the detergent concentration (NP40), with an increase in detergent concentration resulting in higher stringency. Various concentrations of NP40 in both wash 1 (0.2%, Figure 5.13C; 0.3%, Figure 5.13D) and wash 2 (0.4%, Figure 5.14E; 0.5%, Figure 5.14F) were trialled. There were no improvements in the signal to background with increasing NP40 concentration when compared to the standard wash concentration of 0.1% NP40 in wash 1 (Figure 5.13A) and 0.3% NP40 in wash 2 (Figure 5.14A).

*Time and temperature.* Higher stringency washes are generated by increasing either wash time and/or wash temperature. This optimisation method included trialling alterations in wash time (5 mins (standard), Figure 5.13A; 10 mins, Figure 5.13E) and wash temperature in wash 1 (RT (standard), Figure 5.13A; 37°C, 42°C, 48°C, 55°C, 65°C, Figure 5.13F-J). Similarly, alterations in both wash time (3 mins (standard), Figure 5.14A; 2, 2½, 3½, 4, 4½, 5 mins; Figure 5.14G-L) and wash temperature (73°C (standard), Figure 5.14A; 74°C, 75°C,

76°C; Figure 5.14M-0) were also undertaken for wash 2. Overall however, it was found that none of these changes improved the level of signal to background and therefore the standard wash times and temperatures were retained.

*Formamide concentration.* The presence of formamide in wash solutions has been shown to increase the stringency of the washes. Experiments were conducted with different formamide percentages in both wash 1 (10%, 20%, 30%; Figure 5.13K-M) and wash 2 (10%, 20%; Figure 5.14P-Q). However, it was clear that optimal results were achieved with formamide-free wash buffers (Figure 5.13A, Figure 5.14A).

*Additional washes.* The final change to the wash methodology which was tested was the incorporation of additional washes, which would be expected to reduce non-specific binding. However, analysis shows that increasing the number of wash 1 from 1 to 2 (Figure 5.13N) or 3 (Figure 5.13O), or increasing the number of wash 2 from 1 to 2 (Figure 5.14R) resulted in the removal of specific probe binding, thereby reducing signal intensity. In addition, the morphology of the cells was adversely affected by increasing the number of washes, and therefore the standard number of 1 for each wash was maintained (Figure 5.13A, Figure 5.14A).

In conclusion, it was found that increasing the stringency of the washes by reducing the salt concentration, increasing the proportion of NP40, and increasing washing time and temperature, did not improve the specific signal binding of the 17p BAC probe contig. Therefore, the final optimal methodology for washing was as follows: 1x Wash 1 (2X SSC + 0.1% NP40) for 5 mins at RT followed by 1x Wash 2 (0.4X SSC + 0.3% NP40) for 3 mins at 73°C.

**Figure 5.13. Various features of wash 1 were altered in order to optimise the FISH-IS method.**

*(A) Standard conditions: 1x Wash 1 (2X SSC + 0.1% NP40) for 5 mins at RT. (B) 1X SSC. (C) 0.2% and (D) 0.3% NP40. (E) 10 mins wash time. (F) 37°C, (G) 42°C, (H) 48°C, (I) 55°C and (J) 65°C wash temperature. (K) 10%, (L) 20% and (M) 30% formamide concentration. (N) 2X and (O) 3x Wash 1. Data are representative of 3 separate experiments.*

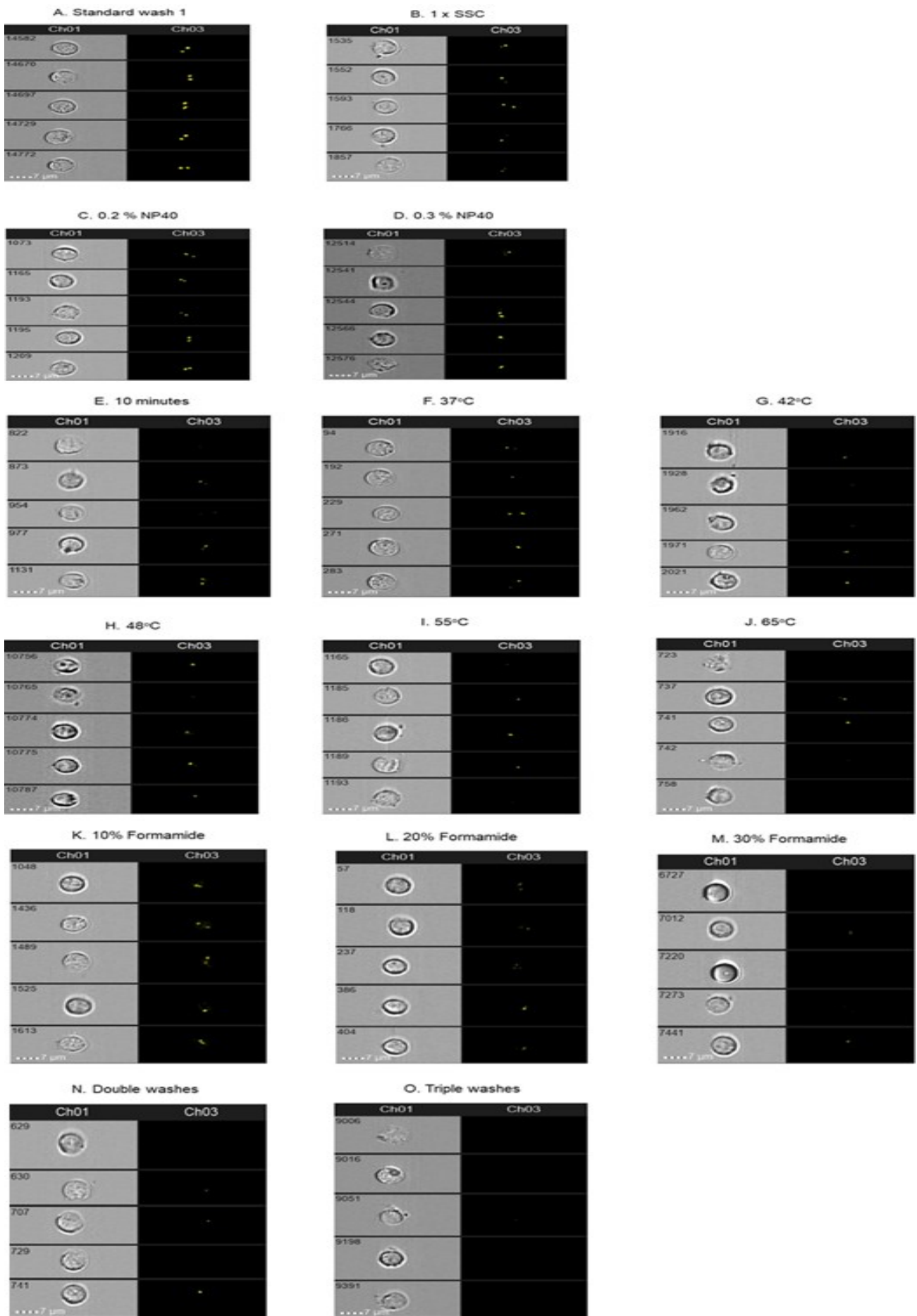
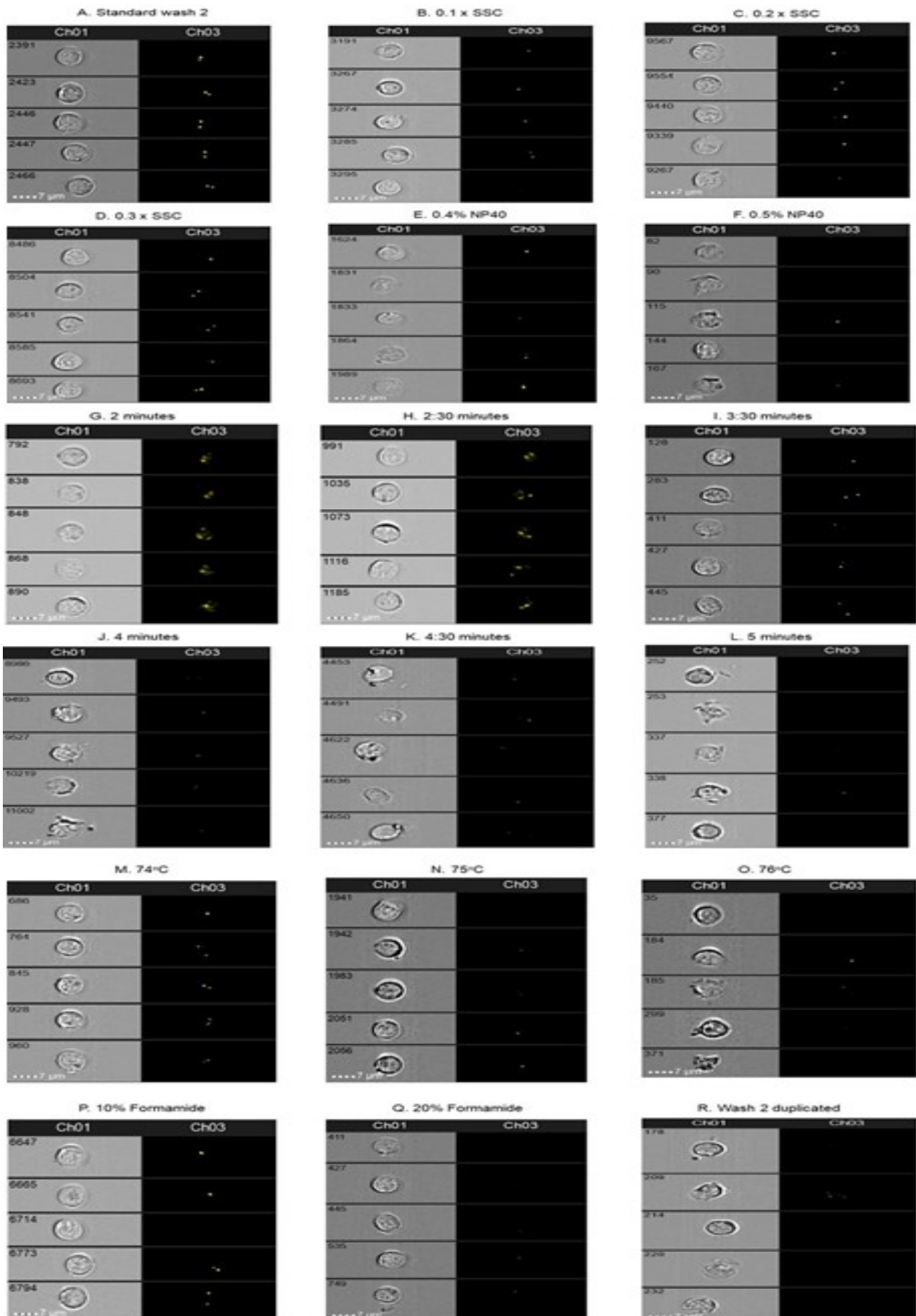


**Figure 5.14. Various features of wash 2 were altered in order to optimise the FISH-IS method.**

*(A) Standard conditions: 1x Wash 2 (0.4X SSC + 0.3% NP40) for 3 mins at 73°C. (B) 0.1X, (C) 0.2X and (D) 0.3X SSC. (E) 0.4% and (F) 0.5% NP40. (G) 2 mins, (H) 2½ mins, (I) 3½ mins, (J) 4 mins, (K) 4 ½ mins and (L) 5 mins wash time. (M) 74°C, (N) 75°C and (O) 76°C wash temperature. (P) 10% and (Q) 20% formamide. (R) 2X Wash 2. Data are representative of 3 separate experiments.*



### 5.3.4.4 Visualisation optimisation

The visualisation of FISH signal, as determined by the INPIRES acquire/acquisition program, was optimised at several points (Figure 5.15): laser power intensity, camera resolution, EDF mode and flow speed. Focus and centering of the cells were set automatically.

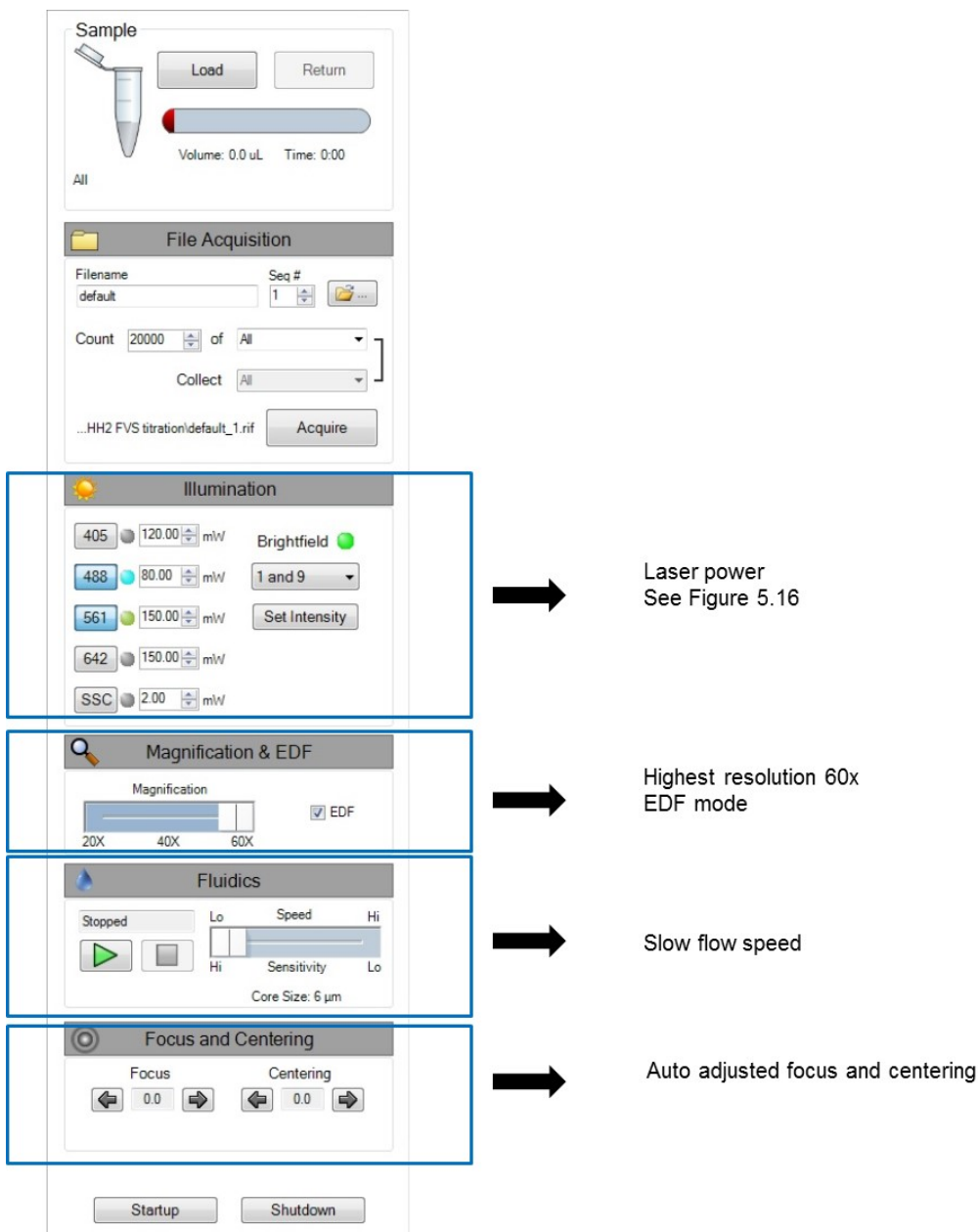


**Figure 5.15. Schematic representation of image acquisition optimisation.**

*Instrument settings of the ImageStreamX machine are indicated.*

1. Laser power intensity. The optimal laser power input was determined in order to maximise the difference between the background fluorescence and the probe intensity. Hybridisations were carried out according to the optimised FISH-IS protocol (see section 5.2.4) on normal karyotype CLL samples with the 17p BAC probe contig which was labelled with spectrum orange and spectrum green. In addition, cells without the 17p BAC probe contig (containing only hybridisation buffer and Cot-1 DNA) were also analysed in order to determine the background fluorescence. Analysis of these samples was performed on the ImageStreamX with the appropriate laser wavelength (561 nm laser for spectrum orange and 488 nm for spectrum green). The largest distance between the geometric mean of signals (cells with probe hybridisation) and background intensity (cells with no probes added) was chosen as the optimal laser power (Figure 5.16). The largest discrepancy between the signal and background was at 80 mW power for the 488 nm laser ( $p=0.01$ ), and 150 mW for the 561 nm laser ( $p=0.03$ ).
2. Camera resolution. The highest level of camera resolution (0.5  $\mu\text{m}$  per pixel) was chosen, which was equivalent to 60x magnification.
3. Extended depth of field (EDF) was applied according to Ortyń et al. (2007); this significantly improves the imagery of FISH probes by removing other variation.



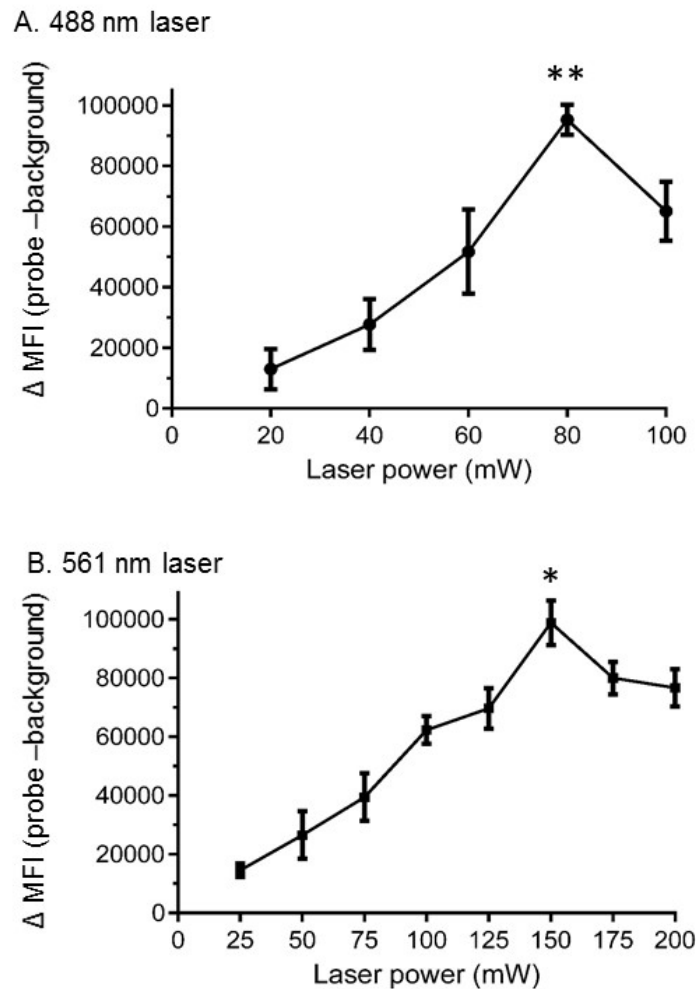


**Figure 5.16. Optimisation of the laser power.**

Each data point represents the  $\Delta$  MFI at a given laser power calculated by the FISH-IS result for a CLL sample (normal karyotype by conventional FISH) hybridised with 17p BAC probe contig minus the same sample with no hybridised probes (background). (A) 488 nm laser; the highest  $\Delta$  MFI (probe to background) was obtained at 80 mW power (\*\* $p=0.001$ ; Students *t*-test). (B) 561 nm laser; the highest  $\Delta$  MFI (probe to background) was achieved at 150 mW power (\* $p=0.03$ , Students *t*-test). Data are the mean of 3 separate experiments  $\pm$  SD.  $\Delta$  MFI: differences between mean fluorescence intensity.

### **5.3.5 FISH-IS is able to distinguish 17p-deleted cells from wild-type 17p cells**

Following FISH-IS with the 17 BAC probe contig, results were analysed by multiple methods in order to determine the optimal analysis which is able to separate different cell populations based on 17p allele(s) status (Figure 5.17). This analysis demonstrated that two populations of cells could be successfully separated based on fluorescence intensity and raw max pixel (Figure 5.17A). This separation was significantly less successful with the other analysis strategies trialled, spot count analysis and bright detail intensity analysis (Figure 5.17B-C). These findings are in agreement with previously published work (Minderman et al. 2012, Fuller et al. 2016)).

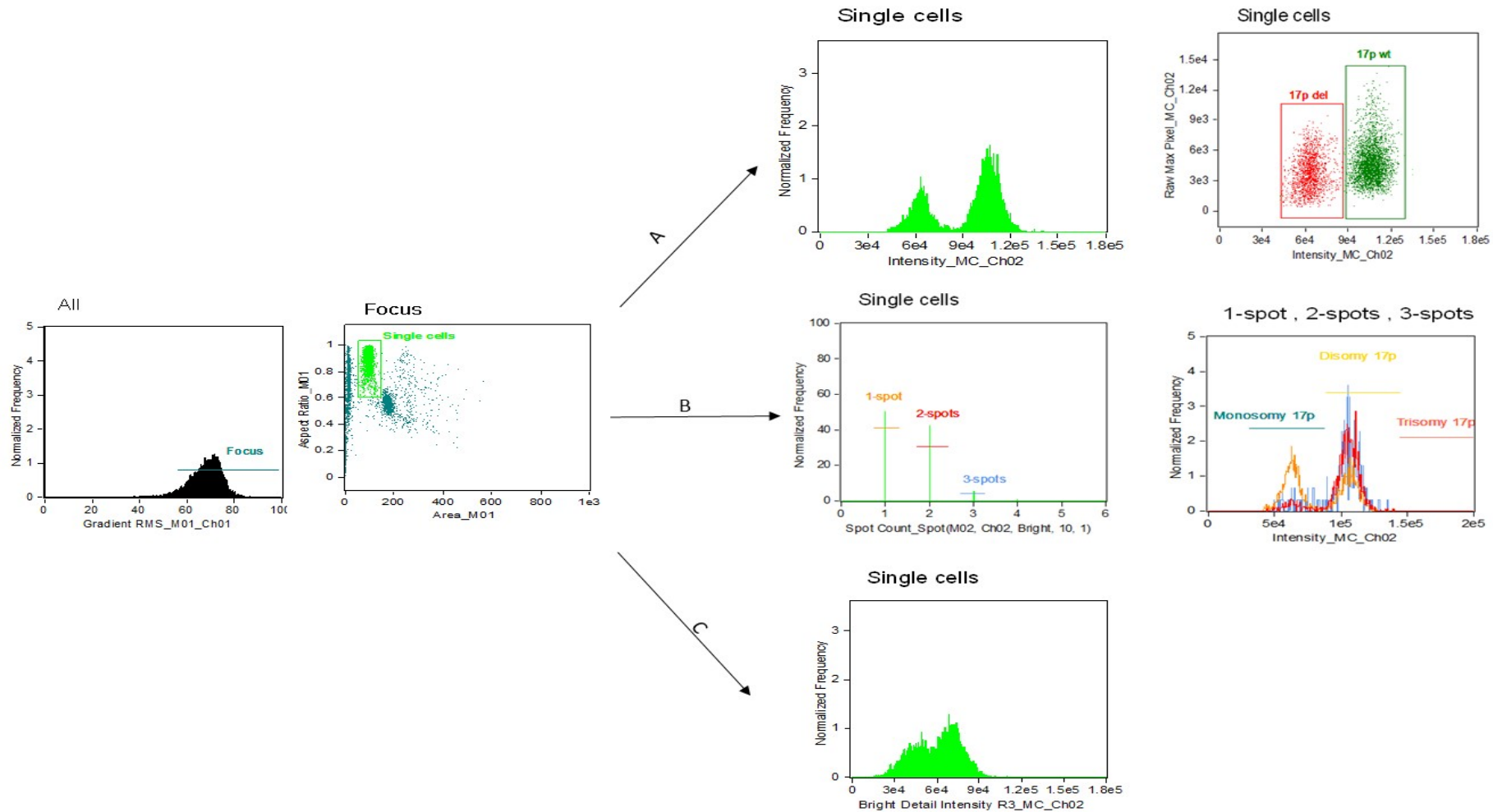
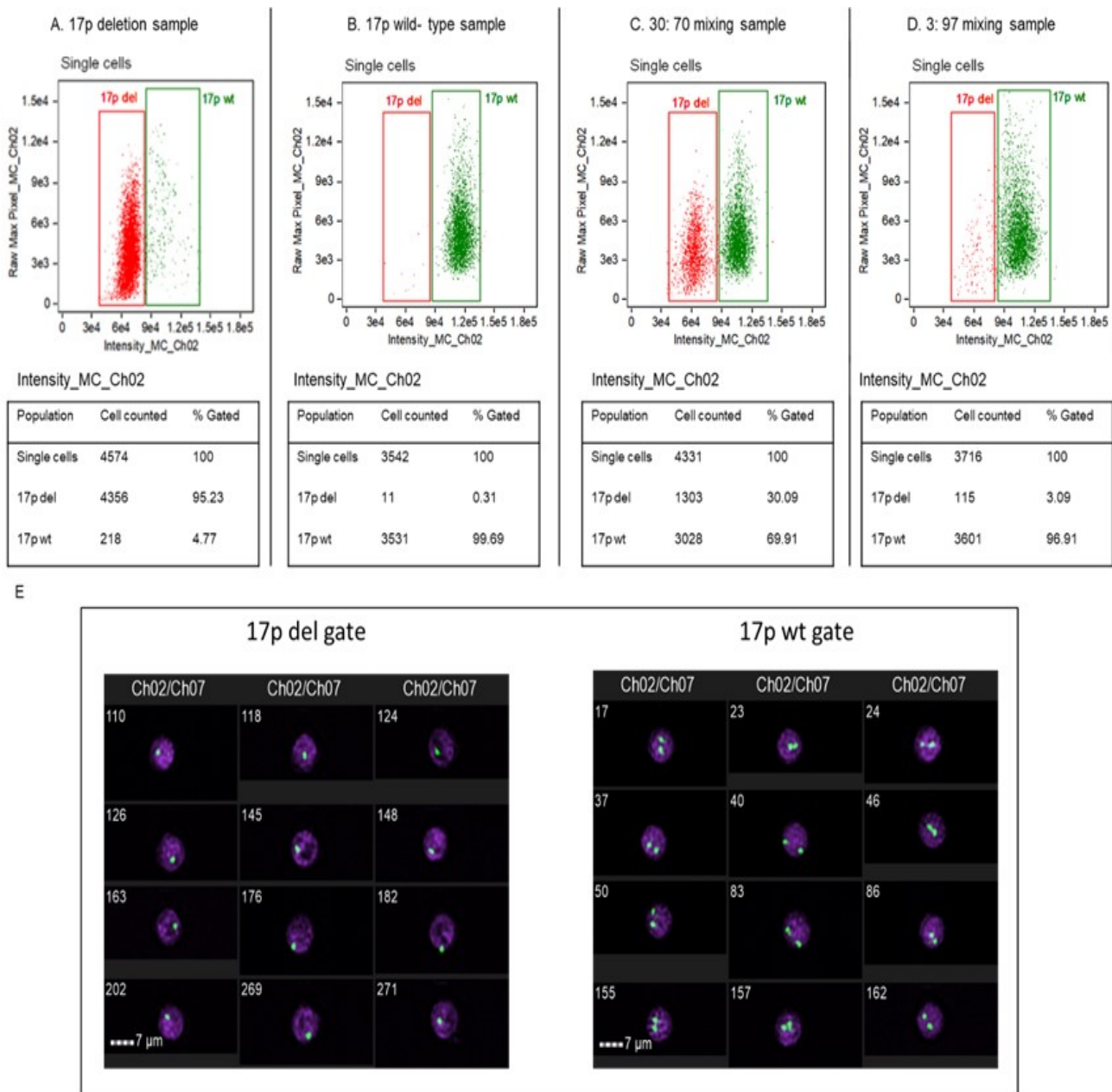


Figure 5.17. Analysis by raw max pixel and fluorescence intensity of the 17p BAC probe contig gives the best discrimination of two separate populations.

(A) Analysis by fluorescence intensity alone or combining with raw max pixel. (B) Analysis by spot count and (C) Analysis by detail intensity analysis. Data are representative of 3 separate experiments.

Although the ultimate purpose of this FISH-IS with the 17p BAC probe contig method is to detect low frequency del17p sub-clones in CLL samples, a fresh CLL sample with a known high frequency del17p sub-clone (95% del17p cells as determined by conventional FISH) was analysed due to the rarity of fresh CLL samples with low frequency del17p sub-clones. This sample analysis showed that 95.23% of cells were 17p deletion (Figure 5.18A) in agreement with 95% by conventional FISH. Furthermore, a 100% wt17p fresh CLL sample (ascertained by FISH) was carried out by FISH-IS to confirm that 99.69% cells were wild-type 17p (2 spots) (Figure 5.18B). As a consequence, these analyses were able to prove that the optimised FISH-IS methodology was capable of discriminating CLL cells based on their 17p status. On the other hand, as multiple fresh CLL samples with different percentages of del17p sub-clones were unavailable, in order to determine the accurate sensitivity of this method the optimised FISH-IS with BAC probe contig technique was applied to controlled mixing CLL samples. This mixing model was generated from combining CLL cells obtained from a patient with a large (95%) 17p-deleted clone size (Figure 5.18A) with cells obtained from a patient with 17p-wild-type CLL cells (Figure 5.18B) in various known ratios (see section 5.2.3). By applying the optimised FISH-IS, it was possible to discriminate between the two populations across various ratios of del17p versus wt17p, including 30:70 (Figure 5.18C) and 3:97 (Figure 5.18D). Visual inspection of the cells confirmed that, as expected, the del17p gate contained cells with 1 spot in their nuclei and the wt17p gate contained cells with 2 spots in their nuclei (Figure 5.18E). These data demonstrate that the 17p BAC probe contig can be used in FISH-IS for the detection of del17p sub-clones in a heterogeneous CLL cell population.



**Figure 5.18. FISH-IS is able to accurately differentiate del17p CLL cells within a mixing model based on fluorescence intensity.**

(A) FISH-IS analysis of a CLL sample with 95% del17p (as determined by conventional FISH analysis). (B) FISH-IS analysis of a CLL sample with 100% wt17p (as determined by conventional FISH). (C, D) FISH-IS analysis of mixed samples generated from combining CLL samples shown in (A), (B) with ratios 30:70 and 3:97. (E) Representative FISH-IS images of cells from the del17p gate and wt17p gate respectively in 30:70 mixing sample. Data are representative of 3 separate experiments in duplicate.

In order to determine the level of sensitivity of detection of del17p CLL cells with the BAC contig in FISH-IS, various ratios of del17p to wt17p CLL cells were analysed by FISH-IS and compared with conventional FISH results (Table 5.7). This analysis showed that this assay is able to accurately detect a del17p sub-clone present at 3%. Where there is less than 3%, FISH-IS results overestimated the del17p percentages.

**Table 5.7. FISH-IS analysis based on fluorescence intensity of CLL controlled mixed samples.**

CLL mixes (%) del17p: wt17p	FISH-IS result (%)		Conventional FISH result (%)	
	del17p (mean $\pm$ SD)	wt17p (mean $\pm$ SD)	del17p (mean $\pm$ SD)	wt17p (mean $\pm$ SD)
0: 100	1.64 $\pm$ 0.50	98.36 $\pm$ 0.50	1.66 $\pm$ 0.62	98.33 $\pm$ 0.62
1: 99	2.70 $\pm$ 0.44	97.21 $\pm$ 0.44	1.83 $\pm$ 0.24	98.17 $\pm$ 0.24
2: 98	2.85 $\pm$ 0.23	97.11 $\pm$ 0.19	2.33 $\pm$ 0.85	97.67 $\pm$ 0.85
3: 97	2.98 $\pm$ 0.16	97.02 $\pm$ 0.16	3.17 $\pm$ 0.62	97.33 $\pm$ 0.62
5: 95	4.99 $\pm$ 0.03	95.00 $\pm$ 0.03	4.67 $\pm$ 1.17	95.33 $\pm$ 1.17
10: 90	9.98 $\pm$ 0.01	90.00 $\pm$ 0.01	10.17 $\pm$ 0.62	89.83 $\pm$ 0.62
20: 80	19.87 $\pm$ 0.12	79.93 $\pm$ 0.12	19.50 $\pm$ 0.82	80.50 $\pm$ 0.82
30: 70	30.00 $\pm$ 0.08	69.90 $\pm$ 0.08	29.50 $\pm$ 0.82	70.50 $\pm$ 0.82
40: 60	39.05 $\pm$ 0.06	59.8 $\pm$ 0.06	39.50 $\pm$ 0.82	60.5 $\pm$ 0.82
50: 50	49.97 $\pm$ 0.05	49.87 $\pm$ 0.05	49.17 $\pm$ 1.02	50.83 $\pm$ 1.02
95: 5	95.10 $\pm$ 0.16	4.76 $\pm$ 0.16	95.50 $\pm$ 1.08	4.50 $\pm$ 1.08

*Data are the mean of 3 separate experiments  $\pm$  SD.*

### 5.3.6 Sanger sequencing confirms that FISH-IS can discriminate del17p sub-clone.

In order to avoid interference with the Sanger sequencing results, in which the primers spanned the BAC containing *TP53* gene (RP11-199F11), this BAC clone was omitted from the 17p BAC probe contig used in this assay. It is noted that the removal of this single clone resulted in a slight signal reduction; however as this reduction was not significant it was determined that analysis with the 16 BAC probe contig was sufficient for sorting (Figure 5.19).

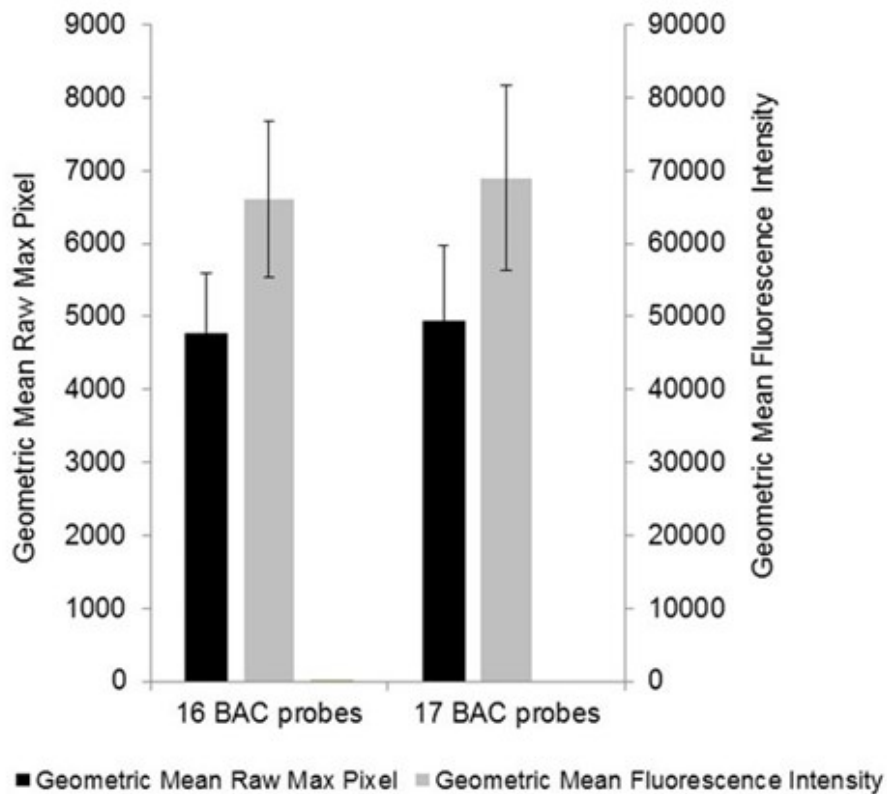


**Figure 5.19. Removal of BAC RP11-199F11 from the probe contig does not significantly affect raw max pixel intensity nor fluorescence intensity when analysed by FISH-IS.**

*Data are the geometric mean of 3 separate experiments  $\pm$  SD on normal karyotype CLL samples.*

The FISH-IS with the 17p BAC probe contig technique was then applied to a fresh CLL sample containing 85% del17p in order to examine whether the 15% of cells with two copies of 17p could be enriched. Again, due to the rarity of low frequency del17p sub-clone CLL samples, the proof-of-principle analysis was carried out on a high frequency del17p sample.

Given that the ImageStreamX machine does not have a sorting function, a BD FACSAria™ Fusion flow sorter was used to sort cells based on 17p BAC probe contig fluorescence intensity. However, due to a lack of distinctly separated fluorescence intensity peaks using the BD FACSAria™ Fusion, the sort fractions for the 85% 17p-deleted cells were determined using the linear mean fluorescence intensity histogram. Clumped cells were contained in fraction 4 and fraction 1 comprised cell fragments and debris. Fraction 2 and fraction 3 were applied according to the percentage of 17p-deleted cells in the conventional FISH (Figure 5.20A). Fluorescence intensity of the 17p-deleted cells was compared to the histogram of the wt17p cells results which were conducted from three experiments using 100% wild-type 17p CLL samples. The histogram overlay of the 17p-deleted cells and 17p-wild-type cells shows an overlap of approximately 15%. This is similar to the percentage of wt17p cells in this 17p deleted sample (Figure 5.20B). Following fractionation, DNA was extracted and two heterozygous SNPs located within *TP53* were analysed by Sanger sequencing (see section 5.2.4). Sanger sequencing of the unsorted sample showed a single nucleotide at both SNPs, confirming the high level of monosomic 17p cells contained within this sample (Figure 5.20C). Fraction 2 also showed a single nucleotide at both sites, confirming that this fraction also contained predominantly del17p cells. However, Sanger sequencing of DNA extracted from fraction 3, which was enriched for the disomic 17p cells, revealed both SNPs as being heterozygous. This confirms the ability to use FISH-IS with the 17p BAC probe contig to enrich the del17p sub-clone based on fluorescence intensity.



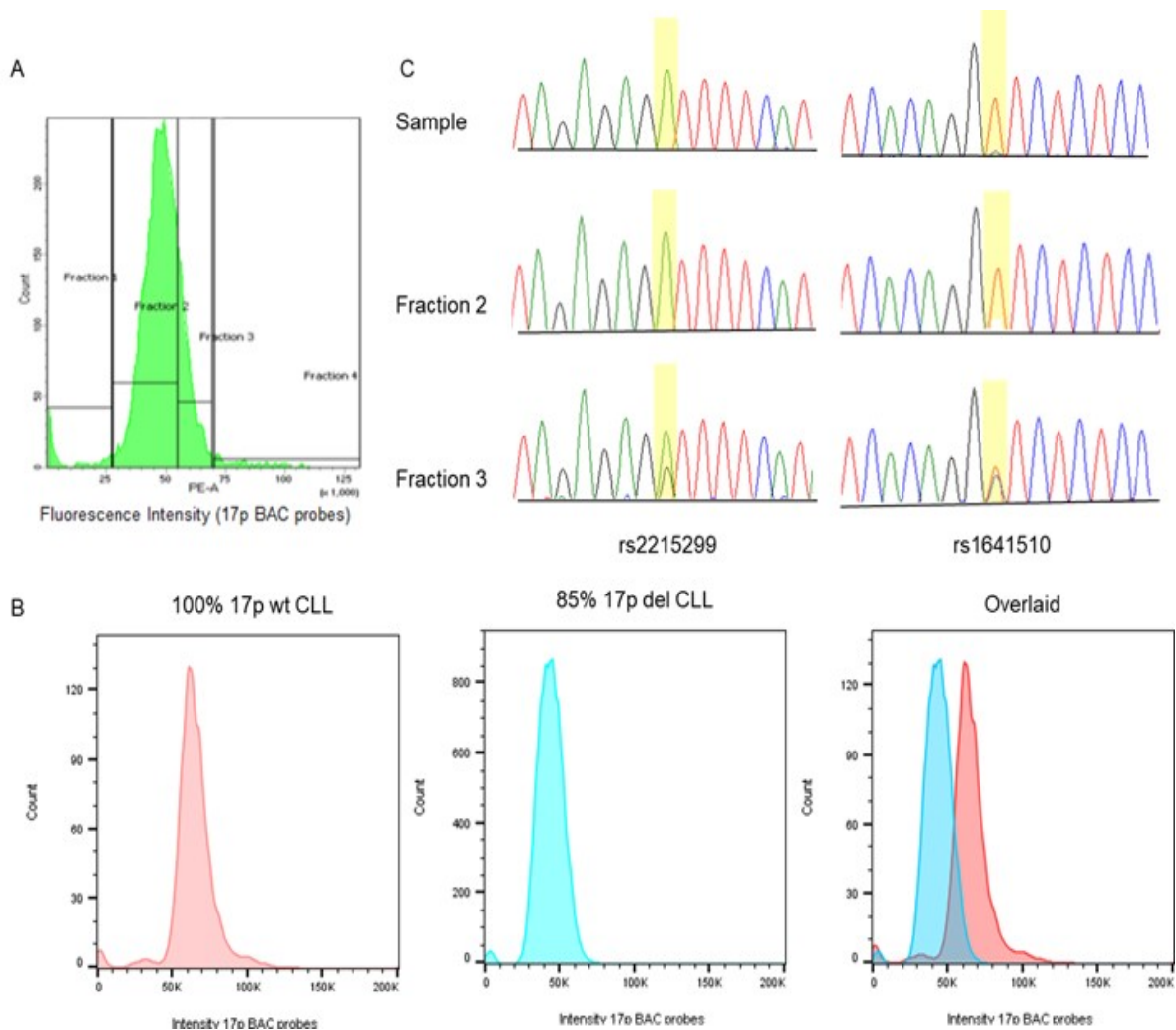


**Figure 5.20. FISH-IS can successfully separate the del17p sub-clone in a CLL sample as confirmed by Sanger sequencing.**

(A) Flow sorting based on fluorescence intensity of 17p BAC probes (spectrum orange). Captured fractions are indicated. (B) Fluorescence intensity histogram of 100% wt17p CLL samples and 85% del17p CLL sample. Overlaid histogram of these 2 samples by FlowJo software reveals that 15% of del17p samples (in blue) were wt17p cells. (C) Two SNPs (rs2215299 and rs1641510) which flank the TP53 gene, were analysed by Sanger sequencing. This SNP analysis validates enrichment of the disomic wt17p sub-clone in fraction 3. The polymorphic nucleotide is highlighted in yellow. Fraction 1 (containing cell debris) and fraction 4 (containing clumping cells) were not analysed. Data are representative of 3 separate experiments.

### **5.3.7 FISH-IS cannot discriminate del17p from wt17p on cryopreserved samples**

Given the rarity of low frequency del17p sub-clones in CLL, it became apparent that the utility of the FISH-IS method would be greatly increased if it was able to be used on cryopreserved samples. In order to determine if this was possible, FISH-IS with the custom 17p BAC probe contig was carried out on cryopreserved CLL samples with known frequencies of del17p sub-clones: 0%, 15%, 22%, 41%, 85% and 95% as determined by conventional FISH.

Figure 5.21 demonstrates a representative example of FISH-IS results on a cryopreserved CLL sample with 41% del17p (as determined by conventional FISH and SNP array). The method was unable to separate the del17p cells from wt17p cells based on the fluorescence intensity scale, despite the presence of bright signals in the captured images (Figure 5.21A) or when viewed through the microscope (Figure 5.21B). Furthermore, Spot Count Wizard was also unable to accurately calculate the del17p proportion, with 56.6% of cells captured in the 1-spot count gate (41% expected; Figure 5.21C).

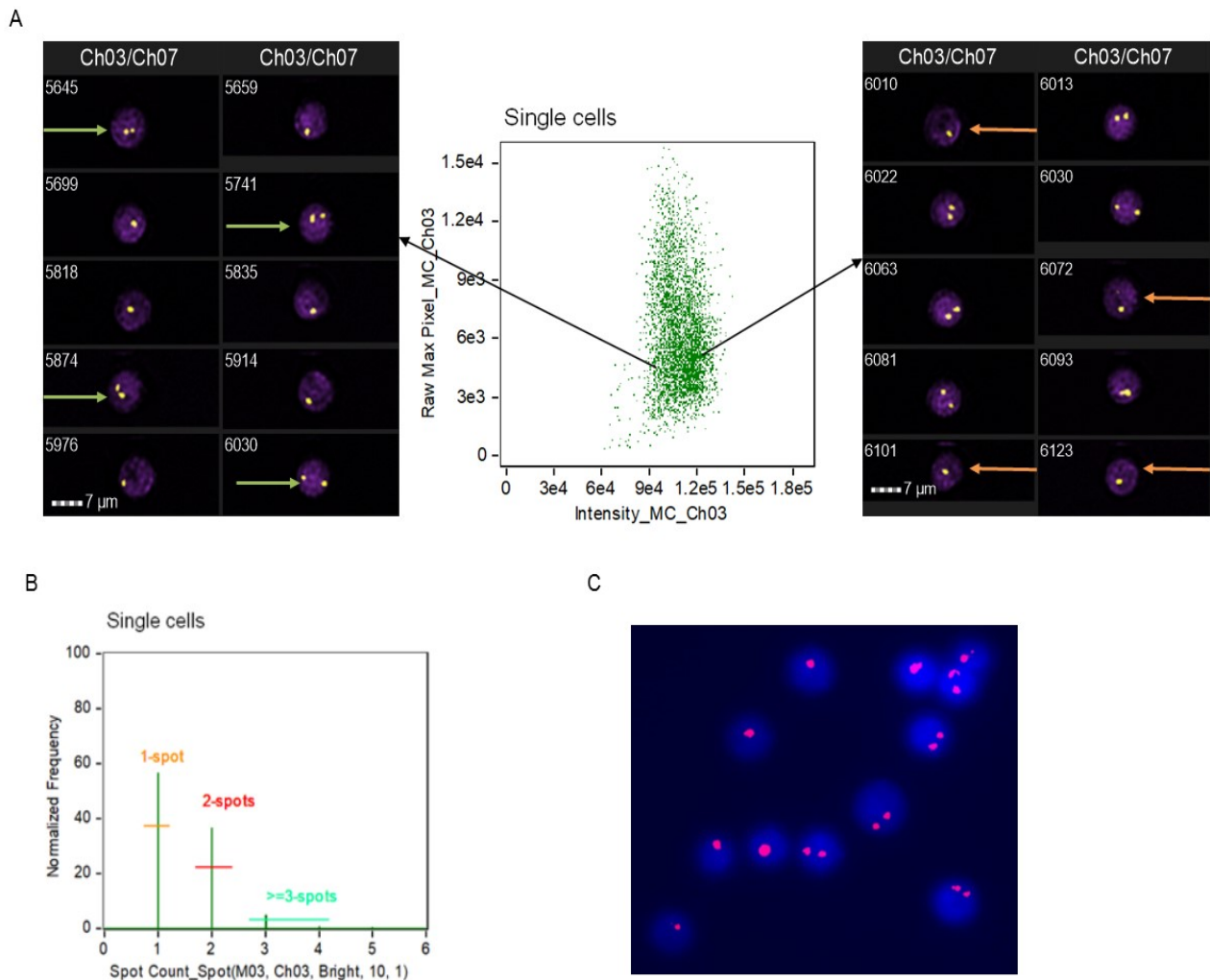


**Figure 5.21. FISH-IS on a cryopreserved CLL with 41% 17p deletion.**

(A) FISH-IS is unable to separate two populations (*del17p* and *wt17p*) based on fluorescence intensity, although the hybridisation signals can clearly be visualised by eye. Purple, DAPI; yellow, 17p BAC probe contig. Green arrows note nuclei with 2 spots located in the *del17p* area and orange arrows point to nuclei with 1 spot located in the *wt17p* area (B) Spot Count Wizard as determined by IDEAS software; 56.6% of nuclei were classified as having 1 spot (41% expected), 36.7% of 2-spots (59% expected) and 5.73% of  $\geq 3$  spots (0% expected). (C) Conventional FISH analysis of the same cells hybridised with 17p BAC probe contig. Blue, DAPI; red, 17p BAC probe contig. Data are representative of 3 separate experiments.

### 5.3.8 Alternative analysis to identify del17p sub-clone on cryopreserved samples

Due to the poor integrity of cryogenically preserved CLL samples, FISH-IS is unable to separate a del17p cell from a wt17p cell based on fluorescence intensity. However, to some extent, the algorithm Spot Count Wizard was able to determine the percentages of 17p-deleted cells, with the caveat that manual curation is then undertaken. A similar analysis to that performed in Chapter 4 with some modification was applied to recalculate the Spot Count Wizard on cryopreserved CLL cells. To illustrate how the Spot Count Wizard combined with manual curation can be applied to cryopreserved CLL cells, a 100% wt17p cryopreserved CLL sample was analysed (Figure 5.22). The algorithm spot count reported 34.5% of cells with 1-spot (0% expected), 58% with pots (100% expected) and 7.3% with  $\geq 3$  spots (0% expected) (Figure 5.22A). The correlation between ploidy and spot count was demonstrated by overlapping the histogram with the 17p BAC probe contig fluorescence intensity for the gates indicated in Figure 5.22A. It is noted that 1-spot nuclei (in green) and nuclei with  $\geq 3$  spots (in purple) were located in the same level of fluorescence intensity with 2-spots gate (in blue) (Figure 5.22B). Furthermore, visual inspection of individual cells confirmed that all nuclei in the 2-spot gate had the expected two signals (Figure 5.22C, middle panel). The incorrect classification of cells as having only 1 spot was found to be mainly due to the 2 signals being located close together or actually overlapping, resulting in an inability to discriminate between them by the current software (Figure 5.22C, top panel). With regards to the  $\geq 3$ -spots gate, the majority of images displayed cells which contained spots outside of the nuclei, which may be due to ruptured cells releasing DNA which then sticks to the cell membrane (Figure 5.22C, bottom panel). Therefore, for future analyses, the true percentage of nuclei within each gate was manually calculated by subtracting false nuclei from each spot gate.



Manual curation of the Spot Count Wizard was then applied to the cryopreserved CLL samples described earlier (0%, 15%, 22%, 41%, 85% and 95% del17p ascertained by conventional FISH). Samples with del17p levels above 41% showed excellent correlation between the FISH-IS curated spot count and conventional FISH percentages (Table 5.8). However there were significant differences between these methods in samples with low frequency del17p (15% by conventional FISH versus 18.07% by spot count; 22% by conventional FISH versus 26.98% by spot count) ( $p < 0.05$ ) (Table 5.8).

**Table 5.8. Results of manual curation of Spot Count Wizard on cryopreserved CLL samples.**

CLL samples	1-spot expected (%)	1-spot observed (%) (mean $\pm$ SD)	p value
Wild-type 17p	0	1.83 $\pm$ 0.53	0.17
15% del(17p)	15	18.07 $\pm$ 1.72	<b>0.03</b>
22% del(17p)	22	26.98 $\pm$ 1.33	<b>0.00</b>
41% del(17p)	41	38.77 $\pm$ 4.71	0.10
85% del(17p)	84	84.33 $\pm$ 1.89	0.61
95% del(17p)	95	95.33 $\pm$ 0.29	0.80

*Data are the mean of 3 separate experiments  $\pm$  SD. The differences between percentages of 1-spot observed and expected were determined by uncorrected Fisher's LSD statistic. Significance ( $p$  value  $< 0.05$ ) is indicated in bold.*

### 5.3.9 Standard media incubation of cryopreserved CLL does not enable FISH-IS analysis

Given the difficulty in using cryopreserved CLL cells for FISH-IS, the protocol for reviving these samples from cryopreservation was addressed. In order to determine the optimal incubation time with respect to cell morphology, cryopreserved CLL cells were thawed and incubated in standard culture conditions and assessed at various time points. Cells were fixed immediately after thawing (0 hours) and at 1, 6, 12, 18 and 24 hours of incubation. Cell morphology was assessed by ImageStreamX brightfield image analysis (Figure 5.23).

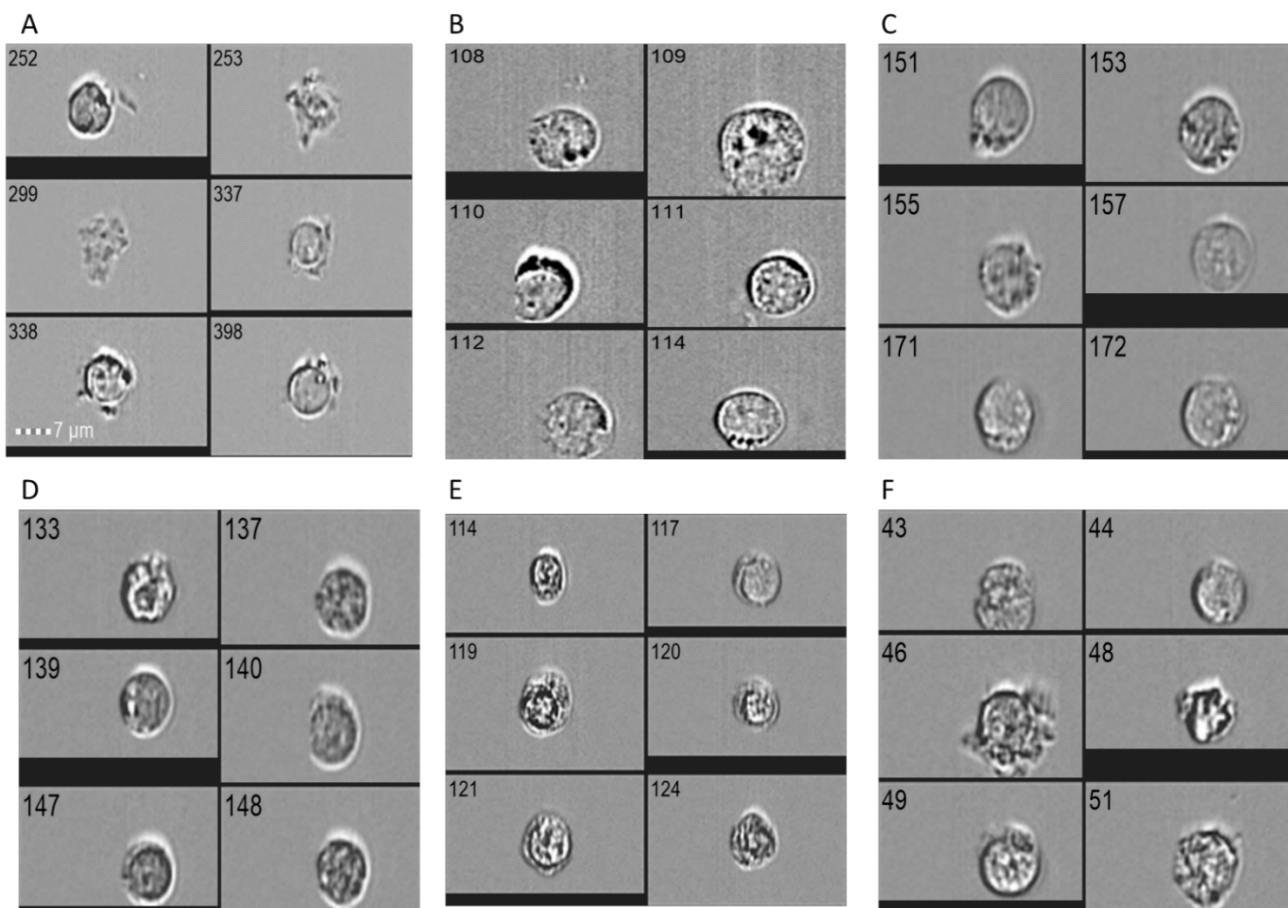


**Figure 5.23. Morphology of CLL samples after Carnoy's fixation as assessed by ImageStreamX with brightfield images.**

*Cells were thawed and fixed immediately (A) or incubated in standard conditions for (B) 1 hour, (C) 6 hours, (D) 12 hours, (E) 18 hours and (F) 24 hours.*

*Data are representative of 3 separate cryopreserved CLL samples in triplicate.*

Immediate fixation (0 hour) and fixation after 1 hour incubation maintains 56.3% and 70.8% intact cells respectively, but the quality of these cells is poor, as evidenced by the presence of numerous fragmented cells seen by brightfield image analysis (Figure 5.23A,B). Cells appeared to have recovered somewhat after 6 hours standard incubation, with an increase in intact cells (79.5%) and improved morphology (Figure 5.23C). Cells proceeded to shrink and rupture with increasing culture times of 12, 18 and 24 hours (Figure 5.23D-F). As shown in Table 5.9, the proportion of intact cells dropped to approximately 40% by the 24-hour-time-point.

**Table 5.9. Intact CLL cells following various time points of standard incubation after cryopreservation.**

Incubation time	Intact cells (%) (mean $\pm$ SD)
0 hour	56.3 $\pm$ 4.11
1 hour	70.8 $\pm$ 4.33
<b>6 hours</b>	<b>79.5 <math>\pm</math> 2.82</b>
12 hours	63.9 $\pm$ 4.53
18 hours	56.6 $\pm$ 6.34
24 hours	40.01 $\pm$ 2.56

*Intact cells were determined by single cells in focus using ImageStreamX. The optimal condition (6 hours incubation) is shown in bold. Data are the mean of 3 separate experiments  $\pm$  SD.*



As the 6-hour incubation appeared to give optimal cell morphology, these cells were hybridised with centromere X probe and analysed by FISH-IS. As a positive control, freshly venesectioned cells were analysed in parallel. This analysis showed that, despite the 6-hour incubation, CLL cryopreserved cells showed high background and low fluorescence intensity, and therefore were not able to be analysed by the FISH-IS protocol developed earlier (Figure 5.24C). Therefore, further experiments assessing various culture conditions were undertaken in an attempt to develop a protocol which would enable analysis of cryopreserved CLL cells by FISH-IS.

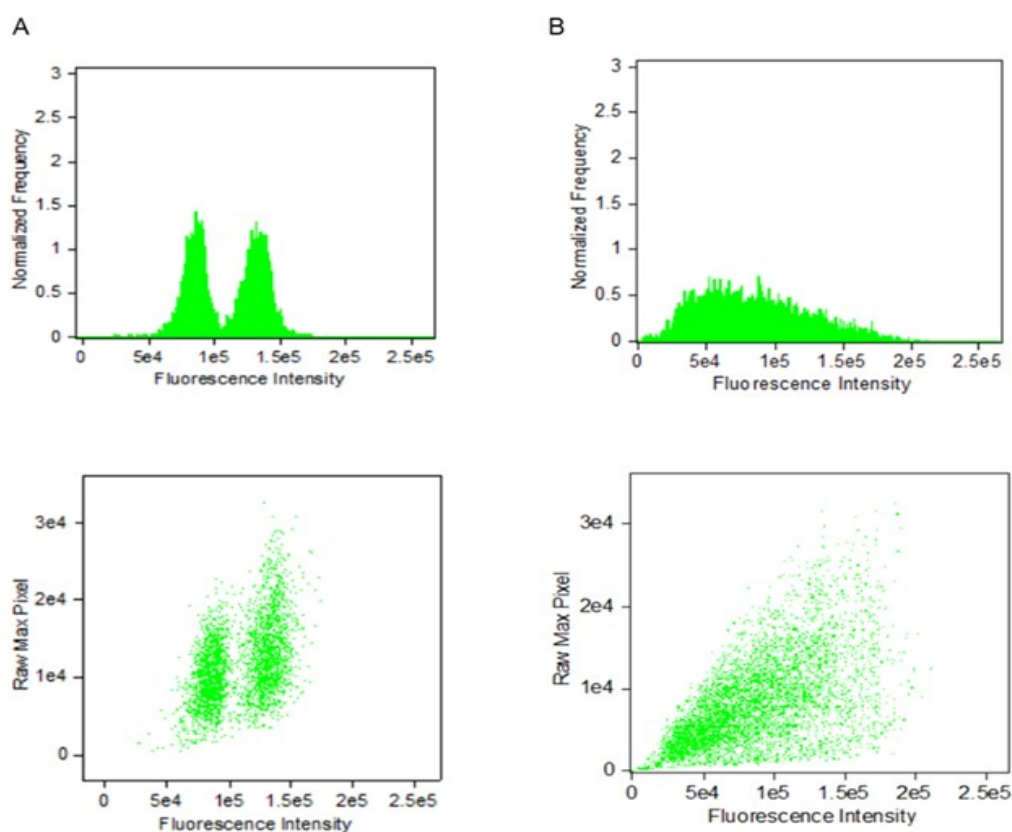


**Figure 5.24. FISH-IS results with centromere X probes on a 50:50 mixture of male and female CLL samples.**

(A) CLL cells fixed directly following venesection. (B) Cryopreserved CLL cells were thawed and incubated in 1640 RPMI 10% FCS media for 6 hours before fixation.

Data are representative of 2 separate experiments.

### **5.3.10 Various culture conditions cannot sufficiently restore cryopreserved CLL**

Several studies have suggested that soluble secreted factors from HS5 (human bone marrow stroma) or cell-cell interactions can significantly promote both the short- and long-term survival and/or recovery of CLL cells in culture (Gehrke et al. 2011, Burgess et al. 2012). Therefore, incubation of cryopreserved CLL cells with HS5 co-culture, HS5 cells - conditioned media and high-density culture conditions were analysed (Figure 5.25A). In addition to standard media, two nutrient-rich media, AIM-V (serum-free) (Levesque et al. 2001) and McCoy's media (Godinez et al. 2012) were also investigated to determine if an increase in nutrients would improve thawed CLL cell viability (Figure 5.25A). Low density incubation was used as a negative control samples (Figure 5.25A).

Using the inverted EVOS™ microscope (ThermoFisher, Australia), an investigation of these six cultured conditions was generated at every time-point (see detail method in section 5.2.5). The EVOS™ images at 48 hours (Figure 5.25B) showed that most of the cells in McCoy's media were dead.

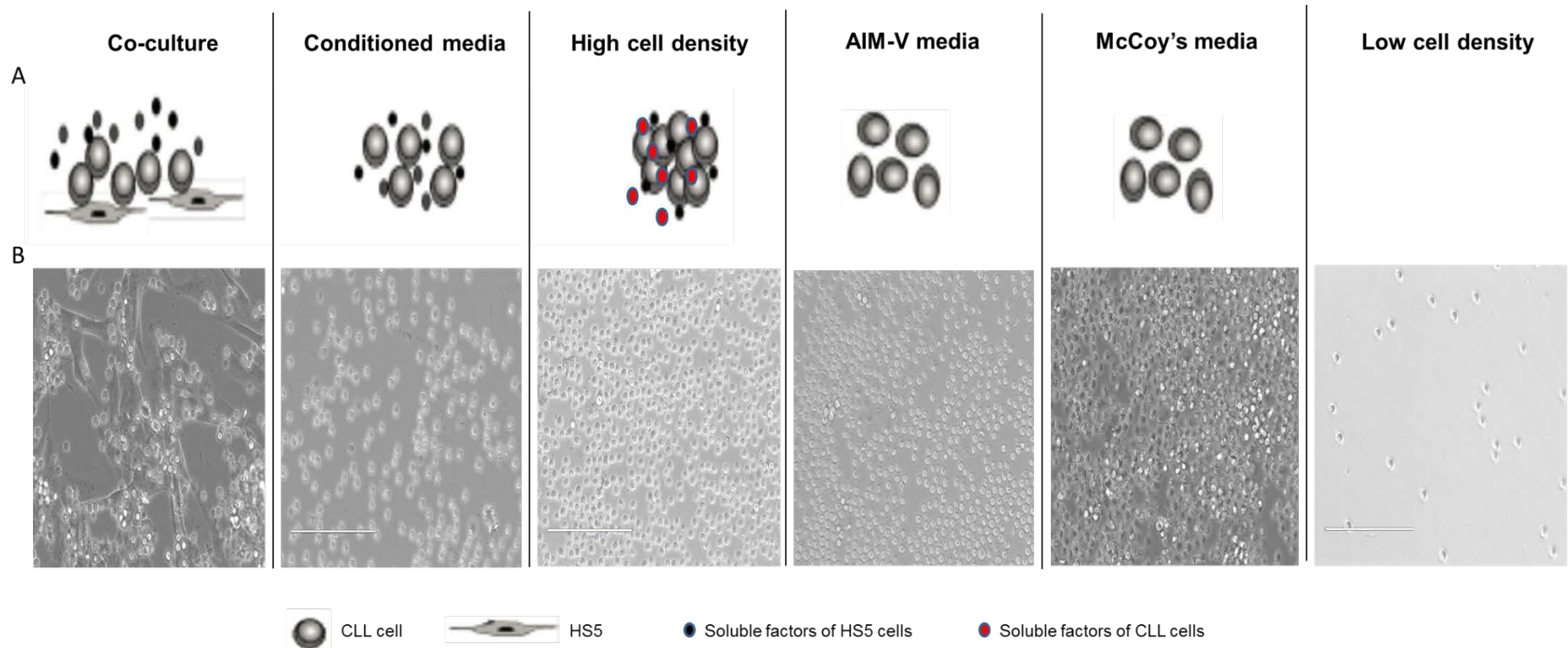


**Figure 5.25. Schematic overview of six different culture conditions assessed and EVOS™ images.**

*(A) Schematic representation of various CLL culture conditions. (B) Representative brightfield images of cells cultured in 24 well-plates at 48 hours by EVOS™ microscope using phase-contrast with 40x objective lens.*

The viability of CLL cells was determined by annexin V/PI assay following various culturing conditions described in Figure 5.26. In general, this analysis demonstrated that co-culture with HS5 cells resulted in the highest viability of CLL cells, followed by incubation in conditioned media, high-density culture and AIM-V media. As expected, the negative control of low cell density incubation displayed the lowest viability (Figure 5.26 A-B). The 2-way ANOVAR statistic test for multiple comparison was applied to determine the significance of differences between the four various culturing conditions: co-culture, conditioned media, high-density and AIM-V media at different time-point. There was no significant difference ( $p > 0.05$ ) between the viability of cells in co-culture and conditioned media ( $p = 0.17$ , Figure 5.26A) and ( $p = 0.14$ , Figure 5.26 B). These two culture conditions accounted for the highest viability amongst the six culture conditions examined ( $p = 0.02 < 0.05$ ) (Figure 5.26C). In addition, there was no significant difference in the viability of cultured high cell density in standard media or in AIM-V media. The worst culture condition for CLL cells was found to be in McCoy's media, with 90% of CLL cells dead by 24 hours (Figure 5.26).

However, it is important to note that the total number of cells declined significantly in all culture conditions (Figure 5.26C). After 120 hours incubation, only half of the number of cells were viable when incubated as co-culture, in conditioned media and in high-density; while low density incubation resulted in a significantly larger decrease in viable cells (Figure 5.26C).

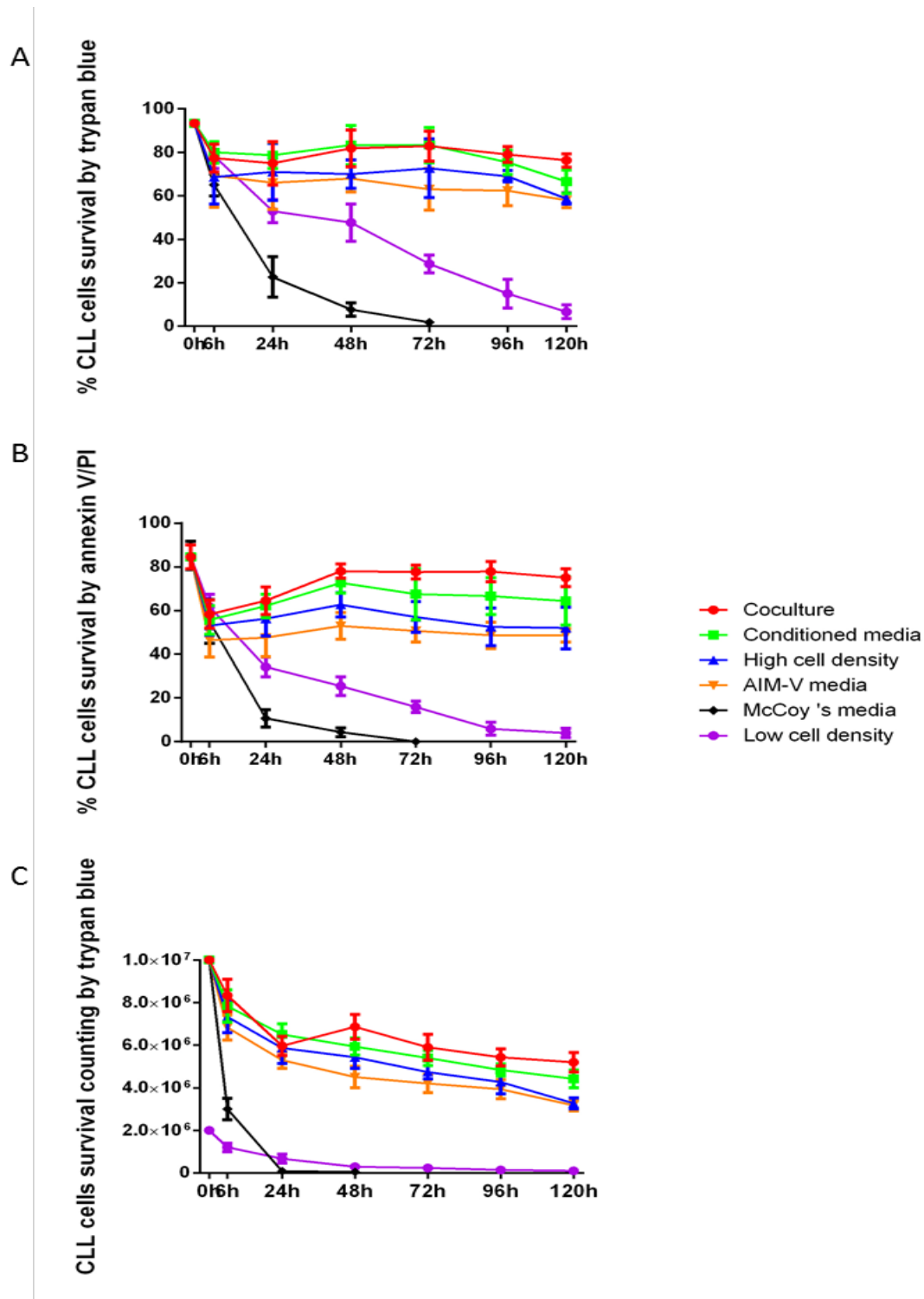


**Figure 5.26.** The impact of *in vitro* supportive culture conditions on CLL cell survival as determined by different methods.

Cell survival as determined by (A) trypan blue and (B) annexin V/PI. (C) Analysis of the actual number of CLL cells by trypan blue analysis demonstrated that survival decreased gradually in all culture conditions. Data are the mean of 3 separate experiments  $\pm$  SD (n=5).

### 5.3.11 FISH-IS results after maintenance in supportive *in vitro* conditioned media.

Co-culture and conditioned media both showed the highest viability (up to 80%; Figure 5.26 A, B) and the greatest overall number of cells alive ( $\sim 7 \times 10^6$  cells; Figure 5.26C) after 48 hours incubation. There was however a technical concern with the availability of CLL cells following co-culture incubation (see section 5.3.12 below), and therefore cryopreserved CLL cells cultured in conditioned media were chosen to be analysed by the FISH-IS protocol. Unfortunately, as seen in Figure 5.27A-B the fluorescence intensity of probe hybridisation within these cells was not sufficient for FISH-IS analysis. The majority of cells started to shrink or showed some degree of damage. As a result, relatively few cells were observed with specific hybridisation (Figure 5.27C), with the majority of cells showing either no hybridisation (Figure 5.27D) or non-specific background hybridisation (Figure 5.27E-F). These factors resulted in a non-uniform fluorescence background that failed to separate cell populations based on fluorescence.

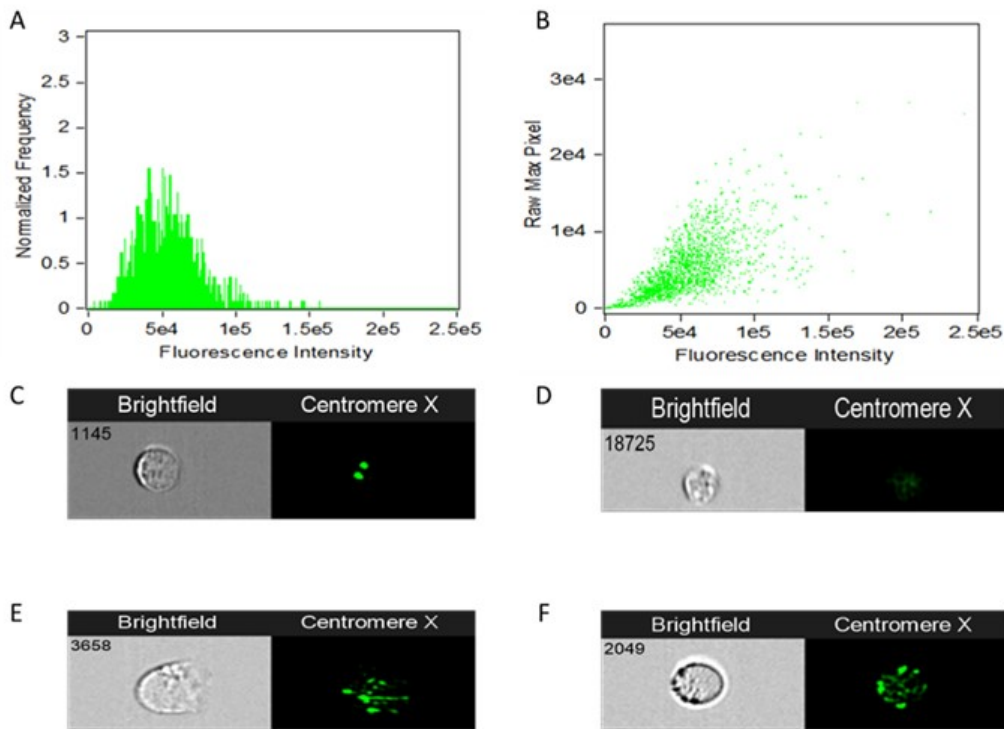


**Figure 5.27. Evaluation of cryopreserved CLL cells with FISH-IS procedure after maintaining in supportive *in vitro* conditioned media.**

(A) Histogram and (B) dot plot showing the fluorescence intensity of centromere X probe on cryopreserved CLL cells after 48 hours incubation in conditioned media. (C) Representative image of an intact cell with specific hybridisation signals and no background. (D) Representative image of a cell which has undergone shrinkage, as can be seen in the brightfield image, resulting in an absence of hybridisation. (E) and (F) Representative images demonstrating non-specific hybridisation of probes on partially damaged cells, resulting in non-uniform background.

Data are representative of 2 separate experiments with the centromere X probe on male and female cryopreserved CLL cells combined in equal proportions (50:50).

### 5.3.12 CLL cells incubated in HS5 co-culture acquired pseudo-nodes

Visualisation of the various culture conditions revealed that after 48 hours of co-culture, CLL cells resulted in “clumping” of cells, hereafter referred to as pseudo-nodes (Figure 5.28A). The formation of these cellular bodies warranted further analysis because they had the potential to lead to an incorrect calculation of CLL cell viability, as CLL cells may be trapped within these structures and therefore not available for analysis, resulting in an underestimation of viability.

Experiments were carried out in order to compare viability between cells in suspension and total cells (both in suspension and in pseudo-nodes) following co-culture incubation (see method 5.2.7). In order to exclude contamination from HS5 cells, CLL and HS5 cells were separated based on side scatter and forward scatter as shown in Figure 5.28B-C. HS5 cells are larger than CLL cells and therefore are shifted to the right-hand side. As expected, Figure 5.28D-E confirm that collection of both suspension cells and pseudo-nodes resulted in an increase from 3% to 16% within the HS5 cell gate. Importantly, assessment of viability by annexin V/PI assay revealed that there was no significant difference in percentage viability between these different methods of isolating CLL cells ( $p= 0.56$ ) (Figure 5.28F).

The biological significance and formation of these pseudo-nodes was not directly related to this research project and was further explored by a fellow PhD candidate, Ms. Lara Escane.



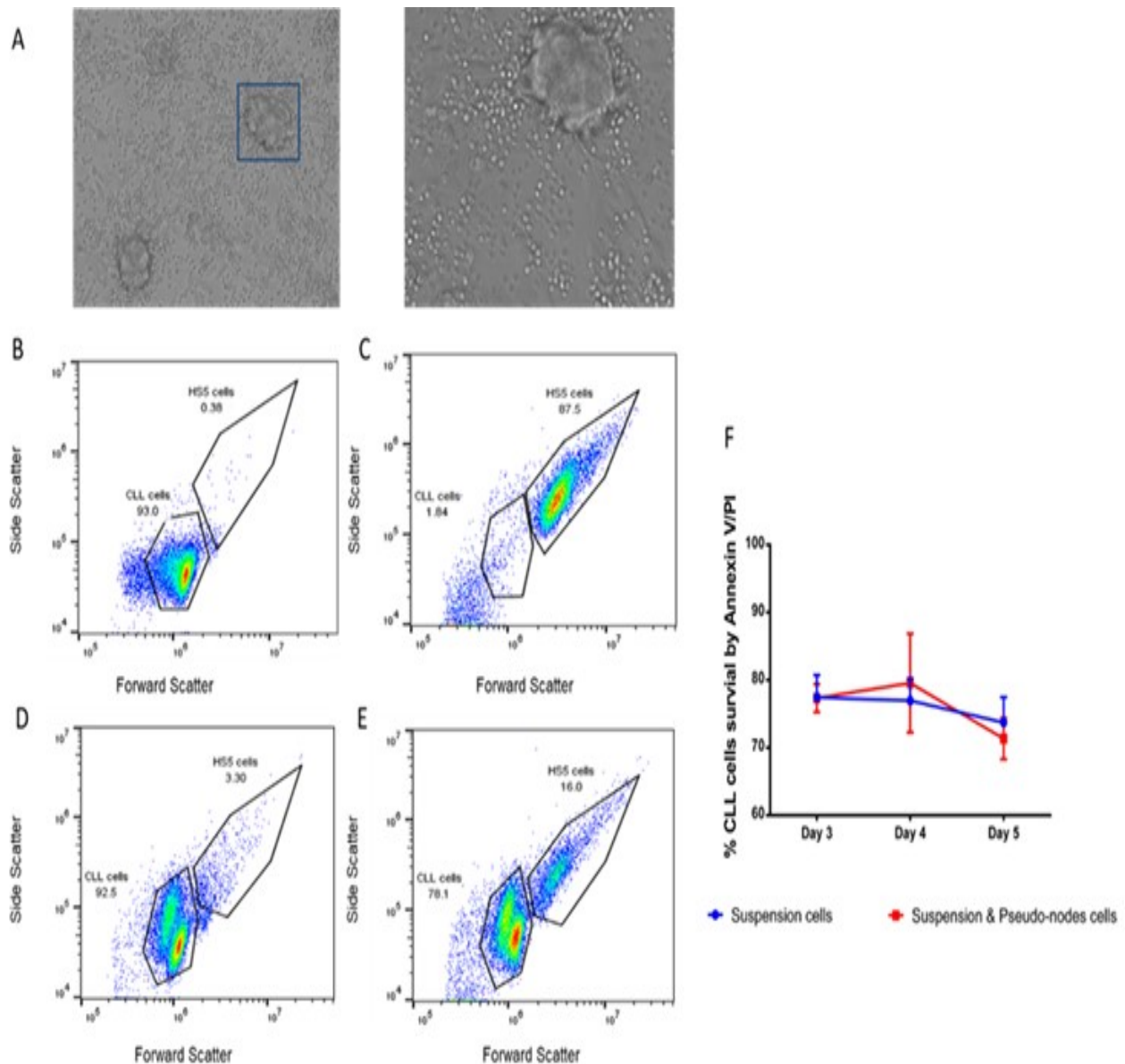


**Figure 5.28. Comparison of CLL cell survival between cells in suspension and cells contained inside the pseudo-nodes.**

(A) EVOS™ phase-contrast microscope images at 10x (left panel) and 40x (right panel) magnification reveal the pseudo-nodes (blue box) which appear at day 3 of co-culture of CLL and HS5 cells. (B) Gating strategy of CLL cells based on forward and side scatter. (C) Gating strategy of HS5 cells based on forward and side scatter. (D) Separation of suspension cells and (E) all cells (suspension cells and those contained within the pseudo-nodes) using the gating strategies shown in (B) and (C). (F) Correlation of CLL cell survival rate as determined by annexin V/PI of suspension cells (blue line) or all cells (red line) ( $p=0.56$ ). Data are the mean of 3 separate experiments  $\pm$  SD ( $n=3$ ).

## 5.4 Discussion

This chapter described my investigation of the application of 17p locus-specific commercially available FISH probes and a custom-made BAC probe contig for the detection of del17p sub-clones in CLL cells. This comprehensive analysis found that the constructed 17p BAC probe contig was superior to the commercial probes in signal intensity, and enabled detection of the del17p sub-clones from a heterogeneous CLL cell population.

The data presented in Chapter 4 established that FISH-IS can accurately distinguish aneuploidy CLL sub-clones with several commercially available centromere probes. However, the 17p LSI commercial probes were unsatisfactory for use in FISH-IS. This is almost certainly due to the relatively small size of the target region of these commercial probes (145 to 172kb). As a result, signals with a lower spot intensity are achieved due to the small amount of fluorescence intensity from minimal probe binding (Smoley et al. 2010). The result is that the signal is not sufficiently bright for high-throughput analysis by the imaging flow cytometry machine. Therefore, in order to analyse del17p sub-clones with the FISH-IS method, this method required generation of a homemade BAC probe contig, targeting 2.5Mb of unique sequence on 17p. It was hypothesised that the target sequence length approached that of the centromere probes which target approximately 3 Mb of repetitive centromeric sequence (Cleveland et al. 2003), and therefore the BAC contig would give a comparable signal. However, analysis revealed that the 17p BAC probe contig was approximately 50% as bright as a centromere probe. This is most likely due to the fact that the repetitive satellite sequences of centromeres are relatively uniform and highly compact, compared with 17p13 sequences spanning the *TP53* gene. The 17p13 region covered by the BAC contig contains a variety of dispersed short/long interspersed elements (SINEs, LINEs), which account for approximately 50% of the entire length of the target sequence.

These repeats were either blocked by the Cot-1 DNA, or if not successfully blocked, would have resulted in non-specific probe binding. Considering that 17 BACs were used in this contig, the level of non-specific background became relatively high. This finding is in accordance with findings of Lawrence et al. (1986), who reported that larger probes, such as BACs, cause high background due to non-specific binding. The role of Cot-1 DNA in the hybridisation is discussed below.

Given that the 17p BAC probe contig was of similar length (2.5 Mb) to centromeric probes (3 Mb), it was expected that the fluorescence signal intensity would be similar. However, the signal intensity achieved with the 17p BAC probe contig was only approximately 50% of that observed for the centromeric probe. This difference may be due to non-specific binding of the BAC probe. Unfortunately, attempting to increase the signal by increasing the number of BAC probes is problematic due to the commensurate increase in background signal, although it has been reported that the level of incorporation and the hybridisation fluorescence signal increase in parallel when the length of the targeted sequences is increased (Zhu et al. 1994).

The labelling method used in this analysis is based on that described by Rigby et al. (1977), and utilises nick translation to incorporate fluorochromes (spectrum green or spectrum orange) into the dsDNA BAC template. This labelling is then followed by ethanol precipitation of the labelled DNA with salmon sperm carrier DNA. There are other methods available to generate fluorescently labelled dsDNA probes such as random-primed labelling (Feinberg et al. 1983), DIG-PCR (Garratt et al. 2002), and PNA-directed padlock probes (Yaroslavsky et al. 2013). It is possible that an alternative labelling method would result in an improved signal to background ratio, however due to time limitations, these alternative methods were not trialled.

In addition to the above direct labelling methods, there are also several indirect labelling methods which have the potential to generate greater fluorescence signal. The disadvantage of these methods is that several additional incubation steps are required, as these methods incorporate reagents such as antibodies or biotin- avidin detection, resulting in increased fluorescence background (Morrison et al. 2003).

When attempting to optimise the FISH-IS protocol for the 17p BAC probe contig, it was considered infeasible to attempt to optimise every single point in the FISH-IS protocol, as the entire methodology is extremely complex and takes three days to complete, with over 100 potential points which can be optimised. Therefore, due to the practical limitations of both time and expense (primarily the cost of labelling the probes), the four main steps in the method were focussed on for optimisation: fixation, hybridisation, washes, and visualisation.

Fixation is the first step which needed to be optimised in the FISH-IS method. The role of this step is to stabilise the nucleus and maintain cell morphology, in addition to protecting cells against degradation by inactivating any internal metabolising enzymes (Huang et al. 2015). Following lymphocyte isolation (Chapter 2, section 2.3) and prior to fixation, cells are incubated in a hypotonic solution which swells the cells in order to counteract the shrinkage effect caused by alcoholic fixatives (Claussen et al. 2002, Deng et al. 2003). The process of fixation was optimised in several steps, including the make-up of the fixative solution, and the temperature and time of fixation. There is a vast array of literature concerning the effects of various fixation solutions. This study demonstrated that the Carnoy fixative (methanol and acetic acid) was optimal for downstream FISH assays.

Multiple studies have indicated that alcohol-based fixatives can result in protein precipitation and denaturation (Giannella et al. 1997, Noguchi et al. 1997). The two main alcohols used for this purpose in the literature are methanol (CH<sub>3</sub>OH) and ethanol (CH<sub>3</sub>CH<sub>2</sub>OH), which

both replace water in the cell, thereby denaturing the protein structure and resulting in shrinkage. Whilst essentially interchangeable in this role, ethanol and methanol each have their own advantages and disadvantages. For instance, methanol is closer to water in structure than ethanol, therefore methanol has been proposed to be better than ethanol in preserving cell morphology (Kumarasinghe et al. 1997, St-Laurent et al. 2006). Conversely, ethanol is a stronger reagent for denaturing structures than methanol, hence the speed of fixation using methanol is slower than that for ethanol (Eltoum et al. 2001). Acetic acid (CH<sub>3</sub>COOH) alone does not fix the protein within cells but it works with the alcohol fixative to help prevent the loss of nucleic acids by countering the shrinkage effect from ethanol (Eltoum et al. 2001) and also acts as a permeabiliser (Fernández et al. 2013). This allows the optimal preservation of cell morphology, while improving permeabilisation to probes entering the cell membrane more rapidly. Acetic acid therefore is the preferred fixative for FISH-IS despite the fact that it cleaves the cell surface antigens (Howat et al. 2014) and as a result, is not a suitable fixative for downstream immuno-phenotyping assays (see discussion in Chapter 6).

The fixative solution used in this study, consisting of 75% methanol and 25% acetic acid (known as chloroform-free Carnoy's fixative) provides optimal fixation to preserve intact cells, subcellular structures and the integrity of nucleic acids. Compared with other fixatives it is commonly used in diagnostic conventional FISH protocols (Urieli-Shoval et al. 1992, Murrell-Bussell et al. 1998, Srinivasan et al. 2002, Chao et al. 2011). In the FISH-IS protocol described by Minderman et al. (2012), cells were fixed with Carnoy's fixative by adding approximately 1 mL per 15 seconds combined with gentle vortexing, followed by incubation at room temperature for 10 mins to complete the fixation process. However, significantly better results were achieved with the full fixation method (Carnoy's fixative was added for 10 mins, and repeated three times); steps are detailed in section 2.6.2. The results

presented here are that the fast fixation method generated less single intact cells, causing less hybridised signals. It is assumed that this is because this method does not allow an adequate period for complete fixation and permeabilisation of the cells, especially when using methanol which has a slow reaction time (Start et al. 1992, Srinivasan et al. 2002).

The cells clumping issue following fixation may be due to cell-cell adhesion mediated by DNA being released from dead and decaying cells (Renner et al. 1993). Therefore DNase I has been used in several published studies in order to avoid clumping of cells (Campbell et al. 1980, Machalinski et al. 1999, Garcia-Pineros et al. 2006). However, here it was found that the addition of this enzyme to the samples did not reduce the amount of cell clumping, implying that free DNA is not the major cause of clumping cells in these samples. Therefore, the clumping might have resulted from the cations (for example, Ca<sup>++</sup>) (Zarkowsky et al. 2011), or due to the fact that cells burst and clump easily due to the hydrolysis bond of the membrane damaged after fixation, etc. The reasons for this clumping issue require further investigation.

The addition of proteinase K has been shown by Pineau et al. (2006) to improve the specific hybridisation efficiency of labelled probes. This is most likely because proteinase K perforates cells and destabilises the histone proteins, thereby increasing exposure of the target nucleotide sequence to the probes (Hilz et al. 1975). However, the addition of proteinase K did not significantly improve the hybridisation efficiency of the probes used here. One possible reason is that proteinase K has been shown to improve hybridisation particularly in tissue samples (Andersen et al. 2001, Schurter et al. 2002), while individual cells do not go through the same initial fixation process and as a consequence tissues may achieve better permeabilisation.

The second main area of optimisation was in the hybridisation process, which again contained numerous steps that required optimisation. In 1987, Landegent et al. (1987) reported that Cot-1 DNA is able to efficiently suppress the nonspecific hybridisation of BAC probes in FISH. Currently the majority of commercial probes contain Cot-1 DNA at a concentration which is based on the company's optimisation experiments, but the exact concentration is not disclosed to the consumer. Therefore, it was not possible to use this information to estimate how much Cot-1 should be added to the 17p BAC probe contig. The literature on standard conventional FISH indicates that the optimal Cot-1 DNA: probe concentration ranges from 20- to 100-fold, but suggests that this ratio should be increased when applied to a flow cytometry application with low copy number (Trask et al. 1988, Rauch et al. 2000, Dugan et al. 2005, Trifonov 2009). Other reports have found that concentrations of 50- to 100-fold Cot-1 DNA relative to the amount of labelled probe promotes high efficiency and specificity of probe binding (Hozier et al. 1998, Vermeesch et al. 2005). In accordance with these reports, the results presented here demonstrated that a 50-fold excess of Cot-1 relative to the labelled BAC probes gave the highest signal to background ratio.

There are several choices for probe denaturation, including temperature denaturation, chemical denaturation or both carried out simultaneously. Mladinic et al. (2014) reported that chemical denaturation alone, or combined with temperature denaturation, resulted in lower probe binding specificity and a lower hybridisation success rate, presumably due to the fact that acid denaturation may result in damage to the fluorophores of the labelled probes. This publication also showed that temperatures higher than 75°C (and up to 90°C) and longer denaturation times (up to 5 mins) resulted in better signal to background noise. Chin et al. (2003) also noted that denaturation for 10 mins at 80°C resulted in improved FISH results. In general, a balance in denaturation temperature needs to be achieved in order to

generate good FISH-IS results: the temperature should be high enough to sufficiently unmask the target sequence enabling probe binding, but not to the extent that it causes damage to cell morphology and integrity.

Formamide concentration can modulate denaturation temperature, such that an increase in formamide concentration can result in DNA denaturation at a reduced temperature. This is reflected in the fact that the formamide concentration in the commercial hybridisation buffer for centromere probe is 55%, while the LSI hybridisation buffer is 50% formamide, as this type of probe does not require the high stringency required for the centromere probes. To reduce the melting point of DNA denaturation, formamide is also used at different concentrations (McConaughy et al. 1969, Gerhard et al. 1981, Berndt et al. 1996, Blake et al. 1996, Liedl et al. 2007, Matthiesen et al. 2012). Denaturation conditions of 75°C-80°C for 2-5 mins are widely used in conventional FISH protocols (Serakinci et al. 2009, Liehr et al. 2017).

The amount of probe required for conventional FISH analysis is determined by the small area under the coverslip and the requirement to assess only 200 cells. However, the FISH-IS method requires a significantly larger amount of probe due to the increased hybridisation volume and the larger number of cells to be analysed. There are several different sources of locus-specific probes used in conventional FISH, ranging from plasmids (1-10 kb) to larger vectors such as PACs, YACs and BACs, which range in size from 80 kb to 1 Mb (Gozzetti et al. 2000, Kearney 2001, Bishop 2010).

For visualisation, the highest camera resolution of 60x (0.5 µm per pixel) was chosen because CLL cells are small lymphocytes with an approximate diameter of 6 µm, which suggests that an EDF of 10 µm would produce adequately high resolution images of these small lymphocytes, with the FISH spots in focus (Basiji et al. 2007). Therefore, magnification



of 60x was selected. In addition, even though the slowest flow speed on the ImageStreamX was used, resulting in approximately 1000 cell events being collected per second, this rate results in an exposure time of less than  $1 \times 10^{-3}$  seconds, potentially resulting in a 'weak' signal if hybridisation has been variable.

Whilst there are obvious advantages to the FISH-IS method, there are also some disadvantages. First of all, regardless of the probe used, it was noted that the quality of the CLL sample is critical; the technique is significantly more robust when performed on samples fixed on the day of veno-puncture. This is presumably because it is crucial to maintain both cell integrity and a single cell suspension in order to facilitate entry of probes across cellular membranes to bind to the target DNA. The cryopreserved cells are likely to have incurred cryoinjuries or micro-damage, especially on their cell membrane, and therefore are prone to damage and cell loss during the FISH-IS protocol (Pegg 1987, Adler et al. 1996, Moussa et al. 2008). Therefore, the background fluorescence of these cryopreserved cells was higher and not uniform in FISH-IS assays. Furthermore, due to the fact that the fluorescence intensity of the 17p BAC probe signals were less than half compared with centromere probe signals, only a small increase in background fluorescence can significantly compromise the BAC probe contig signal. This is why the del17p sub-clones could not be separated from the wt17p sub-clones from cryopreserved cells, based on fluorescence intensity when analysed according to the current pipeline. In addition, separation of these sub-clones can be carried out by applying the spot count software. However, as described in Chapter 4, there are also a number of limitations to the FISH-IS IDEAS software when attempting to enumerate signals as part of the spot count process. This method therefore requires manual curation of the cell spot count results by direct visualisation, particularly when cell quality is reduced due to the asymmetrical background of these cells. It is important to note that even though the spot count analysis required manual curation, this process was relatively simple,

consisting of skimming images relatively quickly on the screen. Therefore, it was possible to accurately annotate thousands of cell images. This is considerably faster than analysing cells under a microscope and recording the number of signals, meaning that FISH-IS with the IDEAS software spot count followed by manual curation is still more efficient at analysing large cell numbers than conventional FISH analysis.

The ImageStreamX is a platform which combines the high throughput analysis afforded by flow cytometry with the microscopic capacity of capturing single cell images. One of the principle advances of this technique is that the sensitivity threshold for detecting abnormal genomic cells is lower than alternative methods at 3%, compared with conventional FISH at 5-10% (Sinclair et al. 1997, Campbell et al. 2013) and SNP-array at 20% (Hagenkord et al. 2010). Thus, FISH-IS has a potential application in the monitoring of progressive/relapse patients, where sub-clones which are associated with a poor prognosis are identified at diagnosis and can be accurately followed through subsequent treatment cycles.

MPS has recently emerged as a diagnostic tool that can interpret genomic sub-clone analysis (Meldrum et al. 2011). When designing an MPS assay, a balance between gene panel size and the level of coverage that is required in order for MPS to be accurate and cost-effective needs to be considered. Firstly, regarding amplification-based target enrichment, a primer hybridisation failure resulting from a variant located in a probe binding site will lead to unsuccessful target amplification or allele bias. This is called allele drop-out and is a significant concern in PCR- based techniques (Ikegawa et al. 2002). Secondly, amplicon enrichment refers to the level of enrichment which is achieved at each amplicon. In order to accurately detect very low frequency sub-clones (i.e. <10%) by MPS, ultra-deep sequencing via a high level of amplicon enrichment is required, which is still prohibitively expensive, even for a narrow target range (Goodwin et al. 2016). Therefore,

genomic characterization of sub-clones, if based solely on MPS, is not cost effective due to the large number of amplicons, exhaustive read depth, specialised techniques, software and skills required to detect low level variants, in addition to the time needed to process the enormous amounts of MPS data when attempting to analyse sub-clones (Kim et al. 2013).

However, probably the most relevant limitation to MPS analysis of an unsorted patient sample is that the sequencing information is derived from DNA pooled from a minimum of  $10^5$  cells. Therefore, the sequencing data does not reveal any information about co-existence of more than one mutation within the same clone, regardless of how high the level of amplicon coverage is achieved. Instead, assumptions must be made based on the probability of coexistence of mutations within a clone. This analysis cannot define the genetic landscape of a specific sub-clone, but instead provides an overview of the combined genetic abnormalities found within one patient sample. Whilst this information is still informative, this pooling of data means that critical information on the potential epistasis of mutations within one cell is lost.

An alternative to MPS analysis of pooled cells is to carry out single cell sequencing. Whilst this method can provide a wealth of information on the individual cells analysed, with a heterogeneous disease such as CLL the number of cells needing to be individually analysed to provide a useful picture of the makeup of the disease would be prohibitive particularly from a cost viewpoint. This method is highly technically demanding, and required highly specialised reagents, equipment and bioinformatics algorithms are required (Sun et al. 2015), placing it out of reach of most research groups.

Therefore, the strength of the FISH-IS method described here lies in the fact that it is able to separate a specific sub-clone based on a genomic abnormality. The isolated sub-clone can then be analysed by MPS, which will provide information which is then specific to the

sub-clone containing the original genomic abnormality. Thus, this methodology provides an unbiased approach to sub-clone analysis at a significantly lower monetary expense and reduced labour cost than either pooled or single-cell MPS, while still being a high-throughput method. Specifically, for CLL, flow sorting a sub-clone population based on 17p allele copy number will enable a better understanding of the genetic architecture of these early and untreated del17p sub-clones, which has eluded understanding in the past.

In terms of applicability and general use, flow cytometry-based techniques are now highly developed and widespread, with most laboratories relying on them for both research and diagnostic purposes. Although the technique was developed for analysis by FISH-IS, once it is established that the hybridisation has been successful with sufficient signal from the probes, the sorting can be performed by a standard flow sorting apparatus prior to an MPS approach. At present, this requires a combination of skills in a number of research areas. However, the techniques established in our study may well have broader application.

In cancers, fusion or break-apart genes are generated due to the combination of two unrelated genes, which usually result from a structural rearrangement of the genome. The best-known example is the Philadelphia (Ph) chromosome which is formed by the joining of the ABL oncogene from chromosome 9 to the BCR gene on chromosome 22. This BCR-ABL fusion gene is found in more than 90% of cases of chronic myelogenous leukaemia (CML) (Hagemeijer 1987), and in 25–30% of adult and 2–10% of paediatric cases of ALL (Tomlins et al. 2005, Talpaz et al. 2006, Edwards 2010). Therefore, an efficacious diagnostic test to identify these rearranged fusion genes is crucial and has widespread applicability to many of the above-mentioned cancers. Importantly, the novel FISH-IS technique I developed here on allele-specific probes, could be directly applied to detect these fusion genes because these locus-specific probes would have similar characteristics

of length and brightness. This would assist in the understanding of sub-clonal and clonal populations in a number of cancers outside of the more easily assessed leukemic diseases.

Although a publication by Fuller et al. (2016) described the combining of FISH-IS with immuno-phenotyping, this assay has only been applied to the highly repetitive centromere and telomere probes so far. Therefore, my novel application to single-locus probes can broaden the investigative power of the FISH-IS technique, and immuno-phenotyping FISH can potentially be applied to locus-specific probes, further improving the understanding of novel sub-clone biology.

All FISH-IS data generated to this point have been carried out on fresh-fixed CLL cells. However, there was an abundance of frozen CLL samples stored in liquid nitrogen (at -196°C) which were also available for this research. Significantly, these stores contain several CLL samples with specific genetic aberrations, such as low frequency del17p sub-clones, which are relatively rare. Therefore, I made the effort was made to develop a protocol that works reliably on CLL cells which have been thawed following cryopreservation, and enables the analysis of these samples by FISH-IS.

Even though utilising the current thawing protocol (Yokoyama et al. 2001, Phelan et al. 2015) to revive cryopreserved CLL cells achieves up to 85% viability, it was found that many CLL cells had damaged cell membranes, resulting in cell rupture and apoptosis. The remaining cells were most likely still negatively affected by the freezing/thawing procedure, and therefore it was hypothesised that alterations to the time and culturing conditions may enable improved cell recovery. Therefore, various culture conditions were trialled with cryopreserved CLL cells to determine if an improvement in cell morphology could be achieved.

It is widely accepted that the proliferation rate of CLL cells is low, and the majority are arrested in the cell cycle at the G0/G1 phase (Hozier et al. 1998, Caligaris-Cappio et al. 1999, Ricciardi et al. 2001). Although CLL cells are resistant to apoptosis and able to expand *in vivo*, they rapidly die under *in vitro* culture conditions, presumably because they are not supported by extrinsic factors provided by the local tumour microenvironment (such as bone marrow, secondary lymphoid organs) (Collins et al. 1989, Munk Pedersen et al. 2004). As a result, CLL cells in standard media do not proliferate, and undergo spontaneous apoptosis within 24 hours (Collins et al. 1989, Burgess et al. 2012, Witkowska et al. 2014). Consequently, in addition to several different types of media, incubation with pre-conditioned media and direct cell-cell support in the form of co-culture with HS5 cells were investigated.

In general, a culture media is composed of a complement of inorganic salts, glucose, amino acids, vitamins and serum (containing hormones and growth factors). However, different culture media will contain these fundamental ingredients in different concentrations, meaning that each media preparation will not support optimal growth of all cell types. It has been reported that CLL cells cultured in serum-free AIM-V media have improved viability compared to standard media at day 15 (Levesque et al. 2001). Levesque et al. (2001) also demonstrated that the addition of FCS diminished the viability of CLL cells. Alternatively, McCoy's 5A media is very high in nutrients and has been shown to support fast recovery of poor quality embryonic cells (Godinez et al. 2012, Yang et al. 2012). In the present study, culturing lymphocytes in this media showed that it improves cell viability, but there are no reports in the literature of this media being used in culturing CLL cells. Data from the present study revealed that McCoy's media was not suitable for maintaining viability of cryopreserved CLL cells and was unable to improve the quality of the cells. An additional limitation was found in comparing the quality of cells between time-points and conditions, due to the limitations of brightfield images and low magnification of the EVOS™ microscope.

The confocal microscope (Flinders University microscopy facility) was explored to help distinguish further conditions necessary to improve the culture systems. Unfortunately, the plate design and objective lens were not appropriate to obtain the high-quality images when using the brightfield channel.

The concept of utilising a feeder layer as a cell supportive system in order to protect CLL cells from spontaneous apoptosis is common in the literature; support cells utilised include follicular dendritic cells (Pedersen et al. 2002), nurse-like cells (Burger et al. 2000), non-malignant leukocytes (Gamberale et al. 2001) and stroma cells (Panayiotidis et al. 1996, Kay et al. 2007, Gehrke et al. 2011, Burgess et al. 2012). The bone marrow stroma cell HS5 co-culture has been applied in several studies because the feeder monolayer is highly reproducible, forms without requiring additional growth factors, and enriches the media culture with numerous cytokines (IL-1, IL-3, IL-6, IL-8 and GM-CSF) (Roecklein et al. 1995). As a result, this enriched condition is hypothesised to be similar to the secretome generated by haematopoietic support cells *in vivo*.

In addition, using soluble factors to promote CLL cell survival and stimulate growth have been investigated in many reports, including interleukin-4 (IL-4) (Dancescu et al. 1992), IL-8 (Francia di Celle et al. 1996), IL-13 (Chaouchi et al. 1996), Insulin-like growth factor-1 (IGF-1) (known as anti-apoptotic factor *in vitro* (Schillaci et al. 2005), CXCL12, CXCL13, CXCL19 and CXCL20 (Ticchioni et al. 2007), CCL3 and CCL4 (Burger et al. 2009), and CCL2 and CXCL2 (Burgess et al. 2012). Despite this extensive list, I found that none of these factors were able to maintain CLL cells for longer than 2 weeks, nor were they able to recover functional CLL cells. Therefore, the thawed cells, which were presumably heavily damaged in the cryopreservation and thawing procedure, most likely underwent apoptosis or necrosis before the fixation procedure and surviving cells were still not robust enough to withstand the fixation and permeabilisation processes required for the FISH-IS protocol.

Therefore, in summary, a protocol for appropriate recovery conditions which would enable analysis of cryopreserved CLL cells by FISH-IS remains to be established.

## **5.5 Conclusions**

This chapter has provided a description of my novel technique of FISH-IS with 17p BAC probe contig which enables accurate identification of del17p sub-clones at a level as low as 3%. However, this method was not optimal on cryopreserved CLL samples and unfortunately, fresh CLL samples with rare genetic aberrations were unavailable at the time of undertaking this project. In order to validate the method, fresh CLL samples are needed, especially low frequency del17p CLL samples. In the future, a larger study is required to translate this technique into the diagnostic setting.

Current investigations include the genomic profiles of clones sorted by this technique. These experiments will be performed on the basis of the experiments conducted and optimised in this thesis. The sub-clones will be analysed using whole exome sequencing to discover the early drivers and the clonal architecture associated with 17p deletion in order to better define therapeutic risk in patients. While this was my original intention for this study, time constraints have excluded these experiments. It is clear that the application of this technology and the knowledge achieved through its use will provide a better platform to understand the low frequency del17p clonal architecture and mutational load and ultimately inform clinical decision making in the era of small molecular therapies.



## 6 Chapter 6 - General Discussion and Conclusions

### 6.1 Overview

The aim of this research project was to address the question surrounding the clinical and biological significance of low frequency del17p in CLL and included ways in which to explore the frequency and genetic makeup of this clinically important subset of CLL. In the clinical setting, despite the worst prognosis in CLL residing with del17p, many patients with a sub-clone of del17p demonstrate an indolent disease course. Explanations for this may include: (1) the presence of many other concomitant driving mutations in the del17p sub-clones, which may contribute differently to del17p CLL progression; and (2) the heterogeneous sizes of del17p sub-clones which are apparent in CLL patients. The clinical course of these patients with del17p CLL might be highly variably dependent on the complex clonal evolution as well as the total del17p burden, particularly in low frequency del17p CLL, where the microenvironment and the fitness of other clones may play a significant role.

In order to successfully treat these CLL patients, the biological context of low frequency del17p sub-clones needs to be explored. This is particularly important in the era of novel therapies where for the first time there is non-chemotherapeutic choice for therapy which needs to be employed in the right time-frame and sequence in the CLL population at large. However, at present, this research project is the first to have undertaken investigation *in depth* of low frequency del17p in CLL, in an attempt to address the gap in research in this area. The importance of mutated *TP53* in low frequency has been investigated and demonstrated in a retrospective investigation by Rossi et al. (2014) but this still fails to answer many burgeoning questions.

From the FISH results of the analysis of the CLL5 cohort, three quarters of del17p CLLs were found to be low frequency. This subgroup was further investigated in this thesis. Using high throughput methodology that allows the individual characterisation of thousands of cells by flow cytometric methodology but using DNA probes, I were able to interrogate the sub-clonal architecture of del17p sub-clones. Interestingly, as reported in Chapter 3, is the significant relationship between del13q and del17p in the low frequency clones which combines a traditionally good prognostic genetic finding with a poor prognostic deletion. Analysis of normal individuals and patients with normal-by-FISH karyotype analysis was undertaken using the same methodology. This allowed a more in-depth analysis of sub-clonal frequencies and demonstrated underlying sub-clonal events within these heterogeneous sub-clones, challenging the common belief that the *TP53* gene loss occurs only after del13q clonal development as the second hit of genomic alterations. The coexistence of separate del13q and del17p sub-clones within the total clone raises the possibility that in early stage CLL, due to inherent DNA instability possibly related to the requirement for DNA alterations at an advanced somatic level (including IgHV), multiple sub-clones are vying for domination and the original hierarchical sequencing does not always apply. Hence, del13q and del17p events may be occurring simultaneously but in different sub-clones, leading to sub-clonal heterogeneity. This was demonstrated somewhat imperfectly by the DNA probes used in this study.

At the beginning of this project in 2013, no molecular techniques were available to approach these low frequency del17p sub-clones *in depth* without bias. Single cell approaches were considered using Fluidigm® methodology but there were prohibitively expensive and subject to potential problems inherent to single cell genetic amplification. Therefore, with the emergence of the ImageStreamX machine, a new technique was required, as described in Chapter 5. Thus, the striking feature of this project is the successful development of

a FISH-IS technique with “homemade” custom probes (17p BAC probe contig) and its application to CLL samples. The results in this project demonstrate that FISH-IS can accurately identify the locus-specific deletion of chromosome 17p within sub-clones, and in particular, can potentially isolate the low frequency del17p sub-clones by flow sorting for subsequent profiling of genomic characteristics.

The following sections provide a detailed discussion of the characteristics of low frequency del17p sub-clones, of the features of the FISH-IS method, its other potential applications, and finally, possible future research directions for this work.

## **6.2 Characteristics of low frequency del17p sub-clone**

This project targeted two recent hot topics in CLL research: del17p and sub-clone characteristics in CLL. Although sub-clones and intra-tumour heterogeneity in CLL have been evident for decades, many fundamental questions remain unanswered about their frequencies, their origins, their biology and especially their evolution relationships with other genetic abnormalities. The results, recorded in Chapter 3, once again illustrated the intra-tumour genetic heterogeneity in CLL potentially underlying the clinical discrepancy in outcomes. The results also provided insights into sub-clonal characteristics, including the concomitant low frequency del17p and del13q in CLL. This genomic concomitance may lead to synergistic effects between these two alterations that promote the fitness of these sub-clones and increase the potential for co-occurrent driver mutations (Zhang et al. 2017). Following this theme, mutual exclusivity in cancer and/or co-occurrence of driver mutations have recently been further explored (Babur et al. 2015, Dao et al. 2017, Kim et al. 2017, Martincorena et al. 2017). It has been found that in many types of tumours the concomitant driver mutations in sub-clones can co-exist and expand in parallel, suggesting intra-clonal cooperative interactions (de Bruin et al. 2014, Yates et al. 2015, Davis et al. 2017).

Furthermore, Zhang et al. (2016) demonstrated that significant increase of *TP53* disruption burden in five different cancer types increases with age. This may help to explain the higher than expected incidence of the low frequency del17p seen in the CLL5 cohort when compared with published younger cohorts, (Catovsky et al. 2007, Rossi et al. 2009). However, the incidence of clinically significant del17p (>25%) in the present cohort was equivalent to these previous studies. Additionally, the reporting of the low frequency clones may not have been seen as relevant to the clinical trial process of these studies whereas it was the focus of this study.

### **6.3 The FISH-IS method provides superior monitoring of del17p sub-clones.**

With the available cytogenetic tests, sub-clones were only evaluated at certain time points in treatment due to the limitations in detection of low frequency clones, as these tests only reliably distinguish large changes, for instance, from <10% to 30% and at times when treatment is being reconsidered due to relapsing or progressive disease. There is no real ability to monitor sub-clonal population changes over time to better understand the behaviour of CLL sub-clones and the impact these may have on disease behaviour. This is particularly evident in the post FCR treated patients, where eventual relapse often heralds substantial clonal evolution which clinicians only pick up as they make treatment decisions.

The newly developed technique of FISH-IS in this project, is not only able to detect the differences in 1%-3% of genomic alterations, but also can help to monitor the sub-clones' progression more frequently and more efficiently. If persistent change and progression in the size of sub-clones under treatment can be identified, I would have the capacity to make timely and prompt interventions either with initiation or changing of the current therapy. This novel technique also has the potential to shed further light and understanding on the

heterogeneity of CLL sub-clones with different treatments including BTK and PI3Kinase inhibitors where persistence of the clones occurs for many months but with limited understanding of how the sub-clonal populations are responding in treatment. In addition, if this technique can be combined with immuno-phenotyping, the genotype/immuno-phenotype can be tracked in CLL tumour cells simultaneously during different treatment time points. This knowledge will be critical for developing therapeutic strategies and for understanding individual responses to drugs. It will enable us to anticipate disease responses more accurately in this era of personalized-medicine.

With the enormous development of *in-depth* MPS techniques, some studies have suggested screening of *TP53* mutational load as an early detection tool or biomarker prediction for specific cancers (Krimmel et al. 2016, Silwal-Pandit et al. 2017). However, the order of any two events, including del17p (*TP53* loss) and *TP53* mutations that occur in cancer is still unclear (Soussi 2010). One study of a colorectal cancer model showed that *TP53* alterations occurred usually at a late transformed stage of cancer (Fearon et al. 1990). This model also showed that the order of the *TP53* defect in tumorigenesis may vary. Likewise, the existence of *TP53* aberrations is considered to be a late event in CLL (Lawrence et al. 2013). However, the data in the thesis would suggest that low frequency del17p may in fact not be a late event and may be arising in sub-clonal form earlier in the disease state and in equilibrium, in some cases, with other known CLL drivers (like del13q). Therefore, improved knowledge of the low frequency del17p sub-clones would help to address this problem of event sequence and clonal hierarchy that eventually contributes to disease progression or relapse post-treatment.

## **6.4 The FISH-IS method has the potential to integrate with many other fields**

The ImageStreamX is able to simultaneously acquire up to 12 different images of each cell (with 12 channels), which rapidly provides tens of thousands of multispectral images with high spatial resolution, and collects them in a uniform manner simultaneously (Basiji et al. 2007). This rich information is supported by the algorithm imaging software tool (IDEAS®) which is able to quantify approximately 40 features per single image, providing up to 250 features per single cell (Eliceiri et al. 2012). The FISH-IS method developed in this study would have broader application which is not restricted to genetic characterisation of CLL. The remaining available fluorescence channels of ImageStreamX are able to be used for simultaneous investigation of other biological questions, including improved cellular visualisation, co-localisation of genetic abnormalities in subpopulations of cells with accurate quantification and standard immuno-phenotyping in conjunction with genetic characterisation (Fuller et al. 2016).

ImageStreamX has been used in multiplexed assays to quantify Golgi proteins (Wortzel et al. 2017), to analyse miRNAs and protein targeted in small cell subsets (Ponomarev et al. 2011), to accurately enumerate micro-particles (Vranic et al. 2013, Headland et al. 2014), and to enhance the detection and quantify extracellular vesicles (Erdrügger et al. 2014, Clark 2015). Notably, ImageStreamX has been widely applied in screening for the response to drugs, for instance, in monitoring antimalarial drugs (Lee et al. 2014b). Taken together, the promising FISH-IS method developed here can be integrated with other capacities of imaging flow cytometry instruments such as the analysis of cell cycle (Gillard et al. 2006, Filby et al. 2011), nuclear translocation of NF- $\kappa$ B (George et al. 2006, Maguire et al. 2011), cell signalling pathway interactions (Pham et al. 2005, Nobile et al. 2010) and apoptosis/necrosis (George et al. 2004, Khuda et al. 2008, Wlodkowic et al. 2010,

Pietkiewicz et al. 2015). Integration of the above aspects with FISH-IS will make it a high content screening tool for the discovery/development of potential new drug candidates (Elliott 2009, Chang et al. 2010, Xu et al. 2010, Zanella et al. 2010). For instance, Pawluczko et al. (2009) studied CLL samples using the ImageStreamX (with protein co-localization features) to show that ofatumumab (monoclonal antibody for CD20) is more effective than rituximab by demonstrating that less C1q (complement-dependent) binding to CLL cells was observed.

Recently, different combinations with FISH-IS approaches have been investigated by other groups. Fuller et al. (2016) demonstrated the integration of genetic and immuno-phenotyping (CD) markers (immune-S-FISH). This combination can detect genomic aberrations in different cell subgroups with identification of the immuno-phenotype. However, a notable issue of this combination is that Carnoy 's fixative compromised the integrity of conjugated antibody epitopes with the preservation of fluorescence (Werner et al. 2000). While this is a promising technology, clearly each particular combination of imaging techniques needs to be tested before general application is possible. However, the dual approaches described open a door to better understanding of the biology of individual cells or sub-clonal populations while being able to characterise thousands of cells in a statistically meaningful way.

## 6.5 Future directions for this project – Other approaches to solving the puzzle

Screening one cancer cell or a few cancer cells within a majority of normal cells in a clinical setting or when tracking MRD means that I are looking for rare events (as in the case of this study, cells with *TP53* aberrations), even though the small number of events does not yet impact the behaviour of the whole clone or the individual patient outcome. However, I know that it is from these small sub-clones, often present at diagnosis that the resistant and refractory disease arises. Although standard MPS approaches make it possible to detect low levels of mutation events, there is still the probability of sequencing errors at some level. It is easier to find the needle in the haystack when you know retrospectively what the needle looks like (Akogwu et al. 2016, Park et al. 2017). In response to some of the technical issues surrounding MPS, duplex sequencing was recently launched as a novel method that overcomes the mutation sequencing errors of MPS (Schmitt et al. 2015). This method uses random tagging of ds DNA (barcodes) to detect mutations. Duplex sequencing enables identification of the allele reads derived from each strand of two complementary DNA strands. Schmitt et al. (2012) demonstrated that duplex sequencing can yield 10,000-fold higher accuracy in sequencing data compared with previous MPS methods. In particular, this method has been reported to detect mutation frequency as low as one per billion sequenced nucleotides (Kennedy et al. 2014, Nachmanson et al. 2017). However, this method is still limited by the cost of sequencing and the small size of the target (<1 Mb).

Although the ultra-deep MPS was able to detect the *TP53* mutations in up to  $1/10^7$ , interpretation of what is happening within the same cell/clone is still impossible by this method (Kalisky et al. 2011). Therefore, to fully understand the heterogeneity and the complexity of cancer sub-clones, the need remains for somatic mutations to be analysed at the level of single cells within the bulk of heterogeneous tumour cells (Navin et al. 2011,



Wang et al. 2012a). In addition, an analytical challenge of MPS single cell data interpretation requires modern computational bioinformatics (Harrington et al. 2010, Bankevich et al. 2012). The Fluidigm C1 instrument was released in 2013 for automated processing of single cell sequencing, including isolation, lysis, and nucleic acid pre-amplifications from single cells. Single cells sequencing (e.g. Fluidigm C1) can provide a wealth of information on single cells captured in 96 well-plates single cells. Gawad et al. (2014) from Stanford University (USA) applied targeted resequencing of single cells (Fluidigm C1 systems) to investigate the clonal origins of intra-tumour heterogeneity of acute lymphoblastic leukaemia. This research noted that the amplification step needs to be highly uniform as the limitations of allele dropout or imbalance impeded the accuracy of their interpretation of the sub-clonal structures. Furthermore, Gawad and his group also reported that in order to obtain high fidelity sequencing data, this single cell method may need to start with sequence from a larger part of the genome template in more cells (bulk cells), especially in cases of high sub-clonal heterogeneity in tumours (de Bourcy et al. 2014, Gawad et al. 2016).

Taken together, apart from the above described limitations of the single cell sequencing method, its main disadvantage is that it is a very expensive process. Therefore, currently it cannot be applied in a routine clinical setting. By contrast, the novel technique developed here is more readily applicable, as it is not expensive other than the initial acquisition of the equipment, and is able to facilitate the analysis of sub-clones with sequencing based on the DNA of sub-clones purified by flow sorting. Enrichment of the target clone by this means alleviates the need for single cell sequencing and could equally apply to immuno-phenotypic sub-clones as well as genetic sub-clones. However, the single cell sequencing method would no doubt be applied more widely in the future if its cost drops significantly with advances in its technical development.

Proof-of-principle experiments for *TP53* mutations have been screened down to 0.3% (Rossi et al. 2014). However, no whole genome based technique can lower the limitation of detection in del17p (SNP array is approximately 10-20% depending on the approaches used). Therefore, sensitive low frequency del17p detection serves to deepen the ability of prognostic screening and, importantly, inspire new and different treatment plans for del17p CLL patients in the future. These more and more precise analyses suggest that knowing the clonal architecture of each patient's tumour will be crucial for optimising their treatment particularly when the outcome of chemo-immunotherapy on genetically unstable clones leads to progressively resistant disease.

Going forward, there is a need for translation studies of this technique with larger validation series on more CLL patient samples to address clinically challenging issues. With such studies, this new technique can become a valuable tool in diagnosis, prognosis and especially in monitoring at the early stages of del17p CLL as well as enhancing our understanding as to how these small sub-clones survive therapy and go on to ultimately cause disease relapse.

## 6.6 Conclusion

In summary, this research project has optimised and developed a FISH-IS approach using a 17p BAC contig probe to accurately identify del17p sub-clones at a level as low as 3%. This new technique needs translational studies to fully understand its utility as a diagnostic, prognostic and monitoring tool in the future. Future work in flow sorting and molecular analysis of sub-clones that follows this study will provide further unique sub-clonal information which will hopefully guide us to a better understanding of the biology of low frequency del17p sub-clones in CLL.

## Appendix

**Table 1. CLL5 trial inclusion and exclusion criteria**

Inclusion Criteria	<ul style="list-style-type: none"> <li>- B-CLL confirmed according to NCI Working Group Criteria.</li> <li>- Binet stage B or C, or progressive symptomatic stage A.</li> <li>- Age <math>\geq</math> 65 years old.</li> <li>- Judged to be in need of systemic therapy.</li> <li>- No previous treatment (chemotherapy, radiotherapy or immunotherapy) for CLL.</li> <li>- Alkaline phosphatase and transaminases <math>\leq</math> 2 x ULN.</li> <li>- Creatinine clearance <math>\geq</math> 50 mL/min (as calculated by eGFR; eGFR also calculated by Cockcroft and Gault formula for final analysis).</li> <li>- Females of childbearing potential or fertile males must take contraceptive measures during and at least 6 months after cessation of therapy.</li> <li>- CIRS score &lt; 6.</li> <li>- Life expectancy &gt; 6 months.</li> <li>- Patient's written informed consent.</li> </ul>
Exclusion Criteria	<ul style="list-style-type: none"> <li>- Age &lt; 65 years old.</li> <li>- Non-progressive or stable Binet stage A.</li> <li>- Clinically significant auto-immuno cytopenia, Coombs-positive haemolytic anaemia (as discerned by treating physician).</li> <li>- Active second malignancy currently requiring treatment (except for non-melanoma skin cancer or cervical cancer <i>in situ</i> or tumour treated curatively by surgery &gt; 5 years ago).</li> <li>- Concomitant disease requiring prolonged use of glucocorticoids (&gt; 1 month).</li> <li>- Known hypersensitivity with anaphylactic reaction to humanised monoclonal antibodies or any of the study drugs.</li> <li>- Class III or IV cardiac disease defined by the NYHA.</li> <li>- Severe or debilitating pulmonary disease.</li> <li>- Severe or debilitating central nervous system disease or cerebral dysfunction.</li> <li>- Transformation to aggressive B-cell malignancy, e.g. diffuse large cell lymphoma, Richter's syndrome or prolymphocytic leukaemia.</li> <li>- Active bacterial, viral or fungal infection; patients who have known Human Immunodeficiency Virus (HIV) infection or active hepatitis B virus (HBV) or hepatitis C virus (HCV) infection.</li> <li>- Total bilirubin &gt; 2 x ULN.</li> <li>- Creatinine clearance &lt; 50 mL/min (as calculated by eGFR).</li> <li>- Any coexisting medical or psychological condition that would preclude participation in the required study procedures.</li> <li>- Treatment with any other investigational agent, or participation in another clinical trial within 30 days prior to entering this study.</li> <li>- Pregnancy and lactation.</li> </ul>

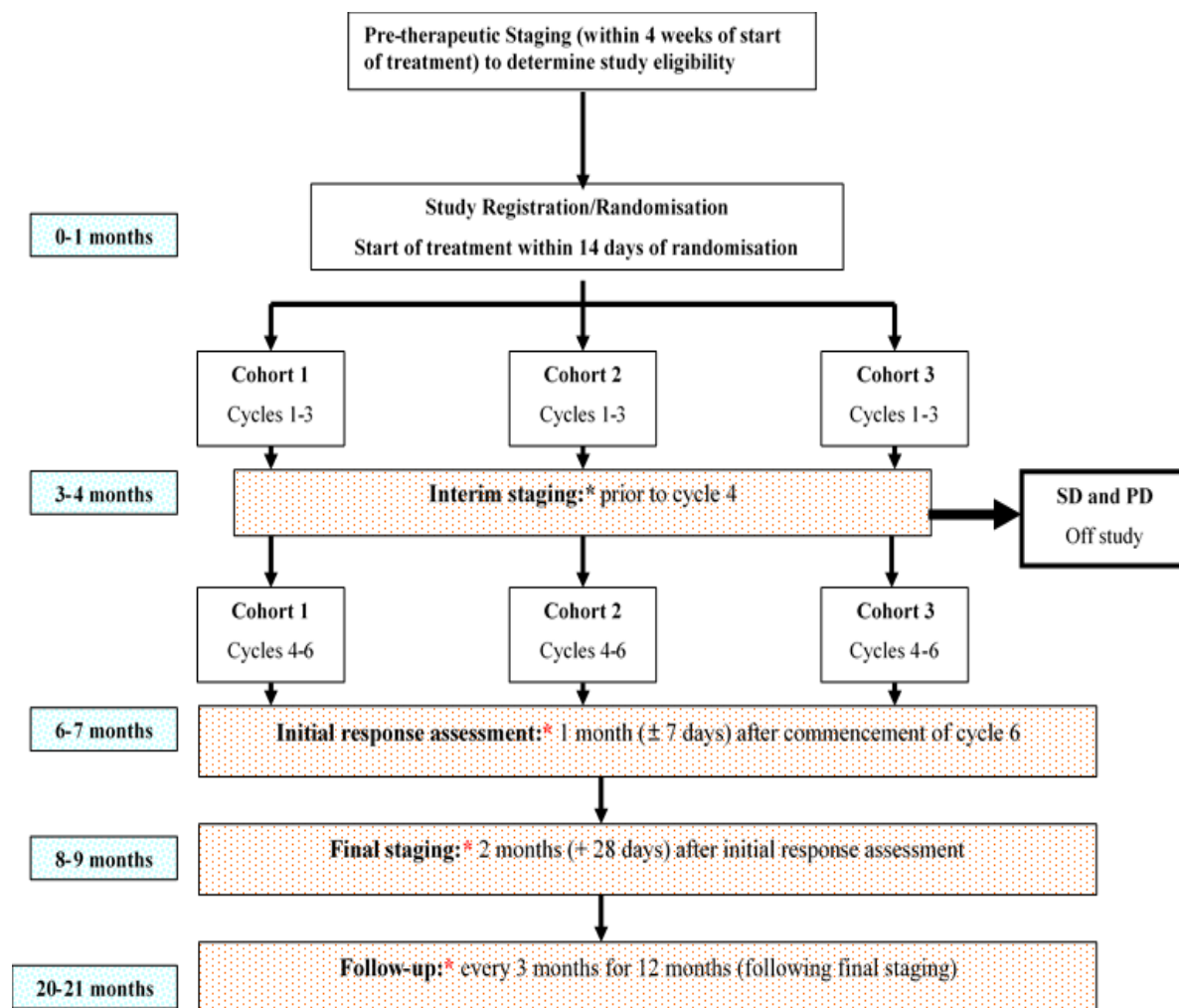
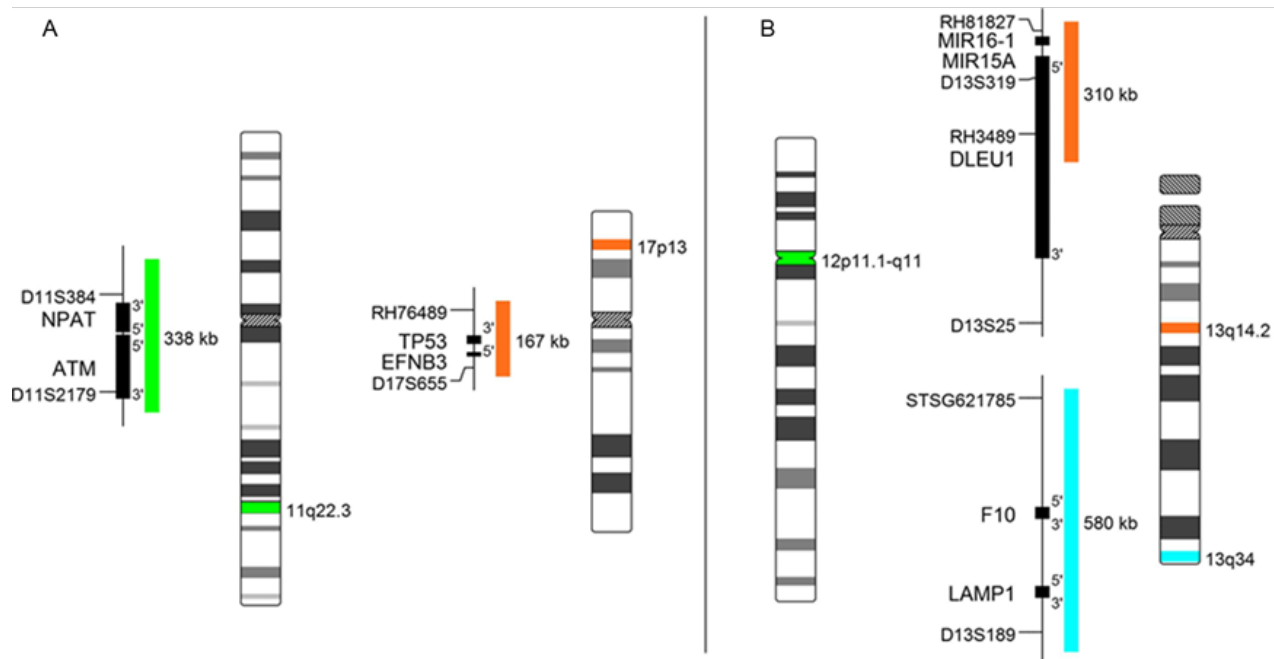


Figure 1. General ARC CLL5 trial cohort treatment schema.

Table 2. CLL5 cohort treatment arms.

Treatment	Oral Fludarabine	Oral Cyclophosphamide	IV Rituximab
Cohort 1 "FR5"	24 mg/m <sup>2</sup> Days 1-5	-	Cycle 1: 375 mg/m <sup>2</sup> D0 Cycles 2-6: 500 mg/m <sup>2</sup> D1
Cohort 2 "FCR3"	24 mg/m <sup>2</sup> Days 1-3	150 mg/m <sup>2</sup> Days 1-3	Cycle 1: 375 mg/m <sup>2</sup> D0 Cycles 2-6: 500 mg/m <sup>2</sup> D1
Cohort 3 "FCR5"	24 mg/m <sup>2</sup> Days 1-5	150 mg/m <sup>2</sup> Days 1-5	Cycle 1: 375 mg/m <sup>2</sup> D0 Cycles 2-6: 500 mg/m <sup>2</sup> D1



**Figure 2. XL CLL commercial probe kit mapping location.**

(A) Vial 1: ATM/TP53 probes. (B) Vial 2: DLEU/LAMP/12 CEN probes.

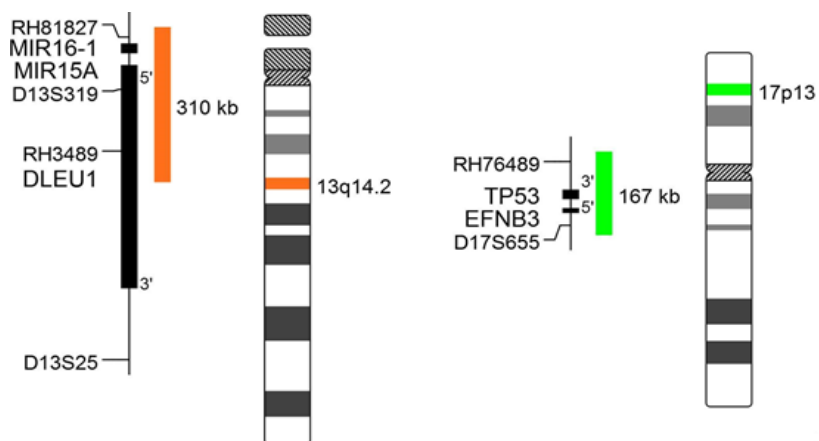


**Figure 3. XL DLEU/TP53 commercial probe kit mapping location.**

**Table 3. All conventional FISH results of CLL5 cohort.**

CLL5 number	Site	D13S319 (13q14.3)	D13S319 (13q14.3)	12p11.1-q11	11q22.3	17p13.1
		(Mono-allelic del13q)	(Bi-allelic deletion)	(Trisomy 12)	(del11q)	(del17p)
001	RMH	2	0	<1	2	5
002	RNS	6	0	2	4	2
003	PAH	73	0	1	95	4
004	STV	9	0	<1	2	7
005	RNS	97	0	2	<1	4
006	RMH	6	0	<1	2	4
007	PAH	4	0	<1	95	5
008	PAH	4	0	2	4	9
009	QEH	94	0	72	4	2
010	RNS	86	0	<1	2	5
011	RNS	4	0	55	2	6
012	HOB	13	0	51	9	7
013	MMN	4	0	4	2	4
014	PAH	8	0	3	4	2
015	RNS	96	0	12	3	3
016	GEE	96	0	3	9	12
017	FRA	3	0	0	4	5
018	SCG	4	93	1	5	12
019	RNS	6	0	2	88	11
020	RNS	95	0	2	2	5
021	RNS	96	0	<1	5	10
022	FRA	4	0	2	4	5
023	PAH	ND	ND	ND	ND	ND
024	PMC	3	0	2	4	3
025	RMH	ND	ND	ND	ND	ND
026	PAH	<1	0	1	1	3
027	HOB	8	0	55	2	5
028	BMO	3	0	43	1	5
029	WES	ND	ND	ND	ND	ND
030	RNS	79	0	<1	2	8
031	HOB	88	0	<1	9	8
032	WES	29	0	1	1	1
033	AUK	N/A	N/A	N/A	N/A	N/A
034	BMO	84	0	3	3	2
035	RNS	4	0	48	2	2
036	STV	ND	ND	ND	ND	ND
037	CAN	95	0	1	4	12
038	RNS	83	0	2	<1	1

039	RMH	10	0	2	93	5
040	HOB	80	0	<1	4	4
041	RMH	3	0	76	4	3
042	CAN	47	52	3	2	5
043	CAN	ND	ND	ND	ND	ND
044	RNS	30	0	1	<1	4
045	?	N/A	N/A	N/A	N/A	N/A
046	MMN	60	27	<1	4	22
047	CHR	N/A	N/A	N/A	N/A	N/A
048	PAH	2	0	<1	2	2
049	RMH	23	0	2	3	2
050	WOL	N/A	N/A	N/A	N/A	N/A
051	RMH	1	0	37	1	3
052	RNS	3	92	<1	3	3
053	CHR	N/A	N/A	N/A	N/A	N/A
054	SCG	2	0	<1	3	88
055	CAN	ND	ND	ND	ND	ND
056	NSH	N/A	N/A	N/A	N/A	N/A
057	STG	ND	ND	ND	ND	ND
058	GCH	4	0	73	5	22
059	STV	4	0	1	9	8
060	CHR	N/A	N/A	N/A	N/A	N/A
061	NSH	N/A	N/A	N/A	N/A	N/A
062	PMC	3	0	1	3	3
063	SCG	4	95	<1	9	41
064	AUS	3	0	85	2	2
065	SCG	ND	ND	ND	ND	ND
066	STG	10	0	<1	4	90
067	PAH	ND	ND	ND	ND	ND
068	AUS	2	0	<1	2	3
069	AUK	N/A	N/A	N/A	N/A	N/A
070	HOB	60	18	<1	4	4
071	COF	3	0	77	3	1
072	NSH	N/A	N/A	N/A	N/A	N/A
073	RNS	80	0	3	18	2
074	AUS	7	0	1	3	1
075	NSH	N/A	N/A	N/A	N/A	N/A
076	HOB	86	0	<1	2	<1
077	AUS	22	12	2	3	2
078	PAH	7	0	3	95	1
079	AUS	3	0	<1	1	1
080	AUS	83	0	<1	1	2
081	GEE	87	0	14	<1	4

082	PMB	ND	ND	ND	ND	ND
083	CON	73	0	<1	3	<1
084	AUS	30	0	3	1	3
085	MMC	1	0	<1	2	91
086	BMO	3	0	1	3	2
087	AUK	N/A	N/A	N/A	N/A	N/A
088	GCH	1	0	76	2	4
089	FMC	0	89	<1	<1	85
090	RDH	2	0	<1	<1	3
091	GOS	4	0	<1	2	4
092	QEH	9	87	<1	96	3
093	CAN	N/A	N/A	N/A	N/A	N/A
094	AUK	N/A	N/A	N/A	N/A	N/A
095	SCG	9	83	60	5	2
096	AUK	N/A	N/A	N/A	N/A	N/A
097	RNS	86	0	1	<1	2
098	HOB	87	10	<1	2	5
099	GEE	88	0	<1	2	2
100	GOS	4	0	<1	1	5
101	QEH	95	0	<1	95	9
102	HOB	4	0	<1	1	3
103	GCH	63	0	<1	18	5
104	RNS	94	0	<1	3	3
105	CAN	84	11	<1	2	4
106	GOS	4	93	<1	2	3
107	RNS	2	0	1	2	4
108	CAN	4	0	63	2	2
109	GEE	1	0	72	2	4
110	FRA	<1	0	66	2	3
111	FMC	45	0	1	1	1
112	AUS	56	0	0	4	3
113	CAN	<1	0	2	4	3
114	LGH	2	71	2	18	4
115	AUS	89	0	0	2	5
116	SCG	75	0	<1	2	4
117	GOS	4	0	0	2	3
118	AUS	85	0	<1	<1	3
119	GOS	7	0	<1	2	5
120	STV	3	87	<1	71	4

All results are displayed in %.

ND: poor sample quality; N/A: no enrolment specimen received by Flinders.



**Table 4. Cumulative Illness Rating Scale (CIRS)**

Rating Strategy of Comorbidity		
0	No problem	Organ system not compromised
1	Mild	Illness/impairment with or without requirement of therapy, excellent prognosis, patients with normal activity.
2	Moderate	Illness/impairment requiring therapy, good prognosis, compromised activity of patient.
3	Severe	Illness/impairment with urgent requirement of therapy, prognosis unclear, marked restriction in activity.
4	Extremely severe	Life threatening illness/impairment, emergency case of therapy, adverse prognosis.

*All organ systems are scored for comorbidity values the above scale and summed.*

**Table 5. Response criteria in CLL5.**

Complete Remission (CR)	<p>Complete remission is present if all the following criteria are fulfilled for at least 2 months:</p> <ul style="list-style-type: none"> <li>• Absence of lymphadenopathy confirmed by physical examination and/or appropriate radiographic techniques (i.e. all lymph nodes &lt; 1 cm in diameter)</li> <li>• No hepato-, splenomegaly by physical examination and/or appropriate radiographic techniques</li> <li>• Absence of constitutional symptoms (= B-symptoms)</li> <li>• No disease symptoms</li> <li>• Normal blood count with: <ul style="list-style-type: none"> <li>○ polymorph nuclear leukocytes (granulocytes) &gt; 1.5 x 10<sup>9</sup>/L.</li> <li>○ Platelets &gt; 100 x 10<sup>9</sup>/L.</li> <li>○ Hb &gt; 110 g/L (without blood transfusion)</li> <li>○ lymphocytes &lt; 5.0 x 10<sup>9</sup>/L</li> </ul> </li> <li>• Bone marrow normocellular for age, &lt; 30 % lymphocytes, no lymphocytic nodules (if the bone marrow is hypo-cellular, a repeat determination should be made in 4 weeks. Samples should be reviewed in conjunction with the prior pathology)</li> <li>• A subset of patients who are otherwise in complete remission but have bone marrow nodules that can be identified histologically are referred to as nodular PR (nPR) and are included in the PRs.</li> </ul>
-------------------------	---

Nodular Partial Remission (nPR)	<p>Some patients fulfil all the above criteria for CR but still have nodules of lymphocytes in the bone marrow histology despite a total lymphocyte count of &lt; 30 %. Although the clonality of these nodules is difficult to determine with the currently available methods these patients nevertheless have a shorter progression-free survival than patients with genuine complete remission without lymphocyte nodules. Therefore these cases are described as nodular partial remission (nPR) and should be listed separately in the evaluation.</p>
Partial Remission (PR)	<p>Partial remission is present if the following criteria are fulfilled for at least 2 months:</p> <ul style="list-style-type: none"> <li>• Reduction in peripheral lymphocyte count by <math>\geq 50\%</math> from pre-treatment value</li> <li>• Reduction in lymph node enlargement by <math>\geq 50\%</math> (sum of products of recorded enlarged lymph nodes)</li> <li>• Reduction of hepato- and/or splenomegaly by <math>\geq 50\%</math> if enlarged at baseline (e.g. a reduction in spleen size from 20 cm to 16 cm on ultrasound and/or a reduction in palpable hepatomegaly from 5 cm to 3 cm)</li> <li>• <i>plus at least one of the following criteria:</i></li> <li>• Polymorphonuclear leukocytes (granulocytes) <math>\geq 1.5 \times 10^9/L</math> or 50% improvement over baseline value</li> <li>• Platelets <math>&gt; 100 \times 10^9/L</math> or 50% improvement over baseline value</li> <li>• Hb <math>&gt; 110 \text{ g/L}</math> or 50 % improvement over baseline value without blood transfusions.</li> </ul>
Progressive Disease (PD)	<p>Progression is present if at least <i>one</i> of the following criteria is fulfilled:</p> <ul style="list-style-type: none"> <li>• <math>\geq 50\%</math> increase in the sum of the products of the diameters of at least two lymph nodes ( at least one node must be <math>\geq 2 \text{ cm}</math>); appearance of new palpable lymph nodes or any new extranodal lesion (regardless of size)</li> <li>• <math>\geq 50\%</math> increase in the size of the liver and/or spleen as determined by measurement below the relevant costal margin or by ultrasound/CT scan; appearance of palpable hepatomegaly or splenomegaly that was not previously present</li> <li>• <math>\geq 50\%</math> increase in the absolute number of circulating lymphocytes to at least <math>5 \times 10^9/L</math></li> <li>• Transformation to a more aggressive histology (e.g. Richter's syndrome or PLL with <math>&gt; 55\%</math> prolymphocytes).</li> </ul> <p>In case of uncertain progression based on lymph node enlargement alone, measurements should be repeated at least 2 weeks later since transient enlargement may occur and does not count as progressive disease.</p>

**Table 6. Hierarchical log linear analysis by SPSS version 22.**

Step Summary						
Step <sup>a</sup>		Effects	Chi-Square <sup>c</sup>	df	Sig.	Number of Iterations
0	Generating Class <sup>b</sup>	del17p*del11q*tri12*del13qmo*del13qbi	.000	0	.	
	Deleted Effect 1	del17p*del11q*tri12*del13qmo*del13qbi	.000	1	1.000	2
1	Generating Class <sup>b</sup>	del17p*del11q*tri12*del13qmo, del17p*del11q*tri12*del13qbi, del17p*del11q*del13qmo*del13qbi, del17p*tri12*del13qmo*del13qbi, del11q*tri12*del13qmo*del13qbi	.000	1	1.000	
	Deleted Effect 1	del17p*del11q*tri12*del13qmo	.000	1	1.000	2
	2	del17p*del11q*tri12*del13qbi	.000	1	1.000	2
	3	del17p*del11q*del13qmo*del13qbi	.000	1	1.000	2
	4	del17p*tri12*del13qmo*del13qbi	.000	1	1.000	2
2	Generating Class <sup>b</sup>	del17p*del11q*tri12*del13qmo, del17p*del11q*tri12*del13qbi, del17p*del11q*del13qmo*del13qbi, del11q*tri12*del13qmo*del13qbi	.000	2	1.000	
	Deleted Effect 1	del17p*del11q*tri12*del13qmo	.000	1	1.000	2
	2	del17p*del11q*tri12*del13qbi	.000	1	1.000	2
	3	del17p*del11q*del13qmo*del13qbi	.000	1	1.000	2
	4	del11q*tri12*del13qmo*del13qbi	.000	1	1.000	2
3	Generating Class <sup>b</sup>	del17p*del11q*tri12*del13qmo, del17p*del11q*tri12*del13qbi, del11q*tri12*del13qmo*del13qbi, del17p*del13qmo*del13qbi	.000	3	1.000	
	Deleted Effect 1	del17p*del11q*tri12*del13qmo	.000	1	1.000	3
4	Generating Class <sup>b</sup>	del17p*del11q*tri12*del13qbi, del11q*tri12*del13qmo*del13qbi, del17p*del13qmo*del13qbi, del17p*del11q*del13qmo, del17p*tri12*del13qmo	.000	4	1.000	
	Deleted Effect 1	del17p*del11q*tri12*del13qbi	.000	1	.999	2
	2	del11q*tri12*del13qmo*del13qbi	.000	1	1.000	2

	3	del17p*del13qmo*del13qbi	.000	1	1.000	3
	4	del17p*del11q*del13qmo	.163	1	.687	5
	5	del17p*tri12*del13qmo	.000	1	1.000	3
5	Generating Class <sup>b</sup>	del17p*del11q*tri12*del13qbi, del11q*tri12*del13qmo*del13qbi, del17p*del11q*del13qmo, del17p*tri12*del13qmo	.000	5	1.000	
	Deleted Effect 1	del17p*del11q*tri12*del13qbi	.000	1	.999	2
	2	del11q*tri12*del13qmo*del13qbi	.000	1	.999	2
	3	del17p*del11q*del13qmo	.163	1	.686	5
	4	del17p*tri12*del13qmo	.000	1	1.000	3
6	Generating Class <sup>b</sup>	del17p*del11q*tri12*del13qbi, del11q*tri12*del13qmo*del13qbi, del17p*del11q*del13qmo	.000	6	1.000	
	Deleted Effect 1	del17p*del11q*tri12*del13qbi	.000	1	.995	2
	2	del11q*tri12*del13qmo*del13qbi	.000	1	1.000	3
	3	del17p*del11q*del13qmo	.164	1	.685	5
7	Generating Class <sup>b</sup>	del17p*del11q*tri12*del13qbi, del17p*del11q*del13qmo, del11q*tri12*del13qmo, del11q*del13qmo*del13qbi, tri12*del13qmo*del13qbi	.000	7	1.000	
	Deleted Effect 1	del17p*del11q*tri12*del13qbi	.000	1	1.000	3
8	Generating Class <sup>b</sup>	del17p*del11q*del13qmo, del11q*tri12*del13qmo, del11q*del13qmo*del13qbi, tri12*del13qmo*del13qbi, del17p*del11q*tri12, del17p*del11q*del13qbi, del17p*tri12*del13qbi, del11q*tri12*del13qbi	.000	8	1.000	
	Deleted Effect 1	del17p*del11q*del13qmo	.178	1	.673	5
	2	del11q*tri12*del13qmo	.000	1	.999	2
	3	del11q*del13qmo*del13qbi	.000	1	1.000	3
	4	tri12*del13qmo*del13qbi	.000	1	1.000	3
	5	del17p*del11q*tri12	.000	1	1.000	3

	6	del17p*del11q*del13qbi	.000	1	1.000	3
	7	del17p*tri12*del13qbi	.000	1	1.000	3
	8	del11q*tri12*del13qbi	.000	1	1.000	3
9	Generating Class <sup>b</sup>	del17p*del11q*del13qmo, del11q*tri12*del13qmo, del11q*del13qmo*del13qbi, tri12*del13qmo*del13qbi, del17p*del11q*tri12, del17p*del11q*del13qbi, del11q*tri12*del13qbi	.000	9	1.000	
Deleted Effect	1	del17p*del11q*del13qmo	.178	1	.673	5
	2	del11q*tri12*del13qmo	.000	1	.999	2
	3	del11q*del13qmo*del13qbi	.000	1	1.000	3
	4	tri12*del13qmo*del13qbi	.000	1	.998	2
	5	del17p*del11q*tri12	.000	1	1.000	3
	6	del17p*del11q*del13qbi	.000	1	1.000	3
	7	del11q*tri12*del13qbi	.000	1	1.000	3
10	Generating Class <sup>b</sup>	del17p*del11q*del13qmo, del11q*tri12*del13qmo, tri12*del13qmo*del13qbi, del17p*del11q*tri12, del17p*del11q*del13qbi, del11q*tri12*del13qbi	.000	10	1.000	
Deleted Effect	1	del17p*del11q*del13qmo	.183	1	.669	5
	2	del11q*tri12*del13qmo	.000	1	1.000	3
	3	tri12*del13qmo*del13qbi	.000	1	1.000	3
	4	del17p*del11q*tri12	.000	1	1.000	3
	5	del17p*del11q*del13qbi	.000	1	.999	3
	6	del11q*tri12*del13qbi	.000	1	1.000	3
11	Generating Class <sup>b</sup>	del17p*del11q*del13qmo, tri12*del13qmo*del13qbi, del17p*del11q*tri12, del17p*del11q*del13qbi, del11q*tri12*del13qbi	.000	11	1.000	
Deleted Effect	1	del17p*del11q*del13qmo	.175	1	.676	5
	2	tri12*del13qmo*del13qbi	.000	1	1.000	3

	3	del17p*del11q*tri12	.000	1	.999	3
	4	del17p*del11q*del13qbi	.000	1	.999	3
	5	del11q*tri12*del13qbi	.000	1	1.000	3
12	Generating Class <sup>b</sup>	del17p*del11q*del13qmo, tri12*del13qmo*del13qbi, del17p*del11q*tri12, del17p*del11q*del13qbi	.000	12	1.000	
	Deleted Effect 1	del17p*del11q*del13qmo	.174	1	.677	5
	2	tri12*del13qmo*del13qbi	.000	1	.998	3
	3	del17p*del11q*tri12	.000	1	1.000	3
13	Generating Class <sup>b</sup>	del17p*del11q*del13qmo, tri12*del13qmo*del13qbi, del17p*del11q*del13qbi, del17p*tri12, del11q*tri12	.000	13	1.000	
	Deleted Effect 1	del17p*del11q*del13qmo	.171	1	.679	5
	2	tri12*del13qmo*del13qbi	.000	1	.998	3
	3	del17p*del11q*del13qbi	.000	1	.997	3
	4	del17p*tri12	.880	1	.348	2
	5	del11q*tri12	.177	1	.674	3
14	Generating Class <sup>b</sup>	del17p*del11q*del13qmo, del17p*del11q*del13qbi, del17p*tri12, del11q*tri12, tri12*del13qmo, tri12*del13qbi, del13qmo*del13qbi	.000	14	1.000	
	Deleted Effect 1	del17p*del11q*del13qmo	.171	1	.679	5
	2	del17p*del11q*del13qbi	.000	1	1.000	3
15	Generating Class <sup>b</sup>	del17p*del11q*del13qmo, del17p*tri12, del11q*tri12, tri12*del13qmo, tri12*del13qbi, del13qmo*del13qbi, del17p*del13qbi, del11q*del13qbi	.000	15	1.000	
	Deleted Effect 1	del17p*del11q*del13qmo	.175	1	.675	5
	2	del17p*tri12	.880	1	.348	3
	3	del11q*tri12	.177	1	.674	3
	4	tri12*del13qmo	5.444	1	.020	2
	5	tri12*del13qbi	1.414	1	.234	3
	6	del13qmo*del13qbi	.931	1	.335	3

	7	del17p*del13qbi	.429	1	.512	3
	8	del11q*del13qbi	.987	1	.320	3
16	Generating Class <sup>b</sup>	del17p*tri12, del11q*tri12, tri12*del13qmo, tri12*del13qbi, del13qmo*del13qbi, del17p*del13qbi, del11q*del13qbi, del17p*del11q, del17p*del13qmo, del11q*del13qmo	.175	16	1.000	
	Deleted Effect 1	del17p*tri12	.872	1	.350	5
	2	del11q*tri12	.168	1	.682	5
	3	tri12*del13qmo	5.436	1	.020	5
	4	tri12*del13qbi	1.415	1	.234	5
	5	del13qmo*del13qbi	.943	1	.331	5
	6	del17p*del13qbi	.441	1	.506	5
	7	del11q*del13qbi	.999	1	.318	5
	8	del17p*del11q	2.528	1	.112	3
	9	del17p*del13qmo	37.329	1	.000	3
	10	del11q*del13qmo	4.682	1	.030	3
17	Generating Class <sup>b</sup>	del17p*tri12, tri12*del13qmo, tri12*del13qbi, del13qmo*del13qbi, del17p*del13qbi, del11q*del13qbi, del17p*del11q, del17p*del13qmo, del11q*del13qmo	.343	17	1.000	
	Deleted Effect 1	del17p*tri12	1.042	1	.307	5
	2	tri12*del13qmo	5.306	1	.021	5
	3	tri12*del13qbi	1.550	1	.213	5
	4	del13qmo*del13qbi	.936	1	.333	5
	5	del17p*del13qbi	.466	1	.495	5
	6	del11q*del13qbi	1.133	1	.287	5
	7	del17p*del11q	2.700	1	.100	3
	8	del17p*del13qmo	37.454	1	.000	3
	9	del11q*del13qmo	4.554	1	.033	3
18	Generating Class <sup>b</sup>	del17p*tri12, tri12*del13qmo, tri12*del13qbi, del13qmo*del13qbi, del11q*del13qbi, del17p*del11q, del17p*del13qmo, del11q*del13qmo	.809	18	1.000	

Deleted Effect	1	del17p*tri12	.945	1	.331	5
	2	tri12*del13qmo	5.288	1	.021	5
	3	tri12*del13qbi	1.453	1	.228	5
	4	del13qmo*del13qbi	2.350	1	.125	5
	5	del11q*del13qbi	.914	1	.339	5
	6	del17p*del11q	2.482	1	.115	3
	7	del17p*del13qmo	38.883	1	.000	3
	8	del11q*del13qmo	4.343	1	.037	3
19	Generating Class <sup>b</sup>	del17p*tri12, tri12*del13qmo, tri12*del13qbi, del13qmo*del13qbi, del17p*del11q, del17p*del13qmo, del11q*del13qmo	1.723	19	1.000	
Deleted Effect	1	del17p*tri12	.987	1	.321	5
	2	tri12*del13qmo	5.295	1	.021	5
	3	tri12*del13qbi	1.495	1	.221	5
	4	del13qmo*del13qbi	2.843	1	.092	5
	5	del17p*del11q	2.525	1	.112	3
	6	del17p*del13qmo	38.920	1	.000	2
	7	del11q*del13qmo	4.804	1	.028	3
20	Generating Class <sup>b</sup>	tri12*del13qmo, tri12*del13qbi, del13qmo*del13qbi, del17p*del11q, del17p*del13qmo, del11q*del13qmo	2.710	20	1.000	

a. At each step, the effect with the largest significance level for the Likelihood Ratio Change is deleted, provided the significance level is larger than .050.

b. Statistics are displayed for the best model at each step after step 0.

c. For 'Deleted Effect', this is the change in the Chi-Square after the effect is deleted from the model.

*The most significant relationship are highlighted in yellow.*



**Table 7. List of Illumina amplicons on chromosome 17, spanning 3 genes (*TP53*, *CD79B* and *GRB2*).**

Target Region Name	Chr	Start Position	End Position	ULSO Sequence
TP53_Exon (8753049)_7424190	17	7590656	7590928	TCAGGAGCTTACCCAATCCAGGGAAGCGTGTACCGTCGTGGAAAGCACGCTCCCAGCCCCGAACGCAAAG TGTCCTCCGGAGCCCAGCAGCTACCTGCTCCCTGGACGGTGGCTCTAGACTTTTGAGAAGCTCAAACTTTT AGCGCCAGTCTTGAGCACATGGGAGGGGAAAACCCCAATCCCATCAACCCCTGCGAGGCTCCTGGCACAA AGCTGGAC
TP53_Exon (8836199)_7424191	17	7577444	7577683	GTCTCCCCAAGGCGCACTGGCCTCATCTTGGGCTGTGTTATCTCCTAGTTGGCTCTGACTGTACCACCA TCCACTACAACTACATGTGTAACAGTTCCTGCATGGGCGGCATGAACCGGAGGCCCATCCTCACCATCATC ACACTGGAAGACTCCAGGTCAGGAGCCACTTGCCACCTGCACACTGGCC
TP53_Exon (8836200)_7424192	17	7573870	7574096	GGAGTAGGGCCAGGAAGGGGCTGAGGTCACCTGGAGTGAGCCCTGCTCCCCCTGGCTCCTTCCC AGCCTGGGCATCCTTGAGTTCCAAGGCCTCATTAGCTCTCGAACATCTCGAAGCGCTCACGCCACGG ATCTGCAGCAACAGAGGAGGGGAGAAGTAAGTATATA
TP53_Exon (8836204)_7424193	17	7571601	7571825	CCTTTTATATCCCATTTTTATATCGATCTCTTATTTTACAATAAACTTTGCTGCCACCTGTGTGTCTGAGGG GTGAACGCCAGTGCAGGCTACTGGGGTCAGCAGGTGCAGGGGTGAGTGAGGAGGTGCTGGGAAGCAGC CACCTGAGTCTGCAATGAGTGTGGGCTGGGGG
TP53_Exon (8836204)_7424194	17	7572281	7572535	AGAGTGCATTGTGAGGGTTAATGAAATAATGTACATCTGGCCTTGAACCACCTTTTATTACATGGGGTCTA GAACCTGACCCCTTGAGGGTGCTTGTCCCTCTCCCTGTTGGTGGTGGGTTGGTAGTTTCTACAGTTGG GCAGCTGGTTAGGTAGAGGGAGTTGTCAAGTCTCTGCTGGCCCAGCCAAACCCTGTCT
TP53_Exon (8836204)_7424195	17	7572479	7572712	TGTGAGGTAGGTGCAAATGCCAGCATTTACAGATATGGGCCTTGAAGTTAGAGAAAATTCAACAGTGAGG GACAGCTTCCCTGGTTAGTACGGTGAAGTGGGCCCTACCTAGAATGTGGCTGATTGTAAACTAACCCCTTA ACTGCAAGAACATTTCTTACATCTCCCAAACAT
TP53_Exon (8836204)_7424196	17	7572653	7572886	TTTGGGTTTTGGGTCTTTGAACCCTTGCTTGCAATAGGTGTGCGTCAGAAGCACCCAGGACTTCCATTTGC TTTGTCCCGGGGCTCCACTGAACAAGTTGGCCTGCACTGGTGTTTTTGTTGTGGGGAGGAGATGGGGAGT AGGACATACCAGCTTAGATTTTAAGTTTTTACTGTGAGGGAT
TP53_Exon (8836204)_7424197	17	7572837	7573073	AATGGCAGGGGAGGGAGAGATGGGGGTGGGAGGCTGTGAGTGGGGAACAAGAAGTGGAGAATGTCAGTC TGAGTCAGGCCCTTCTGTCTTGAACATGAGTTTTTTATGGCGGAGGTAGACTGACCCTTTTTGGACTTCA GGTGGCTGTAGGAGACAGAAGCAGGGAGGAGAGATGACATCACAT
CD79B_Exon (8289983)_7424727	17	62006113	62006375	GGCACTGGAGGCCAGGGCCTCCCTGGGGTGGGAGTGGTTGCGGGAGAGGAATGATGTTCTGTGGCTCT TCTGGGGCCAGTTGGGTCCATGGCCCTTCCCAAGCTCTGCTGGGAGGCCCTCGGCTCCGAGTCCATTTG CGGGCTCTGGACCAGTCTCTGCCTCCCCATCCCATGTGTGGGGACGGATCACCTCATAGCACCCCCAGA AGG
CD79B_Exon (8289983)_7424728	17	62006323	62006564	TGACTGCTTCGGAGCTGCCTGGCTCATGGCCCAACCCCTTTCCTGGACCCCCAGCTGGCCTCTGAAGCT GGCCCACCAGAGCTGCCATTTGTCTCCAGCCCCTGGTCCCAGCTCTTGCCAAAGGGCCTGGAGTAGAAG GACAACAGGGCAGCAACTTGGAGGGAGTTCTCTGGGGATGGACGGGACCCAGCC

CD79B _Exon (8289983)_7424729	17	62006513	62006741	CACTGAGGCCAGGGAGCCTGCACCCAGGTCATGGGGCGACCTGGCTCTCACTCCTGGCCTGGGTGCTCA CCTACAGACCACCTTCACTTCCCCTGTCCGCAGCGTCACTATGTCTCATAGGTGGCTGTCTGGTCAATGTC CAGGCCCTGGAGACATTAAGTGGAACTCAGGCCG
CD79B _Exon (8289983)_7424730	17	62006685	62006916	CAGGGGATGGGGCTGGGGGACACTAACACTCTGATCTCCATCCCTCTCCGCCCCAGGATGACAGCAAG GCTGGCATGGAGGAAGATCACACCTACGAGGTAAGGAGAGGGGCAGGCCAGCAGCTCTGAGTCCTCGG GGTCAGTGGCCACTATCTGCTGGTGTGGTTGGGGTGTGGTCCCG
CD79B _Exon (8289983)_7424731	17	62006865	62007094	CCCCTGCTGGGCCAGGCTGGGGAGGGCCAGGGAGAGGGGTGAGGGGTGAGGAGTGCATTCTGC AAGAACAGCTGAATGAAGGAAGGAAGGAAGGAATGATTGAATTGGTGAGCCAGTGGGGACAGGCTGGACC AAGAAGGCCACAACGAGAGCTGGGGAGATGGAGACCCTGCATATGC
CD79B _Exon (8289983)_7424732	17	62007043	62007274	AGGATTCAGCACCTTGGCACAGCTGAAGCAGAGGAACACGCTGAAGGATGGTATCATCATGATCCAGACG CTGCTGATCATCCTTTCATCATCGTGCCTATCTTCTGCTGCTGGACAAGGTGATCAGGGGACGGGGGAA GCCTGGGGGACCGCAGAGGAGGCCACCGCATAGGCCAGGC
CD79B _Exon (8289983)_7424733	17	62007227	62007454	CTGCGGGGACAGGGGTGGGGTGTGAGCCTGGGCCACAGTCCACCTTTTAGGCCTACAAGGGCAGCTCC CTCAGGTCCCAGTGGCTCTCCTGAGTGTCTAGGGCCATGACCATCACCACAAGAGGCAGGCCGGGCTA GGGTGGGGCGGACAGCTACAGGAGCGTCCCAGCCACCTGGCACACA
GRB2 _Exon (5230232)_7423793	17	73328744	73328991	GCTTAACTTACGGATGTGGTTTCATTTCTATGTAGTTCTTGGGAATGAAGCCGCTTTTTCCATTAAGCTCTG CCTTGTAACAGTTCTGATCACATTCTTCGTTCAAACCTGAAAAGAAATAAGACAACAAAAAACCAATCAT TTCTTTTCCCTTTAAAAAGATAGTTACAAGACAATTATGCTATCTTTTAG
GRB2 _Exon (5230233)_7423794	17	73389493	73389720	TTAAAAGTGTACAATGAAAAACACAGCTTCTTTGTGTGTAATCAGGGCGAAAGAAGGTGGGTGAGCACAGG GAGAGCGATCTCAGCATTGTGCTCGGCATCAGCACTTACCTTGAGGATGTCCCCCTTTTGAAGCTCAGCT CGTCGTCTGCAGTAGCTTTGAAGTCATATTTGGCG
GRB2 _Exon (5230233)_7423795	17	73389671	73389921	GGGTTGCCTTCAATCCTGGCCACTGCTCTTAATCGTCCCTCTCCTGCTTCAGGGTGGCATTGTGTGCCA GAGTGCCGGAGCGAGTCCCAGAAGAGAGGCGAGGCTAAGCCCAGAGCGCTGGGTTGCTTCAGCAGGGAA GACTCCCTTCCCCCTGCTTCAGGCTGCTGAGCACTGAGCAGCGCTCAGAATGGAAGCCATC
GRB2 _Exon (5230234)_7423796	17	73314022	73314246	GCGGATAGCATTGGTAGGTAGTGATTAAGTGTGAATAATAAATACACAATGAATTCTTCACTTGGTATCTTT TTTTCCCTTGCCTGCCTTAAAAATTTAAAAACCGCATCGGGGAGTCAGGAATCTTGGGTCTTATTTTCA CGTGATCACCCAGCTTACATCCCCC
GRB2 _Exon (5230234)_7423797	17	73314176	73314402	AATGCTATCCGCAGAGTTAAAGGATTAAGTACATAGGTCTTTATTTAAACACTGATTTTTTTTTTAAATATATA CACACAAAACCTTAGTTCAGCAAGGCTTCATGATATACACCAATTCCAAAATAAAACAATCAAATGGTCCAGG TGTAAGATGCCAGATTCTTTTAT
GRB2 _Exon (5230234)_7423798	17	73314316	73314540	TCCCTCCGACTCCAGATATGAACAGGGGCCAGGCCTGGAGCGTTTGTGTGCCAGGAGGCGGCAGCTCTT CTGGGCAGAGCCTGTCCCCGCCTTCCCTCACTCTTCTCATCCTGCTTCTTTTTCTCGCAGATGATAAAA GGAATCTGGCATTCTACACCTGGA
GRB2 _Exon (5230234)_7423799	17	73314460	73314687	GGGCCCTGTTTCATATCTGGAGTCGGAGGGAGACTCCCATCGGCCGCTTTGGGACTGAAAGGCCCAAGGC TGTACCAGCTCCCGAAGAGAGGGAGGCAGTCTTGTTTTTGTGTCGTGGGAAGGGGTTTGGGTGGAGAAA AGATTACAGGCACATCACCACAGGGGACCAGAAGTGGAGAG

GRB2_Exon (5230234)_7423800	17	73314606	73314830	TGCTGCTTGTGCCTCCCTTCCCAGTGGGCTGTGTTGACTGCTGCTCCCCACCCCTACCGATGGTCCCAGG AAGCAGGGGAGAGTTGGGGAAGGCAAGATTGGAAAGACAGGAAGACCAAGGCCTCGGCAGAACTCTCTGT CTTCTCTCCACTTCTGGTCCCCTGTGGTGATGT
GRB2_Exon (5230234)_7423801	17	73314902	73315127	CACTGGATCTGGCTTACAGGGGGTTCGGAAGCCTGTCCTCACCGTCTCGGGGGTTGTGGCCCCCGCCCC CTCCCTATATGCACCCCTGGAACCAGCAAGTCCCAGACAAGGAGAGCGGAGGAGGAAGTCATGGGAACG CAGCCTCCAGTTGTAGCAGGTTTCACTATTCC
GRB2_Exon (5230234)_7423802	17	73315046	73315270	CCGACCCCTGTAAGCCAGATCCAGTGGGATGTGGGAGAGCTGGGCGGTACCTTCCCTCTTGCCCCG GTGGCCCATCACACTCACACTGCACCCTGGGCAAGCAGTTCCTGAACCCCAAGGGGCTCACAACCCTT AAAGCTGGAGCTTAAAGCCTCCTGGCTTAGTACAA
GRB2_Exon (5230234)_7423803	17	73315208	73315435	TTTTTTTTTTAATTTGTTTTGTTTTAAAATAAGTTAAAGGCAGTCCAGAGCTTTTCAGCCAATTTGTCTCCT ACTCTGTGTAATAATTTTTCCCTCCGGGCAGGGGAGCCAGGGTAGAGCAAAGGAGACAAAGCAGGAGTGG AAGGTGAGGCGTTCTCCTGCTTGTACTAAGCC
GRB2_Exon (5230234)_7423804	17	73315938	73316162	GCAAAGGCATCGAGCGGCCCTGCCCGCTCCTTTTTGTGTGTATATACGAAGAACACAGGAACAGCTGTTCT TCTTTCAGTCATTCCAATAAAACAGACATTTTGCATAGAGAGAATACCAGCCCACTTGGTTTCTGTTTTT ATTATTGGCGTCAGCTAGGACTATACGTG
GRB2_Exon (5230234)_7423805	17	73316104	73316346	CTCACTTTGGTTGGAACCTTAGGGGGTGGGAGGGGGCGTTGGATTTAAAAATGCCAAAACCTTACCTATAAA TTAAGAAGAGTTTTTATTACAAATTTTCACTGCTGCTCCTCTTTCCCTCCTTTGTCTTTTTTTTTCATCCTTTTT TCTCTTCTGTCCATCAGTGCATGACGTTTAAAGGCCACGTAT
GRB2_Exon (5230234)_7423806	17	73316292	73316520	GAGGGTCACAGGGTGACCCGGCCAGGTGTTCTGCACCTCCCTCACAGGCTGCTGTCAGAGGCAGCTTGTG GGTTTAATTCTTTTGTATGTGTTTTACATTTTCACTTTCTTTAAATAATTGCTTCTTGACTCTTAGACGTTCC GGTTCACGGGGTGACATAATTGCGGGGAAACATGC
GRB2_Exon (5230234)_7423807	17	73316470	73316725	TCTGGCCTCGGAGGTGGCCAGTCACAGACCAGGAATGCAATGTGGGTTTTCTGCTCCTGTTTTGCAGCA GCCGACATACGTCCAGGCCCTCTTTGACTTTGATCCCCAGGAGGATGGAGAGCTGGGCTCCGCCGGGG AGATTTTATCCATGTCATGGATAACTCAGACCCCAACTGGTGGAAAGGAGCTTGCCACGGGCAGACCGG
GRB2_Exon (5230235)_7423808	17	73317703	73317961	TGAGGCTTACCTGTGGCACCTGTTCTATGTCCCAGGAATATCTGCTGGTTTTCTGGAGACAGATGTAGAT CTGTGATAATCCACCAGCTCATTCAAAGAATTGAACTTACCACCCAGAGGAAGTACTTCCCGGCTCCATCT CGGAGCACCTTGAAGTGCTGCACATCGTTTCCAAACCTGGGAGGGACAGAAAGCACATGTGA
GRB2_Exon (5230236)_7423809	17	73321940	73322172	GCAGGAAATACTTACTTGACAGAGAGGGAGAAGTCCCCAGGAGCGCTCTCACTCTCTCGGATAAGAAAGG CCCCATCGTGCCGCTGTTTGTAAAGCATTTCTTCTGCCTTGGCTCTGGGGATTTTGCCAAAAACACCTAA GGAAGGAAGGCAAGCTGGTCAACATCTGCTTCCCCACAAA

**Table 8. Primer sequences and annealing temperatures.**

<b>SNP reference</b>	<b>Primer sequence (5'-3')</b>	<b>Annealing temperature (°C)</b>	<b>Amplicon Size (bp)</b>	<b>Location on Chr 17 (hg18)</b>
rs3803800	GGGACCCTCGCATCTTAACC CCCTGACTCGGGCTTACAAT	58	297	7,403,443 - 7,403,943
rs2302764	TTGTGGCCATGGTAGTGGAC CACTGGCGACCTAGGTGTTG	58	375	7,300,584 - 7,301,084
rs1641510	CCGGCTCTTATTGCTTTGACATTC TACTGTGTGCATTCTAGGCACC	58	352	7,501,971 - 7,502,471
rs2215299	GCTACACATAAGAGAGCGACTTC TATGCTTGTAGGCTTTCGAGG	58	333	14,890,089 - 14,890,589

**Table 9. Name and location of seventeen 17p BAC clones used in the probe contig.**

*BAC RP11-199F11 (indicated with an asterisk) contains TP53. All genomic co-ordinates are based on human genome build NCBI35/hg17.*

	<b>BAC clone</b>	<b>Chr17 Position (hg17)</b>
1	RP11-636N17	6,189,992 - 6,395,815
2	RP11-698N22	6,383,241 - 6,584,761
3	RP11-558E15	6,990,306 - 7,197,567
4	RP11-222J21	7,088,883 - 7,233,441
5	RP11-98D15	7,230,068 - 7,427,689
6	RP11-186B7	7,247,848 - 7,448,344
7	RP11-199F11*	7,441,503 - 7,598,744
8	RP11-63C7	7,621,604 - 7,777,353
9	RP11-441N13	7,743,571 - 7,903,773
10	RP11-613J7	7,873,762 - 8,031,618
11	RP11-1D5	7,944,267 - 8,096,414
12	RP11-1322B12	7,944,267 - 8,101,875
13	RP11-452D1	7,994,103 - 8,170,826
14	RP11-78N21	8,144,297 - 8,327,145
15	RP11-713H12	8,270,682 - 8,444,933
16	RP11-241K13	8,380,249 - 8,556,678
17	RP11-798A22	8,495,270 - 8,702,299

---

## References

- Adler, I. D., Bishop, J., Lowe, X., Schmid, T. E., Schriever-Schwemmer, G., Xu, W., et al. 1996. Spontaneous rates of sex chromosomal aneuploidies in sperm and offspring of mice: a validation of the detection of aneuploid sperm by fluorescence in situ hybridization. *Mutation Research/Fundamental and Molecular Mechanisms of Mutagenesis*, 372, 259-268.
- Akogwu, I., Wang, N., Zhang, C. & Gong, P. 2016. A comparative study of k-spectrum-based error correction methods for next-generation sequencing data analysis. *Human Genomics*, 10, 20.
- Al-Za'abi, A. M., Geddie, W. B. & Boerner, S. L. 2008. Equivalence of laser scanning cytometric and flow cytometric immunophenotyping of lymphoid lesions in cytologic samples. *Am J Clin Pathol*, 129, 780-5.
- Altekruse, S., Kosary, C., Krapcho, M., Neyman, N., Aminou, R., Waldron, W., et al. 2010. SEER cancer statistics review, 1975-2007. *Bethesda, MD: National Cancer Institute*, 7.
- Amann, R. & Fuchs, B. M. 2008. Single-cell identification in microbial communities by improved fluorescence in situ hybridization techniques. *Nat Rev Microbiol*, 6, 339-48.
- Andersen, C. L., Hostetter, G., Grigoryan, A., Sauter, G. & Kallioniemi, A. 2001. Improved procedure for fluorescence in situ hybridization on tissue microarrays. *Cytometry*, 45, 83-6.
- Apostoli, A. J. & Ailles, L. 2016. Clonal evolution and tumor-initiating cells: New dimensions in cancer patient treatment. *Critical Reviews in Clinical Laboratory Sciences*, 53, 40-51.
- Austen, B., Powell, J. E., Alvi, A., Edwards, I., Hooper, L., Starczynski, J., et al. 2005. Mutations in the ATM gene lead to impaired overall and treatment-free survival that is independent of IGVH mutation status in patients with B-CLL. *Blood*, 106, 3175-82.
- Austen, B., Skowronska, A., Baker, C., Powell, J. E., Gardiner, A., Oscier, D., et al. 2007. Mutation status of the residual ATM allele is an important determinant of the cellular response to chemotherapy and survival in patients with chronic lymphocytic leukemia containing an 11q deletion. *J Clin Oncol*, 25, 5448-57.
- Babur, O., Gonen, M., Aksoy, B. A., Schultz, N., Ciriello, G., Sander, C., et al. 2015. Systematic identification of cancer driving signaling pathways based on mutual exclusivity of genomic alterations. *Genome Biol*, 16, 45.
- Badoux, X. C., Keating, M. J., Wang, X., O'Brien, S. M., Ferrajoli, A., Faderl, S., et al. 2011a. Fludarabine, cyclophosphamide, and rituximab chemoimmunotherapy is highly effective treatment for relapsed patients with CLL. *Blood*, 117, 3016-24.
- Badoux, X. C., Keating, M. J. & Wierda, W. G. 2011b. What is the best frontline therapy for patients with CLL and 17p deletion? *Curr Hematol Malig Rep*, 6, 36-46.
- Baerlocher, G. M., Vulto, I., De Jong, G. & Lansdorp, P. M. 2006. Flow cytometry and FISH to measure the average length of telomeres (flow FISH). *Nat Protoc*, 1, 2365-76.
- Balatti, V., Lerner, S., Rizzotto, L., Rassenti, L. Z., Bottoni, A., Palamarchuk, A., et al. 2013a. Trisomy 12 CLLs progress through NOTCH1 mutations. *Leukemia*, 27, 740-3.
- Balatti, V., Pekarky, Y., Rizzotto, L. & Croce, C. M. 2013b. miR deregulation in CLL. *Adv Exp Med Biol*, 792, 309-25.

- 
- Balatti, V., Acunzo, M., Pekarky, Y. & Croce, C. M. 2016. Novel mechanisms of regulation of miRNAs in CLL. *Trends Cancer*, 2, 134-143.
- Baliakas, P., Hadzidimitriou, A., Sutton, L. A., Rossi, D., Minga, E., Villamor, N., et al. 2014a. Recurrent mutations refine prognosis in chronic lymphocytic leukemia. *Leukemia*.
- Baliakas, P., Iskas, M., Gardiner, A., Davis, Z., Plevova, K., Nguyen-Khac, F., et al. 2014b. Chromosomal translocations and karyotype complexity in chronic lymphocytic leukemia: a systematic reappraisal of classic cytogenetic data. *Am J Hematol*, 89, 249-55.
- Bankevich, A., Nurk, S., Antipov, D., Gurevich, A. A., Dvorkin, M., Kulikov, A. S., et al. 2012. SPAdes: A New Genome Assembly Algorithm and Its Applications to Single-Cell Sequencing. *Journal of Computational Biology*, 19, 455-477.
- Bartek, J., Bartkova, J. & Lukas, J. 2007a. DNA damage signalling guards against activated oncogenes and tumour progression. *Oncogene*, 26, 7773-9.
- Bartek, J., Lukas, J. & Bartkova, J. 2007b. DNA damage response as an anti-cancer barrier: damage threshold and the concept of 'conditional haploinsufficiency'. *Cell Cycle*, 6, 2344-7.
- Bartkova, J., Horejsi, Z., Koed, K., Kramer, A., Tort, F., Zieger, K., et al. 2005. DNA damage response as a candidate anti-cancer barrier in early human tumorigenesis. *Nature*, 434, 864-70.
- Bartkova, J., Rezaei, N., Liontos, M., Karakaidos, P., Kletsas, D., Issaeva, N., et al. 2006. Oncogene-induced senescence is part of the tumorigenesis barrier imposed by DNA damage checkpoints. *Nature*, 444, 633-7.
- Bashashati, A., Ha, G., Tone, A., Ding, J., Prentice, L. M., Roth, A., et al. 2013. Distinct evolutionary trajectories of primary high-grade serous ovarian cancers revealed through spatial mutational profiling. *J Pathol*, 231, 21-34.
- Basiji, D. A., Ortyn, W. E., Liang, L., Venkatachalam, V. & Morrissey, P. 2007. Cellular image analysis and imaging by flow cytometry. *Clin Lab Med*, 27, 653-70, viii.
- Basiji, D. & O'gorman, M. R. G. 2015. Imaging flow cytometry. *Journal of Immunological Methods*, 423, 1-2.
- Bauer, K., Rancea, M., Roloff, V., Elter, T., Hallek, M., Engert, A., et al. 2012. Rituximab, ofatumumab and other monoclonal anti-CD20 antibodies for chronic lymphocytic leukaemia. *Cochrane Database Syst Rev*, 11, Cd008079.
- Bauman, J. G., Wiegant, J., Borst, P. & Van Duijn, P. 1980. A new method for fluorescence microscopical localization of specific DNA sequences by in situ hybridization of fluorochromelabelled RNA. *Exp Cell Res*, 128, 485-90.
- Baumgartner, A., Schmid, T. E., Maerz, H. K., Adler, I. D., Tarnok, A. & Nuesse, M. 2001. Automated evaluation of frequencies of aneuploid sperm by laser-scanning cytometry (LSC). *Cytometry*, 44, 156-60.
- Bayani, J. & Squire, J. A. 2004. Fluorescence in situ Hybridization (FISH). *Curr Protoc Cell Biol*, Chapter 22, Unit 22.4.
- Bergmann, M. A., Eichhorst, B. F., Busch, R., Adorf, D., Stilgenbauer, S., Eckart, M. J., et al. Prospective Evaluation of Prognostic Parameters in Early Stage Chronic Lymphocytic Leukemia (CLL): Results of the CLL1-Protocol of the German CLL Study Group (GCLLSG). *ASH Annual Meeting Abstracts*, 2007. 625.
-

- 
- Berndt, A., Kosmehl, H., Celeda, D. & Katenkamp, D. 1996. Reduced formamide content and hybridization temperature results in increased non-radioactive mRNA in situ hybridization signals. *Acta Histochem*, 98, 79-87.
- Best, G., Thompson, P. & Tam, C. S. 2012. Diagnostic techniques and therapeutic challenges in patients with TP53 dysfunctional chronic lymphocytic leukemia. *Leuk Lymphoma*, 53, 2105-15.
- Binet, J. L., Auquier, A., Dighiero, G., Chastang, C., Piguët, H., Goasguen, J., et al. 1981. A new prognostic classification of chronic lymphocytic leukemia derived from a multivariate survival analysis. *Cancer*, 48, 198-206.
- Bishop, R. 2010. Applications of fluorescence in situ hybridization (FISH) in detecting genetic aberrations of medical significance. *Bioscience Horizons: The International Journal of Student Research*, 3, 85-95.
- Blake, R. D. & Delcourt, S. G. 1996. Thermodynamic effects of formamide on DNA stability. *Nucleic Acids Res*, 24, 2095-103.
- Bogomolov, A. G., Karamysheva, T. V. & Rubtsov, N. B. 2014. Fluorescence in situ hybridization with DNA probes derived from individual chromosomes and chromosome regions. *Mol Biol (Mosk)*, 48, 881-90.
- Bottcher, S., Ritgen, M., Fischer, K., Stilgenbauer, S., Busch, R. M., Fingerle-Rowson, G., et al. 2012. Minimal residual disease quantification is an independent predictor of progression-free and overall survival in chronic lymphocytic leukemia: a multivariate analysis from the randomized GCLLSG CLL8 trial. *J Clin Oncol*, 30, 980-8.
- Bozic, I., Antal, T., Ohtsuki, H., Carter, H., Kim, D., Chen, S., et al. 2010. Accumulation of driver and passenger mutations during tumor progression. *Proceedings of the National Academy of Sciences of the United States of America*, 107, 18545-18550.
- Bradley, S., Zamechek, L. & Aurich-Costa, J. 2009. Oligonucleotide FISH Probes. In: Liehr, T. (ed.) *Fluorescence In Situ Hybridization (FISH) — Application Guide*. Berlin, Heidelberg: Springer Berlin Heidelberg.
- Bredemeyer, A. L., Sharma, G. G., Huang, C.-Y., Helmink, B. A., Walker, L. M., Khor, K. C., et al. 2006. ATM stabilizes DNA double-strand-break complexes during V (D) J recombination. *Nature*, 442, 466-470.
- Bullinger, L., Kronke, J., Schon, C., Radtke, I., Urlbauer, K., Botzenhardt, U., et al. 2010. Identification of acquired copy number alterations and uniparental disomies in cytogenetically normal acute myeloid leukemia using high-resolution single-nucleotide polymorphism analysis. *Leukemia*, 24, 438-49.
- Burger, J. A., Tsukada, N., Burger, M., Zvaifler, N. J., Dell'aquila, M. & Kipps, T. J. 2000. Blood-derived nurse-like cells protect chronic lymphocytic leukemia B cells from spontaneous apoptosis through stromal cell-derived factor-1. *Blood*, 96, 2655-63.
- Burger, J. A., Quiroga, M. P., Hartmann, E., Burkle, A., Wierda, W. G., Keating, M. J., et al. 2009. High-level expression of the T-cell chemokines CCL3 and CCL4 by chronic lymphocytic leukemia B cells in nurselike cell cocultures and after BCR stimulation. *Blood*, 113, 3050-8.
- Burgess, M., Cheung, C., Chambers, L., Ravindranath, K., Minhas, G., Knop, L., et al. 2012. CCL2 and CXCL2 enhance survival of primary chronic lymphocytic leukemia cells in vitro. *Leuk Lymphoma*, 53, 1988-98.
-



- 
- Burrell, R. A. & Swanton, C. 2014. The evolution of the unstable cancer genome. *Curr Opin Genet Dev*, 24, 61-7.
- Butler, T. & Gribben, J. G. 2010. Biologic and clinical significance of molecular profiling in Chronic Lymphocytic Leukemia. *Blood Rev*, 24, 135-41.
- Byrd, J. C., Murphy, T., Howard, R. S., Lucas, M. S., Goodrich, A., Park, K., et al. 2001. Rituximab using a thrice weekly dosing schedule in B-cell chronic lymphocytic leukemia and small lymphocytic lymphoma demonstrates clinical activity and acceptable toxicity. *Journal of Clinical Oncology*, 19, 2153-2164.
- Byrd, J. C., Peterson, B. L., Morrison, V. A., Park, K., Jacobson, R., Hoke, E., et al. 2003a. Randomized phase 2 study of fludarabine with concurrent versus sequential treatment with rituximab in symptomatic, untreated patients with B-cell chronic lymphocytic leukemia: results from Cancer and Leukemia Group B 9712 (CALGB 9712). *Blood*, 101, 6-14.
- Byrd, J. C., Smith, L., Hackbarth, M. L., Flinn, I. W., Young, D., Proffitt, J. H., et al. 2003b. Interphase cytogenetic abnormalities in chronic lymphocytic leukemia may predict response to rituximab. *Cancer Res*, 63, 36-8.
- Byrd, J. C., Gribben, J. G., Peterson, B. L., Grever, M. R., Lozanski, G., Lucas, D. M., et al. 2006. Select high-risk genetic features predict earlier progression following chemoimmunotherapy with fludarabine and rituximab in chronic lymphocytic leukemia: justification for risk-adapted therapy. *J Clin Oncol*, 24, 437-43.
- Byrd, J. C., Furman, R. R., Coutre, S. E., Flinn, I. W., Burger, J. A., Blum, K. A., et al. 2013. Targeting BTK with Ibrutinib in Relapsed Chronic Lymphocytic Leukemia. *New England Journal of Medicine*, 369, 32-42.
- Caligaris-Cappio, F. & Hamblin, T. J. 1999. B-cell chronic lymphocytic leukemia: a bird of a different feather. *J Clin Oncol*, 17, 399-408.
- Calin, G. A., Dumitru, C. D., Shimizu, M., Bichi, R., Zupo, S., Noch, E., et al. 2002. Frequent deletions and down-regulation of micro-RNA genes miR15 and miR16 at 13q14 in chronic lymphocytic leukemia. *Proceedings of the National Academy of Sciences*, 99, 15524-15529.
- Campbell, V. W. & Jackson, D. A. 1980. The effect of divalent cations on the mode of action of DNase I. The initial reaction products produced from covalently closed circular DNA. *J Biol Chem*, 255, 3726-35.
- Campbell, L. J., Oei, P., Brookwell, R., Shortt, J., Eaddy, N., Ng, A., et al. 2013. FISH detection of PML-RARA fusion in ins(15;17) acute promyelocytic leukaemia depends on probe size. *Biomed Res Int*, 2013, 164501.
- Campregher, P. V. & Hamerschlak, N. 2014. Novel prognostic gene mutations identified in chronic lymphocytic leukemia and their impact on clinical practice. *Clin Lymphoma Myeloma Leuk*, 14, 271-6.
- Casabonne, D., Almeida, J., Nieto, W. G., Romero, A., Fernandez-Navarro, P., Rodriguez-Caballero, A., et al. 2012. Common infectious agents and monoclonal B-cell lymphocytosis: a cross-sectional epidemiological study among healthy adults. *PLoS One*, 7, e52808.
- Casabonne, D., Almeida, J., Nieto, W. G., Romero, A., Fernandez-Navarro, P., Rodriguez-Caballero, A., et al. 2013. Correction: Common Infectious Agents and Monoclonal B-Cell Lymphocytosis: A Cross-Sectional Epidemiological Study among Healthy Adults. *PLoS One*, 8.
-

- 
- Catovsky, D., Richards, S., Matutes, E., Oscier, D., Dyer, M., Bezares, R., et al. 2007. Assessment of fludarabine plus cyclophosphamide for patients with chronic lymphocytic leukaemia (the LRF CLL4 Trial): a randomised controlled trial. *The Lancet*, 370, 230-239.
- Chang, R. L., Yeh, C. H. & Albitar, M. 2010. Quantification of intracellular proteins and monitoring therapy using flow cytometry. *Curr Drug Targets*, 11, 994-9.
- Chao, Y. & Zhang, T. 2011. Optimization of fixation methods for observation of bacterial cell morphology and surface ultrastructures by atomic force microscopy. *Applied Microbiology and Biotechnology*, 92, 381-392.
- Chaouchi, N., Wallon, C., Goujard, C., Tertian, G., Rudent, A., Caput, D., et al. 1996. Interleukin-13 inhibits interleukin-2-induced proliferation and protects chronic lymphocytic leukemia B cells from in vitro apoptosis. *Blood*, 87, 1022-9.
- Chen, C. Z. 2004. MicroRNAs Modulate Hematopoietic Lineage Differentiation. *Science*, 303, 83-86.
- Chen, S.-Y., Ma, D.-N., Chen, Q.-D., Zhang, J.-J., Tian, Y.-R., Wang, Z.-C., et al. 2017. MicroRNA-200a inhibits cell growth and metastasis by targeting Foxa2 in hepatocellular carcinoma. *Journal of Cancer*, 8, 617-625.
- Chin, K. V., Ueda, K., Pastan, I. & Gottesman, M. M. 1992. Modulation of activity of the promoter of the human MDR1 gene by Ras and p53. *Science*, 255, 459-62.
- Chin, S. F., Daigo, Y., Huang, H. E., Iyer, N. G., Callagy, G., Kranjac, T., et al. 2003. A simple and reliable pretreatment protocol facilitates fluorescent in situ hybridisation on tissue microarrays of paraffin wax embedded tumour samples. *Molecular Pathology*, 56, 275-279.
- Chin, E. L., Da Silva, C. & Hegde, M. 2013. Assessment of clinical analytical sensitivity and specificity of next-generation sequencing for detection of simple and complex mutations. *BMC Genet*, 14, 6.
- Choi, M. Y. & Kipps, T. J. 2012. Inhibitors of B-cell Receptor Signaling for patients with B-cell malignancies. *Cancer journal (Sudbury, Mass.)*, 18, 404-410.
- Chiorazzi, N. & Ferrarini, M. 2003. B cell chronic lymphocytic leukemia: lessons learned from studies of the B cell antigen receptor. *Annu Rev Immunol*, 21, 841-94.
- Chiorazzi, N., Chiorazzi, M. & Ferrarini 2011. Cellular origin(s) of chronic lymphocytic leukemia: cautionary notes and additional considerations and possibilities. *Blood*, 117, 1781-1791.
- Churi, C. R., Shroff, R., Wang, Y., Rashid, A., Kang, H. C., Weatherly, J., et al. 2014. Mutation Profiling in Cholangiocarcinoma: Prognostic and Therapeutic Implications. *PLOS ONE*, 9, e115383.
- Cimmino, A., Calin, G. A., Fabbri, M., Iorio, M. V., Ferracin, M., Shimizu, M., et al. 2005. miR-15 and miR-16 induce apoptosis by targeting BCL2. *Proc Natl Acad Sci U S A*, 102, 13944-9.
- Ciolino, A. L., Tang, M. E. & Bryant, R. 2009. Statistical Treatment of Fluorescence in Situ Hybridization Validation Data to Generate Normal Reference Ranges Using Excel Functions. *The Journal of Molecular Diagnostics : JMD*, 11, 330-333.
- Clark, R. T. 2015. Imaging flow cytometry enhances particle detection sensitivity for extracellular vesicle analysis. *Nat Meth*, 12.
-

- 
- Claussen, U., Michel, S., Muhlig, P., Westermann, M., Grummt, U. W., Kromeyer-Hauschild, K., et al. 2002. Demystifying chromosome preparation and the implications for the concept of chromosome condensation during mitosis. *Cytogenet Genome Res*, 98, 136-46.
- Claytor, R. B., Li, J. M., Furman, M. I., Garnette, C. S., Rohrer, M. J., Barnard, M. R., et al. 2001. Laser scanning cytometry: a novel method for the detection of platelet-endothelial cell adhesion. *Cytometry*, 43, 308-13.
- Cleary, S. P., Jeck, W. R., Zhao, X., Chen, K., Selitsky, S. R., Savich, G. L., et al. 2013. Identification of driver genes in hepatocellular carcinoma by exome sequencing. *Hepatology*, 58, 1693-702.
- Cleveland, D. W., Mao, Y. & Sullivan, K. F. 2003. Centromeres and kinetochores: from epigenetics to mitotic checkpoint signaling. *Cell*, 112, 407-21.
- Cll\_Statistics. 2014. *Cancer Australia*. <http://canceraustralia.gov.au/affected-cancer/cancer-types/leukaemia/chronic-lymphocytic-leukaemia-statistics>. [Online]. [Accessed 27 November 2014].
- Collado, R., Puiggros, A., López-Guerrero, J. A., Calasanz, M. J., Larráyoz, M. J., Ivars, D., et al. 2017. Chronic lymphocytic leukemia with isochromosome 17q: An aggressive subgroup associated with TP53 mutations and complex karyotypes. *Cancer Letters*, 409, 42-48.
- Collins, R. J., Verschuer, L. A., Harmon, B. V., Prentice, R. L., Pope, J. H. & Kerr, J. F. 1989. Spontaneous programmed death (apoptosis) of B-chronic lymphocytic leukaemia cells following their culture in vitro. *Br J Haematol*, 71, 343-50.
- Cordone, I., Masi, S., Mauro, F. R., Soddu, S., Morsilli, O., Valentini, T., et al. 1998. p53 Expression in B-Cell Chronic Lymphocytic Leukemia: A Marker of Disease Progression and Poor Prognosis. *Blood*, 91, 4342-4349.
- Cox, M. C., Panetta, P., Venditti, A., Del Poeta, G., Franchi, A., Buccisano, F., et al. 2003. Comparison between conventional banding analysis and FISH screening with an AML-specific set of probes in 260 patients. *Hematol J*, 4, 263-70.
- Cox, W. G. & Singer, V. L. 2004. Fluorescent DNA hybridization probe preparation using amine modification and reactive dye coupling. *Biotechniques*, 36, 114-22.
- Cramer, P. & Hallek, M. 2010. Prognostic factors in chronic lymphocytic leukemia—what do we need to know? *Nature Reviews Clinical Oncology*, 8, 38.
- Creutzig, U., Van Den Heuvel-Eibrink, M. M., Gibson, B., Dworzak, M. N., Adachi, S., De Bont, E., et al. 2012. Diagnosis and management of acute myeloid leukemia in children and adolescents: recommendations from an international expert panel. *Blood*, 120, 3187-205.
- Dal-Bo, M., Bertoni, F., Forconi, F., Zucchetto, A., Bomben, R., Marasca, R., et al. 2009. Intrinsic and extrinsic factors influencing the clinical course of B-cell chronic lymphocytic leukemia: prognostic markers with pathogenetic relevance. *Journal of Translational Medicine*, 7, 76-76.
- Dameshek, W. 1967. Chronic lymphocytic leukemia--an accumulative disease of immunologically incompetent lymphocytes. *Blood*, 29, Suppl:566-84.
- Damle, R. N., Wasil, T., Fais, F., Ghiotto, F., Valetto, A., Allen, S. L., et al. 1999. Ig V Gene Mutation Status and CD38 Expression As Novel Prognostic Indicators in Chronic Lymphocytic Leukemia Presented in part at the 40th Annual Meeting of The American
-

- 
- Society of Hematology, held in Miami Beach, FL, December 4-8, 1998. *Blood*, 94, 1840-1847.
- Damm, F., Mylonas, E., Cosson, A., Yoshida, K., Della Valle, V., Mouly, E., et al. 2014. Acquired initiating mutations in early hematopoietic cells of CLL patients. *Cancer Discov*, 4, 1088-101.
- Dancescu, M., Rubio-Trujillo, M., Biron, G., Bron, D., Delespesse, G. & Sarfati, M. 1992. Interleukin 4 protects chronic lymphocytic leukemic B cells from death by apoptosis and upregulates Bcl-2 expression. *J Exp Med*, 176, 1319-26.
- Dao, P., Kim, Y. A., Wojtowicz, D., Madan, S., Sharan, R. & Przytycka, T. M. 2017. BeWith: A Between-Within method to discover relationships between cancer modules via integrated analysis of mutual exclusivity, co-occurrence and functional interactions. *PLoS Comput Biol*, 13, e1005695.
- Darzentas, N. & Stamatopoulos, K. 2013. Stereotyped B cell receptors in B cell leukemias and lymphomas. *Methods in molecular biology (Clifton, N.J.)*, 971, 135-148.
- Darzynkiewicz, Z., Smolewski, P., Holden, E., Luther, E., Henriksen, M., François, M., et al. 2011. Laser scanning cytometry for automation of the micronucleus assay. *Mutagenesis*, 26, 153-161.
- Davis, A., Gao, R. & Navin, N. 2017. Tumor evolution: Linear, branching, neutral or punctuated? *Biochim Biophys Acta*, 1867, 151-161.
- Davoli, T., Xu, A. W., Mengwasser, K. E., Sack, L. M., Yoon, J. C., Park, P. J., et al. 2013. Cumulative haploinsufficiency and triplosensitivity drive aneuploidy patterns and shape the cancer genome. *Cell*, 155, 948-62.
- De Bourcy, C. F. A., De Vlaminck, I., Kanbar, J. N., Wang, J., Gawad, C. & Quake, S. R. 2014. A Quantitative Comparison of Single-Cell Whole Genome Amplification Methods. *PLoS ONE*, 9, e105585.
- De Bruin, E. C., Mcgranahan, N., Mitter, R., Salm, M., Wedge, D. C., Yates, L., et al. 2014. Spatial and temporal diversity in genomic instability processes defines lung cancer evolution. *Science*, 346, 251-6.
- Del Giudice, I., Rossi, D., Chiaretti, S., Marinelli, M., Tavolaro, S., Gabrielli, S., et al. 2012. NOTCH1 mutations in +12 chronic lymphocytic leukemia (CLL) confer an unfavorable prognosis, induce a distinctive transcriptional profiling and refine the intermediate prognosis of +12 CLL. *Haematologica*, 97, 437-41.
- Delgado, J., Espinet, B., Oliveira, A. C., Abrisqueta, P., De La Serna, J., Collado, R., et al. 2012. Chronic lymphocytic leukaemia with 17p deletion: a retrospective analysis of prognostic factors and therapy results. *Br J Haematol*, 157, 67-74.
- Delgado, J., Salaverria, I., Baumann, T., Martínez-Trillos, A., Lee, E., Jiménez, L., et al. 2014. Genomic complexity and IGHV mutational status are key predictors of outcome of chronic lymphocytic leukemia patients with TP53 disruption. *Haematologica*, 99, e231-e234.
- Deng, W., Tsao, S. W., Lucas, J. N., Leung, C. S. & Cheung, A. L. M. 2003. A new method for improving metaphase chromosome spreading. *Cytometry Part A*, 51A, 46-51.
- Deng, X., Ljunggren-Rose, A., Maas, K. & Sriram, S. 2005. Defective ATM-p53-mediated apoptotic pathway in multiple sclerosis. *Annals of neurology*, 58, 577-584.
-

- 
- Dewald, G., Stallard, R., Saadi, A. A., Arnold, S., Bader, P. I., Blough, R., et al. 1998a. A multicenter investigation with interphase fluorescence in situ hybridization using X-and Y-chromosome probes. *American Journal of Medical Genetics Part A*, 76, 318-326.
- Dewald, G. W., Wyatt, W. A., Juneau, A. L., Carlson, R. O., Zinsmeister, A. R., Jalal, S. M., et al. 1998b. Highly sensitive fluorescence in situ hybridization method to detect double BCR/ABL fusion and monitor response to therapy in chronic myeloid leukemia. *Blood*, 91, 3357-65.
- Dewald, G., Stallard, R., Alsaadi, A., Arnold, S., Blough, R., Ceperich, T. M., et al. 2000. A multicenter investigation with D-FISH BCR/ABL1 probes. *Cancer Genet Cytogenet*, 116, 97-104.
- Dicker, F., Herholz, H., Schnittger, S., Nakao, A., Patten, N., Wu, L., et al. 2009. The detection of TP53 mutations in chronic lymphocytic leukemia independently predicts rapid disease progression and is highly correlated with a complex aberrant karyotype. *Leukemia*, 23, 117-24.
- Dighiero, G., Maloum, K., Desablens, B., Cazin, B., Navarro, M., Leblay, R., et al. 1998. Chlorambucil in indolent chronic lymphocytic leukemia. French Cooperative Group on Chronic Lymphocytic Leukemia. *N Engl J Med*, 338, 1506-14.
- Dillman, R. O. & Dillman 2008. Immunophenotyping of Chronic Lymphoid Leukemias. *Journal of clinical oncology*, 26, 1193-1194.
- Ding, L., Ley, T. J., Larson, D. E., Miller, C. A., Koboldt, D. C., Welch, J. S., et al. 2012. Clonal evolution in relapsed acute myeloid leukaemia revealed by whole-genome sequencing. *Nature*, 481, 506-510.
- Dohner, H., Fischer, K., Bentz, M., Hansen, K., Benner, A., Cabot, G., et al. 1995. p53 gene deletion predicts for poor survival and non-response to therapy with purine analogs in chronic B-cell leukemias. *Blood*, 85, 1580-1589.
- Döhner, H., Stilgenbauer, S., Benner, A., Leupolt, E., Kröber, A., Bullinger, L., et al. 2000. Genomic Aberrations and Survival in Chronic Lymphocytic Leukemia. *New England Journal of Medicine*, 343, 1910-1916.
- Dong, C. & Yu, B. 2011. Mutation Surveyor: An In Silico Tool for Sequencing Analysis. In: Yu, B. & Hinchcliffe, M. (eds.) *In Silico Tools for Gene Discovery*. Totowa, NJ: Humana Press.
- Dreger, P., Corradini, P., Kimby, E., Michallet, M., Milligan, D., Schetelig, J., et al. 2007. Indications for allogeneic stem cell transplantation in chronic lymphocytic leukemia: the EBMT transplant consensus. *Leukemia*, 21, 12-17.
- Dreger, P., Schetelig, J., Andersen, N., Corradini, P., Van Gelder, M., Gribben, J., et al. 2014. Managing high-risk CLL during transition to a new treatment era: Stem cell transplantation or novel agents? *Blood*, 124, 3841-3849.
- Dugan, L. C., Pattee, M. S., Williams, J., Eklund, M., Sorensen, K., Bedford, J. S., et al. 2005. Polymerase chain reaction-based suppression of repetitive sequences in whole chromosome painting probes for FISH. *Chromosome Res*, 13, 27-32.
- Edelmann, J., Holzmann, K., Miller, F., Winkler, D., Buhler, A., Zenz, T., et al. 2012. High-resolution genomic profiling of chronic lymphocytic leukemia reveals new recurrent genomic alterations. *Blood*, 120, 4783-94.
-

- 
- Edwards, P. A. 2010. Fusion genes and chromosome translocations in the common epithelial cancers. *J Pathol*, 220, 244-54.
- Eichhorst, B. F., Busch, R., Hopfinger, G., Pasold, R., Hensel, M., Steinbrecher, C., et al. 2006. Fludarabine plus cyclophosphamide versus fludarabine alone in first-line therapy of younger patients with chronic lymphocytic leukemia. *Blood*, 107, 885-91.
- Eichhorst, B. F., Busch, R., Stilgenbauer, S., Stauch, M., Bergmann, M. A., Ritgen, M., et al. 2009. First-line therapy with fludarabine compared with chlorambucil does not result in a major benefit for elderly patients with advanced chronic lymphocytic leukemia. *Blood*, 114, 3382-3391.
- Eichhorst, B., Fink, A. M., Bahlo, J., Busch, R., Kovacs, G., Maurer, C., et al. 2016. First-line chemoimmunotherapy with bendamustine and rituximab versus fludarabine, cyclophosphamide, and rituximab in patients with advanced chronic lymphocytic leukaemia (CLL10): an international, open-label, randomised, phase 3, non-inferiority trial. *Lancet Oncol*, 17, 928-942.
- Eliceiri, K. W., Berthold, M. R., Goldberg, I. G., Ibáñez, L., Manjunath, B. S., Martone, M. E., et al. 2012. Biological Imaging Software Tools. *Nature methods*, 9, 697-710.
- Eliyahu, D., Michalovitz, D., Eliyahu, S., Pinhasi-Kimhi, O. & Oren, M. 1989. Wild-type p53 can inhibit oncogene-mediated focus formation. *Proc Natl Acad Sci U S A*, 86, 8763-7.
- Elliott, G. S. 2009. Moving pictures: imaging flow cytometry for drug development. *Comb Chem High Throughput Screen*, 12, 849-59.
- Elter, T., Borchmann, P., Schulz, H., Reiser, M., Trelle, S., Schnell, R., et al. 2005. Fludarabine in combination with alemtuzumab is effective and feasible in patients with relapsed or refractory B-cell chronic lymphocytic leukemia: results of a phase II trial. *Journal of Clinical Oncology*, 23, 7024-7031.
- Elter, T., Gercheva-Kyuchukova, L., Pylypenko, H., Robak, T., Jaksic, B., Rektman, G., et al. 2011. Fludarabine plus alemtuzumab versus fludarabine alone in patients with previously treated chronic lymphocytic leukaemia: a randomised phase 3 trial. *Lancet Oncol*, 12, 1204-13.
- Eltoum, I., Fredenburgh, J., Myers, R. B. & Grizzle, W. E. 2001. Introduction to the theory and practice of fixation of tissues. *Journal of Histotechnology*, 24, 173-190.
- Erdbrügger, U., Rudy, C. K., Etter, M., Dryden, K. A., Yeager, M., Klibanov, A. L., et al. 2014. Imaging flow cytometry elucidates limitations of microparticle analysis by conventional flow cytometry. *Cytometry Part A*, 85, 756-770.
- Eyford, J. E. & Bodvarsdottir, S. K. 2005. Genomic instability and cancer: networks involved in response to DNA damage. *Mutat Res*, 592, 18-28.
- Fabbri, G. & Dalla-Favera, R. 2016. The molecular pathogenesis of chronic lymphocytic leukaemia. *Nat Rev Cancer*, 16, 145-162.
- Fearon, E. R. & Vogelstein, B. 1990. A genetic model for colorectal tumorigenesis. *Cell*, 61, 759-67.
- Feinberg, A. P. & Vogelstein, B. 1983. A technique for radiolabeling DNA restriction endonuclease fragments to high specific activity. *Anal Biochem*, 132, 6-13.
- Feinberg, A. P. & Vogelstein, B. 1984. "A technique for radiolabeling DNA restriction endonuclease fragments to high specific activity". Addendum. *Anal Biochem*, 137, 266-7.
-

- 
- Fernández, J. & Fuentes, R. 2013. Fixation/Permeabilization: New Alternative Procedure for Immunofluorescence and mRNA In Situ Hybridization of Vertebrate and Invertebrate Embryos. *Developmental Dynamics*, 242, 503-517.
- Ferrajoli, A., Shanafelt, T. D., Ivan, C., Shimizu, M., Rabe, K. G., Nouraei, N., et al. 2013. Prognostic value of miR-155 in individuals with monoclonal B-cell lymphocytosis and patients with B chronic lymphocytic leukemia. *Blood*, 122, 1891-9.
- Ferrajoli, A., Wierda, W. G., Lapushin, R., O'Brien, S. M., Faderl, S., Browning, M. L., et al. 2008. Pilot experience with continuous infusion alemtuzumab in patients with fludarabine-refractory chronic lymphocytic leukemia. *Eur J Haematol*, 80, 296-8.
- Filby, A., Perucha, E., Summers, H., Rees, P., Chana, P., Heck, S., et al. 2011. An imaging flow cytometric method for measuring cell division history and molecular symmetry during mitosis. *Cytometry Part A*, 79A, 496-506.
- Finlay, C. A., Hinds, P. W. & Levine, A. J. 1989. The p53 proto-oncogene can act as a suppressor of transformation. *Cell*, 57, 1083-93.
- Fischer, K., Cramer, P., Busch, R., Stilgenbauer, S., Bahlo, J., Schweighofer, C. D., et al. 2011. Bendamustine combined with rituximab in patients with relapsed and/or refractory chronic lymphocytic leukemia: a multicenter phase II trial of the German Chronic Lymphocytic Leukemia Study Group. *J Clin Oncol*, 29, 3559-66.
- Fisher, R., Puzstai, L. & Swanton, C. 2013. Cancer heterogeneity: implications for targeted therapeutics. *Br J Cancer*, 108, 479-85.
- Francia Di Celle, P., Mariani, S., Riera, L., Stacchini, A., Reato, G. & Foa, R. 1996. Interleukin-8 induces the accumulation of B-cell chronic lymphocytic leukemia cells by prolonging survival in an autocrine fashion. *Blood*, 87, 4382-9.
- Fuller, S. J., Papaemmanuil, E., Mckinnon, L., Webb, E., Sellick, G. S., Dao-Ung, L. P., et al. 2008. Analysis of a large multi-generational family provides insight into the genetics of chronic lymphocytic leukemia. *Br J Haematol*, 142, 238-45.
- Fuller, K. A., Bennett, S., Hui, H., Chakera, A. & Erber, W. N. 2016. Development of a robust immuno-S-FISH protocol using imaging flow cytometry. *Cytometry A*, 89, 720-30.
- Furman, R. R., Sharman, J. P., Coutre, S. E., Cheson, B. D., Pagel, J. M., Hillmen, P., et al. 2014. Idelalisib and rituximab in relapsed chronic lymphocytic leukemia. *N Engl J Med*, 370, 997-1007.
- Gall, J. G. & Pardue, M. L. 1969. Formation and detection of RNA-DNA hybrid molecules in cytological preparations. *Proc Natl Acad Sci U S A*, 63, 378-83.
- Gamberale, R., Geffner, J., Arrosagaray, G., Scolnik, M., Salamone, G., Trevani, A., et al. 2001. Non-malignant leukocytes delay spontaneous B-CLL cell apoptosis. *Leukemia*, 15, 1860-7.
- Garcia-Pineros, A. J., Hildesheim, A., Williams, M., Trivett, M., Strobl, S. & Pinto, L. A. 2006. DNase treatment following thawing of cryopreserved PBMC is a procedure suitable for lymphocyte functional studies. *J Immunol Methods*, 313, 209-13.
- Garratt, L. C., McCabe, M. S., Power, J. B. & Davey, M. R. 2002. Detection of Single-Copy Genes in DNA from Transgenic Plants. In: DE MURO, M. A. & RAPLEY, R. (eds.) *Gene Probes: Principles and Protocols*. Totowa, NJ: Humana Press.
-

- 
- Gatenby, R. A. & Brown, J. 2017. Mutations, evolution and the central role of a self-defined fitness function in the initiation and progression of cancer. *Biochim Biophys Acta*, 1867, 162-166.
- Gawad, C., Koh, W. & Quake, S. R. 2014. Dissecting the clonal origins of childhood acute lymphoblastic leukemia by single-cell genomics. *Proceedings of the National Academy of Sciences of the United States of America*, 111, 17947-17952.
- Gawad, C., Koh, W. & Quake, S. R. 2016. Single-cell genome sequencing: current state of the science. *Nat Rev Genet*, 17, 175-88.
- Gehrke, I., Gandhirajan, R. K., Poll-Wolbeck, S. J., Hallek, M. & Kreuzer, K.-A. 2011. Bone Marrow Stromal Cell-Derived Vascular Endothelial Growth Factor (VEGF) Rather Than Chronic Lymphocytic Leukemia (CLL) Cell-Derived VEGF Is Essential for the Apoptotic Resistance of Cultured CLL Cells. *Molecular Medicine*, 17, 619-627.
- Geiger, K. D., Klein, U., Bräuninger, A., Berger, S., Leder, K., Rajewsky, K., et al. 2000. CD5-positive B cells in healthy elderly humans are a polyclonal B cell population. *European journal of immunology*, 30, 2918-2923.
- Genovese, G., Kahler, A. K., Handsaker, R. E., Lindberg, J., Rose, S. A., Bakhoun, S. F., et al. 2014. Clonal hematopoiesis and blood-cancer risk inferred from blood DNA sequence. *N Engl J Med*, 371, 2477-87.
- Gentile, M., Zirlik, K., Ciolli, S., Mauro, F. R., Di Renzo, N., Mastrullo, L., et al. 2016. Combination of bendamustine and rituximab as front-line therapy for patients with chronic lymphocytic leukaemia: multicenter, retrospective clinical practice experience with 279 cases outside of controlled clinical trials. *European Journal of Cancer*, 60, 154-165.
- George, T. C., Basiji, D. A., Hall, B. E., Lynch, D. H., Ortyu, W. E., Perry, D. J., et al. 2004. Distinguishing modes of cell death using the ImageStream® multispectral imaging flow cytometer. *Cytometry Part A*, 59A, 237-245.
- George, T. C., Fanning, S. L., Fitzgerald-Bocarsly, P., Medeiros, R. B., Highfill, S., Shimizu, Y., et al. 2006. Quantitative measurement of nuclear translocation events using similarity analysis of multispectral cellular images obtained in flow. *Journal of Immunological Methods*, 311, 117-129.
- Gerhard, D. S., Kawasaki, E. S., Bancroft, F. C. & Szabo, P. 1981. Localization of a unique gene by direct hybridization in situ. *Proc Natl Acad Sci U S A*, 78, 3755-9.
- Gerlinger, M., Rowan, A. J., Horswell, S., Larkin, J., Endesfelder, D., Gronroos, E., et al. 2012. Intratumor heterogeneity and branched evolution revealed by multiregion sequencing. *N Engl J Med*, 366, 883-92.
- Gerstner, A., Laffers, W., Bootz, F. & Tarnok, A. 2000. Immunophenotyping of peripheral blood leukocytes by laser scanning cytometry. *J Immunol Methods*, 246, 175-85.
- Giachino, C., Padovan, E. & Lanzavecchia, A. 1998. Re-expression of RAG-1 and RAG-2 genes and evidence for secondary rearrangements in human germinal center B lymphocytes. *Eur J Immunol*, 28, 3506-13.
- Giannella, C., Zito, F. A., Colonna, F., Paradiso, A., Marzullo, F., Alaibac, M., et al. 1997. Comparison of formalin, ethanol, and Histochoice fixation on the PCR amplification from paraffin-embedded breast cancer tissue. *Eur J Clin Chem Clin Biochem*, 35, 633-5.
-



- 
- Gillard, G. O. & Farr, A. G. 2006. Features of medullary thymic epithelium implicate postnatal development in maintaining epithelial heterogeneity and tissue-restricted antigen expression. *J Immunol*, 176, 5815-24.
- Gladstone, D. E., Blackford, A., Cho, E., Swinnen, L., Kasamon, Y., Gocke, C. D., et al. 2012. The Importance of IGHV Mutational Status in del(11q) and del(17p) Chronic Lymphocytic Leukemia. *Clinical lymphoma, myeloma & leukemia*, 12, 132-137.
- Godinez, B., Galina, C. S., Moreno-Mendoza, N., Alarcon, M. & Lammoglia, M. A. 2012. Use of a culture medium (McCoy(R)), as a method for evaluating Bos indicus x Bos taurus embryos. *Anat Histol Embryol*, 41, 274-9.
- Goh, A. M. & Lane, D. P. 2012. How p53 wields the scales of fate: Arrest or death? *Transcription*, 3, 240-244.
- Goldin, L. R., Landgren, O., Marti, G. E. & Caporaso, N. E. 2010. Familial Aspects of Chronic Lymphocytic Leukemia, Monoclonal B-Cell Lymphocytosis (MBL), and Related Lymphomas. *European J Clin Med Oncol*, 2, 119-126.
- Gondek, L. P., Tiu, R., O'keefe, C. L., Sekeres, M. A., Theil, K. S. & Maciejewski, J. P. 2008. Chromosomal lesions and uniparental disomy detected by SNP arrays in MDS, MDS/MPD, and MDS-derived AML. *Blood*, 111, 1534-42.
- Gonzalez-Gascon, Y. M. I., Hernandez-Sanchez, M., Rodriguez-Vicente, A. E., Sanzo, C., Aventin, A., Puiggros, A., et al. 2015. A high proportion of cells carrying trisomy 12 is associated with a worse outcome in patients with chronic lymphocytic leukemia. *Hematol Oncol*.
- Gonzalez, D., Martinez, P., Wade, R., Hockley, S., Oscier, D., Matutes, E., et al. 2011. Mutational status of the TP53 gene as a predictor of response and survival in patients with chronic lymphocytic leukemia: results from the LRF CLL4 trial. *J Clin Oncol*, 29, 2223-9.
- Goodwin, S., Mcpherson, J. D. & McCombie, W. R. 2016. Coming of age: ten years of next-generation sequencing technologies. *Nat Rev Genet*, 17, 333-351.
- Gorgoulis, V. G., Vassiliou, L. V., Karakaidos, P., Zacharatos, P., Kotsinas, A., Liloglou, T., et al. 2005. Activation of the DNA damage checkpoint and genomic instability in human precancerous lesions. *Nature*, 434, 907-13.
- Goswami, R. S., Patel, K. P., Singh, R. R., Meric-Bernstam, F., Kopetz, E. S., Subbiah, V., et al. 2015. Hotspot mutation panel testing reveals clonal evolution in a study of 265 paired primary and metastatic tumors. *Clin Cancer Res*, 21, 2644-51.
- Gozzetti, A. & Le Beau, M. M. 2000. Fluorescence in situ hybridization: uses and limitations. *Semin Hematol*, 37, 320-33.
- Grawunder, U., Leu, T. M., Schatz, D. G., Werner, A., Rolink, A. G., Melchers, F., et al. 1995. Down-regulation of RAG1 and RAG2 gene expression in preB cells after functional immunoglobulin heavy chain rearrangement. *Immunity*, 3, 601-8.
- Greaves, M. & Maley, C. C. 2012. Clonal Evolution In Cancer. *Nature*, 481, 306-313.
- Greenwood, J., Clark, M. & Waldmann, H. 1993. Structural motifs involved in human IgG antibody effector functions. *Eur J Immunol*, 23, 1098-104.
- Grever, M., Kopecky, K., Coltman, C., Files, J., Greenberg, B., Hutton, J., et al. 1987. Fludarabine monophosphate: a potentially useful agent in chronic lymphocytic leukemia. *Nouvelle Revue Francaise D'hematologie*, 30, 457-459.
-

- 
- Grimwade, L. F., Fuller, K. A. & Erber, W. N. 2017. Applications of imaging flow cytometry in the diagnostic assessment of acute leukaemia. *Methods*, 112, 39-45.
- Grubor, V., Krasnitz, A., Troge, J. E., Meth, J. L., Lakshmi, B., Kendall, J. T., et al. 2009. Novel genomic alterations and clonal evolution in chronic lymphocytic leukemia revealed by representational oligonucleotide microarray analysis (ROMA). *Blood*, 113, 1294-303.
- Gryshchenko, I., Hofbauer, S., Stoecher, M., Daniel, P. T., Steurer, M., Gaiger, A., et al. 2008. MDM2 SNP309 is associated with poor outcome in B-cell chronic lymphocytic leukemia. *J Clin Oncol*, 26, 2252-7.
- Gunn, S. R., Mohammed, M. S., Gorre, M. E., Cotter, P. D., Kim, J., Bahler, D. W., et al. 2008. Whole-genome scanning by array comparative genomic hybridization as a clinical tool for risk assessment in chronic lymphocytic leukemia. *J Mol Diagn*, 10, 442-51.
- Gunnarsson, R., Mansouri, L., Isaksson, A., Goransson, H., Cahill, N., Jansson, M., et al. 2011. Array-based genomic screening at diagnosis and during follow-up in chronic lymphocytic leukemia. *Haematologica*, 96, 1161-9.
- Gupta, A. K. & Gupta, U. D. 2014. Chapter 19 - Next Generation Sequencing and Its Applications A2 - Verma, Ashish S. In: Singh, A. (ed.) *Animal Biotechnology*. San Diego: Academic Press.
- Hackett, J. A. & Greider, C. W. 2002. Balancing instability: dual roles for telomerase and telomere dysfunction in tumorigenesis. *Oncogene*, 21, 619-26.
- Haferlach, C., Dicker, F., Schnittger, S., Kern, W. & Haferlach, T. 2007. Comprehensive genetic characterization of CLL: a study on 506 cases analysed with chromosome banding analysis, interphase FISH, IgV(H) status and immunophenotyping. *Leukemia*, 21, 2442-51.
- Hagemann, I. S. 2015. Chapter 1 - Overview of Technical Aspects and Chemistries of Next-Generation Sequencing A2 - Kulkarni, Shashikant. In: Pfeifer, J. (ed.) *Clinical Genomics*. Boston: Academic Press.
- Hagemeijer, A. 1987. Chromosome abnormalities in CML. *Baillieres Clin Haematol*, 1, 963-81.
- Hagemeister, F. 2010. Rituximab for the treatment of non-Hodgkin's lymphoma and chronic lymphocytic leukaemia. *Drugs*, 70, 261-72.
- Hagenkord, J. M., Monzon, F. A., Kash, S. F., Lilleberg, S., Xie, Q. & Kant, J. A. 2010. Array-Based Karyotyping for Prognostic Assessment in Chronic Lymphocytic Leukemia: Performance Comparison of Affymetrix 10K2.0, 250K Nsp, and SNP6.0 Arrays. *The Journal of Molecular Diagnostics : JMD*, 12, 184-196.
- Hagman, J. & Grosschedl, R. 1994. Regulation of gene expression at early stages of B-cell differentiation. *Current Opinion in Immunology*, 6, 222-230.
- Haidar, M. A., El-Hajj, H., Bueso-Ramos, C. E., Manshour, T., Glassman, A., Keating, M. J., et al. 1997. Expression profile of MDM-2 proteins in chronic lymphocytic leukemia and their clinical relevance. *Am J Hematol*, 54, 189-95.
- Halazonetis, T. D., Gorgoulis, V. G. & Bartek, J. 2008. An oncogene-induced DNA damage model for cancer development. *Science*, 319, 1352-5.
- Hallek, M. 2013. Chronic lymphocytic leukemia: 2013 update on diagnosis, risk stratification and treatment. *Am J Hematol*, 88, 803-16.
-

- 
- Hallek, M., Cheson, B. D., Catovsky, D., Caligaris-Cappio, F., Dighiero, G., Dohner, H., et al. 2008. Guidelines for the diagnosis and treatment of chronic lymphocytic leukemia: a report from the International Workshop on Chronic Lymphocytic Leukemia updating the National Cancer Institute-Working Group 1996 guidelines. *Blood*, 111, 5446-56.
- Hallek, M. & Eichhorst, B. F. 2004. Chemotherapy combination treatment regimens with fludarabine in chronic lymphocytic leukemia. *Hematol J*, 5 Suppl 1, S20-30.
- Hallek, M., Fischer, K., Fingerle-Rowson, G., Fink, A., Busch, R., Mayer, J., et al. 2010. Addition of rituximab to fludarabine and cyclophosphamide in patients with chronic lymphocytic leukaemia: a randomised, open-label, phase 3 trial. *The Lancet*, 376, 1164-1174.
- Hallek, M., Langenmayer, I., Nerl, C., Knauf, W., Dietzfelbinger, H., Adorf, D., et al. 1999. Elevated serum thymidine kinase levels identify a subgroup at high risk of disease progression in early, nonmolding chronic lymphocytic leukemia. *Blood*, 93, 1732-1737.
- Halling, K. C., King, W., Sokolova, I. A., Meyer, R. G., Burkhardt, H. M., Halling, A. C., et al. 2000. A comparison of cytology and fluorescence in situ hybridization for the detection of urothelial carcinoma. *J Urol*, 164, 1768-75.
- Hamblin, T. J., Davis, Z., Gardiner, A., Oscier, D. G. & Stevenson, F. K. 1999. Unmutated Ig V(H) genes are associated with a more aggressive form of chronic lymphocytic leukemia. *Blood*, 94, 1848-54.
- Han, T., Emrich, L. J., Ozer, H., Reese, P. A., Gajera, R., Gomez, G. A., et al. 1985. Clinical significance of serum lactate dehydrogenase in chronic lymphocytic leukemia. *N Y State J Med*, 85, 685-90.
- Hanahan, D. & Weinberg, R. A. 2000. The Hallmarks of Cancer. *Cell*, 100, 57-70.
- Hanahan, D. & Weinberg, Robert a. 2011. Hallmarks of Cancer: The Next Generation. *Cell*, 144, 646-674.
- Harrington, E. D., Arumugam, M., Raes, J., Bork, P. & Relman, D. A. 2010. SmashCell: a software framework for the analysis of single-cell amplified genome sequences. *Bioinformatics*, 26, 2979-2980.
- Harris, S. L. & Levine, A. J. 2005. The p53 pathway: positive and negative feedback loops. *Oncogene*, 24, 2899-908.
- Harutyunyan, A., Klampfl, T., Cazzola, M. & Kralovics, R. 2011. p53 lesions in leukemic transformation. *N Engl J Med*, 364, 488-90.
- Headland, S. E., Jones, H. R., D'sa, A. S. V., Perretti, M. & Norling, L. V. 2014. Cutting-Edge Analysis of Extracellular Microparticles using ImageStream(X) Imaging Flow Cytometry. *Scientific Reports*, 4, 5237.
- Heit, W., Bunjes, D., Wiesneth, M., Schmeiser, T., Arnold, R., Hale, G., et al. 1986. Ex vivo T-cell depletion with the monoclonal antibody Campath-1 plus human complement effectively prevents acute graft-versus-host disease in allogeneic bone marrow transplantation. *Br J Haematol*, 64, 479-86.
- Heng, H. H., Spyropoulos, B. & Moens, P. B. 1997. FISH technology in chromosome and genome research. *Bioessays*, 19, 75-84.
-

- 
- Henriksen, M., Miller, B., Newmark, J., Al-Kofahi, Y. & Holden, E. 2011. Laser scanning cytometry and its applications: a pioneering technology in the field of quantitative imaging cytometry. *Methods Cell Biol*, 102, 161-205.
- Herling, C. D., Klaumunzer, M., Rocha, C. K., Altmuller, J., Thiele, H., Bahlo, J., et al. 2016. Complex karyotypes and KRAS and POT1 mutations impact outcome in CLL after chlorambucil-based chemotherapy or chemoimmunotherapy. *Blood*, 128, 395-404.
- Hertlein, E., Beckwith, K. A., Lozanski, G., Chen, T. L., Towns, W. H., Johnson, A. J., et al. 2013. Characterization of a new chronic lymphocytic leukemia cell line for mechanistic in vitro and in vivo studies relevant to disease. *PLoS One*, 8, e76607.
- Herzog, S., Reth, M. & Jumaa, H. 2009. Regulation of B-cell proliferation and differentiation by pre-B-cell receptor signalling. *Nat Rev Immunol*, 9, 195-205.
- Hillmen, P., Skotnicki, A. B., Robak, T., Jaksic, B., Dmoszynska, A., Wu, J., et al. 2007. Alemtuzumab compared with chlorambucil as first-line therapy for chronic lymphocytic leukemia. *Journal of Clinical Oncology*, 25, 5616-5623.
- Hilz, H., Wieggers, U. & Adamietz, P. 1975. Stimulation of proteinase K action by denaturing agents: application to the isolation of nucleic acids and the degradation of 'masked' proteins. *Eur J Biochem*, 56, 103-8.
- Holden, E., Luther, E. & Henriksen, M. 2005. New developments in quantitative imaging cytometry. *Nat Meth*, 2.
- Houlston, R. S., Sellick, G., Yuille, M., Matutes, E. & Catovsky, D. 2003. Causation of chronic lymphocytic leukemia--insights from familial disease. *Leuk Res*, 27, 871-6.
- Howat, W. J. & Wilson, B. A. 2014. Tissue fixation and the effect of molecular fixatives on downstream staining procedures. *Methods*, 70, 12-9.
- Hozier, J. C., Scalzi, J. M., Clase, A. C., Davis, L. M. & Liechty, M. C. 1998. Differential destabilization of repetitive sequence hybrids in fluorescence in situ hybridization. *Cytogenet Cell Genet*, 83, 60-3.
- Huang, B. Q. & Yeung, E. C. 2015. Chemical and Physical Fixation of Cells and Tissues: An Overview. In: YEUNG, E. C. T., STASOLLA, C., SUMNER, M. J. & HUANG, B. Q. (eds.) *Plant Microtechniques and Protocols*. Cham: Springer International Publishing.
- Hutchison, I. I. I. C. A. 2007. DNA sequencing: bench to bedside and beyond †. *Nucleic Acids Research*, 35, 6227-6237.
- Ikegawa, S., Mabuchi, A., Ogawa, M. & Ikeda, T. 2002. Allele-specific PCR amplification due to sequence identity between a PCR primer and an amplicon: is direct sequencing so reliable? *Hum Genet*, 110, 606-8.
- International-C.L.L.I.P.I.Group 2016. An international prognostic index for patients with chronic lymphocytic leukaemia (CLL-IPI): a meta-analysis of individual patient data. *Lancet Oncol*, 17, 779-790.
- Irving, J. A., Bloodworth, L., Bown, N. P., Case, M. C., Hogarth, L. A. & Hall, A. G. 2005. Loss of heterozygosity in childhood acute lymphoblastic leukemia detected by genome-wide microarray single nucleotide polymorphism analysis. *Cancer Res*, 65, 3053-8.
- Jaglowski, S. M., Ruppert, A. S., Heerema, N. A., Bingman, A., Flynn, J. M., Grever, M. R., et al. 2012. Complex karyotype predicts for inferior outcomes following reduced-intensity
-

- conditioning allogeneic transplant for chronic lymphocytic leukaemia. *Br J Haematol*, 159, 82-7.
- Jain, N. & O'Brien, S. 2012. Chronic lymphocytic leukemia with deletion 17p: emerging treatment options. *Oncology (Williston Park)*, 26, 1067, 1070.
- Jaiswal, S., Fontanillas, P., Flannick, J., Manning, A., Grauman, P. V., Mar, B. G., et al. 2014. Age-related clonal hematopoiesis associated with adverse outcomes. *N Engl J Med*, 371, 2488-98.
- Jelinek, D. F., Tschumper, R. C., Geyer, S. M., Bone, N. D., Dewald, G. W., Hanson, C. A., et al. 2001. Analysis of clonal B-cell CD38 and immunoglobulin variable region sequence status in relation to clinical outcome for B-chronic lymphocytic leukaemia. *Br J Haematol*, 115, 854-61.
- Jennings, C. D. & Foon, K. A. 1997. Recent advances in flow cytometry: application to the diagnosis of hematologic malignancy. *Blood*, 90, 2863-92.
- Jensen, E. 2014. Technical Review: In Situ Hybridization. *The Anatomical Record*, 297, 1349-1353.
- Jin, L. & Lloyd, R. V. 1997. In situ hybridization: methods and applications. *J Clin Lab Anal*, 11, 2-9.
- Joerger, A. C. & Fersht, A. R. 2008. Structural biology of the tumor suppressor p53. *Annu. Rev. Biochem.*, 77, 557-582.
- Kalisky, T., Blainey, P. & Quake, S. R. 2011. Genomic Analysis at the Single-Cell Level. *Annual Review of Genetics*, 45, 10.1146/annurev-genet-102209-163607.
- Kamentsky, L. A., Burger, D. E., Gershman, R. J., Kamentsky, L. D. & Luther, E. 1997. Slide-based laser scanning cytometry. *Acta Cytol*, 41, 123-43.
- Kamentsky, L. A. & Kamentsky, L. D. 1991. Microscope-based multiparameter laser scanning cytometer yielding data comparable to flow cytometry data. *Cytometry*, 12, 381-7.
- Kamentsky, L. A. 2001. Laser scanning cytometry. *Methods Cell Biol*, 63, 51-87.
- Kandoth, C., McLellan, M. D., Vandin, F., Ye, K., Niu, B., Lu, C., et al. 2013. Mutational landscape and significance across 12 major cancer types. *Nature*, 502, 333-339.
- Kay, D. B., Cambier, J. L. & Wheelless, L. L., Jr. 1979. Imaging in flow. *J Histochem Cytochem*, 27, 329-34.
- Kay, N. E., Shanafelt, T. D., Strege, A. K., Lee, Y. K., Bone, N. D. & Raza, A. 2007. Bone biopsy derived marrow stromal elements rescue chronic lymphocytic leukemia B-cells from spontaneous and drug induced cell death and facilitates an "angiogenic switch". *Leuk Res*, 31, 899-906.
- Kearney, L. 2001. Molecular cytogenetics. *Best Pract Res Clin Haematol*, 14, 645-69.
- Keating, M. J., Flinn, I., Jain, V., Binet, J. L., Hillmen, P., Byrd, J., et al. 2002. Therapeutic role of alemtuzumab (Campath-1H) in patients who have failed fludarabine: results of a large international study. *Blood*, 99, 3554-61.
- Keating, M. J., O'Brien, S., Albitar, M., Lerner, S., Plunkett, W., Giles, F., et al. 2005. Early Results of a Chemoimmunotherapy Regimen of Fludarabine, Cyclophosphamide, and Rituximab As Initial Therapy for Chronic Lymphocytic Leukemia. *Journal of Clinical Oncology*, 23, 4079-4088.

- 
- Keating, G. M. 2010. Rituximab: a review of its use in chronic lymphocytic leukaemia, low-grade or follicular lymphoma and diffuse large B-cell lymphoma. *Drugs*, 70, 1445-76.
- Kempin, S. 2013. Update on chronic lymphocytic leukemia: overview of new agents and comparative analysis. *Curr Treat Options Oncol*, 14, 144-55.
- Kennedy, S. R., Schmitt, M. W., Fox, E. J., Kohn, B. F., Salk, J. J., Ahn, E. H., et al. 2014. Detecting ultralow-frequency mutations by Duplex Sequencing. *Nat Protoc*, 9, 2586-606.
- Kennelly, J. C., Pate, I. & Greenwood, M. R. 1995. The effect of reducing the number of cells scored on the performance of the in vivo rat liver UDS assay. *Mutation Research/Environmental Mutagenesis and Related Subjects*, 334, 91-96.
- Kessler, C., Holtke, H. J., Seibl, R., Burg, J. & Muhlegger, K. 1990. Non-radioactive labeling and detection of nucleic acids. I. A novel DNA labeling and detection system based on digoxigenin: anti-digoxigenin ELISA principle (digoxigenin system). *Biol Chem Hoppe Seyler*, 371, 917-27.
- Kharfan-Dabaja, M. A., El-Asmar, J., Awan, F. T., Hamadani, M. & Ayala, E. 2016. Current state of hematopoietic cell transplantation in CLL as smart therapies emerge. *Best Practice & Research Clinical Haematology*, 29, 54-66.
- Khuda, S. E., Loo, W. M., Janz, S., Van Ness, B. & Erickson, L. D. 2008. Deregulation of c-Myc Confers distinct survival requirements for memory B cells, plasma cells, and their progenitors. *J Immunol*, 181, 7537-49.
- Kikushige, Y., Ishikawa, F., Miyamoto, T., Shima, T., Urata, S., Yoshimoto, G., et al. 2011. Self-renewing hematopoietic stem cell is the primary target in pathogenesis of human chronic lymphocytic leukemia. *Cancer Cell*, 20, 246-59.
- Kim, M., Lee, K.-H., Yoon, S.-W., Kim, B.-S., Chun, J. & Yi, H. 2013. Analytical Tools and Databases for Metagenomics in the Next-Generation Sequencing Era. *Genomics Inform*, 11, 102-113.
- Kim, Y. A., Madan, S. & Przytycka, T. M. 2017. WeSME: uncovering mutual exclusivity of cancer drivers and beyond. *Bioinformatics*, 33, 814-821.
- Klein, E. A. & Silverman, R. 2008. Inflammation, infection, and prostate cancer. *Curr Opin Urol*, 18, 315-9.
- Klein, U. & Dalla-Favera, R. 2010. New insights into the pathogenesis of chronic lymphocytic leukemia. *Seminars in Cancer Biology*, 20, 377-383.
- Kobayashi, Y., Esato, K., Noshima, S., Oga, A. & Sasaki, K. 2000. Detection of 20q13 gain by dual-color FISH in breast cancers. *Anticancer Res*, 20, 531-5.
- Kocks, C., Kocks, K. & Rajewsky 1989. Stable Expression and Somatic Hypermutation of Antibody V Regions in B-Cell Developmental Pathways. *Annual Review of Immunology*, 7, 537-559.
- Kojika, S. & Griffin, J. D. 2001. Notch receptors and hematopoiesis. *Exp Hematol*, 29, 1041-52.
- Krimmel, J. D., Schmitt, M. W., Harrell, M. I., Agnew, K. J., Kennedy, S. R., Emond, M. J., et al. 2016. Ultra-deep sequencing detects ovarian cancer cells in peritoneal fluid and reveals somatic TP53 mutations in noncancerous tissues. *Proceedings of the National Academy of Sciences*, 113, 6005-6010.
-

- 
- Kröber, A., Bloehdorn, J., Hafner, S., Bühler, A., Seiler, T., Kienle, D., et al. 2006. Additional Genetic High-Risk Features Such As 11q Deletion, 17p Deletion, and V3-21 Usage Characterize Discordance of ZAP-70 and VH Mutation Status in Chronic Lymphocytic Leukemia. *Journal of Clinical Oncology*, 24, 969-975.
- Krober, A., Seiler, T., Benner, A., Bullinger, L., Bruckle, E., Lichter, P., et al. 2002. V(H) mutation status, CD38 expression level, genomic aberrations, and survival in chronic lymphocytic leukemia. *Blood*, 100, 1410-6.
- Krull, D. L. & Peterson, R. A. 2011. Preclinical applications of quantitative imaging cytometry to support drug discovery. *Methods Cell Biol*, 102, 291-308.
- Kumarasinghe, M. P., Constantine, S. R. & Hemamali, R. L. 1997. Methanol as an alternative fixative for cytological smears. *Malays J Pathol*, 19, 137-40.
- Kuppers, R., Klein, U., Hansmann, M. L. & Rajewsky, K. 1999. Cellular origin of human B-cell lymphomas. *N Engl J Med*, 341, 1520-9.
- Lai, A. Y. & Kondo, M. 2008. T and B lymphocyte differentiation from hematopoietic stem cell. *Seminars in immunology*, 20, 207-212.
- Landau, D. A., Carter, S. L., Stojanov, P., McKenna, A., Stevenson, K., Lawrence, M. S., et al. 2013. Evolution and impact of subclonal mutations in chronic lymphocytic leukemia. *Cell*, 152, 714-26.
- Landau, D. A., Tausch, E., Taylor-Weiner, A. N., Stewart, C., Reiter, J. G., Bahlo, J., et al. 2015. Mutations driving CLL and their evolution in progression and relapse. *Nature*, 526, 525-30.
- Landegent, J. E., Jansen in De Wal, N., Dirks, R. W., Baao, F. & Van Der Ploeg, M. 1987. Use of whole cosmid cloned genomic sequences for chromosomal localization by non-radioactive in situ hybridization. *Hum Genet*, 77, 366-70.
- Lane, D. P. 1992. p53, guardian of the genome. *Nature*, 358, 15-16.
- Lane, D. P. & Crawford, L. V. 1979. T antigen is bound to a host protein in SV40-transformed cells. *Nature*, 278, 261-3.
- Laurie, C. C., Laurie, C. A., Rice, K., Doheny, K. F., Zelnick, L. R., Mchugh, C. P., et al. 2012. Detectable clonal mosaicism from birth to old age and its relationship to cancer. *Nature Genetics*, 44, 642-650.
- Lawrence, J. B. & Singer, R. H. 1986. Intracellular localization of messenger RNAs for cytoskeletal proteins. *Cell*, 45, 407-15.
- Lawrence, M. S., Stojanov, P., Polak, P., Kryukov, G. V., Cibulskis, K., Sivachenko, A., et al. 2013. Mutational heterogeneity in cancer and the search for new cancer genes. *Nature*, 499, 214-218.
- Le Bris, Y., Struski, S., Guieze, R., Rouvellat, C., Prade, N., Troussard, X., et al. 2016. Major prognostic value of complex karyotype in addition to TP53 and IGHV mutational status in first-line chronic lymphocytic leukemia. *Hematol Oncol*.
- Le Dieu, R. & Gribben, J. G. 2007. Transplantation in chronic lymphocytic leukemia. *Curr Hematol Malig Rep*, 2, 56-63.
- Lee, H., Deignan, J. L., Dorrani, N. & Et Al. 2014a. Clinical exome sequencing for genetic identification of rare mendelian disorders. *JAMA*, 312, 1880-1887.
-

- 
- Lee, Y. Q., Goh, A. S. P., Ch'ng, J. H., Nosten, F. H., Preiser, P. R., Pervaiz, S., et al. 2014b. A High-Content Phenotypic Screen Reveals the Disruptive Potency of Quinacrine and 3',4'-Dichlorobenzamil on the Digestive Vacuole of *Plasmodium falciparum*. *Antimicrobial Agents and Chemotherapy*, 58, 550-558.
- Leitch, I., Leitch, A. & Heslop-Harrison, J. 1991. Physical mapping of plant DNA sequences by simultaneous in situ hybridization of two differently labelled fluorescent probes. *Genome*, 34, 329-333.
- Lengauer, C., Kinzler, K. W. & Vogelstein, B. 1997. Genetic instability in colorectal cancers. *Nature*, 386, 623-7.
- Lens, D., Dyer, M. J. S., Garcia-Marco, J. M., De Schouwer, P. J. J. C., Hamoudi, R. A., Jones, D., et al. 1997. p53 abnormalities in CLL are associated with excess of prolymphocytes and poor prognosis. *British Journal of Haematology*, 99, 848-857.
- Lepretre, S., Aurran, T., Mahe, B., Cazin, B., Tournilhac, O., Maisonneuve, H., et al. 2012. Excess mortality after treatment with fludarabine and cyclophosphamide in combination with alemtuzumab in previously untreated patients with chronic lymphocytic leukemia in a randomized phase 3 trial. *Blood*, 119, 5104-10.
- Levesque, M. C., O'loughlin, C. W. & Weinberg, J. B. 2001. Use of serum-free media to minimize apoptosis of chronic lymphocytic leukemia cells during in vitro culture. *Leukemia*, 15, 1305-7.
- Li, A. H., Rosenquist, R., Forestier, E., Lindh, J. & Roos, G. 2001. Detailed clonality analysis of relapsing precursor B acute lymphoblastic leukemia: implications for minimal residual disease detection. *Leuk Res*, 25, 1033-45.
- Liedl, T. & Simmel, F. C. 2007. Determination of DNA melting temperatures in diffusion-generated chemical gradients. *Anal Chem*, 79, 5212-6.
- Liehr, T., Kreskowski, K., Ziegler, M., Piaszinski, K. & Rittscher, K. 2017. The Standard FISH Procedure. In: Liehr, T. (ed.) *Fluorescence In Situ Hybridization (FISH): Application Guide*. Berlin, Heidelberg: Springer Berlin Heidelberg.
- Lin, K., Manocha, S., Harris, R. J., Matrai, Z., Sherrington, P. D. & Pettitt, A. R. 2003. High frequency of p53 dysfunction and low level of VH mutation in chronic lymphocytic leukemia patients using the VH3-21 gene segment. *Blood*, 102, 1145-6.
- Linzer, D. I. & Levine, A. J. 1979. Characterization of a 54K dalton cellular SV40 tumor antigen present in SV40-transformed cells and uninfected embryonal carcinoma cells. *Cell*, 17, 43-52.
- Lobry, C., Oh, P., Mansour, M. R., Look, A. T. & Aifantis, I. 2014. Notch signaling: switching an oncogene to a tumor suppressor. *Blood*, 123, 2451-9.
- Loeb, L. 1947. The Causes of Cancer. *Bull N Y Acad Med*, 23, 564-80.
- Loeb, L. A. 2011. Human cancers express mutator phenotypes: origin, consequences and targeting. *Nat Rev Cancer*, 11, 450-7.
- Lopez, C., Delgado, J., Costa, D., Conde, L., Ghita, G., Villamor, N., et al. 2012. Different distribution of NOTCH1 mutations in chronic lymphocytic leukemia with isolated trisomy 12 or associated with other chromosomal alterations. *Genes Chromosomes Cancer*, 51, 881-9.
-



- 
- Lorentzen, C. L. & Straten, P. T. 2015. CD19-Chimeric Antigen Receptor T Cells for Treatment of Chronic Lymphocytic Leukaemia and Acute Lymphoblastic Leukaemia. *Scand J Immunol*, 82, 307-19.
- Luther, E., Kametsky, L., Henriksen, M. & Holden, E. 2004. Next-generation laser scanning cytometry. *Methods Cell Biol*, 75, 185-218.
- Machalinski, B., Szolomicka, P., Kijowski, J., Baskiewicz, M., Karbicka, A., Byra, E., et al. 1999. Short-term storage of human haematopoietic cells. Influence of air and deoxyribonuclease I. *Ann Transplant*, 4, 29-36.
- Maguire, O., Collins, C., O'loughlin, K., Miecznikowski, J. & Minderman, H. 2011. Quantifying Nuclear p65 as a Parameter for NF- $\kappa$ B Activation: Correlation Between ImageStream Cytometry, Microscopy and Western Blot. *Cytometry. Part A : the journal of the International Society for Analytical Cytology*, 79, 461-469.
- Maguire, O., Wallace, P. K. & Minderman, H. 2016. Fluorescent In Situ Hybridization in Suspension by Imaging Flow Cytometry. *Methods Mol Biol*, 1389, 111-26.
- Malcikova, J., Smardova, J., Rocnova, L., Tichy, B., Kuglik, P., Vranova, V., et al. 2009. Monoallelic and biallelic inactivation of TP53 gene in chronic lymphocytic leukemia: selection, impact on survival, and response to DNA damage. *Blood*, 114, 5307-14.
- Malcikova, J., Stano-Kozubik, K., Tichy, B., Kantorova, B., Pavlova, S., Tom, N., et al. 2015. Detailed analysis of therapy-driven clonal evolution of TP53 mutations in chronic lymphocytic leukemia. *Leukemia*, 29, 877-85.
- Maloum, K., Sutton, L., Baudet, S., Laurent, C., Bonnemye, P., Magnac, C., et al. 2002. Novel flow-cytometric analysis based on BCD5+ subpopulations for the evaluation of minimal residual disease in chronic lymphocytic leukaemia. *Br J Haematol*, 119, 970-5.
- Mao, X., Young, B. D. & Lu, Y.-J. 2007. The Application of Single Nucleotide Polymorphism Microarrays in Cancer Research. *Current Genomics*, 8, 219-228.
- Marcus, R. & Hagenbeek, A. 2007. The therapeutic use of rituximab in non-Hodgkin's lymphoma. *Eur J Haematol Suppl*, 5-14.
- Marti, G., Abbasi, F., Raveche, E., Rawstron, A. C., Ghia, P., Aurrant, T., et al. 2007. Overview of monoclonal B-cell lymphocytosis. *Br J Haematol*, 139, 701-8.
- Martincorena, I., Raine, K. M., Gerstung, M., Dawson, K. J., Haase, K., Van Loo, P., et al. 2017. Universal Patterns of Selection in Cancer and Somatic Tissues. *Cell*.
- Matthiesen, S. H. & Hansen, C. M. 2012. Fast and Non-Toxic In Situ Hybridization without Blocking of Repetitive Sequences. *PLoS ONE*, 7, e40675.
- Matutes, E. & Polliack, A. 2000. Morphological and Immunophenotypic Features of Chronic Lymphocytic Leukemia. *Reviews in Clinical and Experimental Hematology*, 4, 22-47.
- Maxam, A. M. & Gilbert, W. 1977. A new method for sequencing DNA. *Proceedings of the National Academy of Sciences*, 74, 560-564.
- McConaughy, B. L., Laird, C. D. & McCarthy, B. J. 1969. Nucleic acid reassociation in formamide. *Biochemistry*, 8, 3289-95.
- Mcfadden, D. G., Papagiannakopoulos, T., Taylor-Weiner, A., Stewart, C., Carter, S. L., Cibulskis, K., et al. 2014. Genetic and clonal dissection of murine small cell lung carcinoma progression by genome sequencing. *Cell*, 156, 1298-1311.
-

- 
- Meldrum, C., Doyle, M. A. & Tothill, R. W. 2011. Next-Generation Sequencing for Cancer Diagnostics: a Practical Perspective. *The Clinical Biochemist Reviews*, 32, 177-195.
- Merkel, O., Asslaber, D., Piñón, J. D., Egle, A. & Greil, R. 2010. Interdependent regulation of p53 and miR-34a in chronic lymphocytic leukemia. *Cell Cycle*, 9, 2764-2768.
- Meulmeester, E., Pereg, Y., Shiloh, Y. & Jochemsen, A. G. 2005. ATM-mediated phosphorylations inhibit Mdmx/Mdm2 stabilization by HAUSP in favor of p53 activation. *Cell Cycle*, 4, 1166-70.
- Michael, D. & Oren, M. 2002. The p53 and Mdm2 families in cancer. *Curr Opin Genet Dev*, 12, 53-9.
- Michael, D. & Oren, M. 2003. The p53-Mdm2 module and the ubiquitin system. *Semin Cancer Biol*, 13, 49-58.
- Minderman, H., Humphrey, K., Arcadi, J. K., Wierzbicki, A., Maguire, O., Wang, E. S., et al. 2012. Image cytometry-based detection of aneuploidy by fluorescence in situ hybridization in suspension. *Cytometry A*, 81, 776-84.
- Mizrahi, O., Ish-Shalom, E., Baniyash, M. & Klieger, Y. 2017 Feb 11. doi: 10.1002/cyto.b.21515. [Epub ahead of print]. Quantitative Flow Cytometry: Concerns and Recommendations in clinic and research. *Cytometry B Clin Cytom*.
- Mladinic, M., Kopjar, N., Milic, M., Buljevic Dasovic, A., Huzak, M. & Zeljezic, D. 2010. Genomic instability in a healthy elderly population: a pilot study of possible cytogenetic markers related to ageing. *Mutagenesis*, 25, 455-462.
- Mladinic, M. & Zeljezic, D. 2014. Modification of comet-FISH technique by using temperature instead of chemical denaturation. *MethodsX*, 1, 162-167.
- Montecino-Rodriguez, E. & Dorshkind, K. 2012. B-1 B Cell Development in the Fetus and Adult. *Immunity*, 36, 13-21.
- Montserrat, E., Alcalá, A., Alonso, C., Besalduch, J., Moraleda, J. M., Garcia-Conde, J., et al. 1988. A randomized trial comparing chlorambucil plus prednisone vs cyclophosphamide, melphalan, and prednisone in the treatment of chronic lymphocytic leukemia stages B and C. *Nouv Rev Fr Hematol*, 30, 429-32.
- Montserrat, E. & Dreger, P. 2015. Hope for High-Risk Chronic Lymphocytic Leukemia Relapsing After Allogeneic Stem-Cell Transplantation. *Journal of Clinical Oncology*, 33, 1527-1529.
- Montserrat, E., Sanchez-Bisono, J., Viñolas, N. & Rozman, C. 1986. Lymphocyte doubling time in chronic lymphocytic leukaemia: analysis of its prognostic significance. *British journal of haematology*, 62, 567-575.
- Moreira, A. L., Won, H. H., Mcmillan, R., Huang, J., Riely, G. J., Ladanyi, M., et al. 2015. Massively parallel sequencing identifies recurrent mutations in TP53 in thymic carcinoma associated with poor prognosis. *J Thorac Oncol*, 10, 373-80.
- Moreno-Garcia, M. E., Partida-Sanchez, S., Primack, J., Sumoza-Toledo, A., Muller-Steffner, H., Schuber, F., et al. 2004. CD38 is expressed as noncovalently associated homodimers on the surface of murine B lymphocytes. *Eur J Biochem*, 271, 1025-34.
- Moreno, C., Villamor, N., Colomer, D., Esteve, J., Gine, E., Muntanola, A., et al. 2006. Clinical significance of minimal residual disease, as assessed by different techniques, after stem cell transplantation for chronic lymphocytic leukemia. *Blood*, 107, 4563-9.
-

- 
- Moreno, C., Villamor, N., Colomer, D., Esteve, J., Martino, R., Nomdedeu, J., et al. 2005. Allogeneic stem-cell transplantation may overcome the adverse prognosis of unmutated VH gene in patients with chronic lymphocytic leukemia. *J Clin Oncol*, 23, 3433-8.
- Morrison, L. E., Ramakrishnan, R., Ruffalo, T. M. & Wilber, K. A. 2003. Labeling Fluorescence In Situ Hybridization Probes for Genomic Targets. *In: FAN, Y.-S. (ed.) Molecular Cytogenetics: Protocols and Applications*. Totowa, NJ: Humana Press.
- Moussa, M., Dumont, F., Perrier-Cornet, J. M. & Gervais, P. 2008. Cell inactivation and membrane damage after long-term treatments at sub-zero temperature in the supercooled and frozen states. *Biotechnol Bioeng*, 101, 1245-55.
- Mraz, M., Malinova, K., Kotaskova, J., Pavlova, S., Tichy, B., Malcikova, J., et al. 2009a. miR-34a, miR-29c and miR-17-5p are downregulated in CLL patients with TP53 abnormalities. *Leukemia*, 23, 1159-1163.
- Mraz, M., Malinova, K., Kotaskova, J., Pavlova, S., Tichy, B., Malcikova, J., et al. 2009b. miR-34a, miR-29c and miR-17-5p are downregulated in CLL patients with TP53 abnormalities. *Leukemia*, 23, 1159-1163.
- Mullighan, C. G., Goorha, S., Radtke, I., Miller, C. B., Coustan-Smith, E., Dalton, J. D., et al. 2007. Genome-wide analysis of genetic alterations in acute lymphoblastic leukaemia. *Nature*, 446, 758-64.
- Munk Pedersen, I. & Reed, J. 2004. Microenvironmental interactions and survival of CLL B-cells. *Leuk Lymphoma*, 45, 2365-72.
- Murrell-Bussell, S., Nguyen, D., Schober, W. D., Scott, J., Simpson, J. L., Elias, S., et al. 1998. Optimized fixation and storage conditions for FISH analysis of single-cell suspensions. *J Histochem Cytochem*, 46, 971-4.
- Nabhan, C., Coutre, S. & Hillmen, P. 2007. Minimal residual disease in chronic lymphocytic leukaemia: is it ready for primetime? *Br J Haematol*, 136, 379-92.
- Nachmanson, D., Lian, S., Schmidt, E. K., Hipp, M. J., Baker, K. T., Zhang, Y., et al. 2017. CRISPR-DS: An efficient, low DNA input method for ultra-accurate sequencing. *bioRxiv*.
- Nadeu, F., Delgado, J., Royo, C., Baumann, T., Stankovic, T., Pinyol, M., et al. 2016. Clinical impact of clonal and subclonal TP53, SF3B1, BIRC3, NOTCH1 and ATM mutations in chronic lymphocytic leukemia. *Blood*.
- Navin, N., Kendall, J., Troge, J., Andrews, P., Rodgers, L., Mcindoo, J., et al. 2011. Tumour evolution inferred by single-cell sequencing. *Nature*, 472, 90-4.
- Negrini, S., Gorgoulis, V. G. & Halazonetis, T. D. 2010. Genomic instability--an evolving hallmark of cancer. *Nat Rev Mol Cell Biol*, 11, 220-8.
- Nobile, C., Rudnicka, D., Hasan, M., Aulner, N., Porrot, F., Machu, C., et al. 2010. HIV-1 Nef inhibits ruffles, induces filopodia, and modulates migration of infected lymphocytes. *J Virol*, 84, 2282-93.
- Noguchi, M., Furuya, S., Takeuchi, T. & Hirohashi, S. 1997. Modified formalin and methanol fixation methods for molecular biological and morphological analyses. *Pathol Int*, 47, 685-91.
- Nowell, P. C. E. A. 1976. The clonal evolution of tumor cell populations. *Science*, 194, 23-8.
-

- 
- O'Brien, S. M., Kantarjian, H. M., Cortes, J., Beran, M., Koller, C. A., Giles, F. J., et al. 2001. Results of the fludarabine and cyclophosphamide combination regimen in chronic lymphocytic leukemia. *J Clin Oncol*, 19, 1414-20.
- Okazaki, I. M., Kinoshita, K., Muramatsu, M., Yoshikawa, K. & Honjo, T. 2002. The AID enzyme induces class switch recombination in fibroblasts. *Nature*, 416, 340-5.
- Olivier, M., Hollstein, M. & Hainaut, P. 2010. TP53 Mutations in Human Cancers: Origins, Consequences, and Clinical Use. *Cold Spring Harbor Perspectives in Biology*, 2, a001008.
- Ortyn, W. E., Hall, B. E., George, T. C., Frost, K., Basiji, D. A., Perry, D. J., et al. 2006. Sensitivity measurement and compensation in spectral imaging. *Cytometry A*, 69, 852-62.
- Ortyn, W. E., Perry, D. J., Venkatachalam, V., Liang, L., Hall, B. E., Frost, K., et al. 2007. Extended depth of field imaging for high speed cell analysis. *Cytometry A*, 71, 215-31.
- Oscier, D., Fegan, C., Hillmen, P., Illidge, T., Johnson, S., Maguire, P., et al. 2004. Guidelines on the diagnosis and management of chronic lymphocytic leukaemia. *Br J Haematol*, 125, 294-317.
- Oscier, D., Wade, R., Davis, Z., Morilla, A., Best, G., Richards, S., et al. 2010. Prognostic factors identified three risk groups in the LRF CLL4 trial, independent of treatment allocation. *Haematologica*, 95, 1705-1712.
- Oscier, D. G. 1997. Differential rates of somatic hypermutation in VH genes among subsets of chronic lymphocytic leukemia defined by chromosomal abnormalities. *Blood*, 89, 4153.
- Oscier, D. G., Rose-Zerilli, M. J., Winkelmann, N., Gonzalez De Castro, D., Gomez, B., Forster, J., et al. 2013. The clinical significance of NOTCH1 and SF3B1 mutations in the UK LRF CLL4 trial. *Blood*, 121, 468-75.
- Osoegawa, K., Mammoser, A. G., Wu, C., Frengen, E., Zeng, C., Catanese, J. J., et al. 2001. A bacterial artificial chromosome library for sequencing the complete human genome. *Genome Res*, 11, 483-96.
- Osterborg, A., Dyer, M., Bunjes, D., Pangalis, G. A., Bastion, Y., Catovsky, D., et al. 1997. Phase II multicenter study of human CD52 antibody in previously treated chronic lymphocytic leukemia. European Study Group of CAMPATH-1H Treatment in Chronic Lymphocytic Leukemia. *Journal of Clinical Oncology*, 15, 1567-1574.
- Ouillette, P., Saiya-Cork, K., Seymour, E., Li, C., Shedden, K. & Malek, S. N. 2013. Clonal evolution, genomic drivers, and effects of therapy in chronic lymphocytic leukemia. *Clin Cancer Res*, 19, 2893-904.
- Paganin, M. & Ferrando, A. 2011. Molecular pathogenesis and targeted therapies for NOTCH1-induced T-cell acute lymphoblastic leukemia. *Blood Rev*, 25, 83-90.
- Paik, S., Bryant, J., Tan-Chiu, E., Romond, E., Hiller, W., Park, K., et al. 2002. Real-world performance of HER2 testing--National Surgical Adjuvant Breast and Bowel Project experience. *J Natl Cancer Inst*, 94, 852-4.
- Panayiotidis, P., Jones, D., Ganeshaguru, K., Foroni, L. & Hoffbrand, A. V. 1996. Human bone marrow stromal cells prevent apoptosis and support the survival of chronic lymphocytic leukaemia cells in vitro. *Br J Haematol*, 92, 97-103.
- Parikh, S. A., Keating, M. J., O'Brien, S., Wang, X., Ferrajoli, A., Faderl, S., et al. 2011. Frontline chemoimmunotherapy with fludarabine, cyclophosphamide, alemtuzumab, and rituximab for high-risk chronic lymphocytic leukemia. *Blood*, 118, 2062-2068.
-

- 
- Park, G., Park, J. K., Shin, S.-H., Jeon, H.-J., Kim, N. K. D., Kim, Y. J., et al. 2017. Characterization of background noise in capture-based targeted sequencing data. *Genome Biology*, 18, 136.
- Parkin, B., Ouillette, P., Li, Y., Keller, J., Lam, C., Roulston, D., et al. 2013. Clonal evolution and devolution after chemotherapy in adult acute myelogenous leukemia. *Blood*, 121, 369-77.
- Parkin, B., Ouillette, P., Yildiz, M., Saiya-Cork, K., Shedden, K. & Malek, S. N. 2015. INTEGRATED GENOMIC PROFILING, THERAPY RESPONSE AND SURVIVAL IN ADULT ACUTE MYELOGENOUS LEUKEMIA. *Clinical cancer research : an official journal of the American Association for Cancer Research*, 21, 2045-2056.
- Parry, M., Rose-Zerilli, M. J. J., Ljungström, V., Gibson, J., Wang, J., Walewska, R., et al. 2015. Genetics and Prognostication in Splenic Marginal Zone Lymphoma: Revelations from Deep Sequencing. *Clinical cancer research : an official journal of the American Association for Cancer Research*, 21, 4174-4183.
- Pawluczakowycz, A. W., Beurskens, F. J., Beum, P. V., Lindorfer, M. A., Van De Winkel, J. G., Parren, P. W., et al. 2009. Binding of submaximal C1q promotes complement-dependent cytotoxicity (CDC) of B cells opsonized with anti-CD20 mAbs ofatumumab (OFA) or rituximab (RTX): considerably higher levels of CDC are induced by OFA than by RTX. *J Immunol*, 183, 749-58.
- Pedersen, I. M., Kitada, S., Leoni, L. M., Zapata, J. M., Karras, J. G., Tsukada, N., et al. 2002. Protection of CLL B cells by a follicular dendritic cell line is dependent on induction of Mcl-1. *Blood*, 100, 1795-801.
- Pegg, D. E. 1987. Mechanisms of freezing damage. *Symp Soc Exp Biol*, 41, 363-78.
- Perry, M. J., Chen, X., Mcauliffe, M. E., Maity, A. & Deloid, G. M. 2011. Semi-automated Scoring of Triple-probe FISH in Human Sperm: Methods and Further Validation(1). *Cytometry*, 79, 661-666.
- Pettitt, A. R. 2003. Mechanism of action of purine analogues in chronic lymphocytic leukaemia. *British Journal of Haematology*, 121, 692-702.
- Pham, L. V., Tamayo, A. T., Yoshimura, L. C., Lin-Lee, Y.-C. & Ford, R. J. 2005. Constitutive NF- $\kappa$ B and NFAT activation in aggressive B-cell lymphomas synergistically activates the CD154 gene and maintains lymphoma cell survival. *Blood*, 106, 3940-3947.
- Phelan, K. & May, K. M. 2015. Basic techniques in mammalian cell tissue culture. *Curr Protoc Cell Biol*, 66, 1.1.1-22.
- Pieper, K., Grimbacher, B. & Eibel, H. 2013. B-cell biology and development. *Journal of Allergy and Clinical Immunology*, 131, 959-971.
- Pietkiewicz, S., Schmidt, J. H. & Lavrik, I. N. 2015. Quantification of apoptosis and necroptosis at the single cell level by a combination of Imaging Flow Cytometry with classical Annexin V/propidium iodide staining. *J Immunol Methods*, 423, 99-103.
- Pietsch, E. C., Sykes, S. M., McMahon, S. B. & Murphy, M. E. 2008. The p53 family and programmed cell death. *Oncogene*, 27, 6507-21.
- Pineau, I., Barrette, B., Vallieres, N. & Lacroix, S. 2006. A novel method for multiple labeling combining in situ hybridization with immunofluorescence. *J Histochem Cytochem*, 54, 1303-13.
-

- 
- Pinkel, D., Straume, T. & Gray, J. W. 1986. Cytogenetic analysis using quantitative, high-sensitivity, fluorescence hybridization. *Proc Natl Acad Sci U S A*, 83, 2934-8.
- Pinto, D., Darvishi, K., Shi, X., Rajan, D., Rigler, D., Fitzgerald, T., et al. 2011. Comprehensive assessment of array-based platforms and calling algorithms for detection of copy number variants. *Nat Biotech*, 29, 512-520.
- Ponomarev, E. D., Veremeyko, T. & Barteneva, N. S. 2011. Visualization and quantitation of the expression of microRNAs and their target genes in neuroblastoma single cells using imaging cytometry. *BMC Research Notes*, 4, 517-517.
- Pospisilova, S., Gonzalez, D., Malcikova, J., Trbusek, M., Rossi, D., Kater, A. P., et al. 2012. ERIC recommendations on TP53 mutation analysis in chronic lymphocytic leukemia. *Leukemia*, 26, 1458-61.
- Pozarowski, P., Holden, E. & Darzynkiewicz, Z. 2013. Laser scanning cytometry: principles and applications-an update. *Methods Mol Biol*, 931, 187-212.
- Puente, X. S., Bea, S., Valdes-Mas, R., Villamor, N., Gutierrez-Abril, J., Martin-Subero, J. I., et al. 2015. Non-coding recurrent mutations in chronic lymphocytic leukaemia. *Nature*, 526, 519-24.
- Puente, X. S., Pinyol, M., Quesada, V., Conde, L., Ordonez, G. R., Villamor, N., et al. 2011. Whole-genome sequencing identifies recurrent mutations in chronic lymphocytic leukaemia. *Nature*, 475, 101-5.
- Puiggros, A., Blanco, G. & Espinet, B. 2014. Genetic abnormalities in chronic lymphocytic leukemia: where we are and where we go. *Biomed Res Int*, 2014, 435983.
- Puiggros, A., Collado, R., Calasanz, M. J., Ortega, M., Ruiz-Xivillé, N., Rivas-Delgado, A., et al. 2017. Patients with chronic lymphocytic leukemia and complex karyotype show an adverse outcome even in absence of TP53/ATM FISH deletions. *Oncotarget*, 8, 54297-54303.
- Quesada, V., Conde, L., Villamor, N., Ordonez, G. R., Jares, P., Bassaganyas, L., et al. 2011. Exome sequencing identifies recurrent mutations of the splicing factor SF3B1 gene in chronic lymphocytic leukemia. *Nat Genet*, 44, 47-52.
- Quijano, S., Lopez, A., Rasillo, A., Sayagues, J. M., Barrena, S., Sanchez, M. L., et al. 2008. Impact of trisomy 12, del(13q), del(17p), and del(11q) on the immunophenotype, DNA ploidy status, and proliferative rate of leukemic B-cells in chronic lymphocytic leukemia. *Cytometry B Clin Cytom*, 74, 139-49.
- Rai, K. R., Peterson, B. L., Appelbaum, F. R., Kolitz, J., Elias, L., Shepherd, L., et al. 2000. Fludarabine compared with chlorambucil as primary therapy for chronic lymphocytic leukemia. *N Engl J Med*, 343, 1750-7.
- Rai, K. R., Sawitsky, A., Cronkite, E. P., Chanana, A. D., Levy, R. N. & Pasternack, B. S. 1975. Clinical staging of chronic lymphocytic leukemia. *Blood*, 46, 219-34.
- Raphael, B., Andersen, J. W., Silber, R., Oken, M., Moore, D., Bennett, J., et al. 1991. Comparison of chlorambucil and prednisone versus cyclophosphamide, vincristine, and prednisone as initial treatment for chronic lymphocytic leukemia: long-term follow-up of an Eastern Cooperative Oncology Group randomized clinical trial. *J Clin Oncol*, 9, 770-6.
- Rasi, S., Khiabani, H., Ciardullo, C., Terzi-Di-Bergamo, L., Monti, S., Spina, V., et al. 2016. Clinical impact of small subclones harboring NOTCH1, SF3B1 or BIRC3 mutations in chronic lymphocytic leukemia. *Haematologica*, 101, e135-8.
-

- 
- Rassenti, L. Z., Jain, S., Keating, M. J., Wierda, W. G., Grever, M. R., Byrd, J. C., et al. 2008. Relative value of ZAP-70, CD38, and immunoglobulin mutation status in predicting aggressive disease in chronic lymphocytic leukemia. *Blood*, 112, 1923-1930.
- Rauch, J., Wolf, D., Craig, J. M., Hausmann, M. & Cremer, C. 2000. Quantitative microscopy after fluorescence in situ hybridization - a comparison between repeat-depleted and non-depleted DNA probes. *J Biochem Biophys Methods*, 44, 59-72.
- Rawstron, A. C., Bennett, F. L., O'connor, S. J. M., Kwok, M., Fenton, J. a. L., Plummer, M., et al. 2008. Monoclonal B-Cell Lymphocytosis and Chronic Lymphocytic Leukemia. *New England Journal of Medicine*, 359, 575-583.
- Rehm, H. L., Bale, S. J., Bayrak-Toydemir, P., Berg, J. S., Brown, K. K., Deignan, J. L., et al. 2013. ACMG clinical laboratory standards for next-generation sequencing. *Genet Med*, 15, 733-47.
- Renner, W. A., Jordan, M., Eppenberger, H. M. & Leist, C. 1993. Cell-cell adhesion and aggregation: Influence on the growth behavior of CHO cells. *Biotechnology and Bioengineering*, 41, 188-193.
- Ricci, F., Tedeschi, A., Morra, E. & Montillo, M. 2009. Fludarabine in the treatment of chronic lymphocytic leukemia: a review. *Therapeutics and Clinical Risk Management*, 5, 187-207.
- Ricciardi, M. R., Petrucci, M. T., Gregorj, C., Ariola, C., Lemoli, R. M., Fogli, M., et al. 2001. Reduced susceptibility to apoptosis correlates with kinetic quiescence in disease progression of chronic lymphocytic leukaemia. *Br J Haematol*, 113, 391-9.
- Richards, S., Aziz, N., Bale, S., Bick, D., Das, S., Gastier-Foster, J., et al. 2015. Standards and guidelines for the interpretation of sequence variants: a joint consensus recommendation of the American College of Medical Genetics and Genomics and the Association for Molecular Pathology. *Genet Med*, 17, 405-24.
- Rigby, P. W., Dieckmann, M., Rhodes, C. & Berg, P. 1977. Labeling deoxyribonucleic acid to high specific activity in vitro by nick translation with DNA polymerase I. *J Mol Biol*, 113, 237-51.
- Rigolin, G. M., Saccenti, E., Bassi, C., Lupini, L., Quaglia, F. M., Cavallari, M., et al. 2016. Extensive next-generation sequencing analysis in chronic lymphocytic leukemia at diagnosis: clinical and biological correlations. *Journal of Hematology & Oncology*, 9, 88.
- Robak, T. 2005. Therapy of chronic lymphocytic leukemia with purine analogs and monoclonal antibodies. *Transfus Apher Sci*, 32, 33-44.
- Robak, T., Dmoszynska, A., Solal-Céligny, P., Warzocha, K., Loscertales, J., Catalano, J., et al. 2010a. Rituximab plus fludarabine and cyclophosphamide prolongs progression-free survival compared with fludarabine and cyclophosphamide alone in previously treated chronic lymphocytic leukemia. *Journal of clinical oncology*, 28, 1756-1765.
- Robak, T., Lech-Maranda, E. & Robak, P. 2010b. Rituximab plus fludarabine and cyclophosphamide or other agents in chronic lymphocytic leukemia. *Expert Rev Anticancer Ther*, 10, 1529-43.
- Roecklein, B. A. & Torok-Storb, B. 1995. Functionally distinct human marrow stromal cell lines immortalized by transduction with the human papilloma virus E6/E7 genes. *Blood*, 85, 997-1005.
-

- 
- Rosati, E., Sabatini, R., Rampino, G., Tabilio, A., Di Ianni, M., Fettucciari, K., et al. 2009. Constitutively activated Notch signaling is involved in survival and apoptosis resistance of B-CLL cells. *Blood*, 113, 856-65.
- Rossi, D., Cerri, M., Deambrogi, C., Sozzi, E., Cresta, S., Rasi, S., et al. 2009. The Prognostic Value of TP53 Mutations in Chronic Lymphocytic Leukemia Is Independent of Del17p13: Implications for Overall Survival and Chemorefractoriness. *Clinical Cancer Research*, 15, 995-1004.
- Rossi, D., Bruscaggin, A., Spina, V., Rasi, S., Khiabani, H., Messina, M., et al. 2011a. Mutations of the SF3B1 splicing factor in chronic lymphocytic leukemia: association with progression and fludarabine-refractoriness. *Blood*, 118, 6904-8.
- Rossi, D., Spina, V., Deambrogi, C., Rasi, S., Laurenti, L., Stamatopoulos, K., et al. 2011b. The genetics of Richter syndrome reveals disease heterogeneity and predicts survival after transformation. *Blood*, 117, 3391-3401.
- Rossi, D., Fangazio, M., Rasi, S., Vaisitti, T., Monti, S., Cresta, S., et al. 2012a. Disruption of BIRC3 associates with fludarabine chemorefractoriness in TP53 wild-type chronic lymphocytic leukemia. *Blood*, 119, 2854-62.
- Rossi, D., Rasi, S., Fabbri, G., Spina, V., Fangazio, M., Forconi, F., et al. 2012b. Mutations of NOTCH1 are an independent predictor of survival in chronic lymphocytic leukemia. *Blood*, 119, 521-9.
- Rossi, D., Khiabani, H., Spina, V., Ciardullo, C., Bruscaggin, A., Fama, R., et al. 2014. Clinical impact of small TP53 mutated subclones in chronic lymphocytic leukemia. *Blood*, 123, 2139-47.
- Rossi, D., Terzi-Di-Bergamo, L., De Paoli, L., Cerri, M., Ghilardi, G., Chiarenza, A., et al. 2015. Molecular prediction of durable remission after first-line fludarabine-cyclophosphamide-rituximab in chronic lymphocytic leukemia. *Blood*, 126, 1921-4.
- Rossi, D. & Gaidano, G. 2016. The clinical implications of gene mutations in chronic lymphocytic leukaemia. *Br J Cancer*, 114, 849-54.
- Rowan, W., Tite, J., Topley, P. & Brett, S. J. 1998. Cross-linking of the CAMPATH-1 antigen (CD52) mediates growth inhibition in human B- and T-lymphoma cell lines, and subsequent emergence of CD52-deficient cells. *Immunology*, 95, 427-36.
- Rudenko, H. C., Else, M., Dearden, C., Brito-Babapulle, V., Jones, C., Dexter, T., et al. 2008. Characterising the TP53-deleted subgroup of chronic lymphocytic leukemia: an analysis of additional cytogenetic abnormalities detected by interphase fluorescence in situ hybridisation and array-based comparative genomic hybridisation. *Leuk Lymphoma*, 49, 1879-86.
- Sanger, F., Air, G. M., Barrell, B. G., Brown, N. L., Coulson, A. R., Fiddes, J. C., et al. 1977a. Nucleotide sequence of bacteriophage [phi]X174 DNA. *Nature*, 265, 687-695.
- Sanger, F., Nicklen, S. & Coulson, A. R. 1977b. DNA sequencing with chain-terminating inhibitors. *Proceedings of the National Academy of Sciences*, 74, 5463-5467.
- Schetelig, J., Van Biezen, A., Brand, R., Caballero, D., Martino, R., Itala, M., et al. 2008. Allogeneic hematopoietic stem-cell transplantation for chronic lymphocytic leukemia with 17p deletion: a retrospective European Group for Blood and Marrow Transplantation analysis. *J Clin Oncol*, 26, 5094-100.
-



- 
- Schillaci, R., Galeano, A., Becu-Villalobos, D., Spinelli, O., Sapia, S. & Bezares, R. F. 2005. Autocrine/paracrine involvement of insulin-like growth factor-I and its receptor in chronic lymphocytic leukaemia. *Br J Haematol*, 130, 58-66.
- Schmid, T. E., Lowe, X., Marchetti, F., Bishop, J., Haseman, J. & Wyrobek, A. J. 2001. Evaluation of inter-scorer and inter-laboratory reliability of the mouse epididymal sperm aneuploidy (m-ESA) assay. *Mutagenesis*, 16, 189-95.
- Schmitt, M. W., Fox, E. J., Prindle, M. J., Reid-Bayliss, K. S., True, L. D., Radich, J. P., et al. 2015. Sequencing small genomic targets with high efficiency and extreme accuracy. *Nature methods*, 12, 423-425.
- Schmitt, M. W., Kennedy, S. R., Salk, J. J., Fox, E. J., Hiatt, J. B. & Loeb, L. A. 2012. Detection of ultra-rare mutations by next-generation sequencing. *Proc Natl Acad Sci U S A*, 109, 14508-13.
- Schuh, A., Becq, J., Humphray, S., Alexa, A., Burns, A., Clifford, R., et al. 2012. Monitoring chronic lymphocytic leukemia progression by whole genome sequencing reveals heterogeneous clonal evolution patterns. *Blood*, 120, 4191-6.
- Schurter, M. J., Lebrun, D. P. & Harrison, K. J. 2002. Improved technique for fluorescence in situ hybridisation analysis of isolated nuclei from archival, B5 or formalin fixed, paraffin wax embedded tissue. *Molecular Pathology*, 55, 121-124.
- Schwartz, M., Zlotorynski, E. & Kerem, B. 2006. The molecular basis of common and rare fragile sites. *Cancer Lett*, 232, 13-26.
- Scott, E. W., Simon, M. C., Anastasi, J. & Singh, H. 1994. Requirement of transcription factor PU.1 in the development of multiple hematopoietic lineages. *Science*, 265, 1573-7.
- Scott, L. M. & Rebel, V. I. 2013. Acquired mutations that affect pre-mRNA splicing in hematologic malignancies and solid tumors. *J Natl Cancer Inst*, 105, 1540-9.
- Seifert, M., Sellmann, L., Bloehdorn, J., Wein, F., Stilgenbauer, S., Dürig, J., et al. 2012. Cellular origin and pathophysiology of chronic lymphocytic leukemia. *The Journal of Experimental Medicine*, 209, 2183-2198.
- Serakinci, N. & Kølvråa, S. 2009. Molecular Cytogenetic Applications in Diagnostics and Research: An Overview. In: LIEHR, T. (ed.) *Fluorescence In Situ Hybridization (FISH) — Application Guide*. Berlin, Heidelberg: Springer Berlin Heidelberg.
- Shanafelt, T. D., Witzig, T. E., Fink, S. R., Jenkins, R. B., Paternoster, S. F., Smoley, S. A., et al. 2006. Prospective Evaluation of Clonal Evolution During Long-Term Follow-Up of Patients With Untreated Early-Stage Chronic Lymphocytic Leukemia. *Journal of Clinical Oncology*, 24, 4634-4641.
- Shanafelt, T. D., Hanson, C., Dewald, G. W., Witzig, T. E., Laplant, B., Abrahamzon, J., et al. 2008. Karyotype evolution on fluorescent in situ hybridization analysis is associated with short survival in patients with chronic lymphocytic leukemia and is related to CD49d expression. *J Clin Oncol*, 26, e5-6.
- Shanafelt, T. D., Rabe, K. G., Kay, N. E., Zent, C. S., Jelinek, D. F., Reinalda, M. S., et al. 2010. Age at diagnosis and the utility of prognostic testing in patients with chronic lymphocytic leukemia. *Cancer*, 116, 4777-87.
- Shen, H. M. & Shen 1998. Mutation of BCL-6 Gene in Normal B Cells by the Process of Somatic Hypermutation of Ig Genes. *Science*, 280, 1750-1752.
-

- 
- Shen, Z. 2011. Genomic instability and cancer: an introduction. *J Mol Cell Biol*, 3, 1-3.
- Sher, T., Miller, K. C., Lawrence, D., Whitworth, A., Hernandez-Ilizaliturri, F., Czuczman, M. S., et al. 2010. Efficacy of lenalidomide in patients with chronic lymphocytic leukemia with high-risk cytogenetics. *Leuk Lymphoma*, 51, 85-8.
- Shustik, C., Mick, R., Silver, R., Sawitsky, A., Rai, K. & Shapiro, L. 1988. Treatment of early chronic lymphocytic leukemia: intermittent chlorambucil versus observation. *Hematol Oncol*, 6, 7-12.
- Sieber, O. M., Heinimann, K. & Tomlinson, I. P. 2003. Genomic instability--the engine of tumorigenesis? *Nat Rev Cancer*, 3, 701-8.
- Silber, R., Degar, B., Costin, D., Newcomb, E. W., Mani, M., Rosenberg, C. R., et al. 1994. Chemosensitivity of lymphocytes from patients with B-cell chronic lymphocytic leukemia to chlorambucil, fludarabine, and camptothecin analogs. *Blood*, 84, 3440-6.
- Silwal-Pandit, L., Langerod, A. & Borresen-Dale, A. L. 2017. TP53 Mutations in Breast and Ovarian Cancer. *Cold Spring Harb Perspect Med*, 7.
- Sinclair, P. B., Green, A. R., Grace, C. & Nacheva, E. P. 1997. Improved sensitivity of BCR-ABL detection: a triple-probe three-color fluorescence in situ hybridization system. *Blood*, 90, 1395-402.
- Sinclair, D. A. 2003. Cell biology. An age of instability. *Science*, 301, 1859-60.
- Smoley, S. A., Van Dyke, D. L., Kay, N. E., Heerema, N. A., Dell'aquila, M. L., Dal Cin, P., et al. 2010. Standardization of fluorescence in situ hybridization studies on chronic lymphocytic leukemia (CLL) blood and marrow cells by the CLL Research Consortium. *Cancer genetics and cytogenetics*, 203, 141-148.
- Song, J. & Shao, H. 2016. SNP Array in Hematopoietic Neoplasms: A Review. *Microarrays*, 5, 1.
- Soussi, T., Legros, Y., Lubin, R., Ory, K. & Schlichtholz, B. 1994. Multifactorial analysis of p53 alteration in human cancer: A review. *International Journal of Cancer*, 57, 1-9.
- Soussi, T. 2010. The history of p53: A perfect example of the drawbacks of scientific paradigms. *EMBO Reports*, 11, 822-826.
- Srinivasan, M., Sedmak, D. & Jewell, S. 2002. Effect of Fixatives and Tissue Processing on the Content and Integrity of Nucleic Acids. *The American Journal of Pathology*, 161, 1961-1971.
- St-Laurent, J., Boulay, M. E., Prince, P., Bissonnette, E. & Boulet, L. P. 2006. Comparison of cell fixation methods of induced sputum specimens: an immunocytochemical analysis. *J Immunol Methods*, 308, 36-42.
- Stankovic, T., Hubank, M., Cronin, D., Stewart, G. S., Fletcher, D., Bignell, C. R., et al. 2004. Microarray analysis reveals that TP53- and ATM-mutant B-CLLs share a defect in activating proapoptotic responses after DNA damage but are distinguished by major differences in activating prosurvival responses. *Blood*, 103, 291-300.
- Stankovic, T. & Skowronska, A. 2014. The role of ATM mutations and 11q deletions in disease progression in chronic lymphocytic leukemia. *Leuk Lymphoma*, 55, 1227-39.
- Start, R. D., Layton, C. M., Cross, S. S. & Smith, J. H. 1992. Reassessment of the rate of fixative diffusion. *Journal of Clinical Pathology*, 45, 1120-1121.
-

- 
- Stashenko, P., Nadler, L. M., Hardy, R. & Schlossman, S. F. 1980. Characterization of a human B lymphocyte-specific antigen. *J Immunol*, 125, 1678-85.
- Stengel, A., Schnittger, S., Weissmann, S., Kuznia, S., Kern, W., Kohlmann, A., et al. 2014. TP53 mutations occur in 15.7% of ALL and are associated with MYC-rearrangement, low hypodiploidy, and a poor prognosis. *Blood*, 124, 251-8.
- Stewart, J. C., Villasmil, M. L. & Frampton, M. W. 2007. Changes in fluorescence intensity of selected leukocyte surface markers following fixation. *Cytometry A*, 71, 379-85.
- Stilgenbauer, S., Sander, S., Bullinger, L., Benner, A., Leupolt, E., Winkler, D., et al. 2007. Clonal evolution in chronic lymphocytic leukemia: acquisition of high-risk genomic aberrations associated with unmutated VH, resistance to therapy, and short survival. *Haematologica*, 92, 1242-1245.
- Stilgenbauer, S. & Zenz, T. 2010. Understanding and managing ultra high-risk chronic lymphocytic leukemia. *Hematology Am Soc Hematol Educ Program*, 2010, 481-8.
- Stilgenbauer, S., Schnaiter, A., Paschka, P., Zenz, T., Rossi, M., Dohner, K., et al. 2014. Gene mutations and treatment outcome in chronic lymphocytic leukemia: results from the CLL8 trial. *Blood*, 123, 3247-54.
- Stilgenbauer, S., Eichhorst, B., Schetelig, J., Coutre, S., Seymour, J. F., Munir, T., et al. 2016. Venetoclax in relapsed or refractory chronic lymphocytic leukaemia with 17p deletion: a multicentre, open-label, phase 2 study. *Lancet Oncol*, 17, 768-78.
- Stommel, J. M. & Wahl, G. M. 2004. Accelerated MDM2 auto-degradation induced by DNA-damage kinases is required for p53 activation. *Embo j*, 23, 1547-56.
- Stommel, J. M. & Wahl, G. M. 2005. A new twist in the feedback loop: stress-activated MDM2 destabilization is required for p53 activation. *Cell Cycle*, 4, 411-7.
- Sturm, I., Bosanquet, A. G., Hermann, S., Guner, D., Dorken, B. & Daniel, P. T. 2003. Mutation of p53 and consecutive selective drug resistance in B-CLL occurs as a consequence of prior DNA-damaging chemotherapy. *Cell Death Differ*, 10, 477-84.
- Subramanian, S. & Steer, C. J. 2010. MicroRNAs as gatekeepers of apoptosis. *J Cell Physiol*, 223, 289-98.
- Sun, H.-J., Chen, J., Ni, B., Yang, X. & Wu, Y.-Z. 2015. Recent advances and current issues in single-cell sequencing of tumors. *Cancer Letters*, 365, 1-10.
- Sutton, L. A., Ljungstrom, V., Mansouri, L., Young, E., Cortese, D., Navrkalova, V., et al. 2015. Targeted next-generation sequencing in chronic lymphocytic leukemia: a high-throughput yet tailored approach will facilitate implementation in a clinical setting. *Haematologica*, 100, 370-6.
- Suzuki, H. I., Yamagata, K., Sugimoto, K., Iwamoto, T., Kato, S. & Miyazono, K. 2009. Modulation of microRNA processing by p53. *Nature*, 460, 529-33.
- Takahashi, H., Ruiz, P., Ricordi, C., Miki, A., Mita, A., Barker, S., et al. 2009. In situ quantitative immunoprofiling of regulatory T cells using laser scanning cytometry. *Transplant Proc*, 41, 238-9.
- Talpaz, M., Shah, N. P., Kantarjian, H., Donato, N., Nicoll, J., Paquette, R., et al. 2006. Dasatinib in Imatinib-Resistant Philadelphia Chromosome-Positive Leukemias. *New England Journal of Medicine*, 354, 2531-2541.
-

- 
- Tam, C. S., O'Brien, S., Lerner, S., Khouri, I., Ferrajoli, A., Faderl, S., et al. 2007. The natural history of fludarabine-refractory chronic lymphocytic leukemia patients who fail alemtuzumab or have bulky lymphadenopathy. *Leuk Lymphoma*, 48, 1931-9.
- Tam, C. S., O'Brien, S., Wierda, W., Kantarjian, H., Wen, S., Do, K.-A., et al. 2008. Long-term results of the fludarabine, cyclophosphamide, and rituximab regimen as initial therapy of chronic lymphocytic leukemia. *Blood*, 112, 975-980.
- Tam, C. S. & Khouri, I. 2009a. The role of stem cell transplantation in the management of chronic lymphocytic leukaemia. *Hematol Oncol*, 27, 53-60.
- Tam, C. S., Shanafelt, T. D., Wierda, W. G., Abruzzo, L. V., Van Dyke, D. L., O'Brien, S., et al. 2009b. De novo deletion 17p13.1 chronic lymphocytic leukemia shows significant clinical heterogeneity: the M. D. Anderson and Mayo Clinic experience. *Blood*, 114, 957-964.
- Te Raa, G. D., Derks, I. A., Navrkalova, V., Skowronska, A., Moerland, P. D., Van Laar, J., et al. 2015. The impact of SF3B1 mutations in CLL on the DNA-damage response. *Leukemia*, 29, 1133-42.
- Tegg, E. M., Thomson, R. J., Stankovich, J., Banks, A., Flowers, C., Mcwhirter, R., et al. 2010. Evidence for a common genetic aetiology in high-risk families with multiple haematological malignancy subtypes. *Br J Haematol*, 150, 456-62.
- Thompson, C. B. 1995. New insights into V(D)J recombination and its role in the evolution of the immune system. *Immunity*, 3, 531-539.
- Thompson, P. A., O'Brien, S. M., Wierda, W. G., Ferrajoli, A., Stingo, F., Smith, S. C., et al. 2015. Complex karyotype is a stronger predictor than del(17p) for an inferior outcome in relapsed or refractory chronic lymphocytic leukemia patients treated with ibrutinib-based regimens. *Cancer*, 121, 3612-21.
- Thompson, P. A., Tam, C. S., O'Brien, S. M., Wierda, W. G., Stingo, F., Plunkett, W., et al. 2016. Fludarabine, cyclophosphamide, and rituximab treatment achieves long-term disease-free survival in IGHV-mutated chronic lymphocytic leukemia. *Blood*, 127, 303-309.
- Ticchioni, M., Essafi, M., Jeandel, P. Y., Davi, F., Cassuto, J. P., Deckert, M., et al. 2007. Homeostatic chemokines increase survival of B-chronic lymphocytic leukemia cells through inactivation of transcription factor FOXO3a. *Oncogene*, 26, 7081-91.
- Tirode, F., Surdez, D., Ma, X., Parker, M., Le Deley, M. C., Bahrami, A., et al. 2014. Genomic landscape of Ewing sarcoma defines an aggressive subtype with co-association of STAG2 and TP53 mutations. *Cancer Discov*, 4, 1342-53.
- Tomlins, S. A., Rhodes, D. R., Perner, S., Dhanasekaran, S. M., Mehra, R., Sun, X. W., et al. 2005. Recurrent fusion of TMPRSS2 and ETS transcription factor genes in prostate cancer. *Science*, 310, 644-8.
- Trask, B., Van Den Engh, G., Pinkel, D., Mullikin, J., Waldman, F., Van Dekken, H., et al. 1988. Fluorescence in situ hybridization to interphase cell nuclei in suspension allows flow cytometric analysis of chromosome content and microscopic analysis of nuclear organization. *Hum Genet*, 78, 251-9.
- Travella, A., Ripolles, L., Aventin, A., Rodriguez, A., Bezares, R. F., Caballin, M. R., et al. 2013. Structural alterations in chronic lymphocytic leukaemia. Cytogenetic and FISH analysis. *Hematol Oncol*, 31, 79-87.
- Trbusek, M. & Malcikova, J. 2013. TP53 aberrations in chronic lymphocytic leukemia. *Adv Exp Med Biol*, 792, 109-31.
-

- 
- Treumann, A., Lively, M. R., Schneider, P. & Ferguson, M. a. J. 1995. Primary Structure of CD52. *Journal of Biological Chemistry*, 270, 6088-6099.
- Trifonov, V. A. 2009. FISH with and without COT1 DNA. In: LIEHR, T. (ed.) *Fluorescence in situ hybridization (FISH)*. Springer.
- Truger, M. S., Jeromin, S., Weissmann, S., Dicker, F., Kern, W., Schnittger, S., et al. 2015. Accumulation of adverse prognostic markers worsens prognosis in chronic lymphocytic leukaemia. *Br J Haematol*, 168, 153-6.
- Tzoneva, G. & Ferrando, A. A. 2012. Recent advances on NOTCH signaling in T-ALL. *Curr Top Microbiol Immunol*, 360, 163-82.
- Uchida, J., Lee, Y., Hasegawa, M., Liang, Y., Bradney, A., Oliver, J. A., et al. 2004. Mouse CD20 expression and function. *Int Immunol*, 16, 119-29.
- Uherova, P. 2001. The clinical significance of CD10 antigen expression in diffuse large B-cell lymphoma. *American journal of clinical pathology*, 115, 582.
- Urieli-Shoval, S., Meek, R. L., Hanson, R. H., Ferguson, M., Gordon, D. & Benditt, E. P. 1992. Preservation of RNA for in situ hybridization: Carnoy's versus formaldehyde fixation. *J Histochem Cytochem*, 40, 1879-85.
- Van Bockstaele, F., Verhasselt, B. & Philippe, J. 2009. Prognostic markers in chronic lymphocytic leukemia: a comprehensive review. *Blood Rev*, 23, 25-47.
- Van Der Ploeg, M. 2000. Cytochemical nucleic acid research during the twentieth century. *Eur J Histochem*, 44, 7-42.
- Van Dyke, D. L., Werner, L., Rassenti, L. Z., Neuberg, D., Ghia, E., Heerema, N. A., et al. 2016. The Dohner fluorescence in situ hybridization prognostic classification of chronic lymphocytic leukaemia (CLL): the CLL Research Consortium experience. *Br J Haematol*, 173, 105-13.
- Varghese, A. M., Rawstron, A. C. & Hillmen, P. 2010. Eradicating minimal residual disease in chronic lymphocytic leukemia: should this be the goal of treatment? *Curr Hematol Malign Rep*, 5, 35-44.
- Vassilev, L. T. 2007. MDM2 inhibitors for cancer therapy. *Trends Mol Med*, 13, 23-31.
- Vassilev, L. T., Vu, B. T., Graves, B., Carvajal, D., Podlaski, F., Filipovic, Z., et al. 2004. In vivo activation of the p53 pathway by small-molecule antagonists of MDM2. *Science*, 303, 844-8.
- Vermeesch, J. R., Melotte, C., Froyen, G., Van Vooren, S., Dutta, B., Maas, N., et al. 2005. Molecular karyotyping: array CGH quality criteria for constitutional genetic diagnosis. *J Histochem Cytochem*, 53, 413-22.
- Vousden, K. H. & Lu, X. 2002. Live or let die: the cell's response to p53. *Nat Rev Cancer*, 2, 594-604.
- Vranic, S., Boggetto, N., Contremoulins, V., Mornet, S., Reinhardt, N., Marano, F., et al. 2013. Deciphering the mechanisms of cellular uptake of engineered nanoparticles by accurate evaluation of internalization using imaging flow cytometry. *Particle and Fibre Toxicology*, 10, 2-2.
- Wagner, S., Wagner, M. & Neuberger 1996. SOMATIC HYPERMUTATION OF IMMUNOGLOBULIN GENES. *Annual review of immunology*, 14, 441-457.
-

- 
- Wan, Y. & Wu, C. J. 2013. SF3B1 mutations in chronic lymphocytic leukemia. *Blood*, 121, 4627-34.
- Wang, J. Y. J. 2001. DNA damage and apoptosis. *Cell Death and Differentiation*, 8, 1047-8.
- Wang, X., Zheng, B., Li, S., Zhang, R., Mulvihill, J. J., Chen, W. R., et al. 2009. Automated detection and analysis of fluorescent in situ hybridization spots depicted in digital microscopic images of Pap-smear specimens. *J Biomed Opt*, 14, 021002.
- Wang, L., Lawrence, M. S., Wan, Y., Stojanov, P., Sougnez, C., Stevenson, K., et al. 2011. SF3B1 and other novel cancer genes in chronic lymphocytic leukemia. *N Engl J Med*, 365, 2497-506.
- Wang, J., Fan, H. C., Behr, B. & Quake, S. R. 2012a. Genome-Wide Single-Cell Analysis of Recombination Activity and de novo Mutation Rates in Human Sperm. *Cell*, 150, 402-412.
- Wang, X., Chen, X., Li, Y., Liu, H., Li, S., Zhang, R. R., et al. 2012b. Fluorescence In Situ Hybridization (FISH) Signal Analysis Using Automated Generated Projection Images. *Analytical Cellular Pathology (Amsterdam)*, 35, 395-405.
- Wattel, E., Preudhomme, C., Hecquet, B., Vanrumbeke, M., Quesnel, B., Dervite, I., et al. 1994. p53 mutations are associated with resistance to chemotherapy and short survival in hematologic malignancies. *Blood*, 84, 3148-3157.
- Weise, A., Mrasek, K., Kosyakova, N., Mkrtchyan, H., Gross, M., Klaschka, V., et al. 2009. ISH Probes Derived from BACs, Including Microwave Treatment for Better FISH Results. In: LIEHR, T. (ed.) *Fluorescence In Situ Hybridization (FISH) — Application Guide*. Berlin, Heidelberg: Springer Berlin Heidelberg.
- Wendtner, C., Ritgen, M., Schweighofer, C., Fingerle-Rowson, G., Campe, H., Jäger, G., et al. 2004. Consolidation with alemtuzumab in patients with chronic lymphocytic leukemia (CLL) in first remission—experience on safety and efficacy within a randomized multicenter phase III trial of the German CLL Study Group (GCLLSG). *Leukemia*, 18, 1093-1101.
- Werner, M., Chott, A., Fabiano, A. & Battifora, H. 2000. Effect of formalin tissue fixation and processing on immunohistochemistry. *Am J Surg Pathol*, 24, 1016-9.
- Wierda, W., O'brien, S., Faderl, S., Ferrajoli, A., Wang, X., Do, K. A., et al. 2006. A retrospective comparison of three sequential groups of patients with Recurrent/Refractory chronic lymphocytic leukemia treated with fludarabine-based regimens. *Cancer*, 106, 337-45.
- Wierda, W., O'brien, S., Wen, S., Faderl, S., Garcia-Manero, G., Thomas, D., et al. 2005. Chemoimmunotherapy with fludarabine, cyclophosphamide, and rituximab for relapsed and refractory chronic lymphocytic leukemia. *J Clin Oncol*, 23, 4070-8.
- Wiestner, A. 2015. The role of B-cell receptor inhibitors in the treatment of patients with chronic lymphocytic leukemia. *Haematologica*, 100, 1495-1507.
- Wiktor, A. E., Van Dyke, D. L., Stupca, P. J., Ketterling, R. P., Thorland, E. C., Shearer, B. M., et al. 2006. Preclinical validation of fluorescence in situ hybridization assays for clinical practice. *Genet Med*, 8, 16-23.
- Winkelmann, N., Rose-Zerilli, M., Forster, J., Parry, M., Parker, A., Gardiner, A., et al. 2015. Low frequency mutations independently predict poor treatment-free survival in early stage chronic lymphocytic leukemia and monoclonal B-cell lymphocytosis. *Haematologica*, 100, e237-e239.
-

- 
- Witkowska, M., Nowak, W., Cebula-Obrzut, B., Majchrzak, A., Medra, A., Robak, T., et al. 2014. Spontaneous in vitro apoptosis of de novo chronic lymphocytic leukemia cells correlates with risk of the disease progression. *Cytometry B Clin Cytom*, 86, 410-7.
- Wlodkovic, D., Skommer, J. & Darzynkiewicz, Z. 2010. Cytometry in cell necrobiology revisited. Recent advances and new vistas. *Cytometry A*, 77, 591-606.
- Wojda, A., Zietkiewicz, E., Mossakowska, M., Pawlowski, W., Skrzypczak, K. & Witt, M. 2006. Correlation between the level of cytogenetic aberrations in cultured human lymphocytes and the age and gender of donors. *J Gerontol A Biol Sci Med Sci*, 61, 763-72.
- Wortzel, I., Koifman, G., Rotter, V., Seger, R. & Porat, Z. 2017. High Throughput Analysis of Golgi Structure by Imaging Flow Cytometry. *Scientific Reports*, 7, 788.
- Xu-Monette, Z. Y., Medeiros, L. J., Li, Y., Orlowski, R. Z., Andreeff, M., Bueso-Ramos, C. E., et al. 2012. Dysfunction of the TP53 tumor suppressor gene in lymphoid malignancies. *Blood*, 119, 3668-83.
- Xu, C., Lo, A., Yammanuru, A., Tallarico, A. S., Brady, K., Murakami, A., et al. 2010. Unique biological properties of catalytic domain directed human anti-CAIX antibodies discovered through phage-display technology. *PLoS One*, 5, e9625.
- Yang, Z. & Xiong, H.-R. 2012. *Culture conditions and types of growth media for mammalian cells*, INTECH Open Access Publisher.
- Yaroslavsky, A. I. & Smolina, I. V. 2013. Fluorescence imaging of single-copy DNA sequences within the human genome using PNA-directed padlock probe assembly. *Chemistry & biology*, 20, 445-453.
- Yates, L. R. & Campbell, P. J. 2012. Evolution of the cancer genome. *Nat Rev Genet*, 13, 795-806.
- Yates, L. R., Gerstung, M., Knappskog, S., Desmedt, C., Gundem, G., Van Loo, P., et al. 2015. Subclonal diversification of primary breast cancer revealed by multiregion sequencing. *Nat Med*, 21, 751-9.
- Yokoyama, W. M., Thompson, M. L. & Ehrhardt, R. O. 2001. Cryopreservation and Thawing of Cells. *Current Protocols in Immunology*. John Wiley & Sons, Inc.
- Yokoyama, W. M., Thompson, M. L. & Ehrhardt, R. O. 2012. Cryopreservation and thawing of cells. *Curr Protoc Immunol*, Appendix 3, 3g.
- Yu, H., Chao, J., Patek, D., Mujumdar, R., Mujumdar, S. & Waggoner, A. S. 1994. Cyanine dye dUTP analogs for enzymatic labeling of DNA probes. *Nucleic Acids Research*, 22, 3226-3232.
- Yu, L., Kim, H. T., Kasar, S. N., Benien, P., Du, W., Hoang, K., et al. 2017. Survival of Del17p CLL Depends on Genomic Complexity and Somatic Mutation. *Clin Cancer Res*, 23, 735-745.
- Yuan, J. S., Kousis, P. C., Suliman, S., Visan, I. & Guidos, C. J. 2010. Functions of notch signaling in the immune system: consensus and controversies. *Annu Rev Immunol*, 28, 343-65.
- Zanella, F., Lorens, J. B. & Link, W. 2010. High content screening: seeing is believing. *Trends in Biotechnology*, 28, 237-245.
-

- 
- Zarkowsky, D., Lamoreaux, L., Chattopadhyay, P., Koup, R. A., Perfetto, S. P. & Roederer, M. 2011. Heavy metal contaminants can eliminate quantum dot fluorescence. *Cytometry A*, 79, 84-9.
- Zenz, T., Benner, A., Dohner, H. & Stilgenbauer, S. 2008a. Chronic lymphocytic leukemia and treatment resistance in cancer: the role of the p53 pathway. *Cell Cycle*, 7, 3810-4.
- Zenz, T., Habe, S., Denzel, T., Winkler, D., Dohner, H. & Stilgenbauer, S. 2008b. How little is too much? p53 inactivation: from laboratory cutoff to biological basis of chemotherapy resistance. *Leukemia*, 22, 2257-8.
- Zenz, T., Krober, A., Scherer, K., Habe, S., Buhler, A., Benner, A., et al. 2008c. Monoallelic TP53 inactivation is associated with poor prognosis in chronic lymphocytic leukemia: results from a detailed genetic characterization with long-term follow-up. *Blood*, 112, 3322-9.
- Zenz, T., Habe, S., Denzel, T., Mohr, J., Winkler, D., Buhler, A., et al. 2009a. Detailed analysis of p53 pathway defects in fludarabine-refractory chronic lymphocytic leukemia (CLL): dissecting the contribution of 17p deletion, TP53 mutation, p53-p21 dysfunction, and miR34a in a prospective clinical trial. *Blood*, 114, 2589-97.
- Zenz, T., Mohr, J., Edelmann, J., Sarno, A., Hoth, P., Heuberger, M., et al. 2009b. Treatment resistance in chronic lymphocytic leukemia—the role of the p53 pathway. *Leukemia & Lymphoma*, 50, 510-513.
- Zenz, T., Eichhorst, B., Busch, R., Denzel, T., Habe, S., Winkler, D., et al. 2010a. TP53 mutation and survival in chronic lymphocytic leukemia. *J Clin Oncol*, 28, 4473-9.
- Zenz, T., Vollmer, D., Trbusek, M., Smardova, J., Benner, A., Soussi, T., et al. 2010b. TP53 mutation profile in chronic lymphocytic leukemia: evidence for a disease specific profile from a comprehensive analysis of 268 mutations. *Leukemia*, 24, 2072-9.
- Zhang, W., Edwards, A., Flemington, E. K. & Zhang, K. 2017. Significant Prognostic Features and Patterns of Somatic TP53 Mutations in Human Cancers. *Cancer Informatics*, 16, 1176935117691267.
- Zhang, W., Flemington, E. K. & Zhang, K. 2016. Mutant TP53 disrupts age-related accumulation patterns of somatic mutations in multiple cancer types. *Cancer Genet*, 209, 376-380.
- Zhao, H., Traganos, F. & Darzynkiewicz, Z. 2008. Kinetics of histone H2AX phosphorylation and Chk2 activation in A549 cells treated with topotecan and mitoxantrone in relation to the cell cycle phase. *Cytometry A*, 73, 480-9.
- Zhu, Z., Chao, J., Yu, H. & Waggoner, A. S. 1994. Directly labeled DNA probes using fluorescent nucleotides with different length linkers. *Nucleic Acids Res*, 22, 3418-22.
- Zucchetto, A., Bomben, R., Bo, M. D., Nanni, P., Bulian, P., Rossi, F. M., et al. 2006. ZAP-70 expression in B-cell chronic lymphocytic leukemia: Evaluation by external (isotypic) or internal (T/NK cells) controls and correlation with IgVH mutations. *Cytometry Part B: Clinical Cytometry*, 70, 284-292.